

Field Monitoring of Multiple Roadside Green Infrastructure
Techniques for Water Quality and Water Quantity
Improvements

A

Dissertation

Presented to

the faculty of the School of Engineering and Applied Science
University of Virginia

in partial fulfillment
of the requirements for the degree

Doctor of Philosophy

by

Gail Moruza Hayes

May 2021

APPROVAL SHEET

This
Dissertation
is submitted in partial fulfillment of the requirements
for the degree of
Doctor of Philosophy

Author: Gail Moruza Hayes

This Dissertation has been read and approved by the examining committee:

Advisor: Dr. James A. Smith

Advisor:

Committee Member: Dr. Teresa Culver

Committee Member: Dr. Jon Goodall

Committee Member: Dr. Derek Henderson

Committee Member: Dr. Janet Herman

Committee Member:

Committee Member:

Accepted for the School of Engineering and Applied Science:



Craig H. Benson, School of Engineering and Applied Science

May 2021

Abstract

Stormwater runoff threatens the health of receiving waters through pollution, flooding, and erosion. Urbanization as well as climate change make the need for effective stormwater management techniques a paramount challenge in protecting our waterways and the ecosystems and human industries depending on them. Green infrastructure (GI) is a promising stormwater management technique that returns the hydrology of a developed area to its pre-developed hydrologic conditions through the use of infiltration, evapotranspiration, and onsite storage of runoff. However, there is still much to learn about how well individual GI systems mitigate stormwater runoff in situ and how one GI design compares to another. This dissertation addresses the knowledge gaps on GI through a field study on the performances of four types of GI systems treating road runoff from Lorton Road, a four-lane divided road in Fairfax County, Virginia. The studied GI systems are a bioretention (BR) system, bioswale (BS), compost-amended grass channel (CAGC), and a grass channel (GC). The three objectives of this dissertation are to (1) characterize the runoff volume reductions of the four systems and compare their performances, (2) evaluate the impact of deicing road salts on the capture and mobilization of trace metals in the GI, and (3) determine the extent of fecal contamination and mitigation by each GI system.

Runoff volume reduction of GI systems is an essential step in stormwater management because it reduces risks of flooding and erosion and also reduces the mass load of pollutants carried within runoff. During their first full year of operation, the Lorton GI systems were monitored for runoff volume reduction in every season for a total of 48 rain events with rain depths ranging from 2.8 mm to 97 mm. The GC achieved the largest relative volume reduction and average runoff reduction (78%, 81%), followed by the BR (71%, 73%), BS (56%, 60%), and CAGC (43%, 53%). However, the BR had the narrowest range of reductions, performing predictably well in a variety of conditions while the runoff volume reduction of the three swales (BS, CAGC, and GC) were all significantly inversely correlated with rainfall depth. In several instances, the CAGC and BS actually produced volume, an outcome attributed to particularly intense rainfall and wet soils. Overall, the BR and GC had comparable volume reductions, but selecting either system for a stormwater management plan depends on site-specific requirements such as available space and water treatment goals.

GI systems have been shown to capture trace metals from runoff, but this capture is often only a physical event and can be reversed in the proper conditions such as a sudden influx of road salt laden stormwater. The impact of deicing salts on the capture and mobilization of trace metals was evaluated through analyzing stormwater, soil, and groundwater at the Lorton field site. Flow-weighted composite samples of the stormwater entering and exiting each GI system were collected for 20 – 33 events, in all seasons from the spring of 2018 until the summer of 2020. Measurements of road salt (primarily NaCl) and trace metals (chromium, copper, nickel, and lead) showed no significant trends in the release of metals in the presence of elevated salt contents. In many instances regardless of the salt content, the GI systems were exporting trace metals. This export is attributed to low initial metal concentrations at or near irreducible concentrations. Soil sampling also revealed no significant release of metals in response to salt loading, though the sampling regime occurred over a mild winter season with relatively little road salt application. There was evidence that the mulch of the BR released metals, though the cause cannot explicitly be attributed to salt influx as it could also be a result of mulch decomposition. The groundwater at the BR received a surge of salt in the fall of 2019 in two of its wells with dampened responses in the other wells. The two wells with salt surges did not show evidence of mobilized metals, however. Between the stormwater, soil, and groundwater, there was little evidence of metal mobilization by the deicing salts and it is not believed to be a threat in a climate such as Lorton Road.

Fecal contamination is a leading stormwater pollutant and little is known on how well GI systems mitigate this pollutant. At the Lorton site, fecal contamination of the flow-weighted composite samples was measured using *E. coli* as the fecal indicator bacteria. In spite of the relatively high inflow

concentration of *E. coli* from its contributing drainage area (CDA), the BR reduced *E. coli* concentration and mass loads significantly. The swales received much lower *E. coli* levels from their CDA, but significantly increased its concentration and had no significant impact on *E. coli* loads. Outflow *E. coli* concentrations of all four GI systems were regularly above recommended limits for recreational waters, indicating that GI systems could be a source of *E. coli* in stormwater runoff. Linear correlations found significant relationships between outflow *E. coli* and ambient temperature, dissolved organic carbon (DOC), and total dissolved nitrogen (TDN) (individually). The temperature relationship is attributed to potentially increased wildlife activity in warm weather as well as increased metabolic activity of the bacteria. The links between bacteria and DOC and TDN indicate a potentially significant role that bacteria in stormwater may have in the carbon and nitrogen cycles. Overall, the BR showed good mitigation of fecal contamination while the swales indicated that they might be attracting wildlife which increases *E. coli* occurrence. Improving designs to better reduce DOC and TDN as well as discouraging wildlife activity might help with decreasing fecal contamination in future designs.

This dissertation addresses important questions regarding the runoff volume and water quality improvements offered by GI systems. By investigating the pressing questions of volume reduction, interactions of salts and metals, and prevalence of fecal contamination, the findings of this dissertation can be applied to improve future GI system designs and performance expectations. In a changing climate and spreading urbanization, it is more important than ever to protect our water resources and GI systems are a promising tool to reach these goals.

Table of Contents

Abstract	iv
List of Figures.....	ix
List of Tables.....	x
Acknowledgements	xi
Related Publications	xii
Related Presentations	xiii
1. Introduction	1
1.1 Threats of Stormwater	1
1.2 Green Infrastructure Overview	1
1.3 Runoff Volume Reduction	3
1.4 Metals and Road Salts	6
1.5 Fecal Contamination in Green Infrastructure	9
1.6 Research Objectives	13
1.7 References	13
2. Runoff reduction by four green stormwater infrastructure systems in a shared environment. 20	
2.1 Abstract.....	20
2.2 Introduction	21
2.3 Materials and Methods.....	24
2.3.1 Field Site	24
2.3.2 Rain Data	28
2.3.3 Flow Monitoring	29
2.3.4 Performance Metrics and Quality Assurance.....	30
2.3.5 Statistical Analyses	31
2.4 Results and Discussion	31
2.4.1 Rainfall Data	31
2.4.2 Overall Volume Reduction.....	32
2.4.3 Volume Reduction and Rainfall Characteristics	37
2.4.4 Volume Reductions and Seasonal Influences.....	40
2.4.5 Volume Reductions and Loading Ratios	42
2.4.6 Outflow Volume and Impervious Contributing Drainage Areas.....	43
2.5 Conclusions	44
2.6 References	46
3. Mobilization of trace metals by road salt application	49
3.1 Abstract	49

3.2 Introduction.....	50
3.3 Methods	52
3.3.1 Field Site and Data Collection.....	52
3.3.2 Analytical Methods.....	55
3.3.3 Data Analysis	57
3.4 Results	58
3.4.1 Stormwater Overview	58
3.4.2 Bioretention Stormwater	61
3.4.3 Bioswale Stormwater	63
3.4.4 Compost-Amended Grass Channel Stormwater	65
3.4.5 Grass Channel Stormwater.....	66
3.4.6 Partition Test Results.....	67
3.4.7 Winter 2019 – 2020 Soil Salt Contents.....	68
3.4.8 Winter 2019 – 2020 Soil and Mulch Metal Contents	71
3.4.9 Bioretention Groundwater.....	75
3.5 Discussion	76
3.5.1 Intra-Event Stormwater Metal Mobilization	76
3.5.2 Metal Mobilization in Soil.....	80
3.5.3 Transport to Groundwater	84
3.6 Conclusion	85
3.7 References.....	86
4. Export of fecal contamination from roadside green infrastructure	90
4.1 Abstract	90
4.2 Introduction.....	91
4.3 Methods and Materials	93
4.3.1 Field Site	93
4.3.2 Field Data Collection.....	94
4.3.3 Groundwater Monitoring and Creek Sampling	96
4.3.4 Laboratory Analytical Methods	96
4.3.5 Performance Metrics and Data Analysis	97
4.4 Results	98
4.4.1 Overview of Monitoring	98
4.4.2 Road Runoff EC Content	100
4.4.3 Bioretention.....	100
4.4.4 Grass Channel	103

4.4.5 Compost-Amended Grass Channel.....	104
4.4.6 Bioswale.....	105
4.4.7 Direct Comparison of all GI Systems	106
4.5 Discussion	108
4.5.1 EC Levels in Road Runoff	108
4.5.2 GI Outflow Concentrations.....	109
4.5.3 Environmental and Water Quality Correlations.....	109
4.5.4 Water Quality Improvements: Concentration Reductions.....	112
4.5.5 Water Quality Improvements: Load Reductions.....	114
4.5.6 Comparing Performances.....	115
4.6 Conclusion	115
4.7 References.....	116
5. Dissertation Conclusions.....	120
6. Appendices.....	123
6.1 Appendix A: GI Design Details and Monitoring Methods.....	123
6.4 Appendix B: Flow Data for Reported Events	127
6.2 Appendix C: Application of Curve Number Method.....	133
6.3 Appendix D: Flow Data Repair.....	133
6.5 Appendix E: Design to Avoid Flow Bypass at the Grass Channel.....	134
6.7 Appendix F: Well Data	135
6.8 Appendix G: Event Monitoring Results (Chapter 3)	139
6.9 Appendix H: Irreducible Concentrations	147
6.10 Appendix I: Soil Data	150
6.11 Appendix J: Bacteria Data.....	153

List of Figures

Figure 2.1. Aerial images of compost-amended grass channel (top), grass channel (bottom left), and bioswale (bottom right) with arrows representing surface flow, dotted line inside bioswale representing perforated underdrain, overland flow collector situated between the grass channel and bioswale. Photos taken by Gail Hayes.....	27
Figure 2.2. Aerial image of bioretention with piped flow represented by dark arrows, surface flow represented by light grey arrows, and perforated underdrain represented by dotted lines.	28
Figure 2.3. Rain data for all 48 monitored events including event depth, duration, intensity, and 5-day antecedent rainfall.....	32
Figure 2.4. Sample hydrographs from July 30, 2018 (24 mm) with swale inflows shown as extrapolated flow from the overland flow collector.....	33
Figure 2.5. Overall volume reductions for each system including relative volume reduction and unweighted averages (mean \pm standard deviation).	35
Figure 2.6. Relative volume reductions for each system divided into 10-mm rain event depths with the design rainfall event depth (68.6 mm) enclosed with a dotted line.	38
Figure 2.7. Relative volume reductions for each system divided into growing season (May 20 – Sept 20) and dormant season (Sept 21 – May 19) as well as unweighted averages for each season.	41
Figure 2.8. Performances of each system normalized according to expected inflow (impervious contributing drainage areas).....	43
Figure 3.1. Location of wells around bioretention. Well 1 and Well 2 were drilled manually by auger and all others drilled mechanically.....	55
Figure 3.2. Bioretention metal (chromium, copper, nickel, lead) EMC % reductions with respect to chloride inflow concentrations. Overlaid triangle indicates grab sample at outlet (February 20, 2019).....	62
Figure 3.3. Bioswale metal (chromium, copper, nickel, lead) EMC % reductions with respect to chloride inflow concentrations.....	64
Figure 3.4. Compost-amended grass channel metal (chromium, copper, nickel, lead) EMC % reductions with respect to chloride inflow concentrations.	66
Figure 3.5. Grass channel metal (chromium, copper, nickel, lead) EMC % reductions with respect to chloride inflow concentrations.....	67
Figure 3.6. Partition test results with chloride inflow EMC on the x-axis and the Partition Fraction on the y-axis.	68
Figure 3.7. Chloride and sodium content of GI soils in the top soil and sub-surface, split between Oct-2019 (red) and 2020-Mar (blue).....	70
Figure 3.8. Metal content of bioretention mulch in pre-winter and post-winter samples with error bars showing one standard deviation.....	71
Figure 3.9. Metal content of the top soils of the GI systems, split between Oct-2019 (pink) and 2020-Mar (teal). Dotted lines are historic data (Copper not shown, 86 mg/kg).....	73
Figure 3.10. Metal content of the top soils of the GI systems, split between Oct-2019 (red) and 2020-Mar (blue).....	74
Figure 3.11. Chloride contents of wells at the bioretention.....	75
Figure 3.12. Metal content of the wells at the bioretention.	76
Figure 4.1. Road runoff concentrations of E. coli from the contributing drainage areas of the bioretention and swales. Dashed line: 30-day geometric mean limit. “ – “ not analyzed.	100
Figure 4.2. EC EMC at the bioretention inlet, outlet, and bypass. Dashed line: 30-day geometric mean limit.....	102
Figure 4.3. Grass channel EC results. February 23, 2019 received no measurable EC as inflow from the road runoff. Dashed line: 30-day geometric mean limit.....	104
Figure 4.4. Compost-amended grass channel EC performance. February 23, 2019 received no measurable EC as inflow from the road runoff. Dashed line: 30-day geometric mean limit.	105
Figure 4.5. Bioswale EC performance. February 23, 2019 received no measurable EC as inflow from the road runoff. Dashed line: 30-day geometric mean limit.....	106

List of Tables

Table 2.1. Design specifications and other characteristics for monitored GI systems. (ESM: Engineered soil media, CDA: contributing drainage area, GC: Grass channel, CAGC: Compost-amended grass channel, BS: Bioswale, BR: Bioretention.).	26
Table 2.2. P-values and slopes (m) for simple linear regression analysis of % runoff volume reduction and specified site condition ($\alpha = .05$). AMC: antecedent moisture conditions (rainfall in preceding 5 days)...	39
Table 3.1. Water quality results for events of interest presented as average \pm standard deviation (SD) and range [minimum, maximum] with event mean concentration (EMC) and % reduction of EMC. ^a Bioretention EMC reductions calculated using only inflow and outflow (no bypass).....	60
Table 3.2. Linear regression analysis results of slope and (P-value significance, R^2) with salts, DOC, and TSS as the explanatory variables and outflow concentration and EMC reduction as the response variables at the bioretention. Dash (-) indicates no significance.....	63
Table 3.3. Linear regression analysis results of slope and (P-value significance) with salts, DOC, and TSS as the explanatory variables and outflow concentration and EMC reduction as the response variables at the bioswale.	65
Table 4.1. Event and EC data for monitored events.....	99
Table 4.2. Linear regression analyses of GI system outflows and water quality constituents. N/S = not significant. Response variables are outflow log EMC at each GI while explanatory include environmental factors and water quality parameters at the outlets.....	103
Table 4.3. EC content entering and exiting each GI and environmental conditions during the nine shared events.....	107

Acknowledgements

First, I'd like to thank my advisor, Dr. Jim Smith, for your guidance on this research and the opportunity to join this project. I am grateful for the guidance and feedback of my other committee members, Dr. Teresa Culver, Dr. Jon Goodall, Dr. Derek Henderson, and Dr. Janet Herman. To my entire committee, thank you for supporting my research endeavors, especially in light of the challenges brought on by COVID-19. Special thanks to Dr. Derek Henderson for your guidance in getting this research off the ground and your continued assistance with the field and lab work.

Thank you to Dr. Mike Fitch and Mr. Lewis Lloyd of the Virginia Transportation Research Council for your support of and interest in the success of this research.

Wuhuan Zhang and Dr. Charles Burgis provided invaluable hands-on help as fellow doctoral students on the Lorton research team. Thank you for your unwavering enthusiasm and willingness to go the extra mile.

Undergraduate research assistants from the University of Virginia and George Mason University helped greatly in the field and lab work. To Cecil Johnson, Brett Conklin, Mellany Ona Ayala, Leah Scully, Tyler Privott, and Meredith Sutton, thank you!

Thank you to the Smith Water Quality Research Group members at large. Your kindness and encouragement have meant so much to me.

To my family and friends, thank you for your steady support over the years. To my preborn daughter, thank you for providing hope and joy in a difficult year. To my husband, Thomas; you have walked beside me every step of the way, giving vital encouragement, support, and helping me to stay light-hearted. (Thank you especially for making me dinner almost every night for the last six months of this degree!)

Last but not least, I'd like to acknowledge my late grandmother, Dr. Jacqueline Rorabeck Kasun, for planting the seed of academic endeavors in the young and impressionable little girl you helped with her daily lessons. Though our doctoral topics were decades and fields apart, your example of persistent hard-work was inspirational and formational for me.

Related Publications

This dissertation has directly resulted in the following publications.

(Chapter 1) Henderson, D., **Moruza (Hayes), G.M.**, Burgis, C., Smith, J. A. (2019) “Low Impact Development Technologies for Highway Stormwater Runoff.” In *Encyclopedia of Water: Science, Technology, and Society*; Wiley; pp 1–18. <https://doi.org/10.1002/9781119300762.wsts0009>.

(Chapter 2) **Hayes, G.M.**, Burgis, C., Zhang, W., Henderson, D., Smith, J.A. (2021) “Runoff reduction by four green stormwater infrastructure systems in a shared environment.” *J. Sustainable Water in the Built Environment*. <https://doi.org/10.1061/JSWBAY.0000932>.

(Chapter 3) **Hayes, G. M.**, Zhang, W., Burgis, C., Henderson, D., Smith, J.A. (In Preparation) “Evaluating the impact of sodium chloride road salt on the potential mobilization of metals in the runoff, soils, and groundwater associated with highway green infrastructure.” *J. Environmental Engineering*.

(Chapter 4) **Hayes, G.M.**, Zhang, W., Burgis, C., Henderson, D., Smith, J.A. (Under review) “Evaluating the export of fecal contamination from green infrastructure.” *J. Sustainable Water in the Built Environment*.

Other related publications from this research:

Burgis, C.R., **Hayes, G.M.**, Henderson, D.A., Zhang, W., Smith, J.A. (In Preparation) “Evaluation of Green Stormwater Infrastructure Options for Transportation Water Quality Improvement.”

Burgis, C.R., **Hayes, G.M.**, Henderson, D.A., Zhang, W., Smith, J.A. (2020) “Green Stormwater Infrastructure Redirects Deicing Salt from Surface Water to Groundwater.” *Sci. Total Environ.* <https://doi.org/10.1016/j.scitotenv.2020.138736>.

Burgis, C.R., **Hayes, G.M.**, Zhang, W., Henderson, D.A., Macko, S.A., Smith, J.A. (2020) “Tracking Denitrification in Green Stormwater Infrastructure with Dual Nitrate Stable Isotopes.” *Sci. Total Environ.* <https://doi.org/10.1016/j.scitotenv.2020.141281>.

Related Presentations

This dissertation has directly resulted in the following presentations.

Hayes, G.M., Burgis, C.R., Zhang, W., Henderson, D.H., Smith, J.A. “Green Infrastructure Demonstrates Variable Mitigation of Fecal Contamination in Stormwater.” Virtual poster presentation (abstract submission) at WaterJAM (VA AWWA and VWEA). September 2020.

Hayes, G. M., Burgis, C., Zhang, W., Henderson, D., Smith, J.A. “Comparing flow reductions of four green infrastructure systems in a roadside environment and early results from groundwater monitoring receiving infiltrated runoff.” Session 12. Lectern presentation (abstract submission) at the Annual Water Resources Conference. Salt Lake City, Utah, November 2019.

Hayes, G. M., Zhang, W., Burgis, C., Henderson, D., Smith, J.A. “Low Impact Development Performance on Lorton Road.” Lectern presentation at the VDOT Virginia Transportation Research Council: Environmental Research Advisory Committee Meeting. Charlottesville, VA, May 2019.

Hayes, G. M., Burgis, C., Henderson, D., Smith, J.A. “Low-Impact Development for Roadside Stormwater Management: Performance of Several Stormwater Control Techniques in a Shared Watershed.” P19-20488. Lectern presentation (abstract submission) at Transportation Research Board Annual Meeting. Washington, DC, January 2019.

Hayes, G. M., Burgis, C., Henderson, D., Smith, J.A. “Low Impact Development in Highway Stormwater Management”. Lectern presentation (abstract submission) at the University of Virginia Global Water Initiative Graduate Research Symposium. Charlottesville, VA, October 2018.

Hayes, G., Henderson, D., Burgis, C., Fitch, G.M., Smith, J.A. “Low Impact Development in Highway Stormwater Management: A Virginia Case Study.” Lectern presentation (abstract submission) at Environment & Water Resources Institute (ASCE) Operation & Maintenance of Stormwater Control Measures Conference. Denver, CO, November, 2017.

Other related presentations resulting from this research:

Zhang, W., Burgis, C., **Hayes, G. M.**, Henderson, D., Smith, J.A., “Long-Term Monitoring of Water-Quality Performance of Four Green Infrastructures Receiving Similar Influent Pollutant Loadings.” Lectern presentation at the 2021 World Environmental & Water Resources Congress. May 2021. Milwaukee, WI.

Zhang, W., Burgis, C., **Hayes, G. M.**, Henderson, D., Smith, J.A., “Potential of Vegetation to Mitigate Deicing Salt Loading in Green Infrastructure.” Poster presentation at the 2021 World Environmental & Water Resources Congress. May 2023. Milwaukee, WI.

Burgis, C.R., **Hayes, G.M.**, Zhang, W., Smith, J.A. “Tracking Denitrification in Green Stormwater Infrastructure with Nitrogen and Oxygen Stable Isotopes.” Lectern presentation at ASCE International Low Impact Development Conference. July 19-22, 2020, Bethesda, MD.

Burgis, C.R., **Hayes, G.**, Henderson, D.A., Zhang, W., Smith, J.A. “Green Stormwater Infrastructure Buffers Surface Water from Deicing Salt Loading.” Lectern presentation at ASCE International Low Impact Development Conference. July 19-22, 2020, Bethesda, MD.

Burgis, C. R., **Hayes, G.**, Zhang, W., Smith, J.A., “Tracking Denitrification in Green Stormwater Infrastructure.” Lectern presentation at the University of Virginia Global Water Initiative Graduate Research Symposium. Charlottesville, VA, November 2019.

Zhang, W., Burgis, C., **Hayes, G. M.**, Henderson, D., Smith, J.A., “Water Quality Performance of Green Stormwater Infrastructure along Lorton Road.” Session 11. Poster presentation at the American Water Resources Association’s Annual Water Resources Conference. Salt Lake City, Utah, November 2019.

Burgis, C.R., **Hayes, G.**, Henderson, D.A., Smith, J.A. “Assessment of Green Stormwater Infrastructure Practices on Lorton Road, Fairfax County, VA.” Lectern presentation at the ASCE International Low Impact Development Conference. August 12-15, 2018, Nashville, TN.

Burgis, C.R., **Hayes, G.**, Henderson, D.A., Smith, J.A., Fitch, M. “Assessment of Green Stormwater Infrastructure Performance on Lorton Road.” Lectern presentation at the VDOT Virginia Transportation Research Center Environmental Research Advisory Council. June 8, 2018, Richmond, VA.

Burgis, C.R. “How Does Green Stormwater Infrastructure Handle Road Salt?” Poster presentation at the University of Virginia Engineering Research Symposium. March 22, 2018, Charlottesville, VA.

Burgis, C.R., **Hayes, G.**, Henderson, D.A., Smith, J.A., Fitch, M. “Assessment of the Low Impact Development Strategies Used for the Lorton Road Widening Project.” Lectern presentation at the VDOT Virginia Transportation Research Center Environmental Research Advisory Council. June 12, 2017, Richmond, VA.

1. Introduction

Work from this chapter is published in the Encyclopedia of Water article:

Henderson, D., Gail Moruza (Hayes), Charles Burgis, James A. Smith, “Low Impact Development Technologies for Highway Stormwater Runoff.” In *Encyclopedia of Water: Science, Technology, and Society*; Wiley, 2019; pp 1–18. <https://doi.org/10.1002/9781119300762.wsts0009>.

1.1 THREATS OF STORMWATER

Runoff from rainfall and snowmelt, or stormwater runoff, is a vital part of the water cycle that returns precipitation to water bodies and soils. In an undisturbed or balanced environment, runoff naturally infiltrates, evapotranspires, or is stored in surface or subsurface reservoirs. However, when natural spaces are replaced with buildings, pavement, or other impervious surfaces, stormwater runoff is not mitigated with these natural processes and becomes a nuisance through flooding, erosion, and contaminant transfer to receiving waters. Common contaminants in stormwater include metals, nutrients, oil and grease, suspended solids, road salts, and bacteria (USEPA 2019b). The changing climate is resulting in more rain events of increasing intensity and volume which can overwhelm natural, balanced landscapes (NOAA 2014). The United States Environmental Protection Agency (US EPA) predicts a \$750 million increase in flood damage by the year 2100, a direct result of rain events increasing in intensity and volume and also landscapes unequipped to mitigate the greater volumes of runoff (US EPA 2020).

1.2 GREEN INFRASTRUCTURE OVERVIEW

The adverse effects of stormwater runoff can be mitigated with low impact development, a technique that seeks to return the hydrology of a developed space to its pre-developed conditions by encouraging infiltration and creating additional opportunities for on-site storage (Ahiablame et al. 2012). Infiltrating or storing stormwater reduces the previously mentioned risks as well as loads of entrained pollutants and energy costs at downstream water treatment facilities (Flynn and Traver 2013; Line and Hunt 2009). Installations of low impact development include green infrastructure (GI), primary examples

of which are bioretention systems and swales. Designs of specific GI installations are determined by site characteristics such as climate, soil type, contributing drainage area type and size, typical pollutant, and regulations (Henderson et al. 2019).

A bioretention system is a shallow, vegetated and mulched basin that encourages ponding of runoff as it infiltrates the basin soil. The sand, soil, and organic amendments of the bioretention soils are designed to filter the runoff as it seeps into the underlying stone sump. Underdrains are frequently included in the stone sump to allow quick discharge of the filtered influent (DEQ 2011a). Bioretention systems, also known as rain gardens when constructed on a small scale, excel at capturing or slowing large volumes of quickly moving runoff through ponding and infiltrating runoff (DEQ 2011a). The infiltrate is stored in the soil pores, can exfiltrate to the surrounding soils, or exit through an underdrain (DEQ 2011a; Winston et al. 2016). Minimum volume reductions by bioretention systems mandated by the Virginia Department of Environmental Quality (VA DEQ) are 40% and 80% depending on the inclusion of an underdrain (DEQ 2011a). Other requirements by the VA DEQ include removal of nutrients (total phosphorus and total nitrogen) and total suspended solids through reductions of event mean concentration (EMC) and mass loading (DEQ 2011a).

Another common type of GI installation is a swale, or an engineered channel comprised of various types of soils and vegetation selected according to treatment goals. Swales are typically expected to convey rather than treat or store runoff (Davis et al. 2011). Grass channels are the simplest swale design and typically include native soils and vegetation but can be designed for increased infiltration rates by incorporating compost-amended soils (DEQ 2011c). Minimum volume reductions established by the VA DEQ for grass channels with no soil amendments are 10% for soils with moderate to high infiltration rates (hydrologic soil groups A/B) and 20% for very slow to slow infiltration rates (hydrologic soil groups C/D) and increase to 30% when including compost-amended soils (DEQ 2011c). A grass channel with compost-amended soils is known as a compost-amended grass channel and is a second type of swale.

The bioswale, also known as a dry swale, is a third type of swale and is similar to the bioretention system in that it incorporates engineered soil media and often an underdrain situated on or within a stone sump (DEQ 2011b). VA DEQ requirements of volume reductions for the bioswale are similar to the bioretention system (40% and 60%) and depend on the inclusion of an underdrain. Bioswale designs typically includes turf or similar vegetation (DEQ 2011b). Check dams are frequently used in all three types of swales to reduce the effective slope of the channel and water velocity and also provide additional, temporary storage (DEQ 2011c; A. Davis et al. 2011).

While GI has been in use for several decades, its placement in the natural environment produces a myriad of factors and conditions that influence performance in managing stormwater. Over the last few decades, progress has been made in understanding the performance of GI in the field, but data are still lacking in essential areas of volume and water quality control. First, there are still gaps in understanding how different GI designs in similar environmental conditions reduce runoff volumes. Runoff volume reduction is the primary building block on which much of stormwater management functions because it allows for mass load reductions of contaminants and also reduces the risks of flooding and erosion. Second, recent concerns for the effects of road salt in runoff have led to questions about its impact on trace metals due to concerns that dissociated road salt ions could mobilize trace metals from the GI soils, but more data are needed to understand this event on the full scale of a GI system. Third, increased awareness of fecal contamination in water bodies used for recreation, industry, or drinking water purposes has led to expanded efforts to minimize the release of fecal contamination with stormwater. The natural landscape that GI provides may be encouraging wildlife traffic which may ultimately increase fecal contamination in the outflows of GI systems, but robust methodologies have not yet been employed to examine this.

1.3 RUNOFF VOLUME REDUCTION

GI for stormwater management is relatively novel and there is a need for more field studies evaluating multiple systems in shared environments, particularly with regards to runoff volume reduction. In field studies conducted on bioretention systems and swales, where environmental conditions such as rainfall and temperature are not easily manipulated, research typically focuses on a single type of control measure. However, even in field research, a few conditions can be manipulated, albeit in limited ways.

Bioretention systems have demonstrated high runoff volume reductions in field and lab studies and frequently capture 100% of runoff in smaller events. Shrestha et al. (2018) found average volume reductions of 75% (ranging 48% – 96%) and complete capture in 31% of the events by their roadside bioretention systems in Vermont. Likewise, Cording et al. (2018) reported average volume reductions of 79% in their experimental bioretention systems with varying vegetation types and soil conditions. Examples of moderate volume reductions include Davis (2008), Winston et al. (2016), and Komlos and Traver (2012) which observed volume reduction ranging from 36% to 59% and peak volume reduction ranging from 49% to 58%. Volume reductions of bioretention systems are compromised when groundwater intrudes the basin soils or additional flow enters the basin that is not accounted for in the inflow monitoring. An example of this occurred in Line and Hunt (2009) which reported up to 82% increase in volume due to these factors. However, this same study found that volume reductions could be as high as 77%, presumably if the extraneous sources of water were limited. Other factors of concern in bioretention volume reduction include normal wear over time such as fine sediment accumulation as well as basin depth at initial installation. While Brown and Hunt (2011) determined that bioretention systems with deeper basins reduced runoff volumes to a greater extent than their shallower counterparts, Jenkins et al. (2010) found that 9 years of sediment accumulation did not significantly alter infiltration (and related runoff reductions) significantly.

Several studies have collected data on swale performance within a single season, but used synthetic runoff rather than naturally occurring rain for their site (Yousef et al. 1987; Deletic and Fletcher 2006; García-Serrana et al. 2017). The studies that have examined the runoff reduction performance of swales have found sufficient volume reduction for smaller rain events, less reduction in larger events, perforated underdrains assisting in volume reduction, and antecedent moisture conditions influencing water storage capacity (Knight et al. 2013; Davis et al. 2011; Abida and Sabourin 2006; Shafique et al. 2018; Rujner et al. 2017). Knight et al. (2013) found volume reduction of 23% over 30 analyzed events with no mention of check dams while Davis et al. (2011) found 27% - 63% reduction by swales with check dams. Other factors to consider are the incorporation of an underground storage trench, shown to assist volume reduction with reductions of 40 – 75%, and also antecedent moisture conditions, the greater of which reduce volume retention (Shafique et al. 2018; Rujner et al. 2017).

Short-term studies (less than one year) comparing GI methods to one another include a 2009 comparison between bioretention and a level spreader-grass filter strip wherein the filter strip was shown to have relatively more effective contaminant (total suspended solids and total nitrogen) control but runoff volume was heavily influenced through seasonal conditions (Line and Hunt 2009). Other studies on water quality improvements include variations in vegetation type and presence rather than GI method (Leroy et al. 2016; Valtanen et al. 2017). Other studies do focus on long-term performance of multiple sites, but with the stipulations of zero maintenance over the life-time, limited seasonal testing, or limited time of study in general (Winston et al. 2016; Al-Rubaei et al. 2015; Li et al. 2014; Li et al. 2016; Yu et al. 2013; Cording et al. 2017; Maniquiz et al. 2010).

Several literature reviews have been written on infiltration-based stormwater control measures, such as bioretention and swales, focusing on reviewing runoff reduction performances (water quality and quantity) as well as identifying needs for future research. Common research needs identified among these literature reviews include monitoring over extended time periods (greater than a single season),

incorporating expected performance variations such as seasonal shifts or impacts of maintenance work, and availability of data for modeling or related purposes (Tedoldi et al. 2016; Eger et al. 2017; Eckart et al. 2017; Lucke et al. 2017; Roy-Poirier et al. 2010; Liu et al. 2017). In addition to these acknowledged gaps in the literature, there is room for investigations into the necessity of varying complexity of GI designs. Chapter 2 of this dissertation addresses these gaps in the knowledge on GI for stormwater management through the characterization and comparison of the runoff reduction performances of four independent GI of varying complexity and footprint sizes over one year in shared climate conditions.

1.4 METALS AND ROAD SALTS

Trace metals are a common stormwater pollutant but are also found naturally in the environment. Metals are often necessary for biological processes, but disturbances of metal-rich soils as well as deposits from anthropogenic activity can increase the presence of toxic metals and in some cases their bioavailability as well (Alloway 1995). Six metals in particular are often cited as problematic because of their adverse impacts on organisms: chromium, nickel, copper, zinc, cadmium, and lead. Sources of metals include atmospheric deposition, rainfall, agricultural fertilizers, organic waste, vehicle wear and tear, and mineral (lithogenic) sources (USEPA 2019a; Brown and Peake 2006; Alloway 1995). The impacts which metals have on organisms varies by metal, organism, and environmental conditions. For example, metals on the surfaces or in the roots of plants have been shown to often have minimal impact on plant growth, but potentially amplified food-chain effects through the microflora inhabiting the plant surface (Koeppel 1981). Marine environments are also impacted by stormwater runoff and the metals carried therein. Organisms in these environments can accumulate metals in their tissues, leading to problems with cellular function that ultimately harm growth and reproduction as well as immune and metabolic systems (Jakimska et al. 2011).

GI has been shown to capture metals from stormwater through adsorption and physical capture, thus limiting the adverse impacts of metals on the environment (Ernst et al. 2016). However, because

the removal of metals is typically a physical event rather than a chemical transformation, the metals are still capable of being released if given the proper conditions. One example of such a condition is the introduction of road salt ions that have been shown to mobilize trace metals from their capture in soils. Anti-icing and de-icing agents maintain safe winter driving conditions on roads across the Commonwealth of Virginia and are typically in the form of salt. Sodium chloride is the most common de-icing road salt, but magnesium chloride and calcium chloride are other salts that can be used. Typically, dry sodium chloride is applied, but often it is either in the form of a brine solution or mixed with sand to increase abrasiveness (VDOT 2009).

When dissociated sodium chloride in stormwater infiltrates roadside soils, the mobile chloride travels through the soils due to its negative charge repelling the negative charge of the soil (Ramakrishna and Viraraghavan 2005). Chloride has been shown to reach the groundwater in some areas, potentially risking the quality of drinking water by itself and also through chlorocomplexes formed with certain metals (Bauske and Goetz 1993). Chloride can also reach surface water through surface and subsurface flow, endangering the local biota (Ramakrishna and Viraraghavan 2005). While the chloride ion will typically travel through the soil relatively unabated, the positively charged sodium ion engages in cation exchange with the negatively charged soil, displacing calcium and magnesium, dispersing organic and inorganic particles, decreasing permeability, and mobilizing nutrients and metals (Amrhein et al. 1992; Ramakrishna and Viraraghavan 2005; Sørensen et al. 2017; Norrström 2005). When sodium mobilizes metals, it can increase the metal bioavailability, creating health hazards for plants and animals with which they come into contact (Novotny et al. 1998; USEPA 2019a; Brown and Peake 2006).

When road salts are present, the mobilization mechanisms of chromium, copper, and nickel tend to be attributed to the mobilization of organic content through the influence of sodium ions, though there is evidence that copper forms chlorocomplexes as well (Amrhein et al. 1992; Nelson et al. 2009). Cadmium is typically relatively mobile in soil and has been found to be mobilized through cation-

exchange with sodium and the resulting chlorocomplexes formed with chloride from dissolved road salts (Amrhein et al. 1992; Bauske and Goetz 1993; Bäckström et al. 2004; Ann Catrine Norrström 2005; Nelson et al. 2009; Li et al. 2015). Zinc mobilization is mostly credited to ion exchange and partially to chlorocomplex formation (Norrström 2005; Bäckström et al. 2004). Lead is typically known as the least mobile of these metals due to its tendency to sorb strongly to soil, but it can be mobilized when sodium disperses clay and oxides and it is carried in colloidal form (Nelson et al. 2009; Sjøberg et al. 2017).

The physicochemical interactions between sodium, chloride, and metals in soils are well documented with early investigations focusing on roadside environments with minimal if any stormwater management techniques in use. Most of these studies found evidence that dissociated sodium chloride increased mobility of at least two of the six metals commonly investigated in stormwater studies through characterizing soil content of metals, sodium, and chloride as well as through leaching tests in columns (Amrhein et al. 1992; Bauske and Goetz 1993; Warren and Zimmerman 1994; Norrström 2005; Novotny et al. 1998; Lofgren 2001; Bäckström et al. 2004; Merrikhpour and Jalali 2013; Li et al. 2015). These studies focused primarily on surface water, soil water, and the soil itself, and just Norrström and Jacks (1998) investigated the groundwater, finding elevated levels of lead which they attributed to road salt activity.

When GI gained popularity, the focus of studies on the interactions of road salts and metals in the environment shifted to these systems specifically designed for infiltration. However, much of this research has been in controlled laboratory column experiments leaching typical and experimental bioretention media. In accordance with previous research unrelated to GI systems, most of these column studies have found evidence that road salts could negatively affect GI mediation of metals through mobilization (Sjøberg et al. 2017; Norrström 2005; Nelson et al. 2009; Paus et al. 2014; Huber et al. 2016), though Kakuturu and Clark (2015) found insufficient evidence for such claims. Where field analyses on the interactions between metals and road salts do happen, the GI types are bioretention

systems, infiltration trenches, or ponds with no research on swales. Two field studies on bioretention systems found no evidence for metal leaching in the presence of road salts (Muthanna et al. 2007; Géhéniau et al. 2015), but one on infiltration trenches did (Mullins et al. 2020). Several swale studies have addressed salts and metals individually, but as of yet, nobody has investigated them together (Stagge et al. 2012; Revitt et al. 2017; Boger and Ahiablame 2019). Moreover, there is a shortage of such investigations on multiple types of GI systems in a shared environment.

The lack of consistency in field study results, lack of data altogether on swales, and lack of reporting on multiple types of GI systems in a shared environment provides a good opportunity for this dissertation and the Lorton Road field site provides an excellent location for such a study. Furthermore, studies that have investigated road salts and metal mobility recommend further research on the impacts of these interactions on groundwater (Norrström 2005; Denich et al. 2013). Given the shallow groundwater at the Lorton Road site, there may be measurable trends in road salts mobilizing metals to the water table. Chapter 3 of this dissertation addresses these needs for research through reporting on metal and salt levels in stormwater, groundwater, and soil at the Lorton Road bioretention and swales.

1.5 FECAL CONTAMINATION IN GREEN INFRASTRUCTURE

Fecal contamination in stormwater runoff can introduce pathogens to receiving waters used for recreation, industry, and drinking water purposes. In 2010, the International Stormwater Best Management Practice (BMP) Database reported that pathogens, typically resulting from fecal contamination, were the leading cause for stream impairment in the United States (Wright Water Engineers 2010). Exposure to these pathogens can cause serious diseases such as cholera, typhoid fever, diarrhea, and dysentery (Bain et al. 2014). Every year, fecal contamination is detected at thousands of beaches in the United States alone, risking human health and loss of income due to limitations on tourism and industrial activities (EARPC 2020). Common sources of fecal contamination in stormwater include sanitary sewer overflows, combined sewer overflows, illegal and improper dumping of waste,

wastewater treatment plants, and waste from warm-blooded wild and domesticated animals (Wright Water Engineers 2010). Detection of fecal contamination is conducted through measurements of fecal indicator bacteria, or easily enumerated bacteria that are known to come from warm-blooded animal waste (Wright Water Engineers 2010). Regulations in the United States recommend two species of bacteria to indicate the presence of fecal contamination: enterococcus is used primarily in marine environments and *Escherichia coli* (EC) is used only in freshwater (Wright Water Engineers 2010). Recreational water quality limits for the United States establish a 30-day geometric mean of 126 MPN/100 mL for EC in freshwater and 33 MPN/100 mL for enterococci in salt water (Wright Water Engineers 2010).

Reported levels of fecal contamination that enter GI systems vary widely due to characteristics of bacteria reproduction and differences in selections of fecal indicator bacteria. Even though the EPA recommends EC for freshwater monitoring, some studies measure total or fecal coliform, which includes EC. Other studies may report both enterococci and EC levels to include both freshwater and marine environments. In Passeur et al. (2009), road runoff fecal coliform concentrations entering the bioretention systems ranged from 220 to 20,000 coliforms/100 mL while in Willard et al. (2017), inflow concentrations of EC from a parking lot ranged from less than 2 to over 1000 most probable number (MPN)/100 mL. Parker et al. (2010) reported EC levels in untreated urban stormwater reaching 1.2×10^5 MPN/100 mL and Hathaway et al. (2010) reported EC levels in residential stormflow ranging from 700 to 8.4×10^4 MPN/100 mL. Krometis et al. (2007) reported similarly high levels of bacteria in stormflows from university and residential areas with fecal coliforms averaging over 1.8×10^4 and 9.1×10^4 MPN/100 mL and EC averaging over 3000 and 2.7×10^4 MPN/100 mL at two monitored streams. Treated wastewater effluent typically has much lower levels of bacteria than stormwater, reported by Petersen et al. (2005) to be 5 MPN/100 mL, on average.

GI has been shown to remove fecal contamination from stormwater to some degree in certain designs, but most studies reporting this have not used robust sampling methods and were unable to compute mass loading of organisms. This limitation is due to concerns with contaminated autosamplers harboring organisms and also cost restrictions for this equipment. Therefore, bacteria levels are frequently measured with manually captured grab samples. With these monitoring methods, bioretention systems have been shown to generally remove fecal contamination from runoff, but effectiveness depends on soil depth. Additionally, reported removal rates can vary due to the sensitivity of bacteria to its environment. The removal rate of EC by a bioretention system 1.2 m in depth was reported by Hunt et al. (2008) as approximately 70% for concentration reductions. In Hathaway et al. (2011), two bioretention systems of different depths were monitored and found to reduce EC concentrations depending on their respective depths; the deeper bioretention system (60 cm) reduced EC concentration by 70% while the shallower bioretention system (25 cm) increased EC by 119%. The bioretention system monitored by Hathaway et al. (2009) reduced EC concentration by almost 90%, but no soil depth was reported. Studies which used more robust sampling methods of flow-weighted composite sampling that allow for loading computations include Li and Davis (2009) and Willard et al. (2017). Li and Davis (2009) reported on two bioretention systems of approximately the same depth (0.5 – 0.9 m) that achieved median EC concentration reductions of 57% and 0% but median loading reductions of 94% and 100% (due to volume reductions). Willard et al. (2017) studied a deeper bioretention system with a soil depth of 1.8 m and found average concentration reductions of -18% (median of 100%) and average loading reductions of 100% (also due to volume reductions).

Compared to bioretention systems, there are far fewer studies on swale performance in reducing fecal contamination in stormwater. Swales work well for channeling stormwater to additional treatment systems and do not have the same treatment expectations as bioretention systems, but have been shown to mitigate stormwater in some instances (Davis et al. 2011; Hayes et al. Forthcoming). While

Barrett et al. (1998) reported a 192% increase in fecal coliform concentration in their roadside swales, Mallin et al. (2016) reported reductions in fecal contamination concentrations. However, Mallin et al. (2016) did not directly measure swale outflows and reports only on the water quality of an entire watershed by a series of newly installed BMPs. These contradicting results and small number of studies emphasize the need for more data on swale performance in reducing fecal contamination.

While GI systems have demonstrated the capacity to remove fecal contamination from stormwater runoff, the large variation in results indicate that they also regularly export fecal contamination. These variations in performance and inevitable export are due to the ability of bacteria to increase in number with no external addition of organisms (Wright Water Engineers 2010) and also a result of favorable climate conditions and GI design (Rippy 2015; Clary et al. 2008). Some studies have investigated conditions impacting variations in fecal contamination in GI systems, but there is room for more research on the export of fecal contamination from GI. General conditions commonly cited for affecting EC survival (within GI or in environments absent of GI systems) include temperature, moisture, nutrient and carbon availability, organic content, and sediment level and type (Wright Water Engineers 2010; Rippy 2015; Jeng et al. 2005; Hathaway et al. 2010; Kawasaki et al. 2013). Linking these factors with mass and concentration export of fecal contamination from GI would be a valuable asset to further understanding and optimizing GI designs.

There are still significant data gaps on how well GI reduces the presence of fecal contamination in stormwater runoff. The vast majority of these studies use single grab samples to represent fecal contamination of an entire rain event. However, if proper cleaning procedures and quality assurance plans are followed, it is possible to use autosamplers to create a more robust sampling regime with flow-weighted composite sampling (Hathaway et al. 2014). Chapter 4 of this dissertation addresses these needs through robust sampling methods that use flow-weighted composite samples and loading calculations. Analyses include the evaluation of environmental conditions and key water quality

parameters with respect to the export of fecal contamination from a bioretention system and several types of swales.

1.6 RESEARCH OBJECTIVES

The goal of this dissertation is to evaluate the performance of four types of GI systems for roadway stormwater management in areas of runoff volume control and water quality improvements. The three specific research objectives are (1) to characterize runoff volume reduction by four types of GI systems (Chapter 2), (2) to assess the potential antagonistic impact of road salts on the capture of trace metals in the GI systems (Chapter 3), and (3) evaluate the mitigation and export of fecal contamination by GI systems (Chapter 4).

1.7 REFERENCES

- Abida, H., and J.F. Sabourin. 2006. "Grass Swale-Perforated Pipe Systems for Stormwater Management." *JOURNAL OF IRRIGATION AND DRAINAGE ENGINEERING* 132 (1): 55–63. <https://doi.org/10.1061>.
- Ahiablame, Laurent M., Bernard A. Engel, and Indrajeet Chaubey. 2012. "Effectiveness of Low Impact Development Practices: Literature Review and Suggestions for Future Research." *Water, Air, & Soil Pollution* 223 (7): 4253–73. <https://doi.org/10.1007/s11270-012-1189-2>.
- Alloway, Brian J. 1995. "Heavy Metals in Soils: Trace Metals and Metalloids in Soils and Their Bioavailability." In , 3rd ed. *Environmental Pollution* 22. Springer. https://www.google.com/books/edition/_/Soovc_GOk48C?hl=en&gbpv=1&bsq=bioavailability.
- Al-Rubaei, Ahmed, Maria Viklander, and Godecke-Tobias Blecken. 2015. "Long-Term Hydraulic Performance of Stormwater Infiltration Systems." *Urban Water Journal* 12 (8): 660–71.
- Amrhein, Christopher, James E. Strong, and Paul A. Mosher. 1992. "Effect of Deicing Salts on Metal and Organic Matter Mobilization in Roadside Soils." *Environmental Science & Technology* 26: 703–9.
- Bäckström, Mattias, Stefan Karlsson, Lars Bäckman, Lennart Folkesson, and Bo Lind. 2004. "Mobilisation of Heavy Metals by Deicing Salts in a Roadside Environment." *Water Research* 38 (3): 720–32. <https://doi.org/10.1016/j.watres.2003.11.006>.
- Bain, Robert, Ryan Cronk, Jim Wright, Hong Yang, Tom Slaymaker, and Jamie Bartram. 2014. "Fecal Contamination of Drinking-Water in Low- and Middle-Income Countries: A Systematic Review and Meta-Analysis." *PLOS Medicine*, May. <https://doi.org/10.1371/journal.pmed.1001644>.
- Barrett, Michael E., Patrick M. Walsh, Joseph F. Malina, and Randall J. Charbeneau. 1998. "Performance of Vegetative Controls for Treating Highway Runoff." *Journal of Environmental Engineering* 124 (11): 1121–28. [https://doi.org/10.1061/\(ASCE\)0733-9372\(1998\)124:11\(1121\)](https://doi.org/10.1061/(ASCE)0733-9372(1998)124:11(1121)).
- Bauske, B., and D. Goetz. 1993. "Effects of Deicing-Salts on Heavy Metal Mobility." *Acta Hydrochimica et Hydrobiologica* 21 (1): 38–42. <https://doi.org/10.1002/ahch.19930210106>.
- Boger, Alex, and Laurent Ahiablame. 2019. "Characterization of Nutrient and Metal Leaching in Roadside Ditches Maintained with Cool and Warm Season Grasses." *Hydrology* 6 (2): 47. <https://doi.org/10.3390/hydrology6020047>.

- Brown, Jeffrey N., and Barrie M. Peake. 2006. "Sources of Heavy Metals and Polycyclic Aromatic Hydrocarbons in Urban Stormwater Runoff." *Science of The Total Environment* 359: 145–55.
- Brown, Robert A., and William F. Hunt. 2011. "Impacts of Media Depth on Effluent Water Quality and Hydrologic Performance of Undersized Bioretention Cells." *Journal of Irrigation and Drainage Engineering* 137 (3): 132–43. [https://doi.org/10.1061/\(ASCE\)IR.1943-4774.0000167](https://doi.org/10.1061/(ASCE)IR.1943-4774.0000167).
- Clary, Jane, Jonathan Jones, Ben Urbonas, Marcus Quigley, Eric Strecker, and Todd Wagner. 2008. "Can Stormwater BMPs Remove Bacteria?" *Stormwater Magazine*, June 2008.
- Cording, Amanda, Stephanie Hurley, and Carol Adair. 2018. "Influence of Critical Bioretention Design Factors and Projected Increases in Precipitation Due to Climate Change on Roadside Bioretention Performance." *Journal of Environmental Engineering* 144 (9): 04018082. [https://doi.org/10.1061/\(ASCE\)EE.1943-7870.0001411](https://doi.org/10.1061/(ASCE)EE.1943-7870.0001411).
- Cording, Amanda, Stephanie Hurley, and David Whitney. 2017. "Monitoring Methods and Designs for Evaluating Bioretention Performance." *Journal of Environmental Engineering* 143 (12): 05017006. [https://doi.org/10.1061/\(ASCE\)EE.1943-7870.0001276](https://doi.org/10.1061/(ASCE)EE.1943-7870.0001276).
- Davis, Allen P., James Stagge, Eliea Jamil, and Hunho Kim. 2011. "Hydraulic Performance of Grass Swales for Managing Highway Runoff." *Water Research* 46 (20): 6775–86.
- Davis, Allen P. 2008. "Field Performance of Bioretention: Hydrology Impacts." *Journal of Hydrologic Engineering* 13 (2): 90–95. [https://doi.org/10.1061/\(ASCE\)1084-0699\(2008\)13:2\(90\)](https://doi.org/10.1061/(ASCE)1084-0699(2008)13:2(90)).
- Deletic, Ana, and Tim D. Fletcher. 2006. "Performance of Grass Filters Used for Stormwater Treatment— a Field and Modelling Study." *Journal of Hydrology* 317 (3–4): 261–75. <https://doi.org/10.1016/j.jhydrol.2005.05.021>.
- Denich, Chris, Andrea Bradford, and Jennifer Drake. 2013. "Bioretention: Assessing Effects of Winter Salt and Aggregate Application on Plant Health, Media Clogging and Effluent Quality." *Water Quality Research Journal* 48 (4): 387–99. <https://doi.org/10.2166/wqrjc.2013.065>.
- DEQ. 2011a. "Bioretention." Stormwater Design Specification 9. VA Department of Environmental Quality. http://www.vwrrc.vt.edu/swc/documents/2013/DEQ%20BMP%20Spec%20No%209_BIORETENTION_FinalDraft_v1-9_03012011.pdf.
- DEQ. 2011b. "Dry Swales." Stormwater Design Specification 10. VA Department of Environmental Quality. http://www.vwrrc.vt.edu/swc/documents/2013/DEQ%20BMP%20Spec%20No%2010_DRY%20SWALE_Final%20Draft_v1-9_03012011.pdf.
- DEQ. 2011c. "Grass Channels." Stormwater Design Specification 3. VA Department of Environmental Quality. http://www.vwrrc.vt.edu/swc/documents/2013/DEQ%20BMP%20Spec%20No%203_GRASS%20CHANNELS_Final%20Draft_v1-9_03012011.pdf.
- EARPC. 2020. "Safe for Swimming?" Environment America: Research & Policy Center. 2020. <https://environmentamericacenter.org/reports/ame/safe-swimming-1>.
- Eckart, Kyle, Zach McPhee, and Tirupati Boliseti. 2017. "Performance and Implementation of Low Impact Development – A Review." *Science of The Total Environment* 607–608 (December): 413–32. <https://doi.org/10.1016/j.scitotenv.2017.06.254>.
- Eger, Caitlin G., David G. Chandler, and Charles T. Driscoll. 2017. "Hydrologic Processes That Govern Stormwater Infrastructure Behaviour." *Hydrological Processes* 31 (25): 4492–4506. <https://doi.org/10.1002/hyp.11353>.
- Ernst, Clayton, Lynn Katz, and Michael Barrett. 2016. "Removal of Dissolved Copper and Zinc from Highway Runoff via Adsorption." *Journal of Sustainable Water in the Built Environment* 2 (1): 04015007. <https://doi.org/10.1061/JSWBAY.0000803>.

- Flynn, Kevin M., and Robert G. Traver. 2013. "Green Infrastructure Life Cycle Assessment: A Bio-Infiltration Case Study." *Ecological Engineering* 55 (June): 9–22. <https://doi.org/10.1016/j.ecoleng.2013.01.004>.
- García-Serrana, María, John S. Gulliver, and John L. Nieber. 2017. "Infiltration Capacity of Roadside Filter Strips with Non-Uniform Overland Flow." *Journal of Hydrology* 545 (February): 451–62. <https://doi.org/10.1016/j.jhydrol.2016.12.031>.
- Géhéniau, Nicolas, Musandji Fuamba, Valérie Mahaut, Mario R. Gendron, and Marie Dugué. 2015. "Monitoring of a Rain Garden in Cold Climate: Case Study of a Parking Lot near Montréal." *Journal of Irrigation and Drainage Engineering* 141 (6): 04014073. [https://doi.org/10.1061/\(ASCE\)IR.1943-4774.0000836](https://doi.org/10.1061/(ASCE)IR.1943-4774.0000836).
- Granato, Greg, Peter Church, and Victoria Stone. 1995. "Mobilization of Major and Trace Constituents of Highway Runoff in Groundwater Potentially Caused by Deicing Chemical Migration." *TRANSPORTATION RESEARCH RECORD*, 92–104.
- Hathaway, J. M., W. F. Hunt, A. K. Graves, and J. D. Wright. 2011. "Field Evaluation of Bioretention Indicator Bacteria Sequestration in Wilmington, North Carolina." *Journal of Environmental Engineering* 137 (12): 1103–13. [https://doi.org/10.1061/\(ASCE\)EE.1943-7870.0000444](https://doi.org/10.1061/(ASCE)EE.1943-7870.0000444).
- Hathaway, J. M., W. F. Hunt, R. M. Guest, and D. T. McCarthy. 2014. "Residual Indicator Bacteria in Autosampler Tubing: A Field and Laboratory Assessment." *Water Science and Technology* 69 (5): 1120–26. <https://doi.org/10.2166/wst.2014.035>.
- Hathaway, J. M., W. F. Hunt, and S. Jadlocki. 2009. "Indicator Bacteria Removal in Storm-Water Best Management Practices in Charlotte, North Carolina." *Journal of Environmental Engineering* 135 (12): 1275–85. [https://doi.org/10.1061/\(ASCE\)EE.1943-7870.0000107](https://doi.org/10.1061/(ASCE)EE.1943-7870.0000107).
- Hathaway, J. M., W. F. Hunt, and O. D. Simmons. 2010. "Statistical Evaluation of Factors Affecting Indicator Bacteria in Urban Storm-Water Runoff." *Journal of Environmental Engineering* 136 (12): 1360–68. [https://doi.org/10.1061/\(ASCE\)EE.1943-7870.0000278](https://doi.org/10.1061/(ASCE)EE.1943-7870.0000278).
- Hayes, Gail M., Charles R. Burgis, Wuhuan Zhang, Derek Henderson, and James A. Smith. Forthcoming. "Runoff Reduction by Four Green Stormwater Infrastructure Systems in a Shared Environment." *Journal of Sustainable Water in the Built Environment*.
- Henderson, Derek, Gail Hayes, Charles Burgis, and James A. Smith. 2019. "Low Impact Development Technologies for Highway Stormwater Runoff." In *Encyclopedia of Water: Science, Technology, and Society*, 1–18. Wiley. <https://doi.org/10.1002/9781119300762.wsts0009>.
- Huber, Maximilian, Harald Hilbig, Sophia C. Badenberger, Julius Fassnacht, Jörg E. Drewes, and Brigitte Helmreich. 2016. "Heavy Metal Removal Mechanisms of Sorptive Filter Materials for Road Runoff Treatment and Remobilization under De-Icing Salt Applications." *Water Research* 102 (Supplement C): 453–63. <https://doi.org/10.1016/j.watres.2016.06.063>.
- Hunt, W. F., J. T. Smith, S. J. Jadlocki, J. M. Hathaway, and P. R. Eubanks. 2008. "Pollutant Removal and Peak Flow Mitigation by a Bioretention Cell in Urban Charlotte, N.C." *Journal of Environmental Engineering* 134 (5): 403–8. [https://doi.org/10.1061/\(ASCE\)0733-9372\(2008\)134:5\(403\)](https://doi.org/10.1061/(ASCE)0733-9372(2008)134:5(403)).
- Jakimska, Anna, Piotr Konieczka, Krzysztof Skóra, and Jacek Namieśnik. 2011. "Bioaccumulation of Metals in Tissues of Marine Animals, Part I: The Role and Impact of Heavy Metals on Organisms," 10.
- Jeng, Hueiwang C., Andrew England, and Henry B. Bradford. 2005. "Indicator Organisms Associated with Stormwater Suspended Particles and Estuarine Sediment." *Journal of Environmental Science and Health, Part A* 40 (4). <https://pubmed.ncbi.nlm.nih.gov/15792299/>.
- Jenkins, Jennifer K. G., Bridget Wadzuk, and Andrea Welker. 2010. "Fines Accumulation and Distribution in a Storm-Water Rain Garden Nine Years Postconstruction." *Journal of Irrigation and Drainage Engineering* 136 (12): 862–69. [https://doi.org/10.1061/\(ASCE\)IR.1943-4774.0000264](https://doi.org/10.1061/(ASCE)IR.1943-4774.0000264).

- Kakuturu, Sai P., and Shirley E. Clark. 2015. "Effects of Deicing Salts on the Clogging of Stormwater Filter Media and on the Media Chemistry." *Journal of Environmental Engineering* 141 (9): 04015020. [https://doi.org/10.1061/\(ASCE\)EE.1943-7870.0000927](https://doi.org/10.1061/(ASCE)EE.1943-7870.0000927).
- Kawasaki, Nobuyuki, Kazuhiro Komatsu, Ayato Kohzu, Noriko Tomioka, Ryuichiro Shinohara, Takayuki Satou, Fumiko Nara Watanabe, et al. 2013. "Bacterial Contribution to Dissolved Organic Matter in Eutrophic Lake Kasumigaura, Japan." *Applied and Environmental Microbiology* 79 (23): 7160–68. <https://doi.org/10.1128/AEM.01504-13>.
- Knight, E.M.P., W.F. III Hunt, and R.J. Winston. 2013. "Side-by-Side Evaluation of Four Level Spreader-Vegetated Filter Strips and a Swale in Eastern North Carolina." *Journal of Soil and Water Conservation* 68 (1): 60–72. <https://doi.org/10.2489/jswc.68.1.60>.
- Koeppel, David. 1981. "Effect of Heavy Metal Pollution on Plants." In . Vol. 1. Springer.
- Komlos, John, and Robert Traver. 2012. "Long-Term Orthophosphate Removal in a Field-Scale Stormwater Bioinfiltration Rain Garden." *Journal of Environmental Engineering* 138 (10): 991–98. [https://doi.org/10.1061/\(ASCE\)EE.1943-7870.0000566](https://doi.org/10.1061/(ASCE)EE.1943-7870.0000566).
- Krometis, Leigh-Anne H., Gregory W. Characklis, Otto D. Simmons III, Mackenzie J. Dilts, Christina A. Likirdopoulos, and Mark D. Sobsey. 2007. "Intra-Storm Variability in Microbial Partitioning and Microbial Loading Rates." *Water Research* 41 (2): 506–16. <https://doi.org/10.1016/j.watres.2006.09.029>.
- Leroy, Marie-Charlotte, Florence Portet-Kotalo, Marc Legras, Franck Lederf, Vincent Moncond'huy, Isabelle Polaert, and Stéphane Marcotte. 2016. "Performance of Vegetated Swales for Improving Road Runoff Quality in a Moderate Traffic Urban Area." *Science of The Total Environment* 566–567 (October): 113–21. <https://doi.org/10.1016/j.scitotenv.2016.05.027>.
- Li, Fayun, Ying Zhang, Zhiping Fan, and Kokyo Oh. 2015. "Accumulation of De-Icing Salts and Its Short-Term Effect on Metal Mobility in Urban Roadside Soils." *Bulletin of Environmental Contamination and Toxicology* 94 (4): 525–31.
- Li, Haiyan, Kun Li, and Xiaoran Zhang. 2016. "Performance Evaluation of Grassed Swales for Stormwater Pollution Control." *Procedia Engineering*, 12th International Conference on Hydroinformatics (HIC 2016) - Smart Water for the Future, 154: 898–910. <https://doi.org/10.1016/j.proeng.2016.07.481>.
- Li, Hounq, and Allen P. Davis. 2009. "Water Quality Improvement through Reductions of Pollutant Loads Using Bioretention." *Journal of Environmental Engineering* 135 (8): 567–76. [https://doi.org/10.1061/\(ASCE\)EE.1943-7870.0000026](https://doi.org/10.1061/(ASCE)EE.1943-7870.0000026).
- Li, Ming-Han, Mark Swapp, Myung Hee Kim, Kung-Hui Chu, and Chan Yong Sung. 2014. "Comparing Bioretention Designs With and Without an Internal Water Storage Layer for Treating Highway Runoff." *Water Environment Research* 86 (5): 387–97. <https://doi.org/10.2175/106143013X13789303501920>.
- Line, D.E., and W.F. Hunt. 2009. "Performance of a Bioretention Area and a Level Spreader-Grass Filter Strip at Two Highway Sites in North Carolina." *Journal of Irrigation and Drainage Engineering* 135 (2): 217–24. [https://doi.org/\(ASCE\)0733-9437\(2009\)135:2\(217\)](https://doi.org/(ASCE)0733-9437(2009)135:2(217)).
- Liu, Yaoze, Bernard A. Engel, Dennis C. Flanagan, Margaret W. Gitau, Sara K. McMillan, and Indrajeet Chaubey. 2017. "A Review on Effectiveness of Best Management Practices in Improving Hydrology and Water Quality: Needs and Opportunities." *Science of The Total Environment* 601–602 (December): 580–93. <https://doi.org/10.1016/j.scitotenv.2017.05.212>.
- Lofgren, Stefan. 2001. "The Chemical Effects of Deicing Salt on Soil and Stream Water of Five Catchments in Southeast Sweden." *Water, Air, & Soil Pollution* 130: 863–68.
- Lucke, Terry, Peter Nichols, Earl Shaver, James Lenhart, Antje Welker, and Maximilian Huber. 2017. "Pathways for the Evaluation of Stormwater Quality Improvement Devices – the Experience of Six Countries." *CLEAN – Soil, Air, Water* 45 (8): 1600596. <https://doi.org/10.1002/clen.201600596>.

- Mallin, Michael A., Mary I.H. Turner, Matthew R. McIver, Byron R. Toothman, and Hunter C. Freeman. 2016. "Significant Reduction of Fecal Bacteria and Suspended Solids Loading by Coastal Best Management Practices." *Journal of Coastal Research* 320 (July): 923–31. <https://doi.org/10.2112/JCOASTRES-D-15-00195.1>.
- Maniquiz, Marla, So-Young Lee, and Lee-Hyung Kim. 2010. "Long-Term Monitoring of Infiltration Trench for Nonpoint Source Pollution Control." *Water Air Soil Pollution* 212: 13–26.
- Merrikhpour, Hajar, and Mohsen Jalali. 2013. "The Effects of Road Salt Application on the Accumulation and Speciation of Cations and Anions in an Urban Environment: Effects of Road Salt Application." *Water and Environment Journal* 27 (4): 524–34. <https://doi.org/10.1111/j.1747-6593.2012.00371.x>.
- Mullins, Angela R., Daniel J. Bain, Erin Pfeil-McCullough, Kristina G. Hopkins, Sarah Lavin, and Erin Copeland. 2020. "Seasonal Drivers of Chemical and Hydrological Patterns in Roadside Infiltration-Based Green Infrastructure." *Science of The Total Environment* 714 (April): 136503. <https://doi.org/10.1016/j.scitotenv.2020.136503>.
- Muthanna, Tone Merete, Maria Viklander, Godecke Blecken, and Sveinn T. Thorolfsson. 2007. "Snowmelt Pollutant Removal in Bioretention Areas." *Water Research* 41 (18): 4061–72. <https://doi.org/10.1016/j.watres.2007.05.040>.
- Nelson, S.S., D.R. Yonge, and M.E. Barber. 2009. "Effects of Road Salts on Heavy Metal Mobility in Two Eastern Washington Soils." *Journal of Environmental Engineering* 135 (7): 505–10.
- NOAA. 2014. "Heavy Downpours More Intense, Frequent in a Warmer World." Climate.Gov: Science & Information for a Climate-Smart Nation. March 4, 2014. <https://www.climate.gov/news-features/featured-images/heavy-downpours-more-intense-frequent-warmer-world>.
- Norrström, A. C, and G Jacks. 1998. "Concentration and Fractionation of Heavy Metals in Roadside Soils Receiving De-Icing Salts." *Science of The Total Environment* 218 (2–3): 161–74. [https://doi.org/10.1016/S0048-9697\(98\)00203-4](https://doi.org/10.1016/S0048-9697(98)00203-4).
- Norrström, Ann Catrine. 2005. "Metal Mobility by De-Icing Salt from an Infiltration Trench for Highway Runoff." *Applied Geochemistry* 20 (10): 1907–19. <https://doi.org/10.1016/j.apgeochem.2005.06.002>.
- Novotny, Vladimir, Deron Muehring, Daniel Zitomer, Daniel Smith, and Roderick Facey. 1998. "Cyanide and Metal Pollution by Urban Snowmelt: Impact of Deicing Compounds." *Water Science and Technology* 38 (10): 223–30.
- Parker, J.K., D. McIntyre, and R.T. Noble. 2010. "Characterizing Fecal Contamination in Stormwater Runoff in Coastal North Carolina, USA." *Water Research* 44 (14): 4186–94. <https://doi.org/10.1016/j.watres.2010.05.018>.
- Passeport, Elodie, William F. Hunt, Daniel E. Line, Ryan A. Smith, and Robert A. Brown. 2009. "Field Study of the Ability of Two Grassed Bioretention Cells to Reduce Storm-Water Runoff Pollution." *Journal of Irrigation and Drainage Engineering* 135 (4): 505–10. [https://doi.org/10.1061/\(ASCE\)IR.1943-4774.0000006](https://doi.org/10.1061/(ASCE)IR.1943-4774.0000006).
- Paus, Kim H., Joel Morgan, John S. Gulliver, TorOve Leiknes, and Raymond M. Hozalski. 2014. "Effects of Temperature and NaCl on Toxic Metal Retention in Bioretention Media." *Journal of Environmental Engineering* 140 (10): 04014034. [https://doi.org/10.1061/\(ASCE\)EE.1943-7870.0000847](https://doi.org/10.1061/(ASCE)EE.1943-7870.0000847).
- Petersen, T. M., H. S. Rifai, M. P. Suarez, and A. R. Stein. 2005. "Bacteria Loads from Point and Nonpoint Sources in an Urban Watershed." *Journal of Environmental Engineering-Asce* 131 (10): 1414–25. [https://doi.org/10.1061/\(ASCE\)0733-9372\(2005\)131:10\(1414\)](https://doi.org/10.1061/(ASCE)0733-9372(2005)131:10(1414)).
- Ramakrishna, Devikarani M., and Thiruvengkatachari Viraraghavan. 2005. "Environmental Impact of Chemical Deicers – A Review." *Water, Air, and Soil Pollution* 166 (1–4): 49–63. <https://doi.org/10.1007/s11270-005-8265-9>.

- Revitt, D. Michael, J. Bryan Ellis, and Lian Lundy. 2017. "Assessing the Impact of Swales on Receiving Water Quality." *Urban Water Journal* 14 (8): 839–45. <https://doi.org/10.1080/1573062X.2017.1279187>.
- Rippy, Megan A. 2015. "Meeting the Criteria: Linking Biofilter Design to Fecal Indicator Bacteria Removal: Linking Biofilter Design to FIB Removal." *Wiley Interdisciplinary Reviews: Water* 2 (5): 577–92. <https://doi.org/10.1002/wat2.1096>.
- Roy-Poirier, Audrey, Pascale Champagne, and Yves Filion. 2010. "Review of Bioretention System Research and Design: Past, Present, and Future." *Journal of Environmental Engineering* 136 (9): 878–89. [https://doi.org/10.1061/\(ASCE\)EE.1943-7870.0000227](https://doi.org/10.1061/(ASCE)EE.1943-7870.0000227).
- Rujner, Hendrik, Gunther Leonhardt, Jiri Marsalek, and Anne-Marie Perttu. 2017. "The Effects of Initial Soil Moisture Conditions on Swale Flow Hydrographs." *Hydrological Processes* 32: 644–54.
- Shafique, Muhammad, Reeho Kim, and Kwon Kyung-Ho. 2018. "Evaluating the Capability of Grass Swale for the Rainfall Runoff Reduction from an Urban Parking Lot, Seoul, Korea." *International Journal of Environmental Research and Public Health* 15 (3). <https://www.mdpi.com/1660-4601/15/3/537>.
- Shrestha, Paliza, Stephanie Hurley, and Beverley Wemple. 2018. "Effects of Different Soil Media, Vegetation, and Hydrologic Treatments on Nutrient and Sediment Removal in Roadside Bioretention Systems." *Ecological Engineering* 112: 116–31.
- Søberg, Laila C., Maria Viklander, and Godecke-Tobias Blecken. 2017. "Do Salt and Low Temperature Impair Metal Treatment in Stormwater Bioretention Cells with or without a Submerged Zone?" *Science of The Total Environment* 579 (February): 1588–99. <https://doi.org/10.1016/j.scitotenv.2016.11.179>.
- Stagge, James H., Allen P. Davis, Eliea Jamil, and Hunho Kim. 2012. "Performance of Grass Swales for Improving Water Quality from Highway Runoff." *Water Research* 46 (20): 6731–42. <https://doi.org/10.1016/j.watres.2012.02.037>.
- Tedoldi, Damien, Ghassan Chebbo, Daniel Pierlot, Yves Kovacs, and Marie-Christine Gromaire. 2016. "Impact of Runoff Infiltration on Contaminant Accumulation and Transport in the Soil/Filter Media of Sustainable Urban Drainage Systems: A Literature Review." *Science of The Total Environment* 569–570 (November): 904–26. <https://doi.org/10.1016/j.scitotenv.2016.04.215>.
- USEPA. 2019a. "Metals | CADDIS Volume 2 | US EPA." 2019. <https://www.epa.gov/caddis-vol2/metals>.
- USEPA. 2019b. "National Pollutant Discharge Elimination System (NPDES)." National Pollutant Discharge Elimination System (NPDES). 2019. <https://www.epa.gov/npdes/npdes-stormwater-program>.
- USEPA. 2020. "Green Infrastructure: Manage Flood Risk." United States Environmental Protection Agency. September 2020. <https://www.epa.gov/green-infrastructure/manage-flood-risk>.
- Valtanen, Marjo, Nora Sillanpää, and Heikki Setälä. 2017. "A Large-Scale Lysimeter Study of Stormwater Biofiltration under Cold Climatic Conditions." *Ecological Engineering* 100 (March): 89–98. <https://doi.org/10.1016/j.ecoleng.2016.12.018>.
- VDOT. 2009. "Road Anti-Icing, Pre-Treatment and de-Icing." http://www.virginiadot.org/news/resources/snow2009docs/Road_antiicing_pretreatment.pdf.
- Warren, Lesley A., and Ann P. Zimmerman. 1994. "THE INFLUENCE OF TEMPERATURE AND NaCl ON CADMIUM, COPPER AND ZINC PARTITIONING AMONG SUSPENDED PARTICULATE AND DISSOLVED PHASES IN AN URBAN RIVER," 11.
- Willard, L. L., T. Wynn-Thompson, L. H. Krometis, T. P. Neher, and B. D. Badgley. 2017. "Does It Pay to Be Mature? Evaluation of Bioretention Cell Performance Seven Years Postconstruction." *Journal of Environmental Engineering* 143 (9): 04017041. [https://doi.org/10.1061/\(ASCE\)EE.1943-7870.0001232](https://doi.org/10.1061/(ASCE)EE.1943-7870.0001232).
- Winston, Ryan J., Jay D. Dorsey, and William F. Hunt. 2016. "Quantifying Volume Reduction and Peak Flow Mitigation for Three Bioretention Cells in Clay Soils in Northeast Ohio." *Science of The Total Environment* 553 (May): 83–95. <https://doi.org/10.1016/j.scitotenv.2016.02.081>.

- Wright Water Engineers, Inc. 2010. "International Stormwater Best Management Practices (BMP) Database: Pollutant Category Summary: Fecal Indicator Bacteria." International Stormwater BMP Database.
<http://www.bmpdatabase.org/Docs/BMP%20Database%20Bacteria%20Paper%20Dec%202010.pdf>.
- Yousef, Y. A., T. Hvitved-Jacobsen, M. P. Wanielista, and H. H. Harper. 1987. "Removal of Contaminants in Highway Runoff Flowing through Swales." *Science of The Total Environment*, Highway Pollution, 59: 391–99. [https://doi.org/10.1016/0048-9697\(87\)90462-1](https://doi.org/10.1016/0048-9697(87)90462-1).
- Yu, Jianghua, Haixia Yu, and Liqiang Xu. 2013. "Performance Evaluation of Various Stormwater Best Management Practices." *Environmental Science and Pollution Research* 20 (9): 6160–71. <https://doi.org/10.1007/s11356-013-1655-4>.

2. Runoff reduction by four green stormwater infrastructure systems in a shared environment

This chapter has been accepted for publication in the *Journal of Sustainable Water in the Built Environment* (ASCE):

Hayes, Gail M., Charles R. Burgis, Wuhuan Zhang, Derek Henderson, and James A. Smith. (2021) "Runoff Reduction by Four Green Stormwater Infrastructure Systems in a Shared Environment." *Journal of Sustainable Water in the Built Environment*. <https://doi.org/10.1061/JSWBAY.0000932>.

2.1 ABSTRACT

Green infrastructure (GI) imitates the hydrology of undeveloped land to mitigate the impacts of stormwater runoff, but research is lacking that characterizes the performances of different types of independent GI systems in close proximity to each other in terms of runoff volume reduction. To address this gap, the runoff reduction by four GI systems (grass channel (GC), bioretention (BR), bioswale (BS), and compost-amended grass channel (CAGC)) within 1 km of each other along Lorton Road in Fairfax County, Virginia, were monitored for 48 rain events ranging in depth from 2.8 mm to 97 mm with a total rain depth of 1404 mm from June 2018 to July 2019, during their first full year of operation. The GC, BR, and BS were on track to well exceed minimum requirements of the Virginia Department of Environmental Quality with relative runoff reductions of 78%, 71%, and 56%, respectively, but the CAGC performed near its requirement at 43%. Contrary to expectations, the simply designed GC achieved the highest runoff reduction. The BR, with the second highest runoff reduction, had a small footprint relative to its contributing drainage area and demonstrated the least variation in performance in variable rainfall depths, intensities, and durations. The relatively small volume reductions of the BS and CAGC were attributed to their respective design elements of a sloping underdrain and close proximity to the road. This field study explores variations in runoff volume reductions of the four systems in various rainfall and seasonal conditions with respect to their design complexities, providing insights for future design and implementation of GI.

2.2 INTRODUCTION

Stormwater runoff threatens natural and built environments because high volumes of runoff can carry harmful pollutants and cause flooding, scour, combined sewer overflow, and erosion. Low impact development for stormwater management has been in use for a few decades and seeks to return the hydrology of a developed space to its pre-developed conditions by encouraging infiltration of stormwater close to its source and creating opportunities for storage (Ahiablame et al. 2012). Infiltrating and storing stormwater reduces its risks and saves energy costs at downstream water treatment facilities (Flynn and Traver 2013; Line and Hunt 2009). Specific applications of low impact development are green stormwater infrastructure (GI) systems. Two examples of GI systems are bioretention systems and swales, which have received increasing attention over the last decade for their performances in mitigating runoff risks (Ahiablame et al. 2012; Tedoldi et al. 2016; Eckart et al. 2017).

An important metric for performance of GI systems is overall volume reduction, as it is often the metric for government approval and is effective in estimating pollutant load removal (Komlos and Traver 2012; DEQ 2011a). Additionally, evaluation of GI systems with respect to loading ratios (drainage area divided by footprint) provide insight into stormwater management design. Loading ratios are a metric for performance efficiency and maintenance needs that are relevant to stormwater management designs as well as comparisons between individual designs (Winston et al. 2018; PWD 2017). Furthermore, the ratio of outflow volume to impervious contributing drainage area (CDA) demonstrates a system's ability to attenuate its intended inflow for a given rain event and also normalizes performances of GI systems with varying design characteristics. This metric differs from the loading ratio in that it only considers impervious CDA rather than the total CDA and it uses outflow volume rather than footprint size. This difference is important for sites where much of the CDA is pervious, such as the GI systems along Lorton Road used in this study. A larger impervious CDA indicates that a particular system has more volume flowing into it for a given event size and consequently more is likely flowing

out. Therefore, a smaller ratio of outflow volume to impervious CDA indicates that a system demonstrates high efficiency in volume reduction. This ratio minimizes risks associated with calculations and assumptions of non-concentrated overland flow entering a GI system as it compares the GI systems strictly on empirically measured data.

The GI installations of bioretention systems, known as rain gardens when constructed on a small scale, pond and infiltrate runoff through shallow, vegetated and mulched basins consisting of sandy soil and organic amendments above a stone sump (DEQ 2011a). The infiltrated stormwater is stored in the soil pores and if of sufficient volume, exfiltrates laterally or vertically to the surrounding soils, or exits through an underdrain if one is present (DEQ 2011a; Winston et al. 2016). Bioretention system volume reductions are typically in the range of 36% –98% with variations according to rainfall conditions and design characteristics (Winston et al. 2016; Komlos and Traver 2012; Shrestha et al. 2018; Cording et al. 2018; Brown and Hunt 2011; Line and Hunt 2009). In Virginia, the minimum requirement for volume reduction by a bioretention system is 40% – 80% depending on treatment goals and design such that the inclusion of an underdrain lowers expectations of volume reduction (DEQ 2011a).

The GI installations of swales are engineered channels comprising various types of soils and vegetation selected according to treatment goals and are typically designed to convey rather than store runoff. The simplest swale design is a grass channel and usually includes native soils and vegetation, but when the soil of a grass channel is amended with compost, it is known as a compost-amended grass channel (DEQ 2011b). The bioswale, also known as a dry swale, is a linear, channelized bioretention, incorporating engineered soil media and often an underdrain situated on or within a stone sump (DEQ 2011c). One way to reduce the effective slope and water velocity of a swale and also provide temporary storage is to include check dams, 15 – 30 cm wooden walls surrounded by rip-rap distributed along the swale length perpendicular to flow (DEQ 2011c; A. Davis et al. 2011). As with all GI system designs, volume reduction by a swale depends on its design. For example, Knight et al. (2013) found a volume

reduction of 23% over 30 analyzed events with no mention of check dams while Davis et al. (2011) found 27% – 63% reduction by swales with check dams.

In their comprehensive review of low impact development practices, Ahiablame et al. (2012) identified needed research on infiltration-based stormwater management (GI) that quantifies runoff volume reduction performance in various climatic conditions, which is especially important in a changing climate where extreme weather events are increasingly likely to occur. Other suggestions by Ahiablame et al. (2012) that are echoed by Eckart et al. (2017) call for more data on the significance of spatial and temporal trends of runoff volume reduction performance, especially comparing GI systems in close proximity experiencing the same weather and seasons. As modeling of stormwater management including GI systems grows, there is a need for field data for modeling GI systems that will realistically depict these systems over time and in variable rainfall and seasonal conditions (Tedoldi et al. 2016; Eckart et al. 2017; Liu et al. 2017; Ahiablame et al. 2012). The authors of this present study have also noted an absence of literature on examining GI systems of varying design complexity in shared weather conditions.

In 2017, an unprecedented opportunity to address these suggested areas of climatic conditions, data availability, and design complexity arose when Lorton Road in Fairfax County, Virginia was expanded from a two-lane undivided road to a four-lane divided road, at which time dozens of individual GI systems were installed along its 2.6-km roadside. In general, Lorton Road is suburban residential, but the portion of the road in this study is largely undeveloped. Therefore, the objective of this present work was to characterize and compare the runoff volume reduction performances of four GI systems along Lorton Road during their full first year of operation in various rain and seasonal conditions with examination of CDAs and performance normalization according to designed expectations. The results are expected to provide insight into GI systems and inform decision-making by land developers.

2.3 MATERIALS AND METHODS

2.3.1 Field Site

The stormwater management of Lorton Road was designed according to the VDOT Drainage Manual and Virginia Stormwater Management Regulations for a rainfall depth of 68.6 mm (1-year/24-hour event) (VDOT 2017; VSMP 2011). Inflow and outflow were monitored for four Lorton Road GI systems located within 0.8 km of each other at the field site described by Burgis et al. (2020): a bioretention (BR), a grass channel (GC), a compost-amended grass channel (CAGC), and a bioswale (BS). These four GI systems were selected because they represent a diverse selection of stormwater management techniques regularly used by VDOT. Additionally, the inflow for each system is direct road runoff (not from a treatment train) and each is safe to access.

The design specifications and monitoring station characteristics of the four GI systems of interest are given in Table 2.1 and schematics and vegetation of each are included in Appendix A. The as-built documents provided the CDAs, impervious proportions of each CDA, engineered storage capacities, vegetation types, soil specifications for the engineered soil media (ESM) and compost-amended soils, soil layers, and lengths, base widths, grades, side slopes, and check dam counts for the swales. According to the as-built drawings and visual confirmation, the pervious contributing drainage areas of the swales are all directly connected to the swale channel centers with the exception of a 1-m grass strip by the GC and BS that is discussed later. Because of this, the pervious CDA of each swale is considered to be part of its footprint. The GC, CAGC, and BS are all types of trapezoidal swales for linear stormwater management but the BR is non-linear and consists of a forebay for pretreatment and a basin for treatment. Each system is separated from the road by 2 - 3 m of green space (vegetated strips) maintained by a VDOT contractor through mowing several times per year, but the GC and BS are also adjacent to a 1.5-m asphalt path within the green space. The four GI systems are mowed to 10 – 15 cm twice per year, once in the spring and once in the fall seasons, with replanting and mulching as needed.

Native soils in the area along Lorton Road are categorized as Beltsville silt loam, Sassafras-Marumsco complex, and Kingstown sandy clay loam (NRCS 2019).

The GC is a simple, grassy channel comprised of native soils and the CAGC is a simple grassy channel incorporating compost-amended native soils in the top 30.5 cm. The BS is essentially a channelized bioretention system that includes ESM and an underdrain within pea gravel (Fig. 2.1 shows the underdrain as the dotted line). See Appendix A for schematics of each swale design. Compost from agricultural, food, industrial, biosolid (EPA CFR Title 40, Part 503), yard trimmings, source-separated, or mixed solid waste amend the soil of the CAGC. The compost consists of no more than 5% dry weight of sand, silt, clay, or rock and was incorporated within the root zone by tilling into the natural soils to a depth of at least 30 cm with a 16% application rate by volume. ESM particle size is categorized as 91% sand, 6% silt, and 3% clay, with a bulk density of 2 g/cm^3 , porosity of approximately 23%, and is 3% organic content by mass. The determination of the infiltration rates of any of the soils of the GI systems (native or engineered) was outside the scope of this study. The swales include wooden check dams that lessen the effective grade of each swale by providing ponding opportunities. Ponding volume for each system is included in its engineered storage value, but storage from the natural soils is not. The swale labels in each aerial image of Fig. 2.1 point toward the singular outlets for the swales, but inflow for each is non-concentrated overland flow (represented by the arrows in Fig. 2.1).

Table 2.1. Design specifications and other characteristics for monitored GI systems. (ESM: Engineered soil media, CDA: contributing drainage area, GC: Grass channel, CAGC: Compost-amended grass channel, BS: Bioswale, BR: Bioretention).

Specification	GC	CAGC	BS	BR
CDA (m ²)	2,469.0	5,908.0	2,711.0	47,753
% Impervious	39	18	40	35
CDA land use	Lorton Road (suburban, sparse development) + sidewalk + vegetated strips			Lorton Rd + residential
Footprint (m ²)	1,619	4,897	1,821	1,012
Loading ratio (CDA/footprint)	1.52	1.21	1.49	47.2
Engineered storage (m ³) = ponding + subsurface	2.20	8.00	55.0	447
Vegetation type	Appendix A, Table A.1			
Subsurface layers (surface → down)	Native soils	31 cm compost-amended native soils over native soils	46 cm ESM, 40 cm pea gravel + underdrain	76-cm ESM, 10-cm #8 stone (+underdrain), 31-cm #57 stone
Inflow type	Non-concentrated overland flow			1-m culvert
Inflow flume size (min, max flow L/s)	0.12-m (0.005, 2.3)			0.9-m (0.06, 857)
Outflow type	swale flow	swale flow	10-cm underdrain + swale flow	10-cm underdrain + bypass
Outflow flume size (min, max flow L/s)	0.46-m (0.031, 150)	0.46-m (0.031, 150)	0.23-m (0.017, 27.1)	0.15-m (0.011, 9.2) 0.46-m (0.031, 150)
Length (m)	85.0	232	65.0	-
Base-width (m)	1.5	1.5	1.5	-
Grade (%)	4.5	2.0	3.0	-
Side slopes	4:1	5:1	5:1	-
No. wooden check dams (height cm)	3 (31)	6 (15)	6 (31)	-

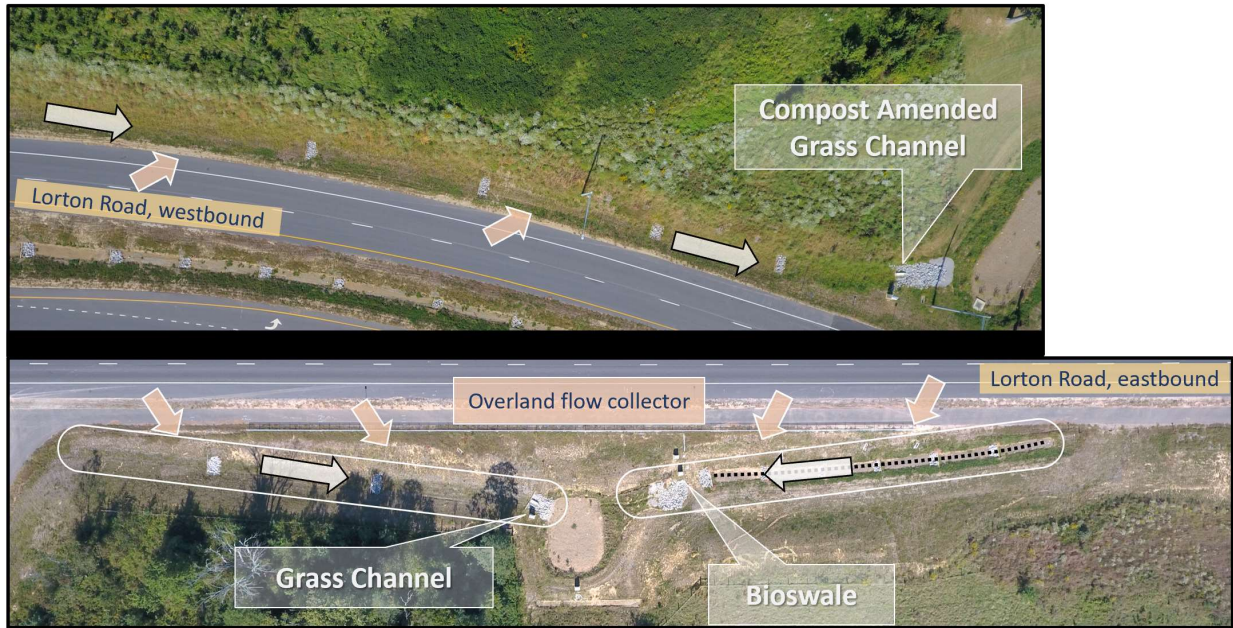


Figure 2.1. Aerial images of compost-amended grass channel (top), grass channel (bottom left), and bioswale (bottom right) with arrows representing surface flow, dotted line inside bioswale representing perforated underdrain, overland flow collector situated between the grass channel and bioswale. Photos taken by Gail Hayes.

The BR consists of a forebay (pretreatment) and basin (treatment) connected by a 0.6-m concrete culvert through an earthen berm that is 5 m in width and 1.5 m in height (Fig. 2.2 and Appendix A). The BR is classified as a gray-green hybrid stormwater control measure because a curb and gutter system provides the only inflow which enters the forebay through a 1-m concrete culvert. After slowing the inflow and capturing large debris, the graded forebay sends most of the stormwater into the basin where it infiltrates the double-shredded hardwood mulch and engineered soil media and eventually exits through the 10.2-cm perforated underdrain that daylights at the outlet (shown as the dotted line/solid arrow in Fig. 2.2). However, the bypass connected to the forebay alleviates large, intense surges of inflow that could damage or displace plants, mulch, and ESM in the basin. The basin and forebay each contain 15-cm ponding depths which account for 124 m³ and 35 m³, respectively, of its 447 m³ storage volume (Table 2.1). The BR outlet flow rate is constrained by the size of the underdrain and fluctuates with increasing or decreasing pressure from the ponded water in the basin, as confirmed

visually. The maximum BR outlet flow rate, limited by the 10.2-cm underdrain, is 7 L/s. Total outflow for the BR for each event is the sum of flow through the outlet and the bypass.



Figure 2.2. Aerial image of bioretention with piped flow represented by dark arrows, surface flow represented by light grey arrows, and perforated underdrain represented by dotted lines.

2.3.2 Rain Data

A tipping bucket rain gauge (Hach™, Loveland, CO) paired to an American Sigma 900 (Hach™, Loveland, CO) located adjacent to the BR collected 10-minute rain data with a precision of 0.25 mm and accuracy of 0.5% at 13 mm/hour. This study included rain events of sufficient depth to create inflow for each system and were separated by a period of no rainfall for at least 14 hours with antecedent dry periods indicated in Appendix D Tables D.1 – D.5. Events included produced detectable outflow from at least one of the four studied GI systems. In addition to rain depth measurements, records on rain intensity, event duration, and antecedent moisture conditions (rainfall in preceding 5 days) were also kept. The rain gauge failed due to a dead battery for the events of July 20, 2018, July 22, 2018, July 23, 2018 (partial), and February 2, 2019. For these dates, Ronald Reagan Washington National Airport Weather Underground Station (23 km away) was used for rain data. This was the closest station with publicly available data for the relevant dates and was verified for accuracy with rain data recorded at our site.

2.3.3 Flow Monitoring

Between the four GI systems, there were seven monitoring stations: three at the BR (inlet, outlet, bypass), one at each of the three swale outlets, and one measuring road runoff that was extrapolated to represent inflows to all three swales. The monitoring stations for the GC and CAGC outlets measured flow exiting these swales and the BS outlet monitoring station was placed at the daylight point of its underdrain, though this flume was positioned to also catch overland flow exiting the BS (Appendix A). Visual examinations of the BS during rain events determined that overland flow exiting the BS was very low if present at all. A monitoring station consisted of an AS950 Autosampler (Hach™, Loveland, CO) with a US9001 ultrasonic depth sensor (Hach™, Loveland, CO) to measure depth of water in a fiberglass H or HS flume (Open Channel Flow© Boise, ID) which it converted to volumetric flow (Equation 2.1). In Equation 2.1, Q is volumetric flowrate (gallons per minute), h is depth (inches), and a , b , c , and d are empirically derived constants specific to each flume size (Appendix A).

$$Q = a + b \times h^{0.5} + c \times h^{1.5} + d \times h^{2.5} \quad \text{Equation 2.1}$$

Overland flow entering the three swales was measured using an adaptation of the method presented in Davis et al. (2011). In this method, the water balance of the swales included inflow generated from both the impervious drainage areas (measured with an overland flow collector) and pervious drainage areas (calculated with the curve number (CN) method). To determine the inflow for the GC, CAGC, and BS resulting from the impervious CDA, an overland flow collector consisting of a 9-m aluminum-HDPE gutter channeled road runoff to a monitoring station between the GC and the BS (Fig. 2.1 and Appendix A). Though the overland flow collector was adjacent to the GC and BS, it was located such that it did not intercept flow that would otherwise enter those swales. The flow data collected from the overland flow collector was extrapolated according to the impervious CDA of the GC, CAGC, and BS by dividing its raw value by the CDA of the overland flow collector (entirely impervious) and then multiplying by the respective swales' impervious CDA values. The strip of unpaved space with very little

vegetation between Lorton Road and the GC and BS visible in Fig. 2.1 was considered part of this contributing area and was removed from the total pervious CDA. In accordance with Davis et al. (2011), the inflow volume attributed to each swale’s pervious CDA was determined from the NRCS CN method using average CN values of 65 (GC and CAGC – brush, good condition, soil type C) and 45 (BS – brush, good condition, soil type A/B), but values were adjusted according to antecedent rainfall as indicated in Appendix B (USDA et al. 1986).

2.3.4 Performance Metrics and Quality Assurance

For this study, “performance” of a GI system is defined as the percent reduction of runoff volume by a particular GI system. Runoff volume reduction performance was calculated with Equation 2.2 and is referred to as “relative volume reduction” as demonstrated in the International Stormwater Best Management Practice Database (GeoSyntec and Wright Water Engineers Inc. 2012). Unweighted averages of individual event flow reductions for each system are also discussed, but this metric overemphasizes the significance of higher performance in low rainfall (less than 15 mm) that produce low flow near the limit of the flumes’ equations (Equation 2.1).

$$\text{Relative volume reduction (\%)} = \frac{(\text{Total study period volume in}) - (\text{Total study period volume out})}{(\text{Total study period volume in})} \quad \text{Equation 2.2}$$

An analysis of the water balance of each GI system is not reported here, but the total inflow of each system was assumed equal to the sum of its outflow, infiltration, evapotranspiration, and storage. The volume unaccounted for in our inflow and outflow measurements is represented as percent volume reduction and would directly infiltrate the surrounding soils, pond in or around the GI systems, evaporate, or be taken up by plants. However, within this volume reduction, the breakdown of each mechanism’s contribution is undetermined.

Flow volume summations began with the rain and ended once the flow reached its pre-event value (no or very low baseflow). The autosamplers were regularly calibrated and flumes cleaned to ensure accurate readings. Flow readings were considered zero flow when the water level fell under the

minimum value for the appropriate use of Equation 2.1 as determined by the flume manufacturer (Table 2.1). Data with interferences from power issues, malfunctioning sensors, user error, extremely flooded flumes, and freezing conditions were not included. Corrections to the flow data of the BS and BR did occur in two scenarios, the first of which was flooding in the BS flume and the second of which was baseflow through the BR inlet and outlet. The specifics of data adjustments for these two scenarios are included in Appendix C.

2.3.5 Statistical Analyses

Normal distribution was not assumed for any data presented herein. Therefore, all statistical analyses were performed using non-parametric tests, specifically the Mann-Whitney (M-W) test for two independent samples, reported with confidence of 95% ($\alpha = .05$). All analyses in this chapter were performed using Microsoft Excel.

2.4 RESULTS AND DISCUSSION

2.4.1 Rainfall Data

Between June 2018 and July 2019, 48 rain events totaling a depth of 1,404.1 mm were monitored at the GC, CAGC, BS, and BR. Typical annual rainfall in Virginia ranges from 966 to 1168 mm (NCICS 2020) with an average intensity of 1.5 mm/h (Greeley and Hansen 2014), but 2018 was a particularly wet year for much of the Commonwealth (Boyer 2019). Each system was monitored with a complete set of inflow and outflow data during every reported rain event with the exception of July 17, 2018, July 20, 2018, and July 22, 2018 where flow monitoring at the BR bypass failed because of damaged equipment. Rainfall depth (mm), intensity (mm/h), duration (h), and rainfall in the preceding 5 days for these 48 events, are presented in Fig. 2.3 with **X** marking the respective means. Minimum rainfall to produce inflow to the swales from the road was 2.8 mm, but minimum rainfall to produce flow from the pervious portions of each swale's CDA was 7.4 mm, 2.8 mm, and 3.6 mm for the GC, CAGC, and BS, respectively. The BR inflow was also initiated with 2.8 mm of rain. Depths of rainfall during the growing season and

dormant season totaled 864.4 mm and 539.8 mm, respectively, with average event depths (\pm standard deviation) of 27.0 ± 23.8 mm and 33.7 ± 23.7 mm. The 48 monitored events were split as 32 during the growing season and 16 during the dormant season. The M-W test for two independent samples indicated no significant difference in event depth or intensity between the two seasons with $P = .2$ and $P = .7$, but duration between the two seasons did vary significantly with $P = .03$ such that the dormant season events were longer.

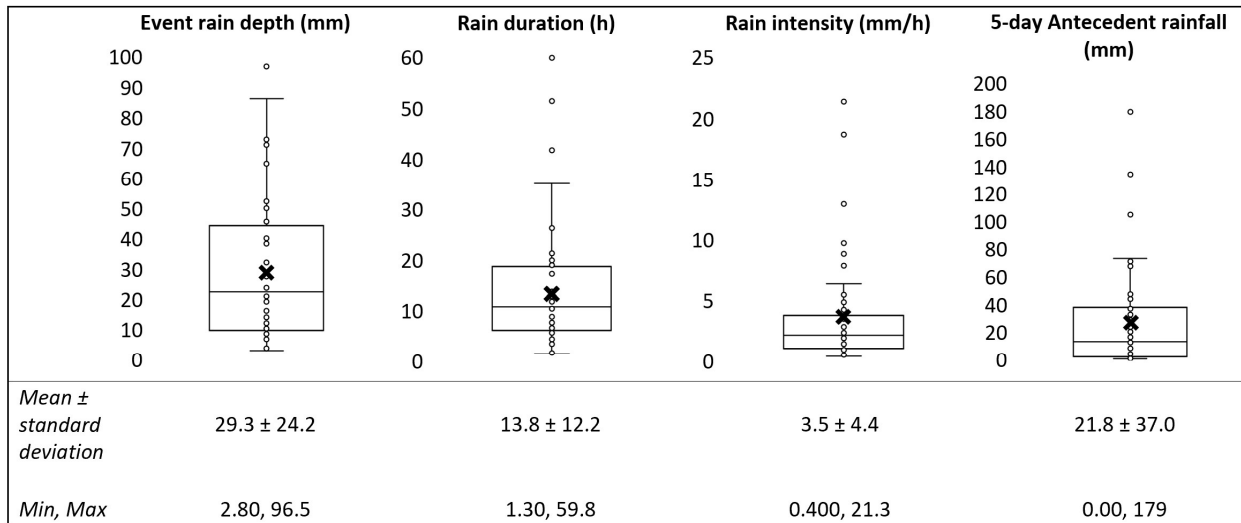


Figure 2.3. Rain data for all 48 monitored events including event depth, duration, intensity, and 5-day antecedent rainfall.

2.4.2 Overall Volume Reduction

A key purpose of GI systems is to reduce sudden and intense (flashy) runoff to less intense flows of lower volume, which the Lorton Road GI systems generally did well. Swale outflow would end within 1 – 3 hours of the rain event ending, but the peak outlet flow (7 L/s) of the BR could continue for several hours after the rain ended and would drop to baseflow (approximately 0.3 L/s or less) when the basin no longer held ponded runoff. Additionally, the BR inlet often had baseflow entering at approximately 1.3 L/s. These baseflows are accounted for in the data analysis with the procedure explained in Appendix C. The BR bypass flow was flashy, but less so than the inflow, and would end before or with the rain. Fig. 2.4 contains hydrographs from each of the monitored systems from July 30, 2018 included as a

demonstration of typical flow data. The event in Fig. 2.4 had a depth of 24 mm and an intensity of 3 mm/hr. The flows in Fig. 2.4 are adjusted for baseflow and instrument sensitivity and the overland flow in each swale graph is extrapolated to represent road runoff into each swale.

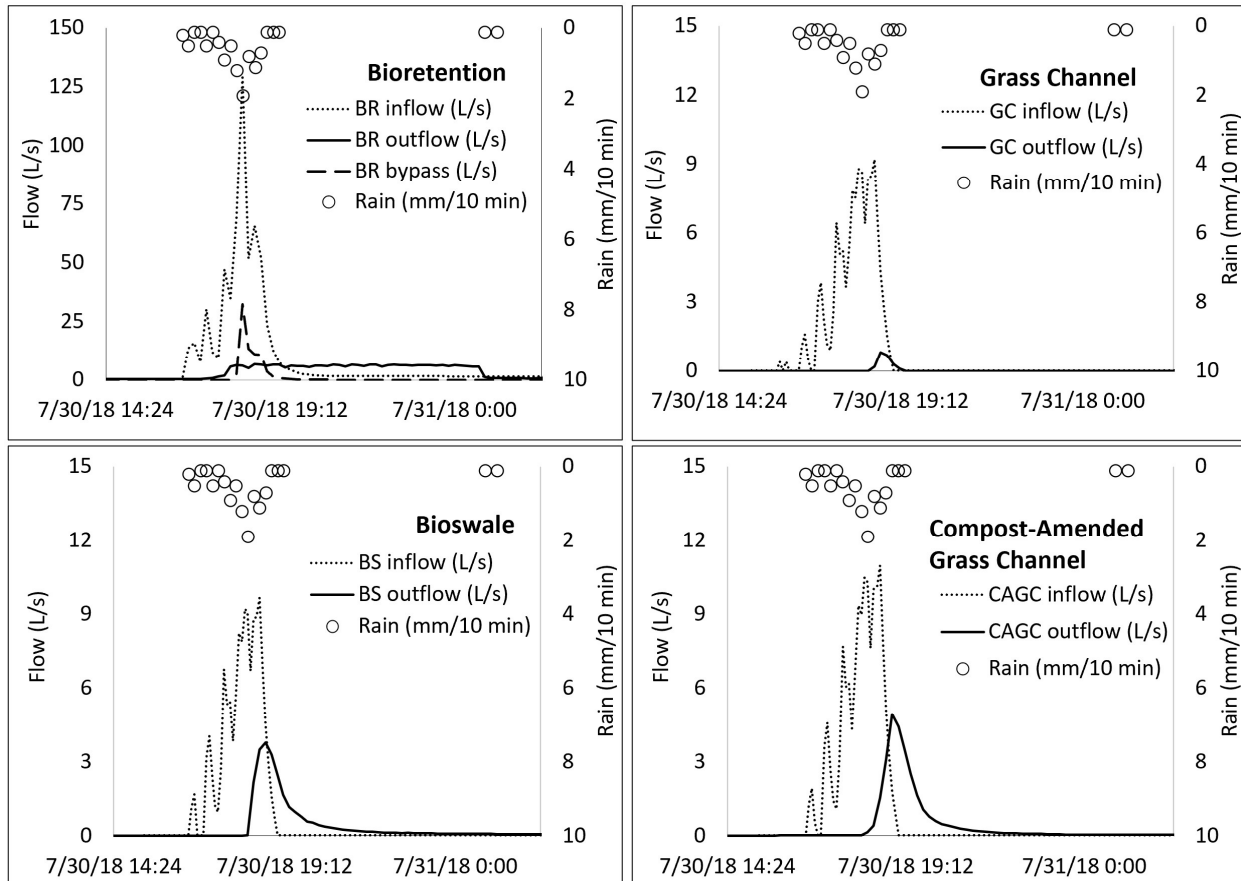


Figure 2.4. Sample hydrographs from July 30, 2018 (24 mm) with swale inflows shown as extrapolated flow from the overland flow collector.

Summary flow and rain data is also included in Appendix D, but Fig. 2.5 gives overall volume reductions for the 1-year study period. The GC had the highest relative volume reduction at 78%, followed by the BR, BS, and CAGC at 71%, 56%, and 43%, respectively. Data points outlying the box and whisker plots for the swales in Fig. 2.5 (July 23, 2018, July 25, 2018, September 8, 2018, and September 25, 2018) are medium to large events of depths 45.5 mm, 49.8 mm, 28.4 mm, and 70.9 mm, respectively. July 23, 2018 and July 25, 2018 had particularly high AMC levels (130 and 179 mm, respectively), September 8, 2018 had the highest intensity of all the monitored events (21.3 mm/h), and

September 25, 2018 simply had a lot of rain. The negative volume reductions of these extraordinary rain events were attributed to drainage areas that became hydraulically connected to the swales in saturated conditions, expanding the contributing drainage area and increasing volume flowing into the swale for which the overland flow collector could not account (Davis et al. 2011; Darboux et al. 2002). Though the determination of the exact cause of negative volume reductions by the swales was not pursued in this study, several other studies on swales have reported increases in volume during larger events, though with varying degrees of certainty (Davis et al. 2011; Schueler 1994; Knight et al. 2013). The unweighted average volume reductions (not accounting for event rain depth) of each system were also computed, but were uniformly larger than their relative volume reduction counterparts with the discrepancies generally increasing with increasing ranges of reductions. The unweighted average GC performance was significantly higher than the other systems (M-W $P \leq .001$), but there were no significant differences among the CAGC, BS, and BR.

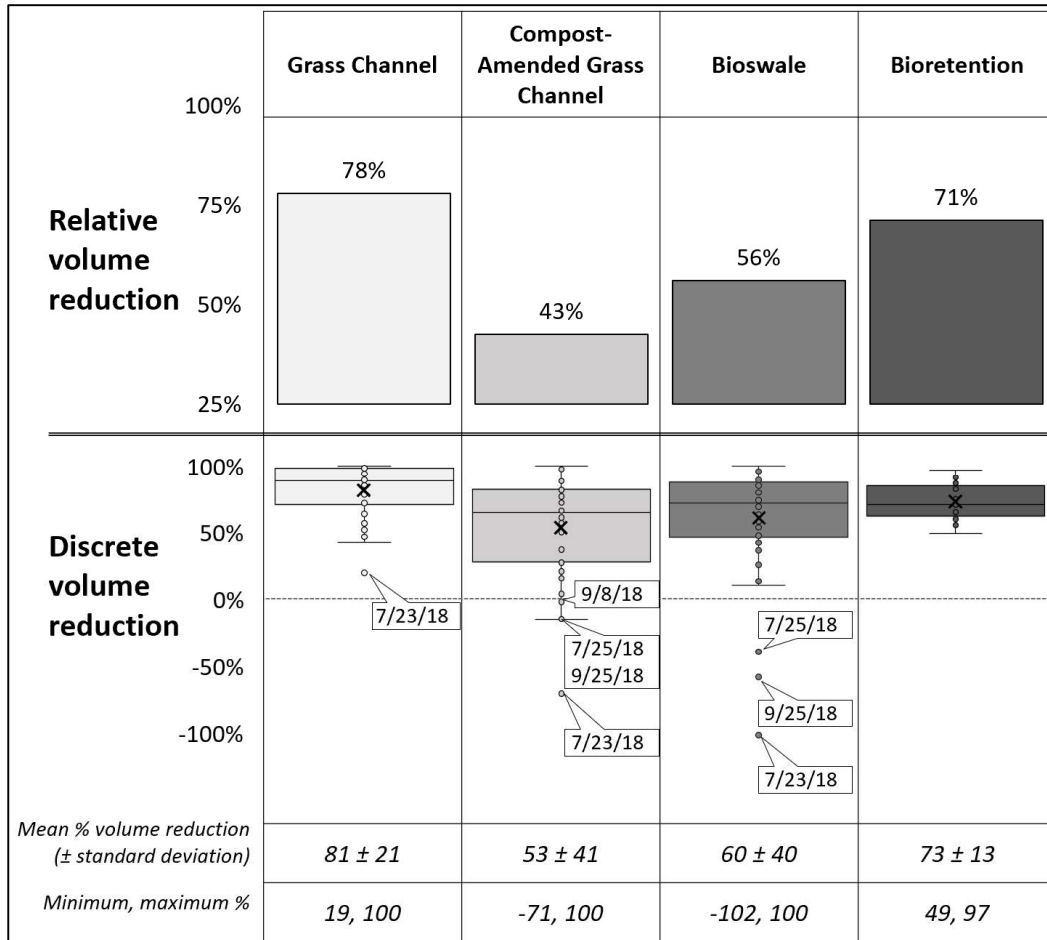


Figure 2.5. Overall volume reductions for each system including relative volume reduction and unweighted averages (mean ± standard deviation).

Given its simple design, it might be surprising that the GC reduced runoff volume so well and with much less variation than the other two swales. It is unlikely that the GC was overflowing around the flume because there was a physical barrier of cinderblocks and soil bags preventing water from the channel bypassing the flume (Appendix E). The inquiry here is not why the GC performed so well overall, but rather why the other swales performed so poorly. A major quality of the CAGC, for example, was its closeness to the road; the pervious areas connected to the GC and BS center lines are 3 – 10 m in width while the CAGC is at most 4 m for its entire length, so the CAGC had less buffer between its channel center and the road runoff. Additionally, the sloped underdrain of the BS prevented the stormwater from slowing and infiltrating into surrounding soils. While the BR also had this underdrain, its slope was

not as steep and it was also in combination with a much larger subsurface storage capacity, allowing for a greater overall volume reduction performance.

The overall runoff volume reductions of this study were similar to comparable systems. Davis (2008) found runoff volume reductions up to 63% for bioretention systems while Winston et al (2016) found 36 – 59%. Ahiablame et al. (2012) reviewed Davis (2008) and several other field and laboratory-scale studies on bioretention systems and reported reductions between 40% and 97%, a range that is wider than but overlapping that of the International Stormwater BMP Database report on bioretentions with underdrains (33% – 73%) (GeoSyntec and Wright Water Engineers, Inc. 2012). In general, the primary intention of swales is not volume reduction, though they have been shown to produce no outflow in rain events less than 6 mm in a swale with no check dams (Abida and Sabourin 2006). In Davis et al. (2011), swales with check dams performed better than swales without check dams when considering all rain events, though both types typically completely captured the smallest 40% of rain events (A. Davis et al. 2011). Other studies summarized in the International Stormwater BMP Database have shown swales with no underdrains can reduce volume by 35 – 65% with an average of 48%, though this report does not clarify if check dams were present (GeoSyntec and Wright Water Engineers, Inc. 2011). In terms of regulatory performance, the Virginia Department of Environmental Quality requires annual relative volume reduction of at least 10% for GC, 30% for CAGC, and 40% for BS and BR systems, all of which were on course to be satisfied, though the CAGC was close to its minimum requirement (DEQ 2011a; 2011b; 2011c).

Previous research on the volume reduction of minimally engineered infiltration-based stormwater management, or vegetated filter strips, was conducted by Henderson et al. (2016) at a nearby field site on Lorton Road. This study examined the difference in volume reduction performance of an unmanaged vegetated strip and a managed vegetated strip (vegetation manually trimmed to 10 cm one time in late summer) in reducing runoff volume from the adjacent road. Managed vegetated strips reduced runoff

volume by 81% while the unmanaged vegetated strips reduced volume by 87%. These results in conjunction with the high GC runoff volume reduction capability, suggest that minimally engineered systems are able to sufficiently decrease runoff volume as well as, if not better than, a more engineered system such as a BS or BR.

2.4.3 Volume Reduction and Rainfall Characteristics

The relative volume reduction of each swale decreased as event depth increased (Fig. 2.6) which is consistent with the performances of roadside swales of Davis et al. (2011) wherein swales behaved as green conduits during larger events rather than sinks for runoff. In Fig. 2.6, relative volume reduction of each GI system is shown in 10-mm increments of event rain depth. Events under 50 mm composed over 80% of the events monitored, but event sizes in each 10-mm increment were still represented, including the design event depth of 68.6 mm, which demonstrated satisfactory volume reductions. When considering all events up to and including the design depth, all systems performed satisfactorily. For this range of depths (2.8 – 70 mm), the relative volume reduction of the GC, CAGC, and BS were all greater than their overall volume reductions (83%, 45%, and 59%, respectively), but the BR was actually lower in performance (68%).

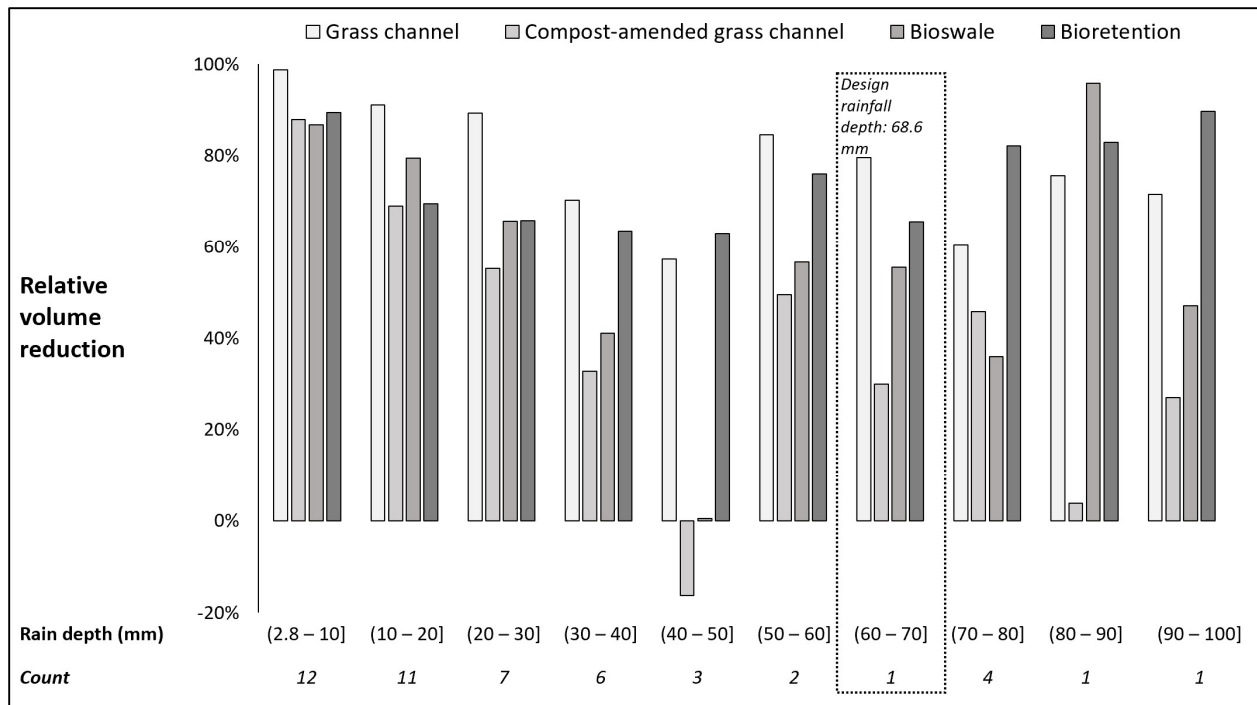


Figure 2.6. Relative volume reductions for each system divided into 10-mm rain event depths with the design rainfall event depth (68.6 mm) enclosed with a dotted line.

Using a linear regression analysis, rainfall depth was significantly correlated with performance for all systems except the BR (Table 2.2). Other rainfall characteristics (intensity, duration, antecedent rainfall, and the sum of antecedent rainfall and event depth) had significant correlation with volume reduction in some cases, but not all, and are attributed for variations in performance for events of the same depth (Table 2.2). The sum of rainfall in the preceding 5 days and event depth was the only predictor variable to be significantly correlated with volume reduction for all four GI systems monitored. Intensity was significant for all systems except the BR. Antecedent rainfall depth was significant for the CAGC and BS and duration was significant for only the BS.

Table 2.2. P-values and slopes (m) for simple linear regression analysis of % runoff volume reduction and specified site condition ($\alpha = .05$). AMC: antecedent moisture conditions (rainfall in preceding 5 days).

		Event depth	AMC	Event Duration	Event rain intensity	AMC + event depth
Grass channel	<i>P</i>	.0001	.06	.2	7.3×10^{-4}	.0001
	<i>m</i>	-0.01	-	-	-0.02	-0.003
Compost-amended grass channel	<i>P</i>	.0001	.02	.3	2.6×10^{-6}	4.1×10^{-5}
	<i>m</i>	-0.01	-0.004	-	-0.06	-0.01
Bioswale	<i>P</i>	.001	.0003	.03	.02	3.1×10^{-7}
	<i>m</i>	-0.01	-0.01	-0.011	-0.03	-0.01
Bioretention	<i>P</i>	.1	.2	.4	.3	.04
	<i>m</i>	-	-	-	-	-0.001

The system most resilient to varying rain characteristics in terms of volume reduction was the BR (high robustness), which is reflective of its narrow range in performance (Fig. 2.6); most of the rain conditions that significantly affected the performance of the other systems had no such impact on the BR because of its ponding and subsurface storage capabilities that could accommodate flashy events. However, the summation of antecedent rainfall and event rainfall did have a significant inverse linear correlation with BR performance; forebay soils saturated from a previous rain would lead to less infiltration of inflow prior to the basin, allowing more volume to reach the basin and the outlet or be sent straight to the bypass.

It is surprising that the GI system which was most impacted by varying rain conditions (least robust), was the BS. It would be expected that the BS would have comparable performance to the BR because of their overlapping designs (engineered soil media, underdrain), but the grade of the BS in combination with its underdrain allowed faster evacuation of runoff that otherwise might have infiltrated surrounding soils of the BS if allowed to remain idle. The other two swales, the GC and CAGC, had no underdrain and were more robust than the BS with respect to varying conditions, though only marginally so for the CAGC because of its proximity to the road.

2.4.4 Volume Reductions and Seasonal Influences

Growing season in Virginia is spring and summer, or May 20th - September 20th while dormant season is autumn and winter, or September 21st - May 19th. For all systems, relative volume reduction decreased from the growing season to the dormant season (Fig. 2.7). The GC and BR relative volume reduction changes were comparable in dropping 4% and 5%, respectively, the BS fell 9%, and the CAGC performance decreased by less than 1%. Likewise, unweighted average volume reductions decreased significantly from growing to dormant season for all systems except for the CAGC with *P*-values of .004, .04, .04, and .06 for the GC, BS, BR, and CAGC respectively (M-W). Within the growing season, as with the overall volume reduction performance, the unweighted average GC growing season volume reduction outperformed the BR, BS, and CAGC with *P*-values of .001, .004, and .01, respectively (M-W test), but there were no significant differences between the other systems during this season. Within the dormant season, the GC continued to outperform the others though its unweighted average was statistically comparable to the BR.

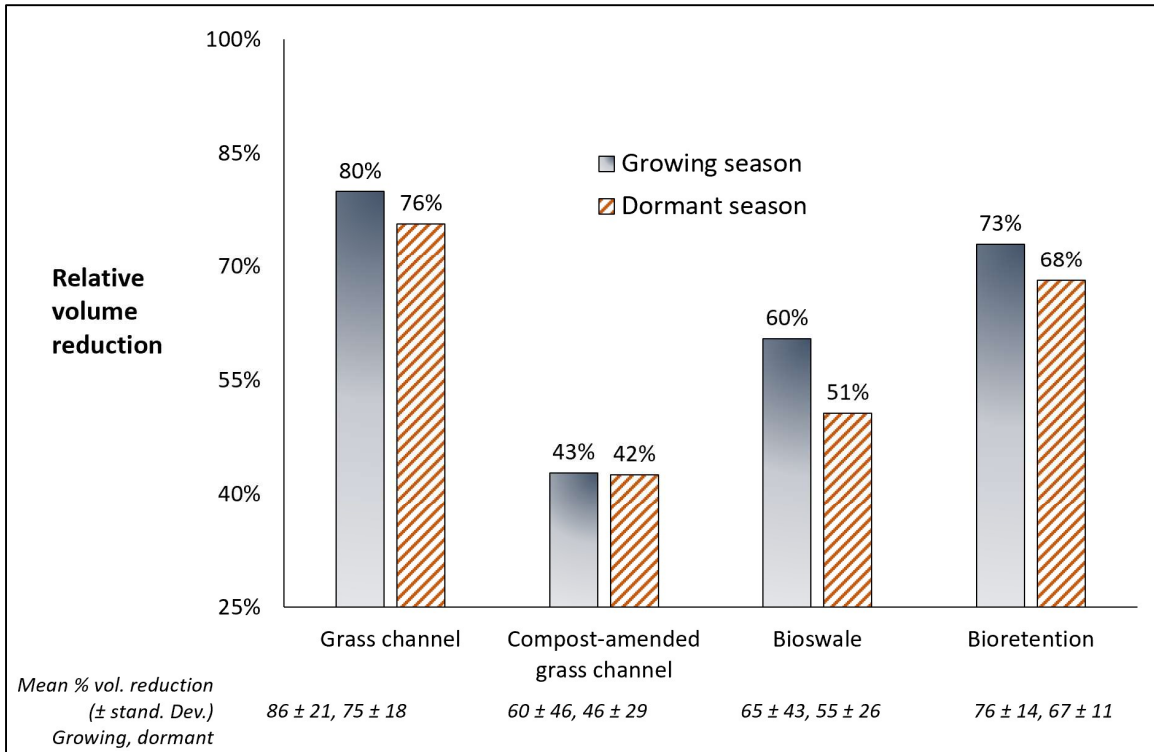


Figure 2.7. Relative volume reductions for each system divided into growing season (May 20 – Sept 20) and dormant season (Sept 21 – May 19) as well as unweighted averages for each season.

The phenomenon of lower performance in colder seasons has been attributed to reduced vegetation activity and decreased hydraulic conductivity during cold seasons, though neither were explicitly measured in this present study (Valtanen et al. 2017; Emerson and Traver 2008). Plant growth during the growing season slowed, absorbed, and transpired runoff while roots encouraged infiltration and increased retention. In addition to plant inactivity during the dormant season, decreasing hydraulic conductivity would discourage infiltration and encourage runoff from the swales. But in the case of the BR, decreasing hydraulic conductivity would have had the opposite effect on performance because of its 15-cm ponding depth, if it had any effect at all, because it would create a less permeable surface of the basin and therefore longer storage time. Consequently, the decreasing performance of the BR in the dormant season was attributed to inactivity of vegetation such that the influent moved quickly from the surface to the underdrain with little interference from vegetation that would remove water through evapotranspiration.

The growing season and dormant season did not differ significantly in rain intensity or depth, but the dormant season did contain significantly longer events. Event duration had no significant influence on GC or CAGC performance in either season, so the explanation for changes in their performances must be another factor such as vegetation inactivity or lowered hydraulic conductivity. However, duration in the dormant season was significant for the BR and BS such that both system performances were significantly inversely correlated with the longer event durations of the dormant season (M-W, P -value = .02 (BR) and .01 (BS)). Given the design similarities between these two systems, it is possible that one or more of their design elements as well as plant dormancy were susceptible to longer event durations – perhaps high infiltration capabilities of the ESM in combination with their underdrains.

2.4.5 Volume Reductions and Loading Ratios

The loading ratios for the GC, CAGC, and BS are similar with values of 1.52, 1.21, and 1.49, respectively, but the BR is much higher at 47.2 (Table 2.1). The large loading ratio of the BR indicates that it is expected to handle volume from an area much larger than its footprint, a characteristic allowed by its 15-cm ponding depth in its forebay and bypass. For example, for the 24.4 mm rain event of January 19, 2019, the BR received 426 m³ and a total of 168 m³ (39%) was outflow. For this same event, the GC, CAGC, and BS each received 152 m³, 146 m³, and 152 m³ respectively, while 17 m³ (11%), 92 m³ (63%), and 84 m³ (55%), respectively were outflow. Examining the performances of all four systems with respect to their loading ratios, the BR was the best “value” for volume reduction given its high loading ratio and strong volume reduction, though the selection of a swale is useful if a green alternative to gray piped infrastructure is desired. However, the similar ratios of the three types of swales indicate that the extra effort of implementing and maintaining the more complex CAGC and BS may not be warranted when the performance of the simple GC amounts to greater runoff volume reduction in all the conditions explored thus far.

2.4.6 Outflow Volume and Impervious Contributing Drainage Areas

In this study, the GI system performances were normalized by dividing outflow volumes for each event for each GI system by their respective impervious surface CDA values (Fig. 2.8). For events under 15 mm, the swales had near-zero ratios of outflow to impervious CDA, but these ratios grew with event depth. This reflects the swales' ability to absorb flows from low rainfall depths. The BS and CAGC had similarly shaped graphs with maximum values of approximately 200 while the GC remained lower with a maximum of approximately 100. However, the BR by far had the lowest ratios which made it the more efficient system according to this metric. The large subsurface and ponding storage capacity of the BR allowed it to mediate the larger flows that would overwhelm the swale systems. In fact, the BR ratios are so low that it raises concerns that the system is much larger than it needs to be, though it provides a performance buffer in extreme events.

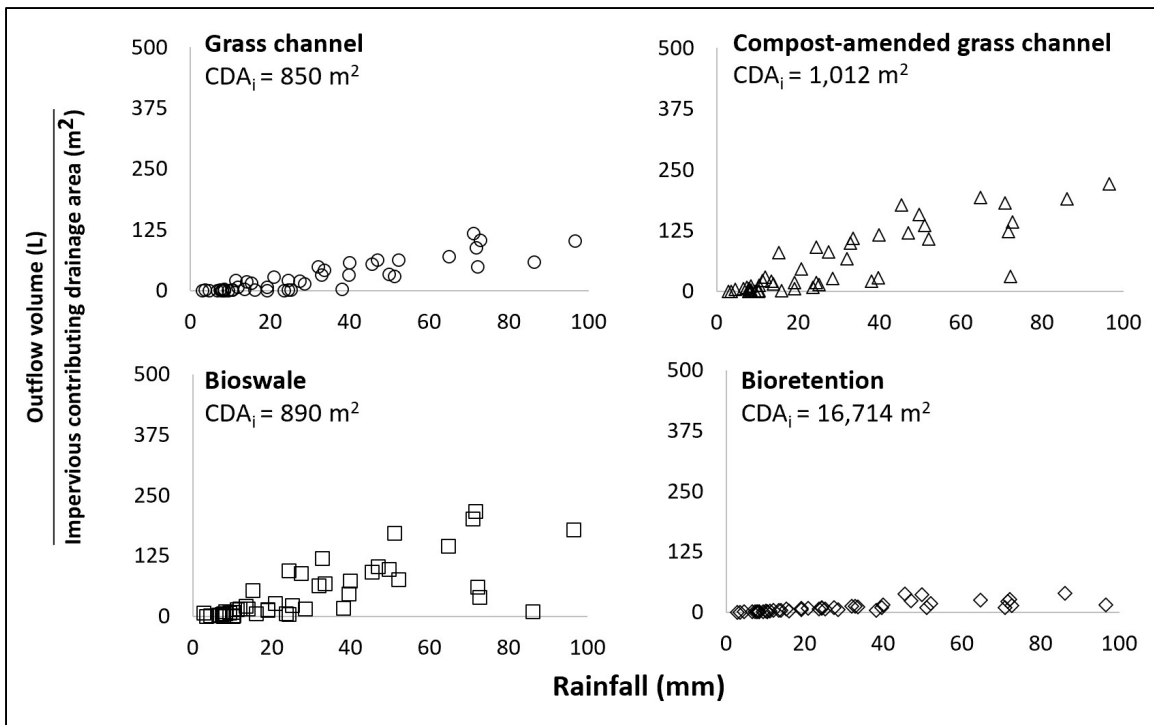


Figure 2.8. Performances of each system normalized according to expected inflow (impervious contributing drainage areas).

2.5 CONCLUSIONS

Runoff volume reduction performances of four types of newly installed and closely located green stormwater infrastructure, a grass channel, compost-amended grass channel, bioswale, and bioretention, were evaluated over their first year of operation. Performances of these systems overall were satisfactory if not well above expectations in some cases, though they varied with rainfall conditions and season. Recommendations for selecting one GI system over another depend on site-specific characteristics and project needs such as the available land for implementation and water quality control requirements.

The results of this study suggest that the simplest swale design of the grass channel could perform just as well as (if not better than) the more heavily engineered swale types, but not necessarily better than a bioretention. Given the large volume reduction of the grass channel, it could be an excellent choice over more engineered swale designs. For example, the grass channel could function well where a single large GI system is not practical, but where multiple dispersed systems will fit and piped infrastructure could be replaced with a GI system. The bioretention system, on the other hand, worked well in reducing large volumes of water and would do well in areas that fit a single large system rather than several distributed systems, such as an intersection. The compost-amended grass channel and bioswale had mediocre volume reductions overall with the widest variations in performances, indicating that they would perform best as green conduits rather than volume control in most circumstances. The relatively low volume reductions of these two are attributed to design characteristics such as a sloped underdrain within highly permeable soils (bioswale) and narrower pervious space between the channel center and the road (compost-amended grass channel).

Specific conclusions on volume reduction performances during this first year include:

- The relative and unweighted average runoff volume reduction of the grass channel, when considering no other factors, was the highest (78%, 81%) followed by the bioretention (71%, 73%), bioswale (56%, 60%), and compost-amended grass channel (43%, 53%).
- As rainfall depth increased, all performances fell in varying amounts. In general, the bioretention volume reduction was the least susceptible to varying rainfall conditions and the bioswale was the most susceptible.
- Volume reductions for all systems decreased from the growing season to the dormant season. Potential explanations for this change include decreased plant activity, lowered hydraulic conductivity of soils, and longer events during the dormant season.
- The loading ratios of the swales were similar (1.21 - 1.52) but the bioretention ratio was 47.2. Given the comparable values of the swale ratios and the relatively high runoff reduction by the grass channel, the results suggest that the more complex swale designs including underdrains and soil amendments are not necessarily merited.
- The bioretention had the lowest ratios of outflow volume to impervious contributing drainage area for all rain events, indicating that it reduced volume well for its expected inflow, though it is potentially larger than it needs to be for its designed performance.

Suggestions for further research on field performance of GI systems include studies on runoff volume reductions with respect to age of the systems and maintenance efforts and costs. Future studies should also address water quality issues as well as runoff reduction, exploring load reduction of pollutants of concern.

2.6 REFERENCES

- Abida, H., Sabourin, J.F. 2006. "Grass Swale-Perforated Pipe Systems for Stormwater Management." *J Irr. and Drain. Eng.* 132 (1): 55–63. <https://doi.org/10.1061>.
- Ahiablame, L. M., Engel, B.A., Chaubey, I. 2012. "Effectiveness of Low Impact Development Practices: Literature Review and Suggestions for Future Research." *Water, Air, & Soil Poll.* 223 (7): 4253–73. <https://doi.org/10.1007/s11270-012-1189-2>.
- Boyer, J. 2019. "Year of Extremes: Richmond and Virginia's Biggest Weather Stories of 2018." *Richmond Times-Dispatch*, January 2019. https://www.richmond.com/weather/year-of-extremes-richmond-and-virginia-s-biggest-weather-stories/article_a2c08eb0-07ec-5f10-b582-b66904c53a08.html. Accessed May 22, 2020.
- Brown, R.A., Hunt III, W.F. 2011. "Impacts of Media Depth on Effluent Water Quality and Hydrologic Performance of Undersized Bioretention Cells." *J Irr. and Drain. Eng.* 137 (3): 132–43. [https://doi.org/10.1061/\(ASCE\)IR.1943-4774.0000167](https://doi.org/10.1061/(ASCE)IR.1943-4774.0000167).
- Burgis, C., Hayes, G.M., Henderson, D., Zhang, W., Smith, J.A. 2020. "Green stormwater infrastructure redirects deicing salt from surface water to groundwater." *Sci. of the Tot. Env.* 729. <https://doi.org/10.1016/j.scitotenv.2020.138736>.
- Cording, A., Hurley, S., Adair, C. 2018. "Influence of Critical Bioretention Design Factors and Projected Increases in Precipitation Due to Climate Change on Roadside Bioretention Performance." *J Env. Eng.* 144 (9): 04018082. [https://doi.org/10.1061/\(ASCE\)EE.1943-7870.0001411](https://doi.org/10.1061/(ASCE)EE.1943-7870.0001411).
- Darboux, F., Davy, Ph., Gascuel-Oudou, C., Huang, C. 2002. "Evolution of Soil Surface Roughness and Flowpath Connectivity in Overland Flow Experiments." *CATENA* 46 (2–3): 125–39. [https://doi.org/10.1016/S0341-8162\(01\)00162-X](https://doi.org/10.1016/S0341-8162(01)00162-X).
- Davis, A., Stagge, J., Jamil, E., Kim, H. 2011. "Hydraulic Performance of Grass Swales for Managing Highway Runoff." *Water Research* 46 (20): 6775–86.
- Davis, A. 2008. "Field Performance of Bioretention: Hydrology Impacts." *J Hydrologic Eng.* 13 (2): 90–95. [https://doi.org/10.1061/\(ASCE\)1084-0699\(2008\)13:2\(90\)](https://doi.org/10.1061/(ASCE)1084-0699(2008)13:2(90)).
- DEQ. 2011a. "Bioretention." Stormwater Design Specification 9. VA Department of Environmental Quality. http://www.vwrrc.vt.edu/swc/documents/2013/DEQ%20BMP%20Spec%20No%209_BIORETENTION_FinalDraft_v1-9_03012011.pdf. Accessed January 10, 2020.
- DEQ. 2011b. "Grass Channels." Stormwater Design Specification 3. VA Department of Environmental Quality. http://www.vwrrc.vt.edu/swc/documents/2013/DEQ%20BMP%20Spec%20No%203_GRASS%20CHANNELS_Final%20Draft_v1-9_03012011.pdf. Accessed January 10, 2020.
- DEQ. 2011c. "Dry Swales." Stormwater Design Specification 10. VA Department of Environmental Quality. http://www.vwrrc.vt.edu/swc/documents/2013/DEQ%20BMP%20Spec%20No%2010_DRY%20SWALE_Final%20Draft_v1-9_03012011.pdf. Accessed January 10, 2020.
- Eckart, K., McPhee, Z., Bolisetti, T. 2017. "Performance and Implementation of Low Impact Development – A Review." *Sci. of the Tot. Env.* 607–608 (December): 413–32. <https://doi.org/10.1016/j.scitotenv.2017.06.254>.
- Emerson, C., Traver, R.G. 2008. "Multiyear and Seasonal Variation of Infiltration from Storm-Water Best Management Practices." *J Irr. and Drain. Eng.* 134 (5): 598–605. [https://doi.org/10.1061/\(ASCE\)0733-9437\(2008\)134:5\(598\)](https://doi.org/10.1061/(ASCE)0733-9437(2008)134:5(598)).
- Flynn, K.M., Traver, R.G. 2013. "Green Infrastructure Life Cycle Assessment: A Bio-Infiltration Case Study." *Eco. Eng.* 55 (June): 9–22. <https://doi.org/10.1016/j.ecoleng.2013.01.004>.
- GeoSyntec Consultants, and Wright Water Engineers, Inc. 2011. "Volume Reduction." Technical Summary. International Stormwater Best Management Practices (BMP) Database. bmpdatabase.org. Accessed December 30, 2019.

- GeoSyntec Consultants, and Wright Water Engineers, Inc. 2012. "Bioretention Volume Reduction." Addendum 1. International Stormwater Best Management Practices (BMP) Database. bmpdatabase.org. Accessed December 30, 2019.
- Greeley and Hansen. 2014. "Typical Year Selection." CSS Long Term Control Plan Update. City of Alexandria Department of Transportation and Environmental Services. <https://www.alexandriava.gov/uploadedFiles/tes/oeq/info/Typical%20Year%20Selection-FINAL.pdf>. Accessed May 22, 2020.
- Henderson, D., Smith, J.A., Fitch, G.M. 2016. "Impact of Vegetation Management on Vegetated Roadsides and Their Performance as a Low-Impact-Development Practice for Linear Transportation Infrastructure." *Transp. Res. Record*. <https://doi.org/10.3141/2588-19>.
- Knight, E.M.P., Hunt III, W.F., Winston, R.J. 2013. "Side-by-Side Evaluation of Four Level Spreader-Vegetated Filter Strips and a Swale in Eastern North Carolina." *J of Soil and Water Cons.* 68 (1): 60–72. <https://doi.org/10.2489/jswc.68.1.60>.
- Komlos, J., Traver, R. 2012. "Long-Term Orthophosphate Removal in a Field-Scale Storm-Water Bioinfiltration Rain Garden." *J Env. Eng.* 138 (10): 991–98. [https://doi.org/10.1061/\(ASCE\)EE.1943-7870.0000566](https://doi.org/10.1061/(ASCE)EE.1943-7870.0000566).
- Line, D.E., Hunt III, W.F. 2009. "Performance of a Bioretention Area and a Level Spreader-Grass Filter Strip at Two Highway Sites in North Carolina." *J Irr. and Drain. Eng.* 135 (2): 217–24. [https://doi.org/\(ASCE\)0733-9437\(2009\)135:2\(217\)](https://doi.org/(ASCE)0733-9437(2009)135:2(217)).
- Liu, Y., Engel, B.A., Flanagan, D.C., Gitau, M.W., McMillan, S.K., Chaubey, I. 2017. "A Review on Effectiveness of Best Management Practices in Improving Hydrology and Water Quality: Needs and Opportunities." *Sci. of the Tot. Env.* 601–602 (December): 580–93. <https://doi.org/10.1016/j.scitotenv.2017.05.212>.
- Mays, Larry. 2011. In *Water Resources Engineering*, 2nd ed., 304. Wiley-India Edition.
- NCICS. 2020. North Carolina Institute for Climate Studies. "NOAA National Centers for Environmental Information." State Climate Summaries: Virginia. May 18, 2020. <https://statesummaries.ncics.org/chapter/va/>.
- NRCS. 2019. "Web Soil Survey." Natural Resources Conservation Service. 2019. <https://websoilsurvey.sc.egov.usda.gov/App/HomePage.htm>. Accessed December 26, 2019.
- PWD. 2017. "Loading Ratio Requirements." SMGM v 3.1. Philadelphia Water Department. <https://www.pwdplanreview.org/upload/pdf/Loading-Ratio-Requirements-18.03.26.pdf>. Accessed July 8, 2020.
- Schueler, T.R. 1994. "Performance of Grassed Swales Along East Coast Highways." Technical Note #32. Article 114. Watershed Protection Techniques. Center for Watershed Protection. <https://owl.cwp.org/?mdocs-file=4843>. Accessed May 22, 2020.
- Shrestha, P., Hurley, S., Wemple, B. 2018. "Effects of Different Soil Media, Vegetation, and Hydrologic Treatments on Nutrient and Sediment Removal in Roadside Bioretention Systems." *Eco. Eng.* 112: 116–31.
- Tedoldi, D., Chebbo, G., Pierlot, D., Kovacs, Y., Gromaire, M-C. 2016. "Impact of Runoff Infiltration on Contaminant Accumulation and Transport in the Soil/Filter Media of Sustainable Urban Drainage Systems: A Literature Review." *Sci. of the Tot. Env.* 569–570 (November): 904–26. <https://doi.org/10.1016/j.scitotenv.2016.04.215>.
- USDA, NRCS, and CED. 1986. "Urban Hydrology for Small Watersheds (TR-55)." Technical Release 55. https://www.nrcs.usda.gov/Internet/FSE_DOCUMENTS/stelprdb1044171.pdf. Accessed December 26, 2019.
- Valtanen, M., Sillanpää, N., Setälä, H. 2017. "A Large-Scale Lysimeter Study of Stormwater Biofiltration under Cold Climatic Conditions." *Eco. Eng.* 100 (March): 89–98. <https://doi.org/10.1016/j.ecoleng.2016.12.018>.

- VDOT. 2017. Virginia Department of Transportation. "VDOT Governance Document: Drainage Manual." Location and Design Division. [http://www.virginiadot.org/business/resources/LocDes/Drainage Manual/START_VDOT_Drainage_Manual.pdf](http://www.virginiadot.org/business/resources/LocDes/DrainageManual/START_VDOT_Drainage_Manual.pdf). Accessed March 13, 2017.
- Virginia Stormwater Management Program (VSMP). 2011. *Water Quality Compliance. Virginia Administrative Code*. Vol. 9VAC25-870-65. [https://law.lis.virginia.gov/admincode /title9/agency25/chapter870/section65/](https://law.lis.virginia.gov/admincode/title9/agency25/chapter870/section65/). Accessed December 26, 2019.
- Winston, R.J., Dorsey, J.D., Hunt III, W.F. 2016. "Quantifying Volume Reduction and Peak Flow Mitigation for Three Bioretention Cells in Clay Soils in Northeast Ohio." *Sci. of the Tot Env.* 553 (May): 83-95. <https://doi.org/10.1016/j.scitotenv.2016.02.081>.
- Winston, R.J., Dorsey, J.D., Smolek, A.P., Hunt III, W.F. 2018. "Hydrologic Performance of Four Permeable Pavement Systems Constructed over Low-Permeability Soils in Northeast Ohio." *J Hydrologic Eng.* 23 (4): 04018007. [https://doi.org/10.1061/\(ASCE\)HE.1943-5584.0001627](https://doi.org/10.1061/(ASCE)HE.1943-5584.0001627).

3. Mobilization of trace metals by road salt application

This chapter is in preparation to be submitted to the *Journal of Environmental Engineering* (ASCE):

Hayes, Gail M., Charles R. Burgis, Wuhuan Zhang, Derek Henderson, and James A. Smith. (In Preparation.) "Investigating trace metal mobilization by road salts in four green stormwater infrastructure systems." *Journal of Environmental Engineering*.

3.1 ABSTRACT

Trace metals are frequently deposited in receiving waters by stormwater runoff, but green infrastructure (GI) has demonstrated the capability of capturing these pollutants and mitigating their risks. However, the removal of metals from runoff is typically impermanent and the intrusion of road salts can mobilize the metals from soils through cation exchange, formation of chlorocomplexes, and the disintegration of the soil structure. Previous studies on the mobilization of metals by road salts have used soil columns and roadside soils with only one investigating the impact of salts on metals on the scale of an entire GI system. This chapter addresses the need for more research by analyzing the stormwater and soil quality of four GI systems for trends in mobilization by road salts of four trace metals common in stormwater: chromium, copper, nickel, and lead. The four monitored GI systems, a bioretention system, bioswale, compost-amended grass channel, and grass channel, showed no significant trends of metal mobilization by road salts in either intra-event analyses or the pre- and post-winter season soil sampling. While the mulch at the bioretention system significantly decreased in metal content over the winter months, the role of road salts in this is unclear. The groundwater at the bioretention system did show a surge of road salts in the weeks following deicing application, but the response in metal content was minimal. Ultimately, it was determined that road salt application in a climate such as Lorton Road does not pose a significant threat to the mobilization of metals due to infrequency of salt application and small concentrations of trace metals in the runoff. More significant indicators of metal mobilization include the export of total suspended solids, dissolved organic carbon, and pre-existing metal content of the GI soils which created irreducible concentrations.

3.2 INTRODUCTION

Trace metals are common pollutants in stormwater runoff that can have toxic, carcinogenic, and mutagenic effects on organisms in waterways receiving stormwater runoff (USEPA 2019). Among other sources, vehicle wear and tear deposits metals on road surfaces where they are washed away with stormwater runoff (USEPA 2019; Brown and Peake 2006). Through sorption, metals are likely to be captured out of runoff or soil solution, which decreases their bioavailability and mobility (Maniquiz-Redillas and Kim 2014; Jayarathne et al. 2020). Because of this ability to be captured in soils, green infrastructure (GI) such as bioretention systems and swales, are commonly used to mitigate trace metals in stormwater runoff.

Bioretention systems have been shown to mitigate trace metals in runoff by reducing total concentrations of copper by up to 94%, nickel by up to 74%, and lead by up to 98% (Davis et al. 2003; David et al. 2015). But results vary widely and depend on conditions such as prevalence of organic content and natural mobility of a specific metal as explained in Chowdhury and Mohamed (2018) where total lead and chromium were both found to increase in concentration by 29% and 6.5%, respectively. Swales have also demonstrated variable reductions of trace metal concentrations in runoff with studies reporting consistent improvements in water quality (Stagge et al. 2012) or mixtures of reductions and increases (Leroy et al. 2016; Knight et al. 2013). Leroy et al. (2016) found, for example, total lead concentration reductions fluctuated from -24% to 15% and total copper from 4.4% to 44% depending on the type of vegetation cover of the swales.

When metals are captured from runoff, they accumulate within the media of GI systems, with highest concentrations near the media surface (Li and Davis 2008; Jones and Davis 2013; Knight et al. 2013). Removing metals from runoff typically results in physical capture rather than chemical transformation and can be improved by inorganic or organic soil amendments (Lwin et al. 2018), so the metal is capable of re-entering solution in the certain conditions (Bolan et al. 2014). Captured or

immobilized metals have the lowest bioavailability and when metals enter soil solution, this bioavailability and mobility can increase, raising risks to the organisms in contact with the water (Bolan et al. 2014). Metals captured in soils have been shown to be mobilized into solution in the presence of road salts, particularly NaCl, but also MgCl₂ and CaCl₂ (Bauske and Goetz 1993). This mobilization usually occurs through cation exchange with sodium, magnesium, or calcium ions but can also occur through the mobilization of organics, colloids, or suspended solids from the intrusion of the cations (Nelson et al. 2009; Maniquiz-Redillas and Kim 2016; Chapman and Horner 2010). Formation of chlorocomplexes can also occur in some circumstances (Bauske and Goetz 1993). Once mobilized from the soil, the metals are carried with the runoff to receiving waters or remain in the soil solution but with increased bioavailability. Speciation of a metal in solution can be in many different forms with varying levels of bioavailability (Benjamin 2002). Other concerns with metal mobilization with road salts include threats to groundwater quality; if the threat is not only from salt intrusion (Denich et al. 2013) it can also be from both the salts and the metals that they mobilize (Norrström 2005; Norrström and Jacks 1998; Bauske and Goetz 1993).

Previous studies on the mobilizing effects of road salts on metals have primarily been limited to lab studies with mesocosms or soil columns and field studies on roadside soils. Early studies on roadside soils found higher metal mobility in soils directly beside the roadway, a result of the higher salt content of these soils (Bäckström et al. 2004; Zehetner et al. 2009). In the lab, column studies often found evidence of metal mobilization and attributed this to organic content dispersion, ion exchange, and formation of chlorocomplexes, results consistent with road salt presence (McManus and Davis 2020; Sjøberg et al. 2017; Li et al. 2015; Peltier et al. 2010). However, both Paus et al. (2014) and Denich et al. (2013) found limited evidence through their mesocosm and column studies that road salt would actually have this effect. First, the overall capability of the bioretention media to capture metals was greater than the mobilizing impact of the salts (Denich et al. 2013). Second, confounding factors such as organic

content of the soil (compost volume fraction) and ambient temperature were more significant factors in metal retention than salts (Paus et al. 2014). To the author's knowledge, only one study has been conducted on the interaction of salts and metals within stormwater management systems in a field setting. Mullins et al. (2020) studied the salt impacts on an infiltration trench and found increases in lead and copper concentrations as well as the likelihood of legacy contamination mobilization. No other field studies have been pursued on either bioretention systems or swales on this topic.

Due to the contradictory and sparse results, this subject of road salts mobilizing trace metals in GI systems warrants further research. This present study seeks to address this gap in the knowledge, particularly with respect to the need for more field data. Identifying the extent to which road salts impact metal retention would be valuable for future designs of GI systems in regions where road salts are regularly used. The Lorton Road field site is a good opportunity to study the impact of road salts on trace metals because it includes several types of GI systems as well as measurable quantities of both road salts and trace metals. By including data from stormwater, soil, and groundwater from field-scale functioning GI systems, this present study can go a step further than the previous studies on the subject by looking for trends on the scale of the whole GI system in multiple systems. The objective of this study is to evaluate the mobilizing impact of road salts on trace metals within GI systems through examining intra-event mitigation of metals (chromium, copper, nickel, and lead), changes in groundwater salt and metal content, and variations in levels of salts and metals in the GI system soils.

3.3 METHODS

3.3.1 Field Site and Data Collection

This study was conducted at the Lorton Road field site described in Chapter 2. Briefly, this site consists of four individual GI systems, a bioretention (BR), bioswale (BS), compost-amended grass channel (CAGC), and grass channel (GC), that were instrumented for flow monitoring and sample collection. There were seven monitoring stations such that the BR had three (inlet, outlet, bypass), each

swale had one at their respective outlets, and one measured the overland flow entering the three swales. At each monitoring station, flow was monitored in all seasons for the duration of the monitoring period using Hach AS950 autosamplers (Hach™, Loveland, CO) and fiberglass H-flumes (Open Channel Flow© Boise, ID). Flume sizes and manufacturer-provided flow equations are listed with the properties of each GI in Appendix A. Flow-weighted composite samples of inflow and outflow from each GI were collected using flow-pacing numbers set according to rainfall depth predictions. Water quality of the flow-weighted composite samples was interpreted as the event mean concentration (EMC) of a given parameter. Samples were collected in 9.5-L glass bottles and kept on ice until pick-up within 12 – 24 hours of an event finishing. A successful sampling event included at least 5 discrete aliquots of 100 mL each collected over the rising limb and peak of the monitored flow. Prior to sampling an event, sample intake lines were rinsed with at least 600 mL of distilled water and the flumes and ceramic intake tips scrubbed. Field blanks of distilled water passed through the autosampler after the cleaning rinses were periodically collected and analyzed to check the sufficiency of this cleaning procedure.

Soil and mulch samples were collected at the site and refrigerated in plastic air-tight gallon bags until analysis. Early samples of the stock ESM and compost materials for the BR, BS, and CAGC were collected prior to the start of this study in 2015. Native soil samples around the BR were also collected prior to the beginning of this study in 2017 via soil auger. Two more soil sampling sessions occurred: one prior to the 2019 – 2020 winter season in 2019-Oct and one after the winter season in 2020-Mar. For these samples, an aluminum trowel was used to collect approximately 3.5 liters of soil from the top soil (0 – 5 cm) and the sub-surface (15 – 20 cm) in the four GI systems. In 2019-Oct, three sampling points of top soil and sub-surface were collected along the lengths of every GI system. This frequency was repeated in 2020-Mar for the BR and CAGC, but was reduced to two for the GC and BS due to the short length of the swales and destructive nature of the sampling. Mulch samples were collected with the same frequency as the soils in the BR.

Well locations at the BR are shown in Fig. 3.1. Two groundwater monitoring wells were placed manually inside the forebay of the BR in the summer and fall of 2018 and eight were placed by mechanical drilling (Ground Zero Inc., Fredericksburg, MD) on the perimeter of the BR in the spring of 2019. Well depths are listed in Appendix F and range from 3 m to 10 m below the surface of the forebay. The wells were drilled until water was reached except A2 and E2 which extended 2 - 5 m deeper. The hydraulic gradient of the groundwater moves north-east with Well B considered as the most upstream and least impacted by the BR infiltration (Appendix F). Each well consists of 5-cm diameter PVC with the bottom one meter screened with 10 slots per 2.5 cm. The screens are all within sand that rises at least one meter above the top of the screen. Immediately above the screen and sand is bentonite clay which reaches to the soil surface for sealing the well from surface water seepage. Locked steel covers as well as plugs protect each well. Groundwater depth was measured every 7 – 10 days for the study length. Groundwater sampling occurred every 4 – 6 weeks during the monitoring period with one exception in the spring of 2020. This interruption resulted from restrictions due to COVID-19, so sampling occurred in January and then May of 2020. To sample each well, three well volumes were purged from each well using polyethylene bailers. After purging, 500-mL samples were collected with periodic duplicates for procedure verification. Upon return to the lab, the groundwater samples were preserved with the same methods used for the stormwater samples and analyzed for common ions and metals.



Figure 3.1. Location of wells around bioretention. Well 1 and Well 2 were drilled manually by auger and all others drilled mechanically.

Rainfall data was collected with a rain gauge installed at the BR, as described in Chapter 2. When the rain gauge would fail, the local weather station data would be used as replacement. The instances where this replacement occurred for this present study are indicated in Appendix G. Average daily temperature was collected through the same substitute weather station used for the rain gauge, Ronald Reagan National Airport, located 23 km from the site.

3.3.2 Analytical Methods

Inductively-coupled plasma mass spectrometry (ICPMS) (Agilent, Santa Clara, California) quantified total chromium, total nickel, total copper, and total lead in acidified (2% HNO₃) stormwater, groundwater, and acid digested soil samples. Minimum detection on the ICPMS was 0.1 µg/L. Ion chromatography (IC) (Dionex ICS-5000, Thermo Scientific, Sunnyvale, CA) measured ions (sodium, chloride, calcium, and magnesium) to a detection limit of 0.05 mg/L. TOC-L Total Organic Carbon Analyzer (Shimadzu, Kyoto, JPN) quantified DOC in samples acidified to 2% HCl and had a detection limit of 2 mg/L. Samples were filtered with 0.45 µm PTFE syringe filters prior to analysis in the ICP, IC, and TOC-L analyzer. Check standards of known concentrations for the ICP, IC, and TOC-L analyses were also analyzed with each set of samples. Total suspended solids (TSS) of stormwater were measured with gravimetric determination by vacuum filtration of 100 – 300 mL of sample through 0.45 µm filters that

were dried for 24 hours at 100° C. TSS analyses were performed in triplicate and averages of these three values are reported.

To quantify metal content of soils, approximately 1 g of the samples were dried for at least 24 – 48 hours on polystyrene weigh boats in ambient laboratory conditions. The dried soils (0.5 g) were then digested in 10 mL strong acid (70% HNO₃) using a Mars 6 microwave (CEM Corporation Matthews, NC) programmed to follow EPA method 3051 (EPA SW-846). This digestion method has been verified by Lloyd et al. (2019) with the same equipment in the same lab and Link et al (1998) at another lab. Soil digestions were performed in duplicate and averages are reported. Following digestion, samples were diluted with deionized water to 2% HNO₃, filtered with 0.45 µm PTFE syringe filters, and measured with ICP-MS. Microwave blanks consisting of 10 mL of 70% HNO₃ were conducted in every microwave digestion session and analyzed alongside digestions to ensure cleaning efficacy of microwave vials.

Soil extractable chloride was measured using a method demonstrated in Robinson et al. (2017) and Burgis et al. (2020): 10 g of oven dried soil samples were shaken for 15 minutes in a 50-mL vial containing 25 mL of 0.01 M CaNO₃. Prior to analysis in the IC, samples were filtered with 0.45 µm PTFE syringe filters. Waypoint Analytical (Richmond, VA) quantified pH, cation exchange capacity (CEC), and major soil extractable cations (Na⁺, Mg²⁺, Ca²⁺) with an ammonium acetate extraction. The extractable cation method mixes 20 mL of ammonium acetate (1 M, pH=7) with 4 g of dry soil that is shaken on a 2mm sieve for 10 minutes. After filtration with Whatman #1 filters, the cations are quantified with an ICP-OES (Perkin Elmer Optima 8300, Waltham, MA). Sodium adsorption ratio (SAR) was determined to identify build-up of sodium with respect to calcium and magnesium, a sign of deteriorating soil conditions resulting from sodium intrusion. SAR is calculated by dividing the sodium concentration by the square root of one-half of the sum of the calcium and magnesium concentrations (USDA 2017). Organic content of soils (10 g oven dried) was measured by gravimetric determination using the temperature levels delineated in Loss on Ignition ASTM Standard D7348 (ASTM 2013).

To identify impacts of road salts on the partitioning of metals out of the stormwater, a partition test was performed. In the partition test, samples with varying levels of chloride (below 50 mg/L and above 500 mg/L) were selected and split into two aliquots. The levels of chloride were selected based on the findings of other studies which suggested mobilization could occur at the high levels. One aliquot was filtered prior to acidification to 2% HNO₃ (“F-A”) and the other aliquot was acidified prior to filtering (“A-F”). While the A-F sample theoretically contains all metals in the solution as well as those which dissociated from suspended solids after acidification, the F-A sample theoretically contains only the free metals prior to acidification. Impacts of chloride and sodium levels on the metal partitioning were then evaluated through the ratio of the F-A results to the A-F metal contents. The resulting ratio is referred to as the Partition Fraction. A Partition Fraction close to 1 indicates that all measurable metals in the sample were dissociated from suspended solids prior to acidification, which is the result hypothesized in a high salt solution.

3.3.3 Data Analysis

Data analysis was conducted in Microsoft Excel and RStudio (R Version 4.0.2). Normality in data distribution was not assumed, so non-parametric statistical analyses were used. Specifically, Mann-Whitney tests were used for non-paired samples and significance for these results was set at 90% or $\alpha = .1$. Simple linear regression analyses were used for identifying correlations between salt inflow and metal reductions or outflow concentrations and also for soil characteristics. For stormwater, higher concentrations of chloride flowing into the GI system were hypothesized to correlate with more metals flowing out and greater EMC reductions. Secondary mobilization of metals was hypothesized to occur through the release of DOC and TSS upon the introduction of sodium to the soil matrix. Chloride was used to measure road salt content in stormwater and groundwater as the instrument for measuring sodium (IC for cations) was malfunctioning during the study period. EMC percent reductions for the BR were computed using only the inflow and outflow concentrations, though the bypass EMC values are

reported as well. Metal mobilization by salts from the soils was considered as increases in sodium content associated with decreases in metal contents.

3.4 RESULTS

3.4.1 Stormwater Overview

The inflow and outflow concentrations and EMC reductions of salts, metals, DOC, and TSS for each reported event for the four GI system are summarized in Table 3.1. The systems were monitored in all seasons from the spring of 2018 until the summer of 2020, with many events shared between all four systems but several that were monitored at three or fewer of the systems. Therefore, the individual GI stormwater results are presented independent of each other with no direct comparisons made. The inflow to each of the swales was measured at the single overland flow collector, but inflow water quality summaries in Table 3.1 vary for each swale according to which corresponding outflow data was captured. The complete set of results as well as average daily temperature and precipitation data is presented in Appendix G. The winter season of 2018 – 2019 had many more events than the 2019 – 2020 season where road salt was required for driving safety and elevated sodium and chloride levels were measured, so the intra-event stormwater analyses focus on the earlier season. Even though no events with elevated salt levels were captured during the 2019 – 2020 winter season, there were a few wherein road salts were likely applied, as evidenced by the weather records, groundwater data, and some of the soil data (indicated in Appendix G). Because VDOT keeps limited records of road salt application that are not geographically specific, it is impossible to know definitively when and how much salt was applied, though.

As demonstrated in Burgis et al. (2020), sodium chloride was the predominant road salt applied to Lorton Road during the study period and concentrations of sodium and chloride in the road runoff ranged from 4 – 8050 mg/L and 10 – 5000 mg/L, respectively (Table 3.1 and Appendix G). Burgis et al. (2020) demonstrated that surges of chloride could be detected in the BR outlet after a winter event, so

monitoring occurred in all seasons at the GI systems for this study. The salt data of runoff into and out of the BR and BS as well as the groundwater data through October 2019 used in the analyses of this chapter were first reported in Burgis et al. (2020) as part of a study on the road salt mitigation by GI systems. The ranges detected in this study were the same as the road salt that was in synthesized runoff or measured in actual runoff in Sjøberg et al. (2017), McManus and Davis (2020), Paus et al. (2014), and Denich et al. (2013) who used chloride concentrations between 1000 mg/L and 10,000 mg/L. The levels of calcium and magnesium, other common cations used in road salt, were usually at least an order of magnitude lower than those for sodium, including events where deicing road salt was likely applied. Metal concentrations in inflow and outflow had relatively low variability compared to the sodium and chloride results with concentration ranges of 0.24 – 6.9 µg/L, no detect – 23 µg/L, 4.2 – 63 µg/L, and 0.8 – 17 µg/L, for chromium, nickel, copper, and lead, respectively. Cadmium results were consistently at or below the detection limit of the ICPMS, so this element is excluded from the results. Zinc levels were consistently high even after cleaning the intake lines, so these results are excluded as well due to concerns with contamination. Water quality improvements with regards to each parameter in Table 3.1 are minimal as reductions are often negative.

Table 3.1. Water quality results for events of interest presented as average \pm standard deviation (SD) and range [minimum, maximum] with event mean concentration (EMC) and % reduction of EMC. ^a Bioretention EMC reductions calculated using only inflow and outflow (no bypass).

		Bioretention			Bioswale		C-A Grass Channel		Grass Channel		
		Inflow	Outflow	Bypass	Inflow	Out	Inflow	Out	Inflow	Out	
EMC	mg/L	Na	312 \pm 844 [10.2, 4346]	168 \pm 342 [31, 1789]	102 \pm 132 [2.7, 1231]	555 \pm 123 [15, 4976]	428 \pm 123 [27, 3501]	500 \pm 56 [20, 4976]	111 \pm 56 [28, 540]	202 \pm 30 [15, 2420]	25 \pm 30 [5.1, 134]
		Cl	470 \pm 1383 [3.9, 7395]	281 \pm 698 [6.6, 3748]	157 \pm 1383 [2.5, 2299]	692 \pm 1974 [6.5, 8050]	701 \pm 1654 [7.9, 7112]	604 \pm 1892 [6.5, 8050]	129 \pm 249 [2.7, 1050]	278 \pm 926 [6.5, 4270]	30 \pm 69 [0.7, 313]
		DOC	5.9 \pm 3.4 [3.3, 21.4]	7.4 \pm 4.3 [0.5, 18.2]	6.7 \pm 3.4 [0, 23]	5.6 \pm 2.3 [2.8, 12]	9.6 \pm 4.5 [4.1, 22]	5.8 \pm 2.5 [2.9, 12]	17 \pm 7.5 [6.6, 33]	5.2 \pm 2.2 [2.8, 12]	9.9 \pm 5.6 [2.9, 26]
		TSS	66 \pm 65 [9.5, 302]	13.5 \pm 10.7 [1.5, 42.5]	28 \pm 65 [7.2, 100]	108 \pm 71 [45, 341]	28 \pm 22 [5.5, 88.3]	104 \pm 78 [7.0, 341]	50 \pm 30 [18, 136]	97 \pm 73 [7.0, 341]	24 \pm 15 [5.0, 55]
	μ g/L	Cr	1.8 \pm 1.3 [0.7, 6.9]	1.4 \pm 1.1 [0, 4.2]	1.0 \pm 1.3 [0.2, 2.9]	1.7 \pm 1.1 [0.2, 4.5]	1.4 \pm 0.7 [0, 2.5]	1.5 \pm 0.9 [0.2, 4.0]	1.2 \pm 1.0 [0, 5.2]	1.7 \pm 1.0 [0.4, 4.5]	0.7 \pm 0.6 [0.1, 2.4]
		Ni	1.3 \pm 1.0 [0, 4.7]	3.9 \pm 2.3 [0.3, 8.5]	0.9 \pm 1.0 [0.4, 4.4]	1.3 \pm 0.7 [0.4, 2.8]	5.2 \pm 4.9 [1.5, 23]	1.3 \pm 0.7 [0.4, 2.8]	1.6 \pm 1.8 [0.4, 9.4]	1.2 \pm 0.7 [0.4, 2.8]	0.6 \pm 0.4 [0, 1.6]
		Cu	11.2 \pm 5.8 [6.5, 41]	22.6 \pm 15.8 [3.2, 63]	8.1 \pm 5.8 [3.8, 37]	9.2 \pm 2.9 [4.2, 16]	30 \pm 19 [5.5, 61]	8.9 \pm 2.5 [4.2, 16]	14 \pm 16 [3.6, 84]	9.2 \pm 2.8 [5.2, 16]	8.9 \pm 3.3 [4.7, 16]
		Pb	2.6 \pm 1.8 [0.8, 9.5]	3.9 \pm 2.6 [0.5, 9.5]	32 \pm 1.8 [0.6, 254]	3.8 \pm 2.2 [1.0, 9.8]	6.1 \pm 4.9 [0.6, 17.4]	8.4 \pm 23 [1.0, 109]	19 \pm 70 [0.8, 331]	3.7 \pm 2.1 [1.2, 9.8]	3.9 \pm 2.1 [1.2, 8.6]
	% EMC Reduction	Na	-74 \pm 131 [-654, 95] ^a			-126 \pm 123 [-367, 66]		-6.6 \pm 56 [-69, 96]		55 \pm 30 [17, 94]	
		Cl	-80 \pm 268 [-1470, 95] ^a			-91 \pm 150 [-532, 60]		-19 \pm 63 [-141, 94]		77 \pm 21 [-1.0, 93]	
Cr		-5.3 \pm 97 [-314, 100] ^a			-0.35 \pm 71 [-200, 100]		6.8 \pm 84 [-300, 100]		49 \pm 44 [-60, 93]		
Ni		-319 \pm 315 [-1350, 37] ^a			-367 \pm 389 [-1701, 32]		-51 \pm 234 [-1075, 75]		44 \pm 47 [-100, 100]		
Cu		-117 \pm 144 [-511, 68] ^a			-253 \pm 229 [-716, 47]		-52 \pm 136 [-605, 58]		-4.4 \pm 44 [-79, 71]		
Pb		-100 \pm 165 [-475, 92] ^a			-85 \pm 138 [-461, 92]		-37 \pm 126 [-500, 55]		-26 \pm 70 [-173, 81]		
DOC		-41 \pm 74 [-305, 92] ^a			-87 \pm 77 [-286, 35]		-220 \pm 136 [-594, -13]		-101 \pm 83 [-259, 49]		
TSS		65 \pm 43 [-113, 98] ^a			66 \pm 25 [20, 96]		29 \pm 62 [-157, 79]		64 \pm 26 [7, 92]		

3.4.2 Bioretention Stormwater

The inflow and outflow of the BR was monitored for 33 events from March 2018 until August 2020 and is summarized in Table 3.1 with full data in Appendix G. The total rain depth of these events was 1562 mm with individual events ranging from 7.4 to 105 mm while the average daily temperature ranged from 1.7° C to 24° C (overall average of $14 \pm 8.3^\circ$ C). While most of the road salt events were rainfall that followed snow or ice, January 16, 2019 and February 20, 2019 were snowmelt alone. The outlet sampling for the February 20, 2019 event failed, so a grab sample was collected near the completion of the flow.

Fig. 3.2 shows the chloride inflow with respect to metal EMC reduction. The majority of events at the BR received low levels of chloride in the inflow and the system released metals (negative reductions) at these lowest chloride levels. Several regressions between salt inflows and metal outflows or EMC reductions were found to be significant such that increased levels of salt inflow were significantly correlated with lower concentrations of metals in the outflow and increased EMC reductions (Table 3.2). Additional regression analyses were pursued between calcium or magnesium and metal reductions. However, these results were similar to those in Table 3.2, but with larger slopes. The regression analyses were repeated using charge equivalents with the metals and the cations to identify potential trends related to charge density, but this resulted in no significant trends. At the lowest concentrations, the metal EMC reductions were highly variable, even with approximately similar and low inflow concentrations of the corresponding metal. In spite of the variability in EMC reductions, there are significant positive linear correlations between metal inflow concentrations and the corresponding EMC reduction (Appendix H). The arrows in Fig. 3.2 indicate a visual trend with no statistical significance.

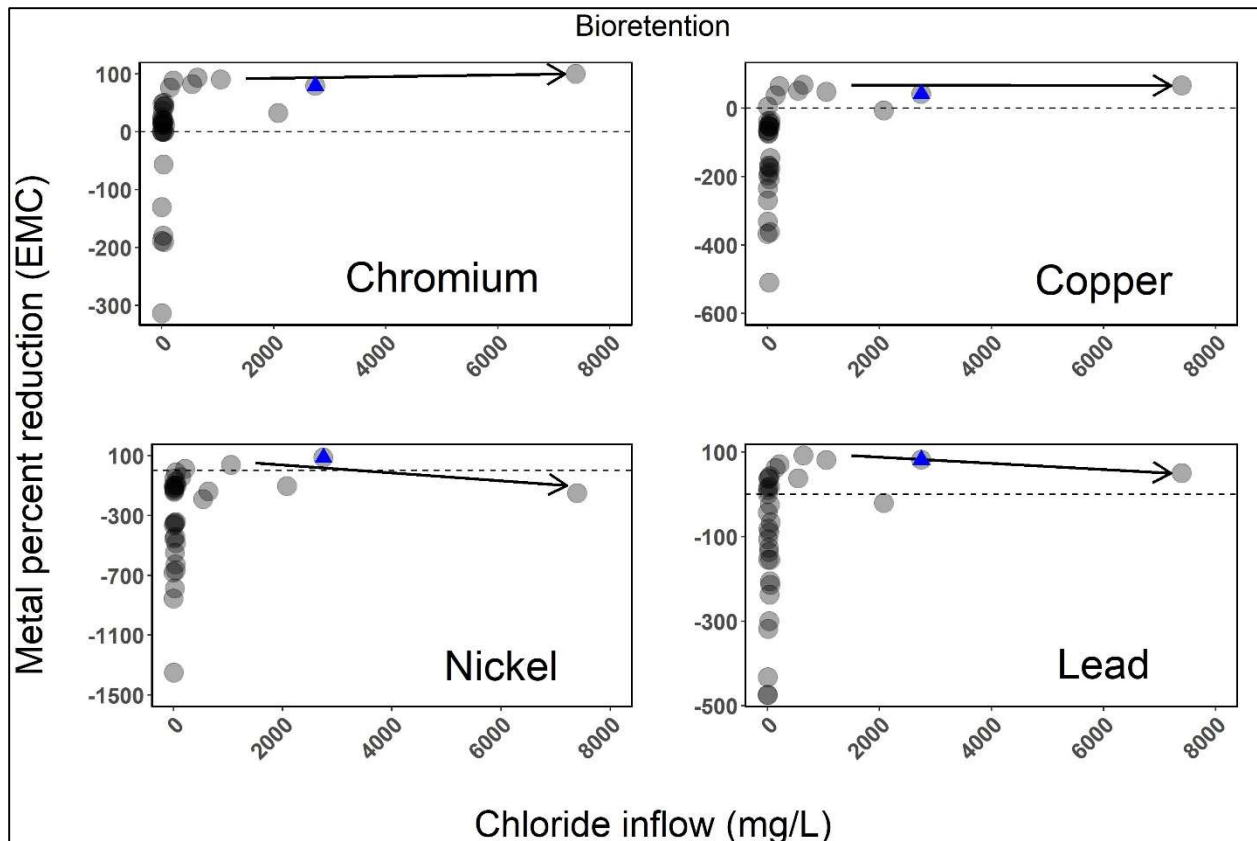


Figure 3.2. Bioretention metal (chromium, copper, nickel, lead) EMC % reductions with respect to chloride inflow concentrations. Overlaid triangle indicates grab sample at outlet (February 20, 2019). Data points are partially transparent such that darker circles indicate overlapping data points. Arrows are for visual reference only.

Results of the intra-event linear regression analyses using inflow and outflow concentrations of sodium, chloride, DOC, and TSS as the explanatory variables and the outflow concentrations and EMC reductions of the metals as the response variables are in Table 3.2. The DOC and TSS inflow levels were significantly positively correlated with outflow metal levels though there was no correlation with metal EMC reduction. DOC and TSS outflow concentrations were also significantly correlated with metal outflow concentrations. No correlation was found between salt inflow and DOC or TSS concentration outflow.

Table 3.2. Linear regression analysis results of slope and (P-value, R²) with salts, DOC, and TSS as the explanatory variables and outflow concentration and EMC reduction as the response variables at the bioretention. Dash (-) indicates no significance.

		Bioretention Inflow EMC (mg/L)				Bioretention Outflow EMC (mg/L)			
		Na	Cl	DOC	TSS	Na	Cl	DOC	TSS
Outflow EMC (ug/L)	Cr	-0.003 (.045, 0.1)	-0.002 (.0497, 0.1)	0.13 (.02, 0.2)	0.01 (.02, 0.2)	-	-	0.14 (2E-3, 0.3)	0.08 (4E-8, 0.7)
	Ni	-	-	0.3 (.01, 0.2)	0.02 (1E-3, 0.4)	-	-	0.22 (.02, 0.1)	0.15 (2E-5, 0.5)
	Cu	-0.046 (.04, 0.1)	-0.03 (.047, 0.1)	2.3 (4E-3, 0.3)	0.11 (.01, 0.2)	-	-	2.2 (6E-4, 0.3)	1.2 (4E-8, 0.7)
	Pb	-0.01 (.03, 0.1)	-0.005 (.03, 0.1)	.28 (.04, 0.1)	-	-	-	0.32 (4E-4, 0.2)	0.18 (1E-5, 0.5)
% EMC Reduction	Cr	0.25 (.02, 0.1)	0.14 (.03, 0.1)	-	-	-	-	-	5.3 (2E-5, 0.5)
	Ni	-	-	-	-	-	-	-36 (.01, 0.2)	-23 (7E-7, 0.6)
	Cu	0.48 (.02, 0.1)	0.27 (.02, 0.1)	-	-	0.40 (.04, 0.1)	0.19 (.03, 0.1)	-13.1 (.03, 0.2)	-9.8 (8E-6, 0.5)
	Pb	0.5 (.02, 0.1)	0.28 (.03, 0.1)	-	-	0.46 (.03, 0.1)	0.21 (.03, 0.1)	-15.4 (.02, 0.2)	-9.9 (1E-4, 0.5)

3.4.3 Bioswale Stormwater

Inflow and outflow of the BS were monitored for 20 events during the study period and are summarized in Table 3.1 with full data in Appendix G. The total rain depth of these events was 812 mm with individual events ranging from 14 mm to 104 mm. Monitoring occurred in all seasons and the average temperature was 13 ± 8.5° C with a range of 1.1 – 27° C. Shown in Fig. 3.3 is the metal EMC reduction plotted with respect to chloride inflow concentration of the BS. Of the four metals, nickel and copper are exported most frequently (negative reductions), followed by lead and chromium. Like the BR, the majority of events exported metals even in the lowest chloride concentrations. The arrows in Fig. 3.3 indicate a visual trend with no statistical significance.

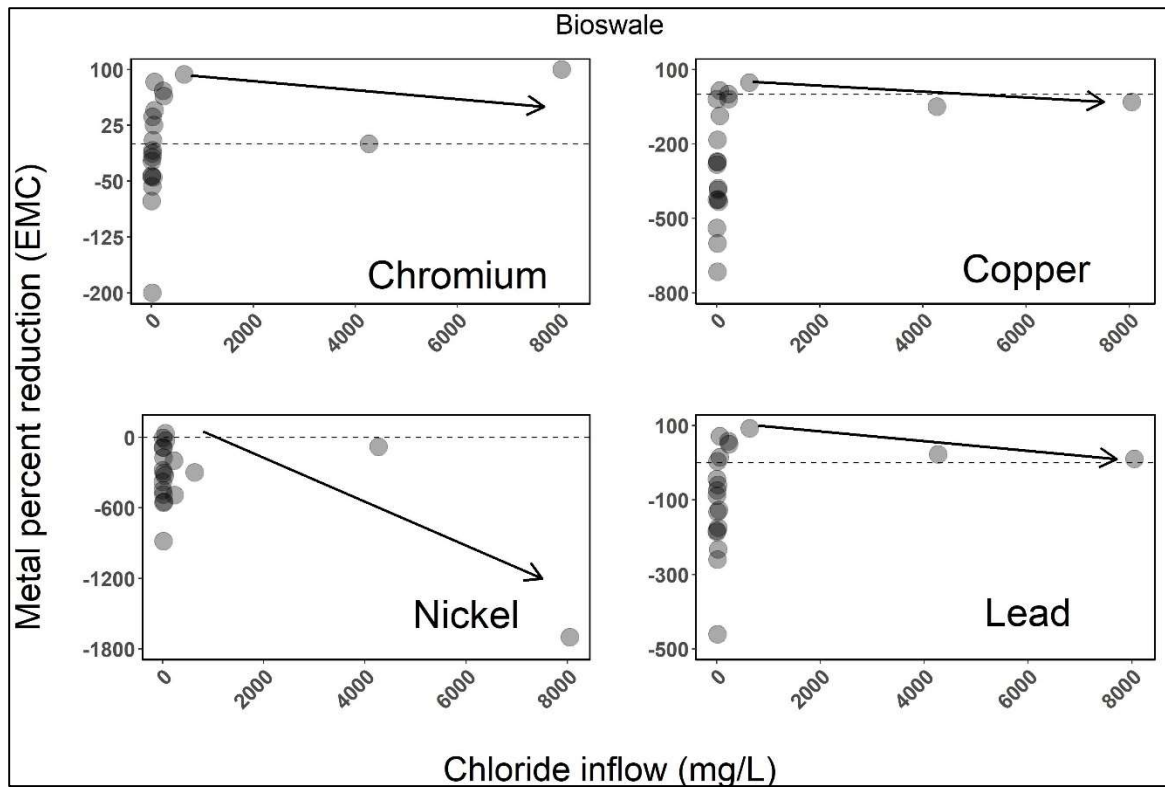


Figure 3.3. Bioswale metal (chromium, copper, nickel, lead) EMC % reductions with respect to chloride inflow concentrations. Data points are partially transparent such that darker circles indicate overlapping data points. Arrows are for visual reference only.

There were no significant correlations between the salt flowing into the BS and outflow metals or with EMC reductions, as summarized in Table 3.2. Only the DOC inflow EMC had significance with metal outflow EMC and this was only for nickel ($P = .001$, $m = 728$). Copper and lead outflow concentrations were significantly inversely correlated with outflow concentrations of sodium and chloride and the EMC reductions of the metals were positively correlated with the salt outflow concentrations. Copper and lead outflow EMC and EMC reductions were positively and inversely (respectively) correlated with DOC outflow concentrations (Table 3.2). No significant correlations were found between salt inflow and DOC and TSS outflow. There were significant positive correlations between inflow metal concentrations and their corresponding EMC reductions for chromium, copper, and nickel (omitting the -1700%), but not for lead (Appendix H).

Table 3.3. Linear regression analysis results of slope and (P-value, R²) with salts, DOC, and TSS as the explanatory variables and outflow concentration and EMC reduction as the response variables at the bioswale.

		Bioswale Inflow EMC				Bioswale Outflow EMC			
		Na	Cl	DOC	TSS	Na	Cl	DOC	TSS
Outflow EMC	Cr	-	-	-	-	-	-	-	-
	Ni	-	-	0.73 (1E-3, 0.2)	-	-	-	-	-
	Cu	-	-	-	-	-0.04 (.02, 0.2)	-0.02 (.02, 0.2)	3.3 (5E-5, 0.7)	-
	Pb	-	-	-	-	-0.01 (.03, 0.2)	-0.004 (.02, 0.2)	0.83 (4E-4, 0.6)	-
% EMC Reduction	Cr	-	-	-	-	0.13 (.049, 0.2)	-	-	-
	Ni	-	-	-	-	-	-	-	-
	Cu	-	-	-	-	0.49 (.02, 0.2)	0.22 (.02, 0.2)	-34 (2E-3, 0.5)	-
	Pb	-	-	-	-	0.29 (.02, 0.3)	0.13 (.03, 0.3)	-19 (.01, 0.4)	-

3.4.4 Compost-Amended Grass Channel Stormwater

The CAGC was monitored in all seasons for inflow and outflow in 22 events over the monitoring period as summarized in Table 3.1 with full data in Appendix G. The average temperature of these reported events was $14 \pm 8.5^\circ \text{C}$ with a range of $1.1 - 27^\circ \text{C}$ and total rainfall depth of 829 mm (range of 7.4 – 105 mm). The plots showing metal EMC reduction with respect to chloride inflow concentration at the CAGC are in Fig. 3.4. Linear regression analyses indicated no significant correlation between inflow and outflow salts, DOC, and TSS and outflow metals or EMC reductions of metals except that chloride was positively correlated with copper reduction ($P = .047$, $m = 290$). There were no significant linear correlations between chloride or sodium flowing into the CAGC and DOC or TSS flowing out. But the

inflow metal concentrations were all significantly correlated with their EMC reductions to varying degrees (Appendix H). The arrows in Fig. 3.4 indicate a visual trend with no statistical significance.

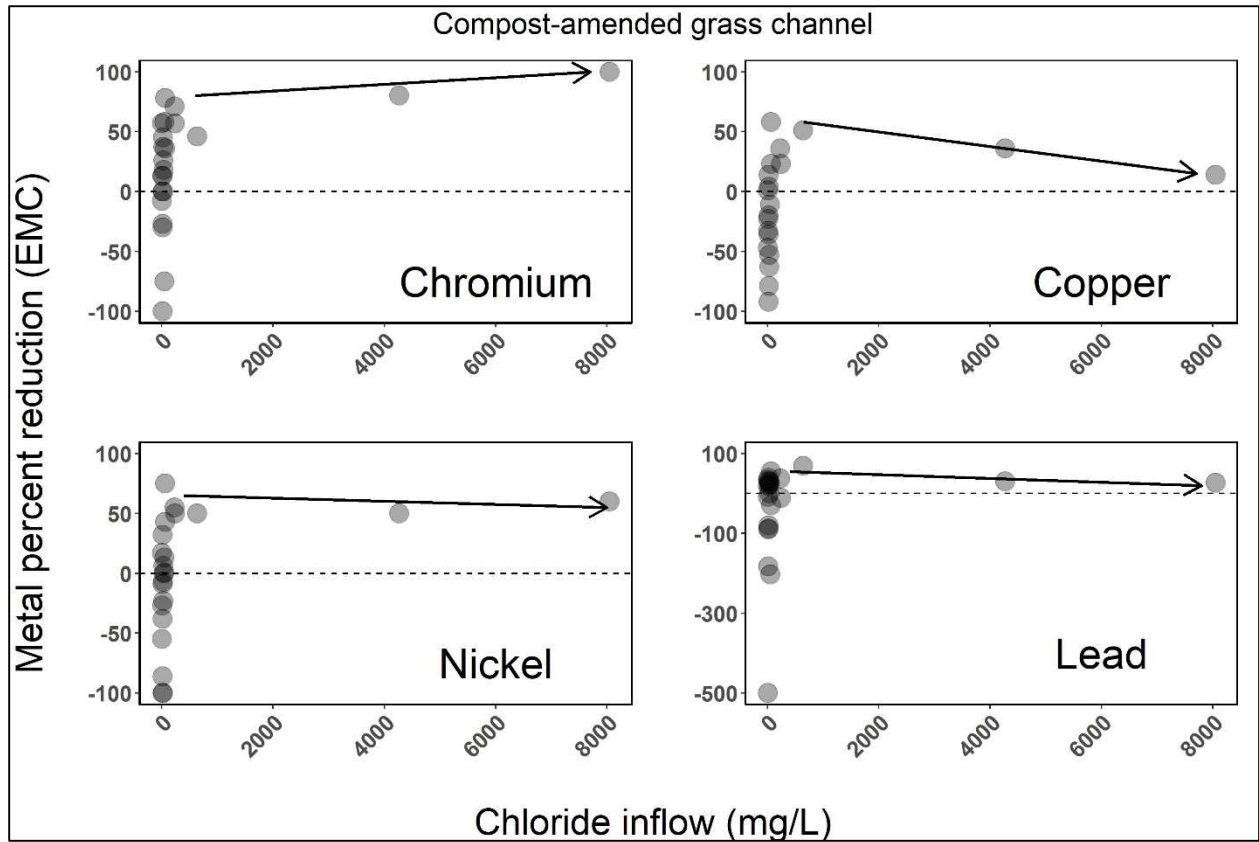


Figure 3.4. Compost-amended grass channel metal (chromium, copper, nickel, lead) EMC % reductions with respect to chloride inflow concentrations. Data points are partially transparent such that darker circles indicate overlapping data points. Arrows are for visual reference only.

3.4.5 Grass Channel Stormwater

Inflow and outflow were monitored for 21 events spanning all seasons at the GC, as summarized in Table 3.1 with full data in Appendix G. Average temperature of these events was $13 \pm 7.7^\circ \text{C}$ and ranged from 2.1°C to 27°C and the total rain depth was 904 mm with individual events ranging from 14 mm to 104 mm. Fig. 3.5 shows metal EMC reduction with respect to chloride inflow concentration in all of the events fully monitored at the GC. Sodium and chloride inflow concentrations had no correlations with metal outflow concentrations or EMC reductions during these 21 events. However, copper and lead EMC reductions were both significantly positively correlated with TSS inflow concentration ($P = .01$ and

.04, respectively). There were no significant correlations between inflow salts and outflow DOC or TSS, but the inflow metals were significantly positively correlated with their respective EMC reductions (Appendix H). The arrows in Fig. 3.5 indicate a visual trend with no statistical significance.

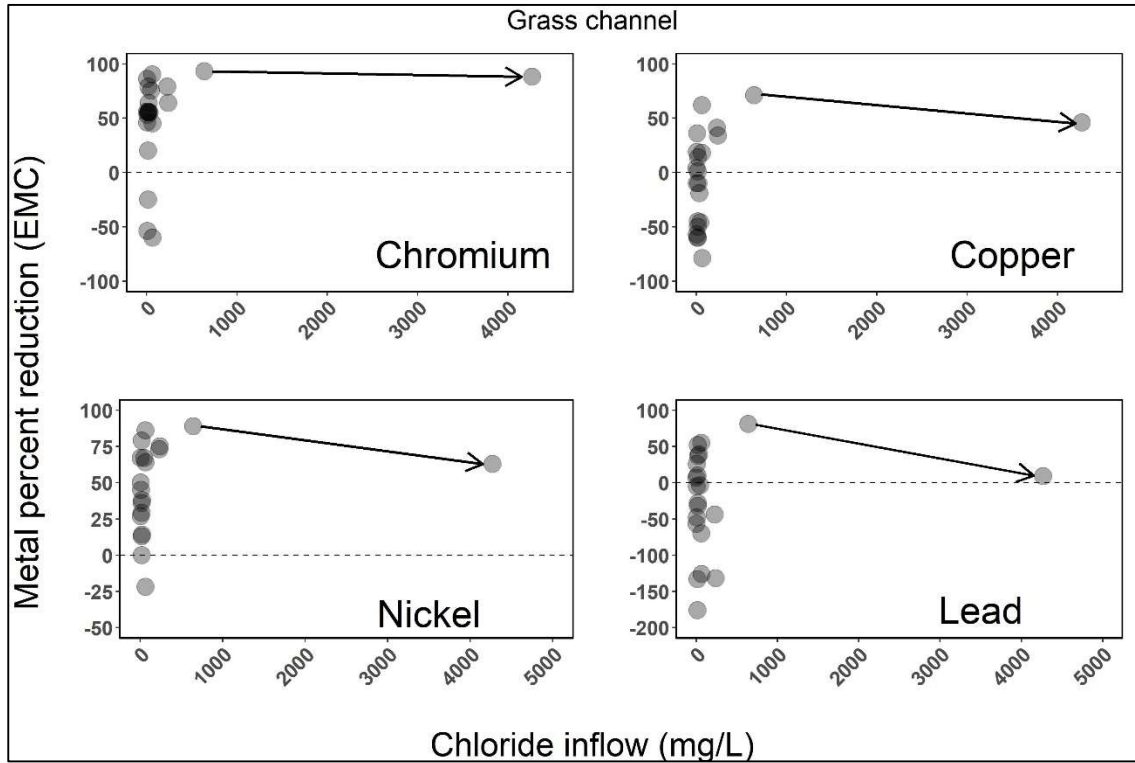


Figure 3.5. Grass channel metal (chromium, copper, nickel, lead) EMC % reductions with respect to chloride inflow concentrations. Data points are partially transparent such that darker circles indicate overlapping data points. Arrows are for visual reference only.

3.4.6 Partition Test Results

The results of the partition test are given in Fig. 3.6. The x-axis gives chloride content of the inflow sample and the y-axis gives the ratio of metal contents of that same sample for the two methods of preparation (partition fraction): F-A (filter followed by acidification) to A-F (acidification followed by filtering). There were no trends in ratios with respect to salt inflow. At the lowest chloride values, the ratios ranged widely with the nickel and lead reaching up to 30 and 7, respectively (not shown), while copper was evenly spread up to 0.6 and chromium up to 1, though most of the chromium ratios were

below 0.5. The two outlying points in nickel and lead with ratios of 30 and 7, respectively, are attributed to instrument or human error because a ratio greater than one is not possible.

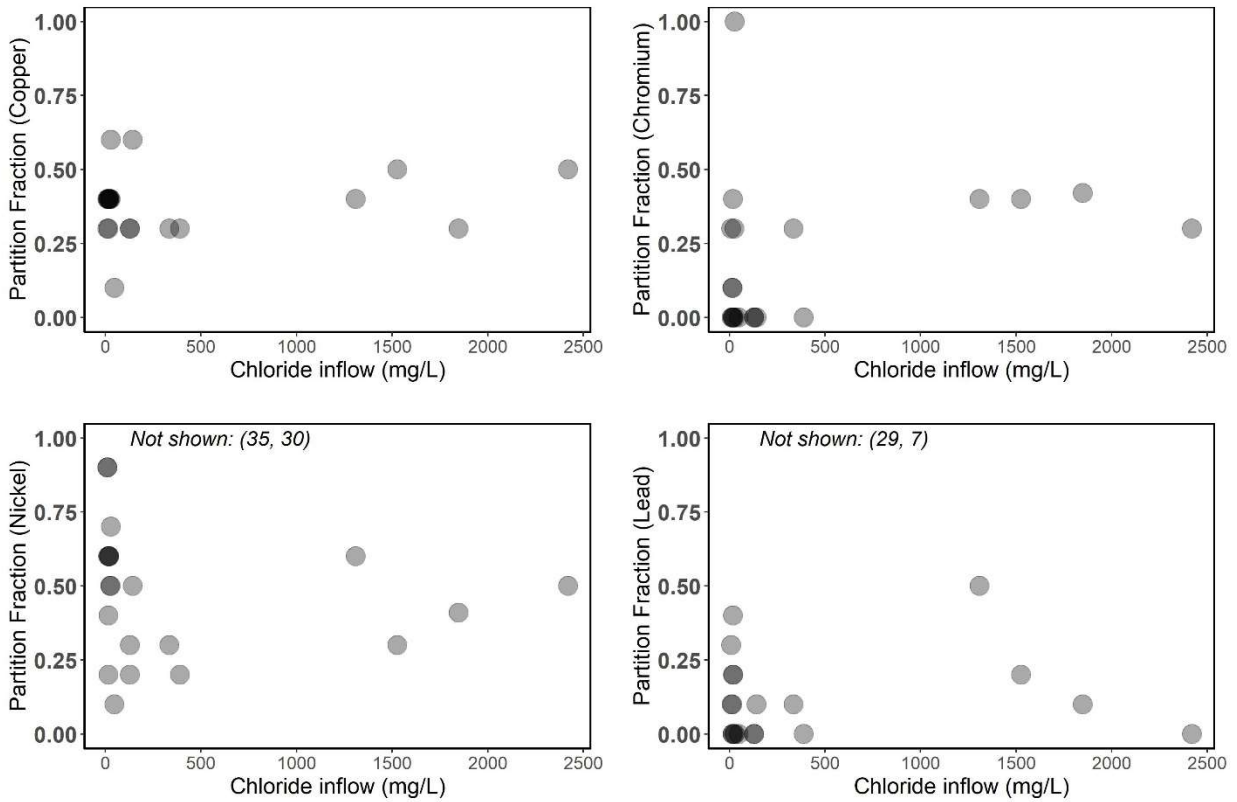


Figure 3.6. Partition test results with chloride inflow EMC on the x-axis and the Partition Fraction on the y-axis. Data points are partially transparent such that darker circles indicate overlapping data points.

3.4.7 Winter 2019 – 2020 Soil Salt Contents

Soil contents of salts and metals as well as pH, cation exchange capacity, organic content, and sodium adsorption ratios are summarized in Appendix I. The soil pH values were acidic overall (5.8 ± 0.6) and ranged from 4.6 to 6.7 while the average organic content was $5.3 \pm 3.2\%$. Specifically, the average pH and organic content in the 2019-Oct sampling for the BR, BS, CAGC, and GC were 6.0 ± 0.5 and $3.0\% \pm 0.6$, 5.7 ± 0.7 and $5.8\% \pm 3.3\%$, 6.1 ± 0.8 and $6.4\% \pm 1.4\%$, 5.6 ± 0.4 and $4.2\% \pm 0.5\%$. The values for the 2020-Mar sampling were 5.9 ± 0.3 and $3.0\% \pm 0.5\%$, 5.7 ± 0.6 and $6.0\% \pm 3.8\%$, 6.2 ± 0.4 and $9.0\% \pm 4.3\%$, 5.1 ± 0.3 and $4.6\% \pm 1.0\%$. While pH and sodium contents were significantly positively correlated when including all GI soils ($P = .01$), there were no statistically significant changes in pH or organic

content over the course of the winter. The chloride and sodium contents of the soils of the four GI systems are shown in Fig. 3.7 with the red bars (left) representing the pre-winter samples and the blue bars (right) representing the post-winter samples. The results are split into top soil and subsurface chloride contents with the same for sodium contents. The numbers in parentheses above the tallest columns indicate the height of the error bar which is not shown in order to allow the smaller bars to be more easily seen. The dashed lines on the BR and BS columns represent the stock ESM sample reported by Burgis et al. (2020) which gives initial concentrations of chloride at 3.2 mg/kg and sodium at 7.0 mg/kg.

The average sodium content of the swales (82 mg/kg) was lower than that of the BR (395 mg/kg). There was no significant addition or removal of sodium or chloride to the BR or BS soils over the 2019 – 2020 winter period. But, the CAGC and GC significantly decreased in chloride when considering both their top soil and sub-surface samples together ($P = .09, .02$). The GC also significantly gained sodium in its total soil content ($P = .03$), though its initial and final levels (18 – 27 mg/kg) were low compared to the other GI systems. There were no significant changes in CEC or SAR values in any single GI system over the course of the winter.

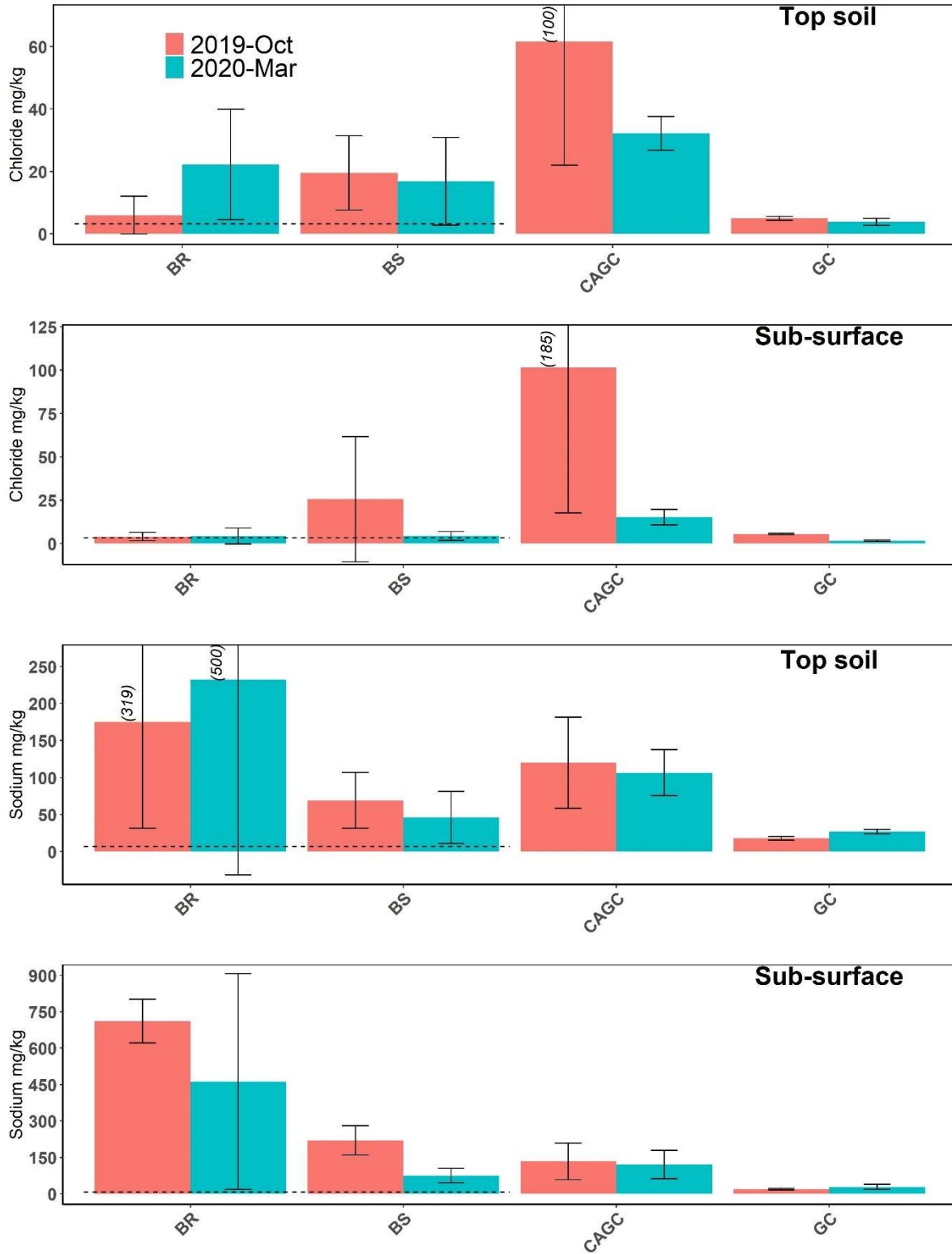


Figure 3.7. Chloride and sodium content of GI soils in the top soil and sub-surface, split between Oct-2019 (red) and 2020-Mar (blue).

3.4.8 Winter 2019 – 2020 Soil and Mulch Metal Contents

The total metal content of the mulch at the BR is shown in Fig. 3.8 in pairs such that pre-winter is in red (left) and post-winter is in blue (right). For each of the measured metals, the mulch metal content for all four metals decreased significantly ($P < .05$) over the winter period. Over the 2019 – 2020 winter, average concentrations of chromium dropped 75%, copper dropped 56%, nickel dropped 55%, and lead dropped 18%.

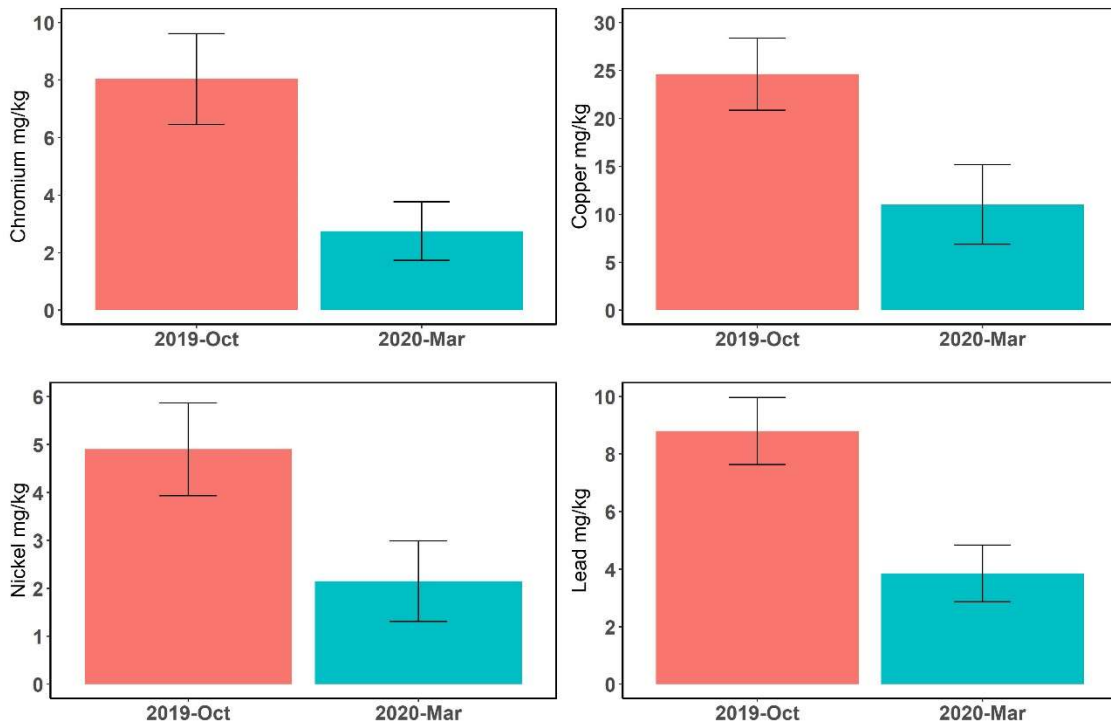


Figure 3.8. Metal content of bioretention mulch in pre-winter and post-winter samples with error bars showing one standard deviation.

Fig. 3.9 and Fig. 3.10 show the metal levels in the soil samples in the pre-winter and the post-winter samples for the top soil and sub-surface samples, respectively. The dashed lines in Fig. 3.9 represent stock or early samples as reference for changes in soil metal content over the life of the GI systems. The initial copper value (86 mg/kg) for the ESM of the BR and BS is too high to show without making the rest of the plot illegible. The line above the CAGC bars is strictly for the compost amendment, not the total

soil content, so the true content of the initial CAGC soil is lower for most metals as it is a combination of the compost and native soils.

In the top soil of the BR and all soils of the CAGC, chromium increased significantly over the season ($P = .04, .01$, respectively). The BS top soil increased in chromium as well during this time and the GC decreased slightly, but neither were significant. The BR also saw a significant increase in lead in both soil depths ($P = .06$) while the CAGC saw a significant increase in copper ($P = .09$). The BR and BS had the highest contents of nickel (8.4 – 12, 6.2 – 9.3 mg/kg) and copper (46 – 65 mg/kg, 32 – 45 mg/kg) of the GI systems and the GC was relatively high in lead content (22 – 44 mg/kg). Linear regression analyses on the soil qualities and metals contents of the soils were performed, but there were no significant correlations between sodium and the metal contents of the soils or the pH or organic contents.

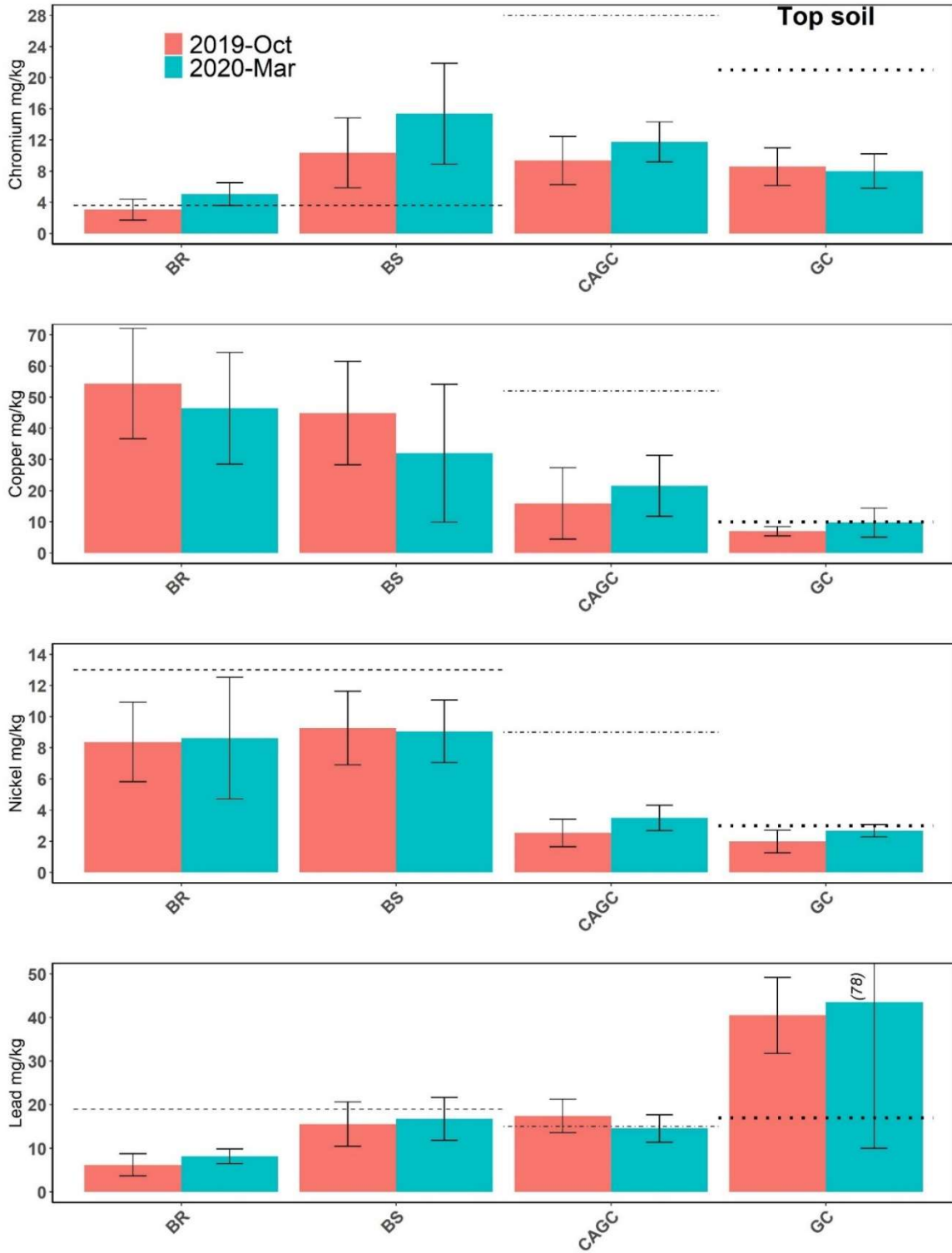


Figure 3.9. Metal content of the top soils of the GI systems, split between Oct-2019 (pink) and 2020-Mar (teal). Dotted lines are historic data (Copper not shown, 86 mg/kg).

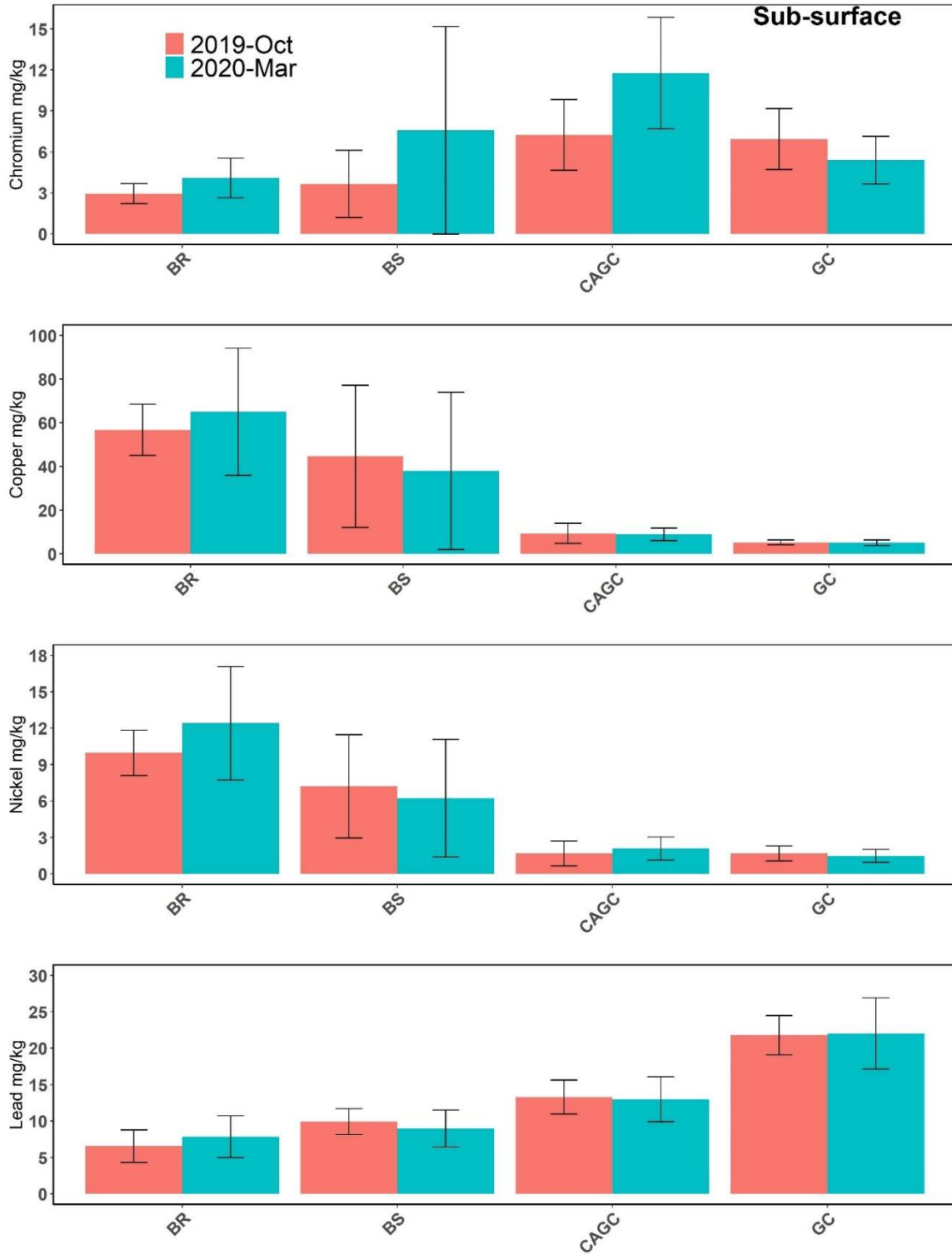


Figure 3.10. Metal content of the top soils of the GI systems, split between Oct-2019 (red) and 2020-Mar (blue).

3.4.9 Bioretention Groundwater

Well depths, salt, and metal contents are provided in Appendix F and their locations around and inside the BR system are shown in Fig. 3.1. Fig. 3.11 shows the chloride content of the groundwater in the vicinity of the BR from late 2018 and spring of 2019 through the autumn of 2020. The gap between 2020-January and 2020-May is due to the sampling interruption resulting from COVID-19 restrictions. Well A and its deeper neighbor, Well A2, are located next to each other near the bypass of the BR. These two wells showed a surge in 2019-Nov in chloride levels from 1115 mg/L and 903 mg/L, to 4503 mg/L and 2922 mg/L, respectively. The other wells also show immediate and dampened responses but are in some cases delayed. In these other wells at this same 2019-Nov sampling time, chloride concentrations range from 167 mg/L to 486 mg/L.

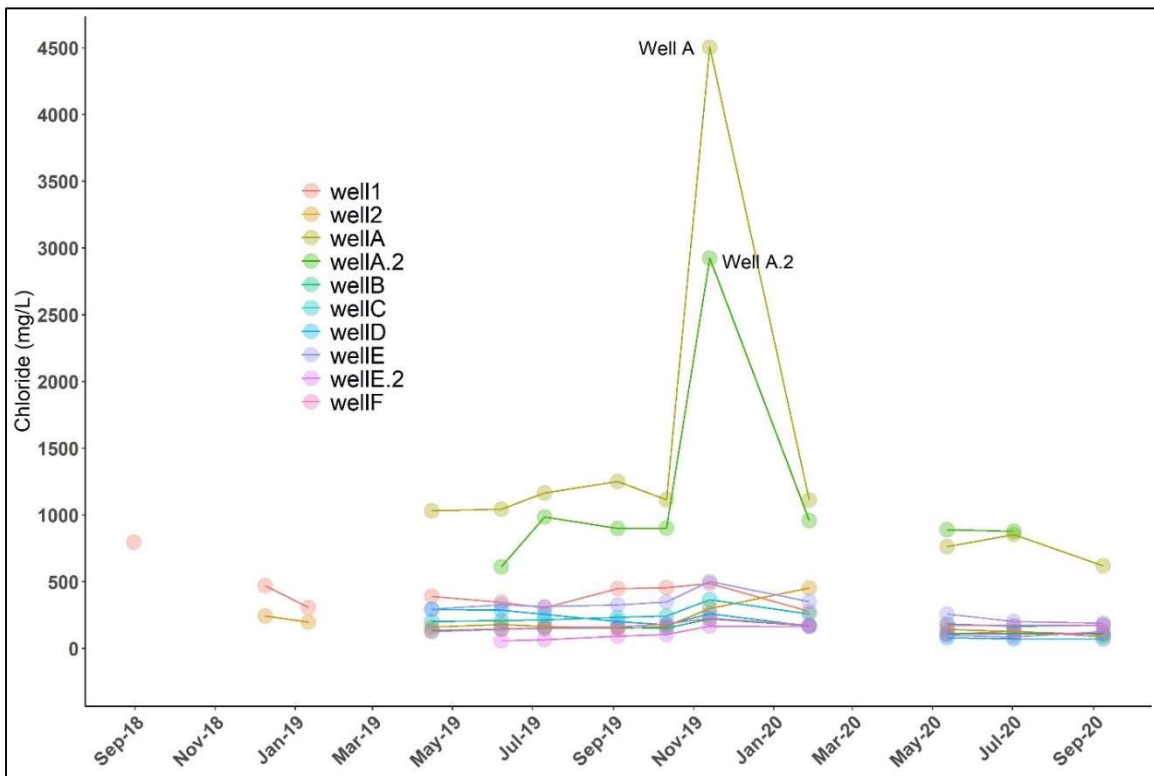


Figure 3.11. Chloride contents of wells at the bioretention.

Shown in Fig. 3.12 are the metal contents of the groundwater wells. The wide range of initial concentrations in Fig. 3.12 are attributed to contamination from the well installation procedure (such as

residue from drill wear and tear) as the concentrations drop quickly in the ensuing months. In Fig. 3.12, the dashed line represents the sampling session where elevated chloride levels were detected in 2019-Nov. The same gap which appeared in Fig. 3.11 is also in Fig. 3.12 due to the monitoring interruptions. Most of the wells increase from 2019-Nov to 2020-Jan in copper and chromium levels. Well 1 has a distinct peak in both copper and chromium for the 2019-Nov sampling session. Lead also showed distinct responses around the 2019-Nov sampling session through peaks in Well 1 and Well 2. Early sampling of Well 2 in 2018-Oct gave a concentration of over 300 mg/L, but the graph is unable to show this value while keeping the other values visible.

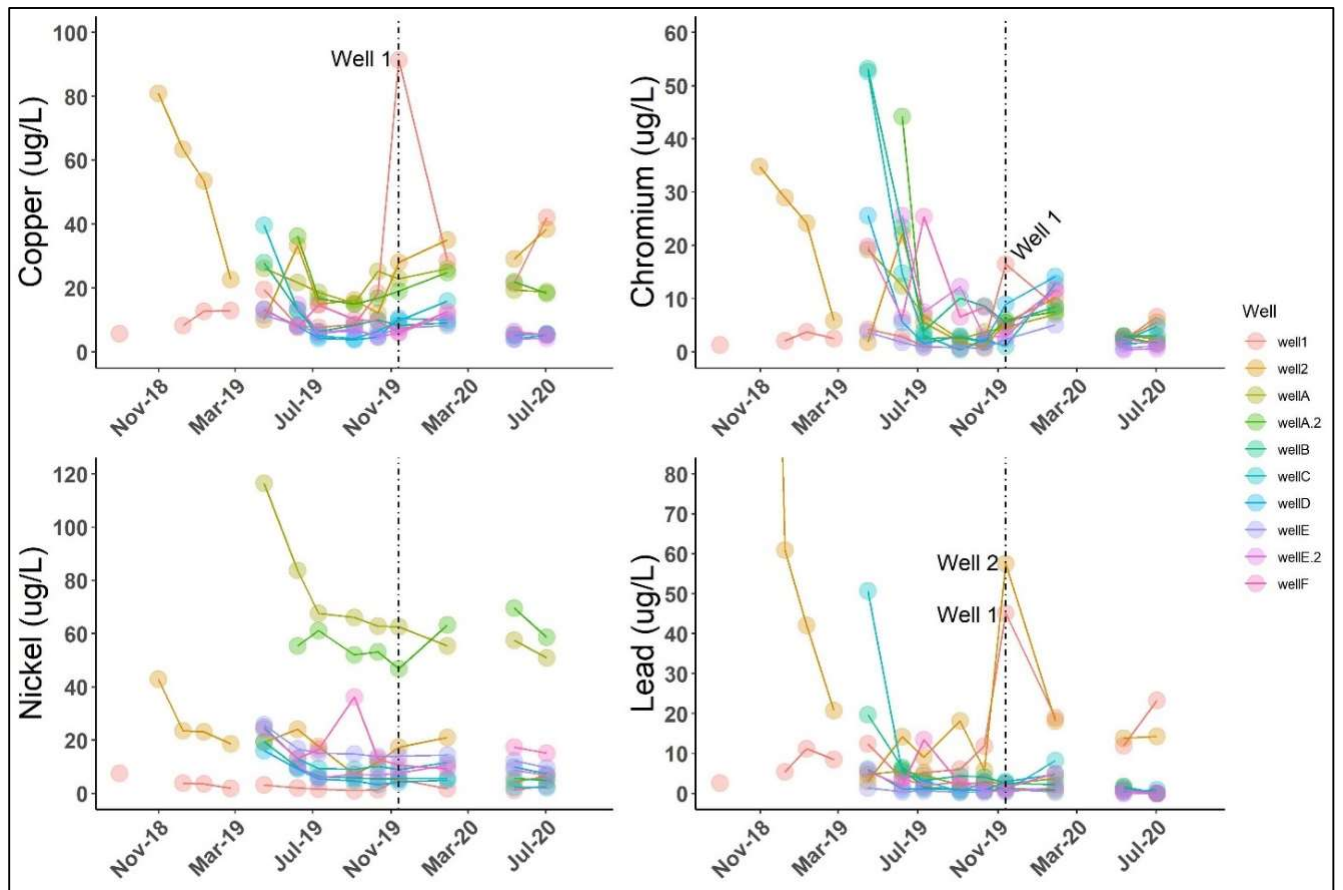


Figure 3.12. Metal content of the wells at the bioretention.

3.5 DISCUSSION

3.5.1 Intra-Event Stormwater Metal Mobilization

The metal concentrations in the road runoff entering the Lorton Road GI systems were often low relative to other similar studies. For example, copper measurements in Ernst et al. (2016), Sjøberg et al. (2017), Henderson et al. (2016), and Maniquiz-Redillas and Kim (2016) were 36.0 µg/L, 149 µg/L, 38.1, µg/L, and 695 µg/L, respectively, while this present study had a mean of 10 µg/L. Lead measurements ranged from 7.9 µg/L to 400 µg/L in Chapman and Horner (2010), Sjøberg et al. (2017), Henderson et al. (2016), Maniquiz-Redillas and Kim (2016) compared to the average of 3.0 µg/L in this study. Chromium measurements ranged from 9.4 to 240 µg/L in Henderson et al. (2016) and Maniquiz-Redillas and Kim (2016) compared to 1.8 µg/L in this study. Nickel measurements reported in Maniquiz-Redillas and Kim (2016) were 110 – 200 µg/L, compared to 1.2 µg/L in this study. The low concentrations of the Lorton Road runoff are attributed for the frequently negative EMC reductions in the intra-event analyses. Maniquiz-Redillas and Kim (2016) found a similar situation in their study with low initial concentrations resulting in lower reductions by the GI systems. The determination of irreducible concentrations was not in the scope of this research, but it is probable that the inflow concentrations on Lorton Road were often close to these limits or the preexisting concentrations of the GI soils. In spite of the large negative reductions in concentration and assisted by the small starting concentrations, outflow values of metals from the GI systems were usually within water quality criteria and did not consistently threaten the receiving waters (TSDR 2015a; 2015b; 2015c; 2015d).

Linear regression analyses showed correlations between the metals and the inflow levels of sodium and chloride, but not in the manner hypothesized; increased levels of salt inflow were significantly correlated with lower concentrations of metals in the outflow and increased EMC reductions. Because of this, the hypothesis that the concentration of inflow chloride is positively correlated with the outflow metal concentrations and inversely correlated with the metal EMC reductions is not supported. The regression analyses were dominated by the lowest concentrations of chloride, though. Examining the highest chloride inflow concentrations in Fig. 3.2, Fig. 3.3, Fig. 3.4, and Fig. 3.5 does show a slight,

though minimal, negative trend in some of the metal reductions, represented by the black arrows. This finding would be in agreement with column and mesocosm studies by Sjøberg et al. (2017), Valtanen et al. (2017), and Amrhein et al. (1992), wherein the intrusion of salty water (> 2000 mg/L) did cause a release of metals from their soil columns, but there is insufficient data to draw any statistical conclusions. Of the four metals and in all GI systems, chromium decreased the least in EMC reduction at the highest chloride levels. At the BR, the chromium inflow concentration for this particular event with high chloride was 2.8 µg/L while at the BS and CAGC, it was 0.24 µg/L. This means that in spite of the variable concentrations flowing in (at possible irreducible concentrations) and the very high chloride in the runoff, the evidence that chromium is mobilized by the road salt within a single event is minimal. Besides chromium, the metals do have a negative or zero slope in EMC reduction from the lower chloride values to the highest values. Regardless of this potential trend, though, the EMC reductions that are associated with the highest chloride values are typically no more negative than those that occur with the lowest chloride values. With the exception of the nickel results at the BS, all of the EMC reductions at these highest values are within the average of the total dataset for that GI. Therefore, if high road salt concentrations are associated with the negative trends seen in Fig. 3.2, Fig. 3.3, Fig. 3.4, and Fig. 3.5, the outcome is average metal reductions seen in much lower chloride conditions.

In addition to direct mobilization of metals through cation exchange (with sodium) and the formation of chlorocomplexes, there is concern with sodium displacing organic content of soils and therefore increasing the probability of metal mobilization (Nelson et al. 2009; Schuler and Relyea 2018). The links between DOC and TSS and metal content were demonstrated at all GI systems except for the CAGC, but most often at the BR. For example, the BR had increases of up to 2.3 µg/L of copper for every 1 mg/L increase of DOC at the BR outflow and a 23% increase in EMC of nickel with 1 mg/L increase of TSS at the outflow. Maniquiz-Redillas and Kim (2016) and Chapman and Horner (2010) also found such significant correlations between metal content and organic content and TSS. Even though the DOC and

TSS were demonstrably positively correlated with metal outflow, the salt inflow concentrations were apparently never large enough to directly impact the DOC or TSS concentrations. This lack of correlation means that an indirect mobilization of metals through sodium mobilizing DOC and TSS was not supported.

Factors that were correlated with metal EMC reductions in each GI system were inflow metal concentration and the inflow and outflow concentrations of DOC and TSS. In a climate such as the one at Lorton, it would appear that a more pressing challenge for mediating metals within rain events would be to address these factors. The first such factor, however, of having too clean of inflow and thus irreducible concentrations will likely not be addressed with conventional GI that uses minimally enhanced soils. For example, soil amendments such as iron oxide and bone meal that have been shown to satisfactorily adsorb metals out of runoff could be a good alternative (Ernst et al. 2016). The ESM used at the BR and BS, on the other hand, is primarily inert sand with a compost additive (Chapter 2). The second factor, of outflowing DOC and TSS, would require more effective physical capture and longer holding times for settling of particles. While metals complexed to organic content have relatively low bioavailability and are not considered ecologically harmful (Amrhein et al. 1992), their mobility decreases the total metal mitigation effectiveness of the GI system.

The inflow salt concentration appeared to have minimal effect on metal mobilization on the event-scale, but it also had minimal effect on the scale of the individual sample as seen in the partition test (Fig. 3.6). It was hypothesized that the high salt content (i.e., sodium) would displace more metals from the suspended solids through cation exchange, leaving more metals in solution, but this was not supported. For chromium, copper, and lead, the lower partition fractions primarily less than 0.5 showed that the metal content of any sample no matter the salt level was mostly associated with particulates greater than 0.45 μm (the filter size) while nickel was more evenly distributed. Lead had the lowest fractions, even at the highest chloride levels, which is consistent with Norrström and Jacks (1998) which

identified it as an immobile metal but contrary to Jayarathne et al. (2020) which reported several studies wherein lead showed relatively high mobility compared to nickel and copper. As with the intra-event stormwater samples in this study, the metal content of the samples used in the partition test were likely too low to meaningfully interact with the sodium ions.

3.5.2 Metal Mobilization in Soil

The purpose of the 2019 – 2020 soil samples was to identify if loss of metal content could be correlated with accumulation of road salt. If sodium significantly increased in the soils over the winter period and metals likewise decreased, it could be evidence of displaced metals from the soil matrix that were released with stormflows as chlorocomplexes or other compounds which were not identified in this study. Additionally, when chloride washes out after deposition, whether it be immediately or later in the year, there is the possibility that it is forming chlorocomplexes with metals, increasing their mobility and possibly eventual bioavailability (Nelson et al. 2009). The winter of 2019 – 2020 was relatively mild with few events that might have required deicing salts, so the changes seen in the soils were small but expected.

At the BR, the average chloride levels of the top soil more than tripled (not significantly) during the winter season, but the subsurface showed little change, so no leaching of chloride was detectable between the two depths over that time period (Fig. 3.7). While the top soil of the BR also increased in sodium content over the 2019 – 2020 winter, these were not statistically significant either. The subsurface of the BR had much higher sodium content than the surface (almost 600 mg/kg vs 200 mg/kg), indicating a long-term leaching of sodium downward from the surface. Additionally, the SAR values of the BR sub-surface soils were larger than those of the top soils, giving further evidence of the leaching of sodium downward. However, the insignificant increase of sodium over the winter period is limited evidence that it leached in any meaningful amount over this particular winter season. The apparent addition of sodium and chloride to the BR soils indicates that there were road salts applied to

the CDA of the BR over the winter and that they did flow into the BR basin. The chloride was deposited in the basin from the stormflows and because of chloride's conservative nature, it is predicted to return to approximately 2019-Oct levels by the beginning of the 2020 – 2021 winter season after being washed out by the spring, summer, and autumn stormflows. This washout was shown to occur at this site by Burgis et al. (2020). The sodium is not expected to wash out in large amounts, though, also as demonstrated by Burgis et al. (2020). Comparing recent levels of sodium to the original level shows a large increase in sodium stored in the ESM of the BR basin from the original ESM concentration of 7.0 mg/kg to over 260 mg/kg. The accumulation of sodium in the BR basin is much higher than the roadside soils tested in Zehetner et al. (2009), who found a maximum sodium value of almost 50 mg/kg. The difference between the Zehetner et al. (2009) study and the Lorton Road site is attributed to the intentional infiltration of stormwater in the basin as it receives large volumes of polluted runoff as opposed to the roadside soils which encounter the polluted runoff for a relatively short amount of time.

Contrary to the BR, each of the swales showed a decline in chloride content in varying significance in both the top soil and sub-surface. While there was no short-term accumulation of sodium over the winter, the ESM of the BS did show an accumulation of sodium compared to the stock sample taken at the time of the GI installation (similar to the BR). An important difference between the BR and the swales that dictates the salt accumulations are their CDA types and areas. The BR CDA consists of Lorton Road as well as a residential area with a total of over 4.5 hectares while the swale CDAs are each less than 1-hectare portions of Lorton Road immediately adjacent to the swales. Therefore, the possibility of the BR receiving more road salt than the swales is high.

The CAGC, while not gaining any salt, had relatively high levels of chloride before and after the winter season compared to all other systems. As-built documents of the compost quality initially used in the construction of the CAGC have no record of chloride or sodium content, but do report electrical conductivity of 4.2 dS/m. According to Gondek et al. (2020), compost electrical conductivity is

considered high when it passes 5 dS/m, so it is possible that the CAGC natural level of chloride might be this high due to its initial quality. While the chloride content of the compost may have been elevated, the compost was applied at a 16% rate by volume, so its salt content is diluted, though still apparently high. The loss of chloride over the winter season was not significant for the top soil and sub-surface of the CAGC individually, but was so when the two depths were combined. This same significance also occurred for the GC, but its levels were very low in both depths anyway. Loss of chloride indicates the potential of mobilized metals exiting the GI systems as chlorocomplexes, but none of the swales showed any positive correlations between outflow chloride and metal concentrations in the stormwater analyses.

While the evidence of road salt application in the soils points to small quantities overall, there is still some evidence of metal mobilization. Specifically, for each of the measured metals, the mulch at the BR decreased significantly ($P < .05$) over the winter period, a potential response of metal mobilization from deicing road salts. The decrease of metal content in the mulch could also have resulted from the natural process of mulch decomposition. Regular maintenance protocol for the site requires adding more mulch, but this did not occur until April of 2020, a month after these samples were collected. While the high organic content of mulch makes it ideal for capturing trace metals (Muthanna et al. 2007), these trends of losing metal content over the winter months indicates that it is an impermanent capture. Due to method constraints, the sodium content of the mulch was unable to be measured, but it is possible that the cation exchange of the high sodium inflows caused these decreases in metal contents in the mulch, especially with the increasing levels in the BR top soil. Mulch is a common and effective addition to GI, but if it is included as a means for increasing contaminant capture, it must be changed prior to the winter months to avoid the release of metals over the winter months. The harvesting of trace metals from GI mulch is suggested as a subject for future study.

In the GI soils, increases in several metal contents were measured over the 2019 – 2020 winter period and none of the metals significantly decreased. This result in addition to the limited salt build-up is insufficient evidence to support the hypothesis that the road salts mobilized a significant amount of metals from the GI soils. The increases in metal content are attributed to a combination of deposition from the runoff (though usually small) as well as the loss of metals from the mulch at the BR. These findings are contrary to Sjøberg et al. (2017), Norrström (2005), Li et al. (2015), and Nelson et al. (2009), who all demonstrated that road salt intrusion into their soil columns would displace metals and increase their mobility. However, these studies applied high concentrations of road salt more frequently than what was applied to Lorton Road during the 2019 – 2020 winter study period. Furthermore, this present study utilized entire GI systems with numerous environmental variations not included in the column studies. It is possible that the mobilization did occur at the Lorton GI systems, but there are enough other factors (such as scale of operation and soil type micro-changes) that the mobilization impact was not evident. Even though the stormwater data showed consistent export of metals, it was not enough to make a difference with the soil content over this winter period.

It is also interesting to note that the BR and BS had the highest contents of nickel and copper of the GI systems and were consistently releasing these metals in the stormwater outflows with respective average reductions of $-319 \pm 315\%$ and $-367 \pm 389\%$ for nickel and $-117 \pm 144\%$ and $-253 \pm 229\%$ for copper. The CAGC and GC, on the other hand, with their lower nickel and copper soil contents were reducing these elements with respective averages of $-51 \pm 234\%$ and $44 \pm 47\%$ for nickel and $-52 \pm 136\%$ and $-4.4 \pm 44\%$ for copper. The GC soils were also relatively high in lead content, but the GC was releasing less lead in the stormwater than the other samples. It is not known why the GC capacity for lead was relatively high, but the GC also has a relatively large footprint with respect to its CDA, so there is more opportunity for inflowing lead to be captured in this area than in the other GI systems, which ultimately results in less lead outflow.

Further investigations into patterns that may have predicted metal content with respect to salt in the soils over the winter were pursued. Specifically, linear regression analyses on the sodium and metal contents of the soils of each GI were performed, but there were no significant correlations overall. In the soils, it was hypothesized that sodium content would have been inversely correlated with metal content due to cation exchange, but this was not supported. There was also no evidence that the changes of pH correlated with sodium content impacted metal content either. Ultimately, there was little evidence that sodium displaced significant amounts of metals from these GI systems over the winter period.

Comparing the metal contents of the 2019 – 2020 winter to the historical values, it appears that the ESM of the BR and BS leached copper, nickel, and lead over the lifetimes of these GI systems as the levels in the recent samples are lower than the historical samples. The CAGC and GC also showed some evidence of leaching in chromium, copper, and nickel, but not lead. It is unclear when this leaching happened, though, and if it was a sudden drop in content or occurred over several years. There is no way to determine if these decreases in concentration are caused by road salt activity, but it at least supports that metals have been leaving the GI systems over time, potentially influencing the large negative EMC reductions seen in the stormwater data.

3.5.3 Transport to Groundwater

Salt from the stormflows was shown to be entering the groundwater in the vicinity of the BR within a month of a significant precipitation event with likely road salt application (Fig. 3.11). Between the sampling session in October and the high-chloride sampling session in November, Lorton Road saw three events of possible “wintry” conditions requiring de-icing salts; two of the events were each less than 2 mm, but the third event on 2019-Nov-1 was 25 mm. A similar event occurred in late 2020-Jan, but due to the COVID-19 sampling break, any surge in chloride in the groundwater was not captured. The intrusion of road salts into groundwater from stormwater has been shown to happen in Ramakrishna and Viraraghavan (2005) as well as a previous study at this site Burgis et al. (2020). The chloride in the

stormwater could be carrying metal chlorocomplexes or create chlorocomplexes in the groundwater, thus increasing mobilization of the metals. One well (Well B in Fig. 3.1) was placed upstream of the BR infiltration area and its levels remained low throughout the study period, indicating the effects seen in these wells resulted from stormwater infiltrating the BR forebay.

Evidence of metal mobilization in groundwater through the intrusion of dissociated road salt ions was hypothesized to be seen through the increased levels of metals in the presence of elevated salt content. The BR inflow would infiltrate the forebay and make its way to the shallow wells very easily. As it infiltrated with the road salt, it is possible that it either carried metals with the chloride or displaced metals through cation exchange as it infiltrated the soils to the groundwater. Such evidence of salts interacting with metals does appear to be present in the wells at the BR (Fig. 3.12), though the evidence is limited and insufficient to support the original hypothesis. Specifically, small increases in copper and chromium are seen in each well in the month following the chloride surge. This delayed increase indicates that there might have been a slower release of metals into the wells initiated by the chloride. Well 1 and Well 2 had surges in copper, chromium, and lead, but these wells were not particularly high in chloride concentration. Norrström (2005) showed that high quantities of lead were mobilized through colloid-assisted transport from soils when low electrolyte water flushed soils after high electrolyte water. Other studies (Novotny et al. 1998; Amrhein et al. 1992; McManus and Davis 2020) have shown similar phenomena where sudden changes in electrolyte content created surges in metals released. It is possible that this is being seen in the Lorton wells, but these fluctuations in metal content could also be a result of stormwater with relatively high metal contents infiltrating the soils with no relation to road salts. Ultimately, these findings are in agreement with Denich et al. (2013) who identified the risk of metal mobilization to groundwater by road salts as low.

3.6 CONCLUSION

This study examined trends in stormwater, soil, and groundwater for evidence of metal mobilization through road salt application in four individual GI systems: a bioretention, bioswale, compost-amended grass channel, and grass channel. In the stormwater, soil, and groundwater, there was little evidence that road salts mobilized a significant amount of metals on the scale of an entire GI system. Rather than the road salts, there was evidence that inflow concentrations of metals as well as DOC and TSS levels were more indicative of metal retention, even in the chloride concentration exceeding 8000 mg/L. The soil analyses were conducted over the 2019 – 2020 winter season, which was unusually mild and therefore required little application of road salt. The soils of the GI systems did show some evidence of accumulating sodium and chloride, but the soils did not show any significant release of metals. However, the mulch of the bioretention did significantly decrease in metal content over this period, which could have resulted from road salt application or the natural decomposition of the mulch. There was evidence of road salt surges in the groundwater, but minimal response in terms of metals release.

The Lorton field site will be active through the spring of 2022, so stormwater and groundwater monitoring will continue through that time. This additional sampling time will allow further analysis of metal mobilization in high-salt flows. Future work should increase frequency of groundwater sampling immediately after a winter event when road salts are applied to capture precise surges in both salts and metals.

3.7 REFERENCES

- Amrhein, Christopher, James E. Strong, and Paul A. Mosher. 1992. "Effect of Deicing Salts on Metal and Organic Matter Mobilization in Roadside Soils." *Environmental Science & Technology* 26: 703–9.
- ASTM. 2013. "Standard Test Methods for Loss on Ignition (LOI) of Solid Combustion Residues." D7348-13. 10.1520/D7348-13.
- Bäckström, Mattias, Stefan Karlsson, Lars Bäckman, Lennart Folkesson, and Bo Lind. 2004. "Mobilisation of Heavy Metals by Deicing Salts in a Roadside Environment." *Water Research* 38 (3): 720–32. <https://doi.org/10.1016/j.watres.2003.11.006>.
- Bauske, B., and D. Goetz. 1993. "Effects of Deicing-Salts on Heavy Metal Mobility." *Acta Hydrochimica et Hydrobiologica* 21 (1): 38–42. <https://doi.org/10.1002/aheh.19930210106>.
- Benjamin, Mark M. 2002. *Water Chemistry*. 1st ed. Long Grove: Waveland Press, Inc.
- Bolan, Nanthi, Anitha Kunhikrishnan, Ramya Thangarajan, Jurate Kumpiene, Jinhee Park, Tomoyuki Makino, Mary Beth Kirkham, and Kirk Scheckel. 2014. "Remediation of Heavy Metal(Loid)s

- Contaminated Soils – To Mobilize or to Immobilize?” *Journal of Hazardous Materials* 266 (February): 141–66. <https://doi.org/10.1016/j.jhazmat.2013.12.018>.
- Brown, Jeffrey N., and Barrie M. Peake. 2006. “Sources of Heavy Metals and Polycyclic Aromatic Hydrocarbons in Urban Stormwater Runoff.” *Science of The Total Environment* 359: 145–55.
- Burgis, Charles, Gail M. Hayes, Derek Henderson, Wuhuan Zhang, and James A. Smith. 2020. “Green Stormwater Infrastructure Buffers Surface Water from Deicing Salt Loading.” *Science of The Total Environment* 729: 138736. <https://doi.org/10.1016/j.scitotenv.2020.138736>.
- Chapman, Cameron, and Richard R. Horner. 2010. “Performance Assessment of a Street-Drainage Bioretention System.” *Water Environment Research* 82 (2): 109–19. <https://doi.org/10.2175/106143009X426112>.
- Chowdhury, Rezaul, and Mohamed M A Mohamed. 2018. “Removal of Heavy Metals in Vegetative Graywater Biofiltration Columns.” *J. Environ. Eng.*, 8.
- David, Nicole, Jon E. Leatherbarrow, Donald Yee, and Lester J. McKee. 2015. “Removal Efficiencies of a Bioretention System for Trace Metals, PCBs, PAHs, and Dioxins in a Semiarid Environment.” *Journal of Environmental Engineering* 141 (6): 04014092. [https://doi.org/10.1061/\(ASCE\)EE.1943-7870.0000921](https://doi.org/10.1061/(ASCE)EE.1943-7870.0000921).
- Davis, Allen P., Mohammad Shokouhian, Himanshu Sharma, Christie Minami, and Derek Winogradoff. 2003. “Water Quality Improvement through Bioretention: Lead, Copper, and Zinc Removal.” *Water Environment Research* 75 (1): 73–82.
- Denich, Chris, Andrea Bradford, and Jennifer Drake. 2013. “Bioretention: Assessing Effects of Winter Salt and Aggregate Application on Plant Health, Media Clogging and Effluent Quality.” *Water Quality Research Journal* 48 (4): 387–99. <https://doi.org/10.2166/wqrj.2013.065>.
- Ernst, Clayton, Lynn Katz, and Michael Barrett. 2016. “Removal of Dissolved Copper and Zinc from Highway Runoff via Adsorption.” *Journal of Sustainable Water in the Built Environment* 2 (1): 04015007. <https://doi.org/10.1061/JSWBAY.0000803>.
- Gondek, Matthew, David C. Weindorf, Carmen Thiel, and Greg Kleinheinz. 2020. “Soluble Salts in Compost and Their Effects on Soil and Plants: A Review.” *Compost Science & Utilization* 28 (2): 59–75. <https://doi.org/10.1080/1065657X.2020.1772906>.
- Henderson, Derek, James A. Smith, and George M. Fitch. 2016. “Impact of Vegetation Management on Vegetated Roadsides and Their Performance as a Low-Impact-Development Practice for Linear Transportation Infrastructure.” *Transportation Research Record*. <https://doi.org/10.3141/2588-19>.
- Jayarathne, Ayomi, Buddhi Wijesiri, Prasanna Egodawatta, Godwin A Ayoko, and Ashantha Goonetilleke. 2020. “Metals in the Urban Stormwater Environment.” In *Transformation Processes of Metals in Urban Road Dust*, by Ayomi Jayarathne, Buddhi Wijesiri, Prasanna Egodawatta, Godwin A Ayoko, and Ashantha Goonetilleke, 1–10. Singapore: Springer Singapore. https://doi.org/10.1007/978-981-15-2078-5_1.
- Jones, Philip Sumner, and Allen P. Davis. 2013. “Spatial Accumulation and Strength of Affiliation of Heavy Metals in Bioretention Media.” *Journal of Environmental Engineering* 139 (4): 479–87. [https://doi.org/10.1061/\(ASCE\)EE.1943-7870.0000624](https://doi.org/10.1061/(ASCE)EE.1943-7870.0000624).
- Knight, E.M.P., W.F. III Hunt, and R.J. Winston. 2013. “Side-by-Side Evaluation of Four Level Spreader-Vegetated Filter Strips and a Swale in Eastern North Carolina.” *Journal of Soil and Water Conservation* 68 (1): 60–72. <https://doi.org/10.2489/jswc.68.1.60>.
- Leroy, Marie-Charlotte, Florence Portet-Kotalo, Marc Legras, Franck Lederf, Vincent Moncond’huy, Isabelle Polaert, and Stéphane Marcotte. 2016. “Performance of Vegetated Swales for Improving Road Runoff Quality in a Moderate Traffic Urban Area.” *Science of The Total Environment* 566–567 (October): 113–21. <https://doi.org/10.1016/j.scitotenv.2016.05.027>.

- Li, Fayun, Ying Zhang, Zhiping Fan, and Kokyo Oh. 2015. "Accumulation of De-Icing Salts and Its Short-Term Effect on Metal Mobility in Urban Roadside Soils." *Bulletin of Environmental Contamination and Toxicology* 94 (4): 525–31.
- Li, Houng, and Allen P. Davis. 2008. "Heavy Metal Capture and Accumulation in Bioretention Media." *Environmental Science & Technology* 42 (14): 5247–53. <https://doi.org/10.1021/es702681j>.
- Link, Dirk D., Peter J. Walter, and H. M. Kingston. 1998. "Development and Validation of the New EPA Microwave-Assisted Leach Method 3051A." *Environmental Science & Technology* 32 (22): 3628–32. <https://doi.org/10.1021/es980559n>.
- Lloyd, Lewis N., G. Michael Fitch, Tony S. Singh, and James A. Smith. 2019. "Characterization of Environmental Pollutants in Sediment Collected during Street Sweeping Operations to Evaluate Its Potential for Reuse." *Journal of Environmental Engineering* 145 (2): 04018141. [https://doi.org/10.1061/\(ASCE\)EE.1943-7870.0001493](https://doi.org/10.1061/(ASCE)EE.1943-7870.0001493).
- Lwin, Chaw Su, Byoung-Hwan Seo, Hyun-Uk Kim, Gary Owens, and Kwon-Rae Kim. 2018. "Application of Soil Amendments to Contaminated Soils for Heavy Metal Immobilization and Improved Soil Quality—a Critical Review." *Soil Science and Plant Nutrition* 64 (2): 156–67. <https://doi.org/10.1080/00380768.2018.1440938>.
- Maniquiz-Redillas, Marla, and Lee-Hyung Kim. 2014. "Fractionation of Heavy Metals in Runoff and Discharge of a Stormwater Management System and Its Implications for Treatment." *Journal of Environmental Sciences* 26 (6): 1214–22. [https://doi.org/10.1016/S1001-0742\(13\)60591-4](https://doi.org/10.1016/S1001-0742(13)60591-4).
- Maniquiz-Redillas, Marla, and Lee-Hyung Kim. 2016. "Evaluation of the Capability of Low-Impact Development Practices for the Removal of Heavy Metal from Urban Stormwater Runoff." *Environmental Technology* 37 (18): 2265–72.
- McManus, Meigan, and Allen P. Davis. 2020. "Impact of Periodic High Concentrations of Salt on Bioretention Water Quality Performance." *Journal of Sustainable Water in the Built Environment* 6 (4): 04020014. <https://doi.org/10.1061/JSWBAY.0000922>.
- Mullins, Angela R., Daniel J. Bain, Erin Pfeil-McCullough, Kristina G. Hopkins, Sarah Lavin, and Erin Copeland. 2020. "Seasonal Drivers of Chemical and Hydrological Patterns in Roadside Infiltration-Based Green Infrastructure." *Science of The Total Environment* 714 (April): 136503. <https://doi.org/10.1016/j.scitotenv.2020.136503>.
- Muthanna, Tone Merete, Maria Viklander, Godecke Blecken, and Sveinn T. Thorolfsson. 2007. "Snowmelt Pollutant Removal in Bioretention Areas." *Water Research* 41 (18): 4061–72. <https://doi.org/10.1016/j.watres.2007.05.040>.
- Nelson, S.S., D.R. Yonge, and M.E. Barber. 2009. "Effects of Road Salts on Heavy Metal Mobility in Two Eastern Washington Soils." *Journal of Environmental Engineering* 135 (7): 505–10.
- Norrström, A. C., and G Jacks. 1998. "Concentration and Fractionation of Heavy Metals in Roadside Soils Receiving De-Icing Salts." *Science of The Total Environment* 218 (2–3): 161–74. [https://doi.org/10.1016/S0048-9697\(98\)00203-4](https://doi.org/10.1016/S0048-9697(98)00203-4).
- Norrström, Ann Catrine. 2005. "Metal Mobility by De-Icing Salt from an Infiltration Trench for Highway Runoff." *Applied Geochemistry* 20 (10): 1907–19. <https://doi.org/10.1016/j.apgeochem.2005.06.002>.
- Novotny, Vladimir, Deron Muehring, Daniel Zitomer, Daniel Smith, and Roderick Facey. 1998. "Cyanide and Metal Pollution by Urban Snowmelt: Impact of Deicing Compounds." *Water Science and Technology* 38 (10): 223–30.
- Paus, Kim H., Joel Morgan, John S. Gulliver, TorOve Leiknes, and Raymond M. Hozalski. 2014. "Effects of Temperature and NaCl on Toxic Metal Retention in Bioretention Media." *Journal of Environmental Engineering* 140 (10): 04014034. [https://doi.org/10.1061/\(ASCE\)EE.1943-7870.0000847](https://doi.org/10.1061/(ASCE)EE.1943-7870.0000847).

- Peltier, Edward, Jamila Saadi, Xiaolu Chen, and Bryan Young. 2010. "Metal Sequestration and Remobilization in Bioretention Media." In . Providence, Rhode Island: ASCE. [https://doi.org/10.1061/41114\(371\)310](https://doi.org/10.1061/41114(371)310).
- Ramakrishna, Devikarani M., and Thiruvengkatachari Viraraghavan. 2005. "Environmental Impact of Chemical Deicers – A Review." *Water, Air, and Soil Pollution* 166 (1–4): 49–63. <https://doi.org/10.1007/s11270-005-8265-9>.
- Robinson, Heather K., Elizabeth A. Hasenmueller, and Lisa G. Chambers. 2017. "Soil as a Reservoir for Road Salt Retention Leading to Its Gradual Release to Groundwater." *Applied Geochemistry* 83 (August): 72–85. <https://doi.org/10.1016/j.apgeochem.2017.01.018>.
- Schuler, Matthew S, and Rick A Relyea. 2018. "A Review of the Combined Threats of Road Salts and Heavy Metals to Freshwater Systems." *BioScience* 68 (5): 327–35. <https://doi.org/10.1093/biosci/biy018>.
- Søberg, Laila C., Maria Viklander, and Godecke-Tobias Blecken. 2017. "Do Salt and Low Temperature Impair Metal Treatment in Stormwater Bioretention Cells with or without a Submerged Zone?" *Science of The Total Environment* 579 (February): 1588–99. <https://doi.org/10.1016/j.scitotenv.2016.11.179>.
- Stagge, James H., Allen P. Davis, Eliea Jamil, and Hunho Kim. 2012. "Performance of Grass Swales for Improving Water Quality from Highway Runoff." *Water Research* 46 (20): 6731–42. <https://doi.org/10.1016/j.watres.2012.02.037>.
- TSDR. 2015a. Agency for Toxic Substances & Disease Registry. "Chromium." 2015. <https://www.atsdr.cdc.gov/substances/toxsubstance.asp?toxid=17>.
- TSDR. 2015b. Agency for Toxic Substances & Disease Registry. "Lead." 2015. <https://www.atsdr.cdc.gov/substances/toxsubstance.asp?toxid=22>.
- TSDR. 2015c. Agency for Toxic Substances & Disease Registry. "Public Health Statement for Copper." 2015. <https://www.atsdr.cdc.gov/phs/phs.asp?id=204&tid=37>.
- TSDR. 2015d. "Public Health Statement for Nickel." 2015. <https://www.atsdr.cdc.gov/phs/phs.asp?id=243&tid=44>.
- USDA. 2017. "Sodium Adsorption Ratio (SAR)." United States Department of Agriculture.
- USEPA. 2019. "Metals | CADDIS Volume 2 | US EPA." 2019. <https://www.epa.gov/caddis-vol2/metals>.
- Valtananen, Marjo, Nora Sillanpää, and Heikki Setälä. 2017. "A Large-Scale Lysimeter Study of Stormwater Biofiltration under Cold Climatic Conditions." *Ecological Engineering* 100 (March): 89–98. <https://doi.org/10.1016/j.ecoleng.2016.12.018>.
- Zehetner, Franz, Ulrike Rosenfellner, Axel Mentler, and Martin H. Gerzabek. 2009. "Distribution of Road Salt Residues, Heavy Metals and Polycyclic Aromatic Hydrocarbons across a Highway-Forest Interface." *Water, Air, and Soil Pollution* 198 (1–4): 125–32. <https://doi.org/10.1007/s11270-008-9831-8>.

4. Export of fecal contamination from roadside green infrastructure

This chapter is under review with the *Journal of Sustainable Water in the Built Environment* (ASCE) for their special collection on fecal contamination in stormwater:

Hayes, Gail M., Wuhuan Zhang, Charles R. Burgis, Derek Henderson, and James A. Smith. (Under review.) "Export of fecal contamination from roadside green infrastructure." *Journal of Sustainable Water in the Built Environment*.

4.1 ABSTRACT

Fecal contamination in stormwater runoff is a leading contributor of waterbody impairment in the United States and green infrastructure (GI) has demonstrated highly variable performances in mitigating fecal contamination. There are still needs for research that uses robust sampling methods to quantify concentration and load reductions as well as evaluate export of fecal contamination with treated effluent. The objectives of this study were to (1) quantify fecal contamination using *E. coli* (EC) as the fecal indicator bacteria entering and exiting GI systems and (2) characterize the export of EC from GI systems. This study was conducted at a field site on Lorton Road in Fairfax County, Virginia where a bioretention, bioswale, compost-amended grass channel, and a grass channel were instrumented for two years in all seasons for flow-weighted composite sampling and volume monitoring. The geometric mean of the road runoff entering the bioretention was 1120 MPN/100 mL while that entering the swales was only 58 MPN/100 mL. Combined sewers are not used in Fairfax County, so the EC inputs to the GI are attributed to wildlife, domesticated animals, and leaky sewers. Outflow concentrations from all GI systems were regularly above recreational water quality standards. Regression analyses indicated that average daily temperature, dissolved organic carbon, total dissolved nitrogen, and chloride were all significantly correlated with the log transformed EC concentrations exiting the GI systems. The bioretention did reduce EC presence even with relatively high levels of inflow EC (up to 98% and 93% reductions for loading and concentrations). The swales all significantly increased EC concentrations (up to 150,000%) but did not change loading significantly. It is concluded that EC export is prevalent in GI

systems but can be understood with analysis of related water quality constituents. The results provide insight into environmental factors and common stormwater quality constituents that might be influencing the export of fecal contamination from GI.

4.2 INTRODUCTION

Stormwater runoff frequently deposits fecal contamination into receiving waterways, impairing stream health and causing public health concerns through the introduction of pathogens (USEPA 2012; Wright Water Engineers 2010; Mallin et al. 2016). Sources of fecal contamination in stormwater runoff include wildlife, domesticated animals, leaky sewers, illicit discharges, treated wastewater effluent, and combined sewer overflows (Wright Water Engineers 2010). The United States Environmental Protection Agency (US EPA) regulates the presence of fecal contamination in waterways through Recreational Water Quality Criteria for safe human exposure (USEPA 2012). These criteria use concentrations of fecal indicator bacteria *Escherichia coli* (EC) for freshwater and enterococci for marine water (USEPA 2012). Additional criteria are implemented through local Municipal Separate Storm Sewer System (MS4) plans that limit watershed-scale exports of fecal contamination loading. To help meet treatment requirements, MS4 plans use green infrastructure (GI), a relatively novel but frequently used stormwater management technique that encourages infiltration, evapotranspiration, and storage of runoff close to its source (Brumley et al. 2018; Dietz and Arnold 2018; Zhang and Chui 2019). Common types of GI systems include bioretention filters and swales. A bioretention filter or system (hereafter referred to as a bioretention (BR)) is a vegetated basin that infiltrates runoff through its soils and often includes an underdrain (DEQ 2011a). Swales are vegetated channels that optionally include underdrains and check dams to slow and infiltrate small amounts of runoff (DEQ 2011b; 2011c).

In water bodies such as rivers and lakes, other common stormwater pollutants have been shown to impact bacteria presence, so it is important to understand these factors with regards to stormwater runoff in order to optimize management techniques such as GI. For example, total suspended solids

(TSS) are of interest because of the tendency of bacteria to sorb to sediments and avoid predation or settle out of the runoff (Krometis et al. 2007; Jeng et al. 2005; Brown et al. 2013). Nitrogen and dissolved organic carbon (DOC) are also of interest because they are energy sources for reproduction and may be indicators of the influence bacteria has on both the nitrogen and carbon cycles (Jetten 2008; Anesio et al. 2004). Chloride is of interest particularly in areas where road salt is applied in winter months because it could potentially expedite bacteria die-off (Hrenovic and Ivankovic 2009).

Environmental factors such as temperature and rainfall can also influence bacterial survival by providing heat and moisture needed for incubation or dormancy (Chandrasena et al. 2014; Hathaway et al. 2010).

GI performance in mitigating fecal contamination varies widely and is evaluated by quantifying reductions of concentrations and mass loads. For example, in Li and Davis (2009), median concentration reductions for their two studied bioretention systems (flow-weighted composite sampling) were 0% and 57% but ranged from -15,550% to almost 100%. This same study found load reductions of 100% and 94% with a range of -9,390% to 100%. In Barrett et al. (1998), swales “reduced” fecal contamination concentration by -192% as indicated by grab samples. In both Hathaway et al. (2011) and Hunt et al. (2008) (both using grab sampling), bacteria concentrations were decreased by 70% or more in two bioretention systems with 0.6 and 1.2 m of soil depth. However, in a shallower bioretention (0.25 m) in Hathaway et al. (2011) it was found that fecal contamination concentration increased by over 100%. Much of the research on GI mitigation of fecal contamination has used single or a few discrete grab samples to represent entire event concentrations, but this introduces error when estimating mass loads, so there is a shortage of data on load reductions of fecal contamination by GI (Gavrić et al. 2019; Wright Water Engineers 2010). Mitigation of fecal contamination by GI systems can vary widely, but can be better understood in light of the previously mentioned factors affecting EC growth and die-off.

This study seeks to address the need for more research on fecal contamination in GI using robust flow-weighted composite sampling that include loading calculations. Additionally, this study explores

possible water quality parameters and environmental factors that may impact GI export of fecal indicator bacteria. Therefore, the objectives of this study were to (1) quantify fecal contamination using *E. coli* (EC) as the fecal indicator bacteria entering and exiting GI systems and (2) characterize the export of EC from GI systems.

4.3 METHODS AND MATERIALS

4.3.1 Field Site

This study was conducted at a field site on Lorton Road in Fairfax County, Virginia that is described in Chapter 2 and Chapter 3 as well as in Hayes et al. (Forthcoming), Burgis et al. (2020a), and Burgis et al. (2020b). Lorton Road is four-lanes with a vegetated divider along its entire length and has an annual average daily traffic count of 100,000 vehicles (VDOT 2018). The 1-km portion of Lorton Road used in this study is largely undeveloped, its roadside consisting of both open fields and wooded areas except for one residential development on the south-west end of the road. Construction of Lorton Road and its stormwater management was completed in 2017, at which time four green infrastructure systems (bioretention (BR), bioswale (BS), compost-amended grass channel (CAGC), and grass channel (GC)) were selected and instrumented for stormwater composite sampling and volume monitoring. These GI systems were selected because they receive runoff directly from the road, are easy to access, and are representative of stormwater management techniques commonly used by the Virginia Department of Transportation (VDOT).

There are seven monitoring stations at the site: two for monitoring road runoff entering the GI systems and five at their respective outflow points. One road runoff monitoring station is used only for the bioretention inflow as it is placed at its inflow culvert. The other road runoff monitoring station is used to represent the overland flow entering the swales. This station consists of a 9-m HDPE and aluminum gutter flush with the ground that directs water to a monitoring station. This collection gutter is adjacent to a 2-m asphalt walkway that is adjacent to Lorton Road. The data from this monitoring

station were extrapolated to represent the road runoff entering the three swales as described in Hayes et al. (Forthcoming).

Table 2.1 (Chapter 2) includes the design specifications of each GI retrieved from the as-built plans. The BR (Fig. 2.2) consists of a forebay and vegetated basin and receives road runoff from a curb and gutter system on Lorton Road. Its 48,000 m² contributing drainage area consists of residential and wooded areas as well as roadway. The runoff initially enters the BR forebay through a 1-m concrete culvert, is slowed, and then is directed into the basin through a second, smaller culvert. A bypass on the forebay allows a portion of runoff to discharge the system untreated. Once in the basin, the inflow infiltrates the engineered soil media and is discharged through a 5-cm perforated underdrain located 0.75-m below the basin surface within gravel. The two outflow monitoring stations at the BR are its underdrain outlet and its bypass. The swales all have much smaller contributing drainage areas (CDAs) than the BR, ranging from 2500 m² to 6000 m². Runoff enters the swales from Lorton Road and the green space between their channel centers and the road. The primary difference between the three swales are their soils and underdrains: the BS contains the same engineered soil media and 5-cm perforated underdrain as the BR, the CAGC contains native soils that are amended with compost, and the GC contains only native soils. The outflows of each swale have their own respective monitoring stations. The BS monitoring station is situated to capture both the underdrain flow and any overland flow exiting the swale, but overland flow here has been observed as minimal.

4.3.2 Field Data Collection

Rain data for the site was collected with a tipping-bucket rain gauge (Hach™, Loveland, CO) paired with an American Sigma 900 (Hach™, Loveland, CO) located at the bioretention. The rain gauge precision was 0.25 mm and recorded data every 10 minutes. Instances where the rain gauge failed are indicated in Appendix J, wherein weather data from the Ronald Reagan airport was used. For this present study, a rain event is defined as a period of rainfall followed by at least 12 hours of no rain. The Ronald Reagan

Airport weather station data was used to compute average daily temperatures for the monitored events as well. Because this study aimed to characterize export of fecal contamination, only rain events large enough to create detectable outflow from the GI systems were used.

Each stormwater monitoring station consists of an AS950 Autosampler (Hach™, Loveland, CO) with a US9001 ultrasonic depth sensor (Hach™, Loveland, CO) used to measure depth of water in a fiberglass H or HS flume (Open Channel Flow© Boise, ID) and convert water depth to volumetric flow. Flume sizes and equations for each monitoring station are in Appendix A. Equal-volume, variable-time sampling regimes were used to collect composite, flow-weighted samples from the monitored events. A successful sample contained at least 5 aliquots (100-mL each) collected over the rising limb and peak flow. The concentration of these composite samples was interpreted as the event mean concentration (EMC) for the respective parameters. Samples were collected using ceramic-tipped polypropylene sampling lines provided by Hach™ (Loveland, CO). Samples were stored in 9.5-liter glass bottles on ice until retrieval which was no more than 12 – 24 hours after the event ended, a method verified by McCarthy et al. (2008) which found that bacteria are unlikely to multiply significantly within 24 hours of collection. Total volume that passed through each monitoring station for each event was calculated as described in Chapter 2 (Hayes et al. Forthcoming). The product of total volume and EMC gave the mass load for the particular pollutant for each event at a particular monitoring station.

Careful sanitation procedures were kept to ensure accurate readings of bacteria and other water quality parameters. Prior to each use, the glass bottles and their Teflon-lined caps were washed with phosphate-free soap and tap water, rinsed with deionized water, soaked in 10% HCl for at least 24 hours, and rinsed with deionized water again. Deionized water rinsed through a cleaned bottle was sampled to ensure sufficient cleaning. Additionally, the ceramic tips of the sample collection lines were scrubbed and the lines rinsed (via grab sample of the autosampler) with at least 600 mL of distilled water prior to each monitored event. The sufficiency of this cleaning procedure was verified periodically

and reported in Appendix J. Additionally, sample collection lines were set up with minimal curves and low spots as suggested in Hathaway et al. (2014). The autosamplers were programmed to purge remaining water in the sample intake lines after each aliquot collected, eliminating idle water in the lines that could foster bacterial reproduction. To verify the presence of EC independent of the autosamplers, periodic grab samples of the constant baseflow at the outlet of the BR were also collected using sterile HDPE bottles.

4.3.3 Groundwater Monitoring and Creek Sampling

Ten groundwater monitoring wells (5-cm diameter PVC) were installed in the vicinity of the BR: eight on the perimeter and two inside the forebay (Fig. 3.1). The perimeter wells are 4 – 9 m below the surface of the forebay while the two wells inside the forebay are 2.5 m. The bottom meter of every well is screened (4 slots per cm) in sand. The 10-cm diameter area surrounding the top meter of each well is sealed with bentonite clay to prevent macropore flow along the length of the casing. Well samples were collected in 500-mL bottles after bailing three well volumes with sterile polyethylene bailers. Well samples were tested for EC in March 2019, July 2019, July 2020, and September 2020.

The BR outflow is approximately 15 m from a small unnamed creek that runs parallel to Lorton Road and the continuous baseflow of the outlet has created a marshy area at the outlet. Therefore, the saturated soils between the BR outlet and the creek are often hydraulically connected. Because of this connection and a potential impact on the creek quality, two samples were collected of the creek during low flow in March 2019: one 20 m upstream of its meeting point with the BR baseflow and one 10 m downstream. Physical access to the stream is very limited due to vegetation and fencing, so equal spacing of sampling was not possible.

4.3.4 Laboratory Analytical Methods

EC concentration was quantified with IDEXX Colilert and Quanti-tray/2000 (IDEXX, Westbrook, ME) which required incubation at 35° C for 24 hours. IDEXX results have a confidence of 95%, accuracy of one

organism per 100 mL, and were verified with a comparator tray provided by IDEXX of known positive results. IDEXX results are reported as most probable number (MPN) of EC per 100 mL. 1:1000 dilutions were performed for all samples and the least diluted result was reported. Total suspended solids (TSS) were measured in triplicate with gravimetric determination after vacuum filtration through a 0.45 µm filter and oven drying at 100° C for 24 h. Total dissolved nitrogen (TDN) and dissolved organic carbon (DOC) were measured with a TOC-L Total Organic Carbon Analyzer (Shimadzu, Kyoto, JPN) after acidification to 2% HCl and filtration through 0.45 µm syringe filter. Chloride was measured with ion chromatography also after filtration through 0.45 µm syringe filter (Thermo Fisher Scientific, Waltham, MA). Standards of known concentrations as well as blanks were analyzed in conjunction with samples to verify accuracy of results.

4.3.5 Performance Metrics and Data Analysis

Performance metrics for each GI system were calculated as their reductions of EMC and mass load of EC. The BR outflows were separated into its bypass and outlet and the changes in EC EMC and load at both points are presented for comparison. EC concentrations and mass load averages were calculated as geometric means and average log and percent reductions of EMC and mass loads were calculated as arithmetic means. Normal distribution was not assumed, so non-parametric tests were used (confidence of 95%): Wilcoxon signed rank test was used to determine significance of EMC and mass load reductions of individual GI systems and the Mann-Whitney test for two samples determined significance of differences between GI systems when direct comparison was possible.

Simple linear regression analyses were performed using log transformed EC EMC at each GI system outlet as the response variable. Explanatory variables included average daily temperature, event rainfall depth, antecedent rainfall (rainfall depth in preceding 5-days), and the corresponding outflow EMC values of TSS, TDN, DOC, and chloride. For simple linear regression, percent increase of EC per one unit increase of explanatory variable was calculated by exponentiating the coefficient, subtracting one from

this number, and multiplying by 100 (Ford 2018). All data analysis was conducted in RStudio (R Version 4.0.2) and Microsoft Excel.

4.4 RESULTS

4.4.1 Overview of Monitoring

Monitoring at the four GI systems on Lorton Road occurred in all seasons from April 2018 through April 2020. During this time, the two road runoff monitoring locations captured 20 events entering the BR and 19 events entering the swales. Of these events monitored at the road runoff locations, corresponding outflow measurements were conducted at the BR for 19 events, the BS for 16 events, the CAGC for 12 events, and the GC for 14 events. The environmental conditions of these events are similar, so individual GI results are presented side by side. However, only nine of these events were monitored at every GI system, so direct comparisons of the GI systems are only given with this data subset. Each composite sample consisted of 9 or more individual samples collected throughout the rain event, including the rising limb and peak. All EC EMC, loads, environmental conditions (average daily temperature, rainfall depth, and antecedent rainfall depth), and other relevant water quality constituents (DOC, TDN, TSS, and chloride) of the monitored events are given in Appendix J. The reductions of EC content by each GI system are summarized in Table 4.1 along with the climate data of the monitored events.

Table 4.1. Event and EC data for monitored events.

	Geometric mean	Minimum	Maximum	Average log $\Delta \pm$ SD, [range]	Average % $\Delta \pm$ SD, [range]	Av. % Vol. $\Delta \pm$ SD, [range]	No. events	Av. Temp. (C), [range]	Total rain depth (mm), [range]	Av. Antecedent rain depth (mm), [range]
Bioretention										
EMC in	1187	32	29,500							
EMC bypass	1219	10	35,500	0.4 ± 0.6^a	-91.7 ± 601^a					
EMC out	539	26	27,900			75 ± 7	19	13.9, [2.1, 25]	890, [14, 96.5]	29.8, [0, 179]
Load in	7.9×10^8	1.7×10^7	1.8×10^{10}							
Load bypass	6.8×10^7	2.0×10^5	4.2×10^9	0.90 ± 0.6^a	48 ± 170^a					
Load out	8.4×10^7	2.5×10^6	3.9×10^9							
Bioswale										
EMC in	42	1	1,414	-0.8 ± 1.3	$-1.5 \times 10^5 \pm 6.1 \times 10^5$					
EMC out	343	16	172,000	$[-4.3, 1.4]$	$[-2.4 \times 10^6, 96]$					
Load in	5.1×10^7	1.2×10^6	1.1×10^9	0.4 ± 1.2	$-2.2 \times 10^3 \pm 9.0 \times 10^3$	76 ± 18	16	11.4, [2.1, 24]	650, [13, 104]	25.6, [0, 179]
Load out	1.9×10^7	9.9×10^5	4.7×10^9	$[-2.6, 2.5]$	$[-3.6 \times 10^4, 100]$					
Compost-amended grass channel										
EMC in	61	1	1414	-0.7 ± 0.8	$-1.6 \times 10^3 \pm 2.4 \times 10^3$					
EMC out	412	13	17,500	$[-1.9, 0.4]$	$[-8.6 \times 10^6, 62]$	25 ± 64	12	10.9, [2.1, 24]	425, [14, 64.8]	29.0, [0, 179]
Load in	6.4×10^7	1.2×10^6	1.1×10^9	-0.6 ± 0.7	$-820 \pm 1 \times 10^3$					
Load out	2.5×10^8	1.1×10^7	4.9×10^9	$[-1.5, 0.6]$	$[-3.5 \times 10^3, 63]$					
Grass channel										
EMC in	31	1	308	-1.1 ± 1.1	$-4.7 \times 10^4 \pm 1.3 \times 10^3$					
EMC out	470	13	44,300	$[-3.7, 0.4]$	$[-6.2 \times 10^5, 60]$	39 ± 35	14	10.0, [2.1, 22]	601, [14, 104]	12.3, [0, 67.3]
Load in	4.4×10^7	1.2×10^6	7.0×10^8	-0.3 ± 0.8	$-656 \pm 1.3 \times 10^3$					
Load out	9.4×10^7	5.2×10^6	4.2×10^9	$[-1.7, 1.1]$	$[-5 \times 10^3, 92]$					

^a Indicates difference between inlet and outlet (no bypass).

4.4.2 Road Runoff EC Content

The geometric mean of EC EMC in road runoff at the BR inlet was 1120 MPN/100 mL while that entering the swales was 58.1 MPN/100 mL (Fig. 4.1). In Fig. 4.1, the dashed line at 2.1 represents the 30-day geometric mean limit of exposure of 126 MPN/100mL. Loads (MPN/event) entering the BR ranged from 1.7×10^7 to 1.8×10^{10} . Loads entering the three swales were as low as 1.2×10^6 and as high as 1.1×10^9 for the BS and CAGC and 7.0×10^8 for the GC.

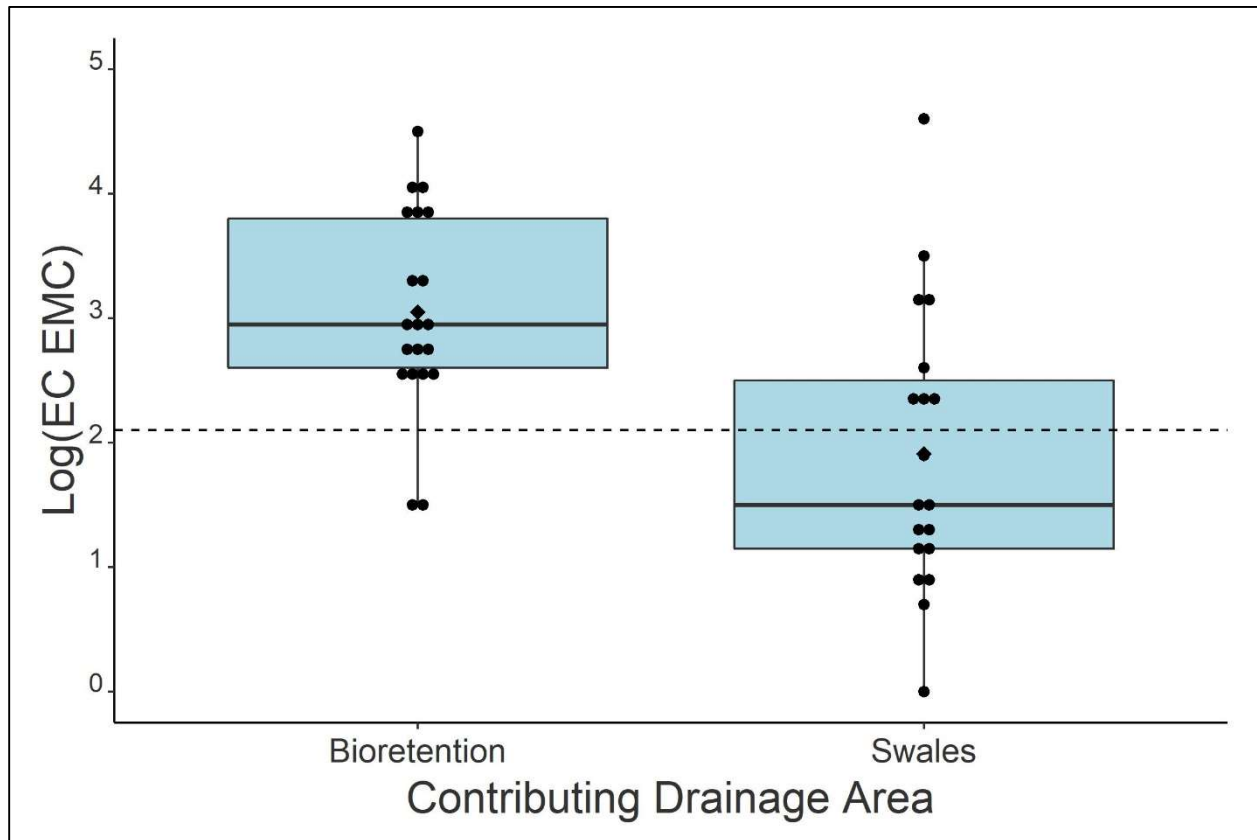


Figure 4.1. Road runoff concentrations of *E. coli* from the contributing drainage areas of the bioretention and swales. Dashed line: 30-day geometric mean limit.

4.4.3 Bioretention

Groundwater sampling from the perimeter of the BR consistently showed no EC in these deeper wells except for one well which had 2 MPN/100 mL in September 2020. However, sampling of the two shallowest wells within the forebay consistently detected EC throughout the study period. Specifically, EC levels detected in the well nearest to the inlet flume were 7.5, 36, 57, and 101 MPN/100 mL in

samples from March 2019, July 2019, and July 2020, and September 2020, respectively. Sampling from the other well within the forebay located west of the bioretention inlet and closer to the bypass reported EC twice with a reading of 31 MPN/100 mL in July 2020 and 13 MPN/100 mL in September 2020.

The performance of the BR is summarized in Table 4.1 and Fig. 4.2 illustrates log EMC of each monitored event. In Fig. 4.2, the dashed line at 2.1 represents the 30-day geometric mean limit of exposure of 126 MPN/100mL. There was one event on October 17, 2019 which produced 2000% increase of EC EMC between the BR inlet and outlet. Of the data collected, there are no unusual features of this event, so it is unknown why this large export occurred. Overall, the EMC at the BR outlet was significantly smaller than that at its inlet (Wilcoxon, $P = .01$), but there was no such difference between the bypass and inlet. The loads of EC exiting at the bypass and outlet were both significantly less than those measured at the inlet (Wilcoxon, $P = 3 \times 10^{-5}$, 2×10^{-4}) and were not different from each other. The average and standard deviation of three grab samples of the BR baseflow taken during the summer and autumn of 2018 were 102 ± 59 MPN/100 mL. The grab sample from the creek upstream of its meeting point with the BR was 649 MPN/100 mL and downstream was 411 MPN/100 mL.

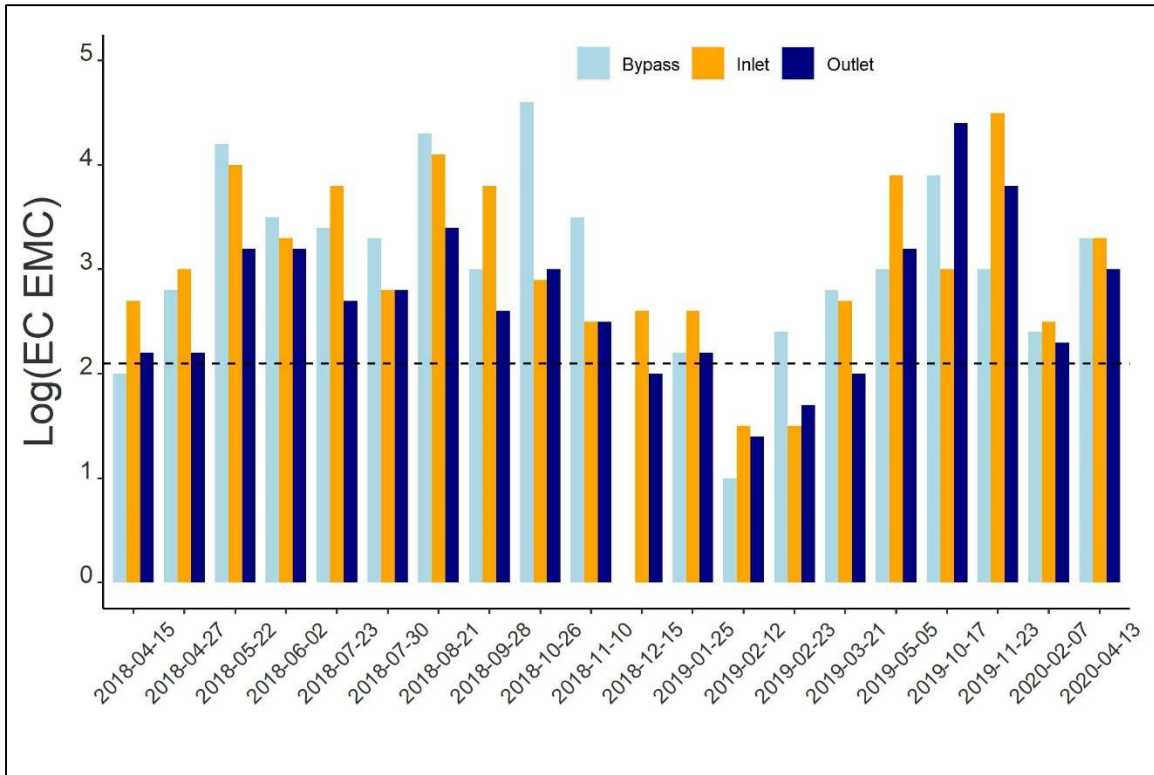


Figure 4.2. EC EMC at the bioretention inlet, outlet, and bypass. Dashed line: 30-day geometric mean limit.

The simple linear regression analyses performed on the log EC EMC exiting the BR are summarized in Table 4.2.

Table 4.2. Linear regression analyses of GI system outflows and water quality constituents. N/S = not significant. Response variables are outflow log EMC at each GI while explanatory include environmental factors and water quality parameters at the outlets. “ - ” not analyzed.

Explanatory variables	Bioretention		Grass Channel		Compost-amended grass channel		Bioswale	
	P-value (R ²)	Slope (% change)	P-value (R ²)	Slope (% change)	P-value (R ²)	Slope (% change)	P-value (R ²)	Slope (% change)
Temperature	.01 (0.3)	0.06 (6%)	.02 (0.3)	0.09 (9.4%)	.02 (0.3)	0.06 (6%)	.01 (0.4)	0.1 (11%)
Rainfall	0.7	N/S	0.7	N/S	0.3	N/S	0.7	N/S
AMC	0.7	N/S	0.4	N/S	0.1	N/S	0.05	N/S
Total suspended solids								
GC	-	-	0.4	N/S	-	-	-	-
CAGC	-	-	-	-	0.5	N/S	-	-
BS	-	-	-	-	-	-	0.7	N/S
BR	0.2	N/S	-	-	-	-	-	-
Total Nitrogen								
GC	-	-	.01 (0.5)	1.2 (232%)	-	-	-	-
CAGC	-	-	-	-	.04 (0.3)	0.99 (169%)	-	-
BS	-	-	-	-	-	-	2E-3 (0.5)	3.2 (2353%)
BR	0.7	N/S	-	-	-	-	-	-
Dissolved Organic Carbon								
GC	-	-	1.2E-5 (0.8)	0.19 (21%)	-	-	-	-
CAGC	-	-	-	-	.002 (0.5)	0.1 (11%)	-	-
BS	-	-	-	-	-	-	4E-4 (0.5)	0.3 (35%)
BR	1.5E-4 (0.5)	1.5 (16%)	-	-	-	-	-	-
Chloride								
GC	-	-	.01 (0.4)	-0.03 (-3%)	-	-	-	-
CAGC	-	-	-	-	.03 (0.3)	-4E-3 (-0.4%)	-	-
BS	-	-	-	-	-	-	0.4	N/S
BR	3.2E-3 (0.4)	-1.3E-3 (-0.1%)	-	-	-	-	-	-

4.4.4 Grass Channel

Table 4.2 summarizes the event data and performance of the GC and Fig. 4.3 illustrates its log EMC values for inflow and outflow. In Fig. 4.3, the dashed line at 2.1 represents the 30-day geometric mean limit of exposure of 126 MPN/100mL. EMC values at the outlet of the GC were significantly larger than

the EMC values of the road runoff entering (Wilcoxon, $P = 3.7 \times 10^{-4}$). While the log reductions of loads were generally positive, these reductions were not significant. The results of the simple linear regression analyses for the log of EC EMC exiting the GC are presented in Table 4.2.

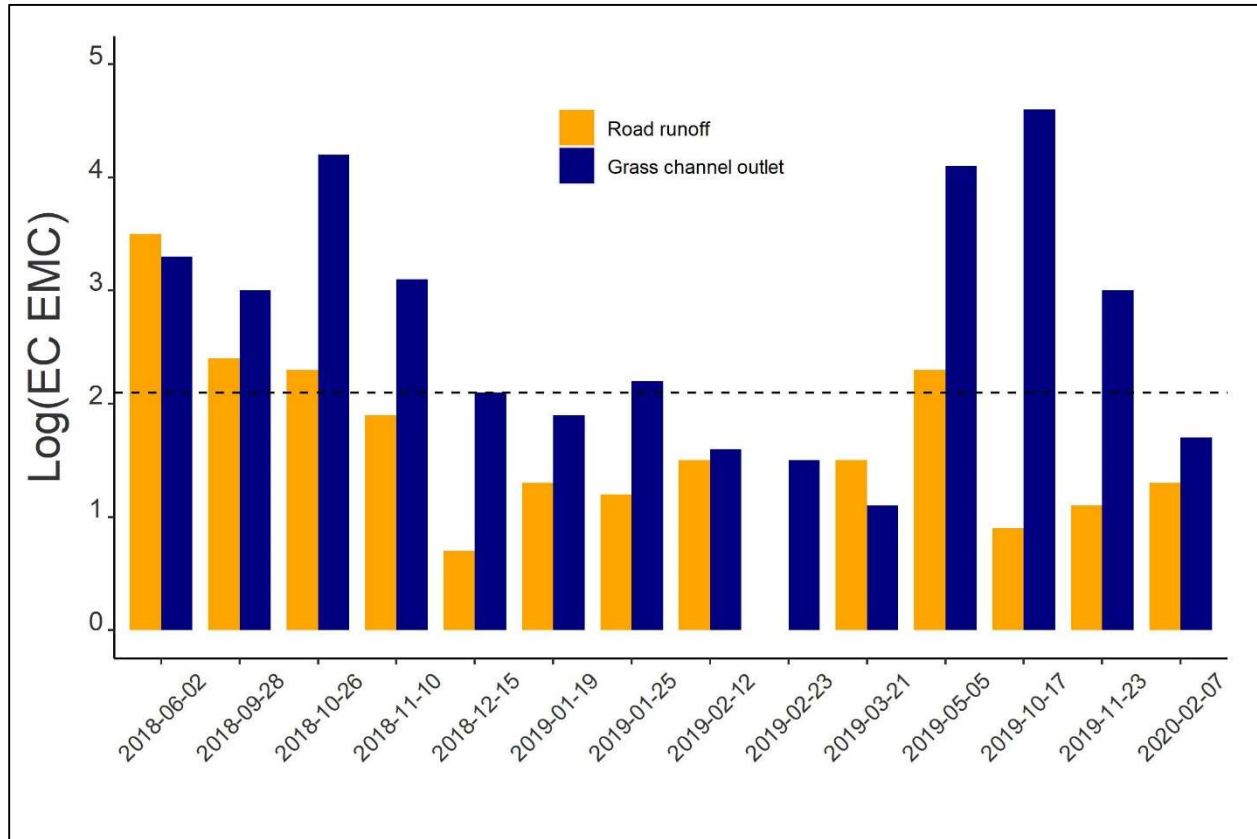


Figure 4.3. Grass channel EC results. February 23, 2019 received no measurable EC as inflow from the road runoff. Dashed line: 30-day geometric mean limit.

4.4.5 Compost-Amended Grass Channel

The performance of the CAGC is presented in Table 4.1 and Fig. 4.4 illustrates the log EMC values. For the monitored events, this GI also significantly increased EMC of EC from the road runoff to its outlet (Wilcoxon, $P = .01$). In Fig. 4.4, the dashed line at 2.1 represents the 30-day geometric mean limit of exposure of 126 MPN/100mL. The average log reduction and range of EC loads were not significant, however. Table 4.2 summarizes the simple linear regression analyses of EC concentration at the outlet with these factors.

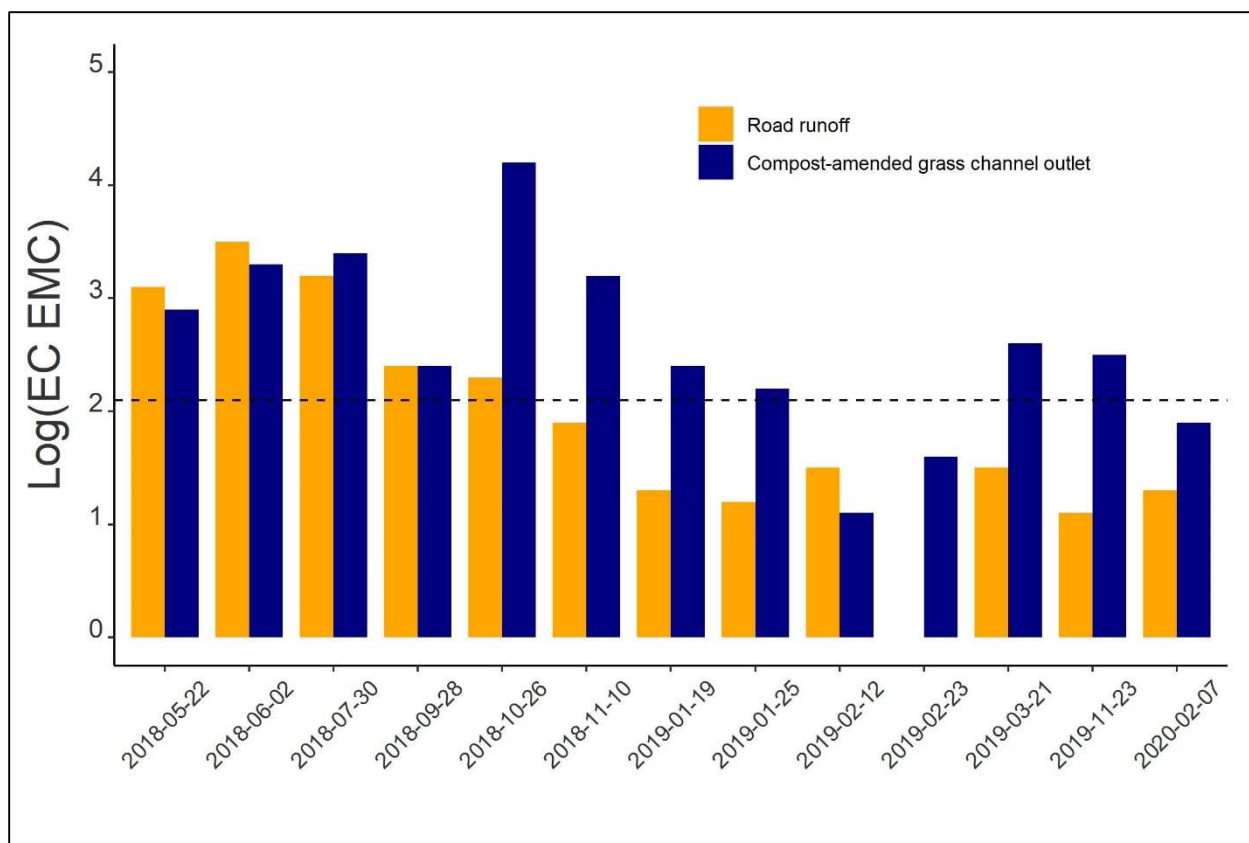


Figure 4.4. Compost-amended grass channel EC performance. February 23, 2019 received no measurable EC as inflow from the road runoff. Dashed line: 30-day geometric mean limit.

4.4.6 Bioswale

The inflow and outflow EMC at the BS are summarized in Table 4.1 and the log EMC are illustrated in Fig. 4.5. In Fig. 4.5, the dashed line at 2.1 represents the 30-day geometric mean limit of exposure of 126 MPN/100mL. The EMC of the BS outlet was also significantly greater than the inflow EMC (Wilcoxon, $P = .01$). The average loading reduction of the BS was typically negative, though the differences between the road runoff load and outflow load of the BS were not significant. Table 4.2 summarizes the results of the simple linear regression analysis of the water quality parameters of interest with log of concentration of EC at the BS outlet.

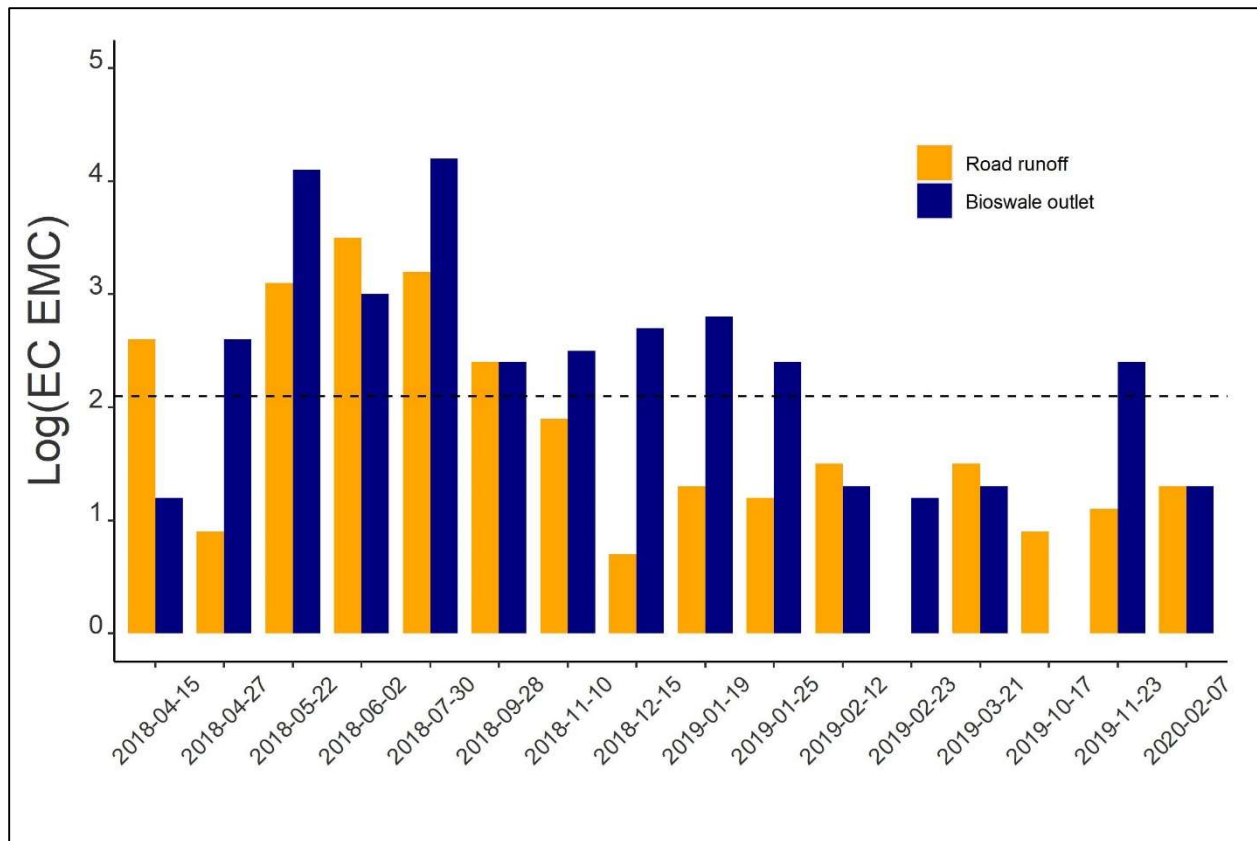


Figure 4.5. Bioswale EC performance. February 23, 2019 received no measurable EC as inflow from the road runoff. Dashed line: 30-day geometric mean limit.

4.4.7 Direct Comparison of all GI Systems

Of all the events monitored at the GI systems during the study period, inflow and outflow for every GI was captured for nine events, making these nine the basis for direct comparison of the four GI systems (Table 4.3). In these events, the BR reduction of EC concentration was significantly greater than that of the GC, CAGC, and BS ($P = 1 \times 10^{-3}$, 3×10^{-3} , 4×10^{-3}). The three swales showed no statistical difference for EMC reduction between each other. The BR and BS (statistically equivalent) had greater load reductions than the GC ($P = .01$ and $.04$) and CAGC ($P = 1 \times 10^{-3}$ for both).

Table 4.3. EC content entering and exiting each GI and environmental conditions during the nine shared events.

	Geometric mean	Minimum	Maximum	Av log reduction \pm SD, [range]	Av % reduction \pm SD, [range]	No. of events	Av. Temp. (C), [range]	Total rain depth (mm), [range]	Av. Antecedent rain depth (mm), [range]
Bioretention						9	9.4 [2.1 - 22]	324 [14, 65]	18, [0, 67]
EMC in	579	32	29,500	0.4 \pm 0.4	35 \pm 46				
EMC bypass	446	10	3100	[-0.2, 1.2]	[-65, 93]				
EMC out	265	26	6300						
Load in	3.1x10 ⁸	1.7x10 ⁷	1.2x10 ¹⁰	1.0 \pm 0.4	84 \pm 13				
Load bypass	1.5x10 ⁷	2.0x10 ⁵	1.2x10 ⁸	[0.3, 1.6]	[53, 98]				
Load out	3.4x10 ⁷	2.5x10 ⁶	4.4x10 ⁸						
Bioswale									
EMC in	31	1	308	-0.5 \pm 0.6	-557 \pm 702				
EMC out	94	16	980	[-1.3, 0.2]	[-1.8 x10 ³ , 40]				
Load in	3.3 x10 ⁷	1.2 x10 ⁶	6.3 x10 ⁸	0.8 \pm 0.6	59 \pm 49				
Load out	6.0 x10 ⁶	9.9 x10 ⁵	1.5 x10 ⁸	[-0.14, 1.5]	[-41, 97]				
Compost-amended grass channel									
EMC in	31	1	308	-0.9 \pm 0.7	-1269 \pm 1273				
EMC out	215	13	2000	[-1.6, 0.4]	[-4.2x10 ³ , 62]				
Load in	3.4x10 ⁷	1.2x10 ⁶	6.1x10 ⁸	-0.7 \pm 0.6	-887 \pm 1052				
Load out	1.7x10 ⁸	1.1x10 ⁷	2.7x10 ⁹	[-1.5, 0.5]	[-3.4 x10 ³ , 63]				
Grass channel									
EMC in	31	1	308	-0.8 \pm 0.6	-1477 \pm 2120				
EMC out	186	13	2000	[-1.9, 0]	[-6.9x10 ³ , 60]				
Load in	3.4x10 ⁷	1.2x10 ⁶	6.3x10 ⁸	-0.1 \pm 0.7	-242 \pm 400				
Load out	4.2x10 ⁷	5.2x10 ⁶	4.8x10 ⁸	[-1.0, 1.1]	[-1.0x10 ³ , 92]				

4.5 DISCUSSION

4.5.1 EC Levels in Road Runoff

The EC EMC values at the two road runoff monitoring stations were highly varied such that the BR inflow EMC values had a geometric mean of 1120 MPN/100 mL and the inflow EMC values to the swales were 58.1 MPN/100 mL (Fig. 4.1). In fact, the concentration of EC at the BR inlet was regularly above the exposure limit for recreational waters established by the EPA (126 MPN/100 mL) (USEPA 2012). The high variability and geometric mean values of these untreated runoff concentrations are consistent with other studies using flow-weighted composite sampling methods that report EC values in untreated stormwater runoff with Li and Davis (2009) reporting geometric means of 5 and 92 MPN/100 mL, Aryal et al. (2012) reporting discrete samples of 100 – 3600 MPN/100 mL, and Willard et al. (2017) reporting discrete samples of 10 – 1100 MPN/100 mL.

Combined sewers are not used in Fairfax County, so the discrepancy between the two road runoff monitoring locations is attributed to their CDAs and the 1-m culvert that flows into the BR as its inflow. This culvert drains an approximately 4.5-hectare CDA consisting of residential area, wooded lots, and roadway, all likely spots of EC deposits from wild animals or other sources. The BR CDA is over four times larger than the CDA for the swales, resulting in a greater time of concentration, which gives additional time for bacterial reproduction. The BR inflow culvert welcomes wildlife such as mammalian species that would deposit EC. Presence of these species in the immediate vicinity of the BR inflow were indicated through visual confirmation of fox and feral cat, raccoon footprints in the inlet flume, and unidentified fecal matter deposited in the BR area during the study period. The source of EC detected at the monitoring point for the swales' inflows is unknown, but given its close proximity to the busy road, it is unlikely to be larger wildlife. However, mice and other small rodents were regularly seen at the swales, so it is suspected that their deposits may be the source. Additionally, the paved path beside the GC and BS is suitable for dog-walking, another potential source. These high influent concentrations of

fecal contamination are to be expected because stormwater runoff as a non-point source pollutant has been shown to contribute significantly more fecal contamination to receiving waters even than treated wastewater effluent or dry weather storm sewer flows (Petersen et al. 2005).

4.5.2 GI Outflow Concentrations

Like the road runoff, the geometric means of all GI outflow EMC values during stormflows were above the 30-day geometric mean limit of 126 MPN/100 mL for human exposure in recreational waters established by the EPA (Table 4.1) (USEPA 2012). Furthermore, the statistical threshold value of EC in recreational waters (410 MPN/100 mL) was overcome in 31 – 50% of the composite samples collected for each event, above the limit of 10% (USEPA 2012). Given that this present study used composite samples of flowing stormwater rather than a body of water, a comparison with the Recreational Water Quality Criteria is indirect but is provided for context. The concentration of EC in the baseflow of the BR was much lower than the typical stormflow, though it was critically high (> 126 MPN/100 mL) in two of three readings. These grab samples of the BR outlet baseflow indicate lingering organisms in the media and a hospitable environment therein. The wildlife traffic could also be contributing EC to the baseflow through fresh deposits on the surface of the basin and forebay. While there was EC detected in the baseflow, its levels were much lower than those of the nearby creek. Furthermore, the baseflow may actually be diluting the EC concentration in the nearby creek. However, only one such sample was collected and very little is known about this creek such that it might be subject to illicit discharge or a gathering area for local wildlife.

4.5.3 Environmental and Water Quality Correlations

At every outlet monitoring station, temperature was significantly positively correlated with the log of EC EMC with 6 – 10% increases in concentration for every one degree increase of temperature (Table 4.2). This is consistent with the findings of Hathaway et al. (2010) who found a statistically significantly greater presence of EC during warmer seasons. Temperature has been shown to be highly impactful for

EC presence, though the relationship depends on competing events and therefore exact cause and effect can be difficult to decipher on a large scale. For example, colder temperatures have been shown to prolong EC survival through encouraging dormancy and discouraging predation while much warmer temperatures can lead to bacteria desiccation (Rippy 2015). However, warmer temperatures below desiccation foster incubation and also encourage wildlife activity that leaves behind fecal deposits. It is the author's understanding that the positive correlation in these results between temperature and EC EMC is a result of the fostered incubation and increased wildlife activity during warmer days. The other environmental factors of rainfall depth and antecedent moisture conditions were not correlated with log of EC EMC at any of the GI outlets.

DOC EMC of the GI outlets were also significantly positively correlated with the log of EC EMC, suggesting EC significance in the carbon cycle in freshwater. These positive correlations ranged from 10% to 35% increases of EC concentration for every 1 mg/L increase of DOC (Table 4.2). The GI systems in this study were regularly exporting DOC as well (Burgis et al. 2020b), potentially a result of EC presence. Dissolved organic content is regularly associated with increased levels of bacteria in freshwater, though most studies showing this have used freshwater systems such as lakes rather than flowing stormwater. Regardless, the behavior of heterotrophic bacteria such as EC remains the same with its demands of energy sources that DOC can provide (Rippy 2015; Kawasaki et al. 2013; Kinnaman et al. 2012). Furthermore, electrosteric repulsive forces of DOC can prevent bacterial sorption to filter media (Aryal et al. 2012; Anesio et al. 2004), decreasing its removal rates in stormwater management systems. In their study on Lake Kasumigaura in Japan, Kawasaki et al. (2013) determined that bacteria can contribute to the pool of recalcitrant carbon given its propensity to both consume carbon and release it in die-off. If fecal contamination is introducing bacteria that ultimately adds to the pool of recalcitrant carbon, it may have a larger impact on the carbon cycle than previously believed and mitigation methods should be researched further.

TDN and EC at each swale outlet were significantly positively correlated such that EC EMC increased between 169% and >2000% for every 1 mg/L increase of TDN (Table 4.2). This finding is contrary to that of Hathaway et al. (2010) who found no significant relationship between fecal contamination and nitrogen, though nitrogen was measured as Total Kjeldahl Nitrogen and no stormwater management techniques were in use. The swales were also regularly exporting TDN during the study period with increases of EMC with increases as much as 400% in some events. However, even though TDN was typically exported, all of the measured concentrations were below 1 - 2 mg/L and not concerning in and of themselves. Like carbon, nitrogen is also assimilated by EC (Bren et al. 2016), so increased concentrations of EC could be expected in the presence of greater concentrations of TDN. Evidence of nitrogen assimilation by plants and microorganisms was identified with nitrogen isotopes by a concurrent study at this site (Burgis et al. 2020b). This positive correlation between TDN and EC concentration indicates that EC could have a significant impact on or be impacted by the nitrogen cycle within GI.

Chloride EMC was found to have significant inverse correlation with EC EMC at the outlets of the BR, GC, and CAGC, but not the BS (Table 4.2). While these correlations were significant, the slopes were small with changes between -0.1% and -3% for every 1 mg/L increase of chloride. The chloride detected at the site mostly resulted from road salt applications which occur during the colder months (Burgis et al. 2020a), so it is possible that this inverse correlation is also attributable to the impact of temperature previously confirmed. Regardless, other studies have examined the relationship between salinity and bacterial survival and found that the relationship is dependent on several factors such as nutrient availability and temperature of the water, but high levels of salinity are generally antagonistic towards survival of EC (Endreny et al. 2012; Hrenovic and Ivankovic 2009; Anderson et al 1979).

The negative charge of bacteria would be attracted to any positive charged suspended particles (such as iron-rich media), so a correlation between suspended solids (positively charged) and EC

concentration could be expected (Wright Water Engineers 2010), but no such correlation was determined at the outlets for any of the GI systems in this study. In Hathaway et al. (2010), similar results were found in the untreated runoff monitored in North Carolina, USA. EC is rod-shaped and is typically 1 – 2 μm in length and 0.5 μm in width (NRC (US) 1999), approximately the same width as the pores of the filters used to measure TSS in this study and close to the limit for the definition of suspended particles. A smaller pore size for the TSS analysis (such as the 0.2 μm typically used for bacteria analysis) may have resulted in a correlation between the two parameters, but would have included dissolved constituents as well as suspended particles.

4.5.4 Water Quality Improvements: Concentration Reductions

In spite of the relatively high EC EMC as inflow, the BR significantly reduced EMC at its outlet for these monitored events (Table 4.1). The overall average percent reduction of EMC (\pm SD) was $-91 \pm 601\%$, but temporarily removing the event on October 17, 2019 which had over 2000% increase of concentration gives a positive average concentration reduction of $46 \pm 47\%$. This value is lower than Hunt et al. (2008) which found a reduction of 70% but between the two bioretentions studied in Hathaway et al. (2011) which ranged from -120% to 89% with the deeper of the two basins studied removing more EC. The mechanisms for reducing EC concentrations were not explored in this present study, but other studies have attributed it to desiccation, physical filtration (Abel et al. 2014), and predation by protozoa (Zhang et al. 2011). Kim et al. (2012) showed that longer hydraulic residence times were also associated with EC removal through increased opportunities for surface sorption and straining. The BR has demonstrated substantial hydraulic residence times (12 – 24 hours) through its extended ponding times in its basin and forebay and constant baseflow (Hayes et al. Forthcoming), so this is primarily attributed for its positive reductions. While the ponding in the BR forebay and basin encourages EC capture, it also is allowing EC to traverse the thin vadose zone to the groundwater table. Thin vadose zones such as what is present at this BR have been shown to transfer bacteria from

stormwater flows to groundwater (Voisin et al. 2018). However, conditions in the groundwater are typically not hospitable for EC survival due to temperature and competition for food sources (USGS 2017), so concentrations are expected to remain low or reduce to zero if no further infiltration from the surface occurs.

The flow path from the BR inlet to its outlet provides several opportunities for decreasing EC presence that is not available in the flow path from its inlet to its bypass. The path to the bypass is partially vegetated but primarily consists of rip-rap for large debris capture, providing very little opportunity for die-off or capture of bacteria. Furthermore, the total distance from the inlet to the bypass is approximately 15 m of surface flow while the distance from the inlet to the outlet at minimum is 30 m of surface flow as well as 1 m of vertical drainage to the underdrain. This lack of treatment explains why the EMC at the bypass was statistically similar to the EMC at the inlet.

For the monitored events, the three swales each increased the EMC significantly from the road runoff to their outflows (Table 4.2). These results are somewhat contrary to Mallin et al. (2016), where the swales reduced fecal contamination concentration, though not statistically significantly due to high variability. Furthermore, the Mallin et al. (2016) study was conducted using grab samples, which introduced some uncertainty. The increases in concentrations at the Lorton swales could be resulting from several causes such as EC reproduction, fresh deposits of EC within the swale structure, a decrease in volume with no organism capture, or a combination of all these. Given the relatively large footprints of the swales compared to the BR (Chapter 2), there is greater opportunity for EC deposits within their structures than for the BR, causing outflows high in EC.

Hunt et al. (2012) and Mohanty et al. (2013) also found that bacteria could be resuspended or remobilized in subsequent flow, resulting in a release of previously captured organisms. The swales in this present study have been shown to perform better as flow conduits rather than treatment devices (Chapter 2), so if there are deposits of fecal contamination within the swale structure, increases in EMC

would be expected. If the flow of runoff were slowed to a greater extent within the swales through smaller slopes and taller, denser vegetation, it could potentially provide more time for settling, filtration, and desiccation on the swale surface, as suggested by Barrett et al. (1998).

4.5.5 Water Quality Improvements: Load Reductions

The BR reduced both volume of runoff and EC EMC, resulting in significant reduction of EC loads (Table 4.1). This result is consistent with Li and Davis (2009) which reported median values near complete reductions in their two BR systems. The volume reductions of the swales, while generally positive, were not large enough to decrease loading, though, due to significant increases in EMC. Therefore, none of the swales achieved significant load reductions (Table 4.1). In fact, the EMC increases in the swales were so large that the average load “reductions” trended negatively (though not statistically significantly), which ultimately exported EC. Because this study only sampled from events which produced measurable outflow, the annual load reductions are likely greater than these, at least for the swales. Generally, the swales have 100% volume reduction in rain events of approximately 10 mm or less (approximately one-quarter of annual rain events at Lorton (Chapter 2), which translates to a complete removal of EC. Regardless, it is important to know that when there was outflow from the swales, EC was being exported.

VDOT MS4 requirements for Fairfax County include load reduction of bacteria in the Occoquan watershed of 94% or 6.8×10^{11} colony forming units per year (Fairfax County 2017). The net removal of EC by the BR during the study period was similar to the MS4 requirement at 6.4×10^{10} MPN but the swales *produced* 3.3×10^8 – 5.9×10^8 MPN even though their average load reductions were not statistically different from zero. It is important to note that these net capture and releases of bacteria are only from individual GI systems, not the entire watershed, since the effects of a single system are less distinct on a larger scale. However, the magnitude of organisms released, particularly from the swales, may create a point source of EC, particularly if the system operates with a single outflow channel such as those

examined at Lorton Road. While the swales in this study do deposit into BR systems for further treatment, this study has shown that even the concentrations of EC leaving a BR system can be too high. The possibility of GI systems acting as point sources for EC may require regulatory action such as placing GI systems with single, channelized outflows in areas that avoid outflowing directly into waterways or including outflow concentration limits in MS4 plans. Determining the impact of EC export from GI on a watershed-scale is suggested for further research.

4.5.6 Comparing Performances

Nine events were shared between the four studied GI systems, so direct comparisons of the systems are limited, but still possible. Directly comparing the GI systems provides insight into performance with respect to shared environmental conditions because the contributing drainage areas of the BR and swales differed greatly, creating different inflow concentrations and loading. These nine shared events were mostly during the cold seasons with two in a warmer season, but the averages and ranges of depths of event rainfall and antecedent rainfall are similar to the whole datasets of each individual GI (Table 4.3). For EMC reductions of this subset of shared monitored events, the BR EMC reductions were significantly greater than any of the swales while the swales themselves did not significantly differ between each other with their negative average reductions. The BR reduced EC EMC relatively well in spite of its high inflow EMC values and contributing drainage area which fosters EC deposits and reproduction. There were differences in loading reductions, though, such that the BS was equivalent to the BR, which both in turn, were greater than the two grass channels (BR = BS > CAGC = GC). The relatively high loading reduction of the BS is attributed to its volume reduction because its EMC reductions were mostly negative like the two grass channels.

4.6 CONCLUSION

In this field study, the export of fecal contamination by four types of GI systems was characterized using flow-weighted composite sampling and *E. coli* (EC) as the fecal indicator bacteria. Each GI system

was monitored for 12 – 19 events in all seasons for two years. Geometric means of outflow concentrations of each GI were above recreational water quality criteria established by the US EPA and were significantly positively correlated with average daily temperature and dissolved organic carbon. Total dissolved nitrogen was significantly positively correlated with the outflows of the three swales while chloride was significantly inversely correlated with all systems except for the bioswale. Overall, GI mitigation of EC varied widely, but correlations of EC event mean concentrations with key water quality and environmental parameters provides insight into optimizing future GI designs. Even with the high concentration of EC outflow, the bioretention significantly reduced EC EMC and load. The swales each significantly increased EC EMC, but had no significant mass load changes. The levels of EC detected at the GI outlets may be indicative of point-sources of EC that are not sufficiently treated.

The Lorton field site will remain active until the spring of 2022, so monitoring of EC will continue until that time. Future studies should evaluate the fecal contamination on the watershed-scale where GI systems are used to identify compliance with MS4 requirements.

4.7 REFERENCES

- Abel, Chol D.T., Saroj K. Sharma, Selamwit A. Mersha, and Maria D. Kennedy. 2014. "Influence of Intermittent Infiltration of Primary Effluent on Removal of Suspended Solids, Bulk Organic Matter, Nitrogen and Pathogens Indicators in a Simulated Managed Aquifer Recharge System." *Ecological Engineering* 64 (March): 100–107. <https://doi.org/10.1016/j.ecoleng.2013.12.045>.
- Anderson, Iris C, Martha Rhodes, and Howard Kator. 1979. "Sublethal Stress in Escherichia Coli: A Function of Salinity." *APPL. ENVIRON. MICROBIOL.* 38: 6.
- Anesio, Alexandre M., Christin Hollas, Wilhelm Granéli, and Johanna Laybourn-Parry. 2004. "Influence of Humic Substances on Bacterial and Viral Dynamics in Freshwaters." *Applied and Environmental Microbiology* 70 (8): 4848–54. <https://doi.org/10.1128/AEM.70.8.4848-4854.2004>.
- Aryal, R, J P S Sidhu, M N Chong, S Toze, J Keller, and W Gernjak. 2012. "Inter-Storm Dissolved Organic Matter Variability and Its Role in Microbial Transport during Urban Runoff Events." In , 8. Melbourne, VIC Australia: Barton, ACT Australia: Engineers Australia.
- Barrett, Michael E., Patrick M. Walsh, Joseph F. Malina, and Randall J. Charbeneau. 1998. "Performance of Vegetative Controls for Treating Highway Runoff." *Journal of Environmental Engineering* 124 (11): 1121–28. [https://doi.org/10.1061/\(ASCE\)0733-9372\(1998\)124:11\(1121\)](https://doi.org/10.1061/(ASCE)0733-9372(1998)124:11(1121)).
- Bren, Anat, Junyoung O. Park, Benjamin D. Towbin, Erez Dekel, Joshua D. Rabinowitz, and Uri Alon. 2016. "Glucose Becomes One of the Worst Carbon Sources for E.Coli on Poor Nitrogen Sources Due to Suboptimal Levels of CAMP." *Scientific Reports* 6 (1). <https://doi.org/10.1038/srep24834>.

- Brown, Jeffrey S., Eric D. Stein, Drew Ackerman, John H. Dorsey, Jessica Lyon, and Patrick M. Carter. 2013. "Metals and Bacteria Partitioning to Various Size Particles in Ballona Creek Storm Water Runoff." *Environmental Toxicology and Chemistry* 32 (2): 320–28. <https://doi.org/10.1002/etc.2065>.
- Brumley, Jessica, Christopher Marks, Alexis Chau, Richard Lowrance, Junqi Huang, Cassie Richardson, Steven Acree, Randall Ross, and Douglas Beak. 2018. "The Influence of Green Infrastructure Practices on Groundwater Quality: The State of the Science." EPA/600/R-18/227.
- Burgis, Charles, Gail M. Hayes, Derek Henderson, Wuhuan Zhang, and James A. Smith. 2020a. "Green Stormwater Infrastructure Buffers Surface Water from Deicing Salt Loading." *Science of The Total Environment* 729: 138736. <https://doi.org/10.1016/j.scitotenv.2020.138736>.
- Burgis, Charles, Gail M Hayes, Wuhuan Zhang, Derek Henderson, and James A. Smith. 2020b. "Tracking Denitrification in Green Stormwater Infrastructure with Dual Nitrate Stable Isotopes." *Science of The Total Environment*. <https://doi.org/10.1016/j.scitotenv.2020.141281>.
- Chandrasena, G. I., A. Deletic, and D. T. McCarthy. 2014. "Survival of Escherichia Coli in Stormwater Biofilters." *Environmental Science and Pollution Research* 21 (8): 5391–5401. <https://doi.org/10.1007/s11356-013-2430-2>.
- DEQ. 2011a. "Bioretention." Stormwater Design Specification 9. VA Department of Environmental Quality. http://www.vwrrc.vt.edu/swc/documents/2013/DEQ%20BMP%20Spec%20No%209_BIORETENTION_FinalDraft_v1-9_03012011.pdf.
- DEQ. 2011b. "Dry Swales." Stormwater Design Specification 10. VA Department of Environmental Quality. http://www.vwrrc.vt.edu/swc/documents/2013/DEQ%20BMP%20Spec%20No%2010_DRY%20SWALE_Final%20Draft_v1-9_03012011.pdf.
- DEQ. 2011c. "Grass Channels." Stormwater Design Specification 3. VA Department of Environmental Quality. http://www.vwrrc.vt.edu/swc/documents/2013/DEQ%20BMP%20Spec%20No%203_GRASS%20CHANNELS_Final%20Draft_v1-9_03012011.pdf.
- Dietz, Michael, and Chester Arnold. 2018. "Can Green Infrastructure Provide Both Water Quality and Flood Reduction Benefits?" *Journal of Sustainable Water in the Built Environment* 4 (2): 02518001. <https://doi.org/10.1061/JSWBAY.0000856>.
- Endreny, Theodore, David J. Burke, Kathleen M. Burchhardt, Mark W. Fabian, and Annette M. Kretzer. 2012. "Bioretention Column Study of Bacteria Community Response to Salt-Enriched Artificial Stormwater." *Journal of Environmental Quality* 41 (6): 1951–59. <https://doi.org/10.2134/jeq2012.0082>.
- Fairfax County. 2017. "Bacteria TMDL Action Plan: Final Submittal to DEQ." TMDL Permit VA0088587.
- Ford, Clay. 2018. "Interpreting Log Transformations in a Linear Model." University of Virginia Library: Research Data Services + Sciences. August 17, 2018. <https://data.library.virginia.edu/interpreting-log-transformations-in-a-linear-model/>.
- Gavrić, Snežana, Günther Leonhardt, Jiri Marsalek, and Maria Viklander. 2019. "Processes Improving Urban Stormwater Quality in Grass Swales and Filter Strips: A Review of Research Findings." *Science of The Total Environment* 669 (June): 431–47. <https://doi.org/10.1016/j.scitotenv.2019.03.072>.
- Hathaway, J. M., W. F. Hunt, A. K. Graves, and J. D. Wright. 2011. "Field Evaluation of Bioretention Indicator Bacteria Sequestration in Wilmington, North Carolina." *Journal of Environmental Engineering* 137 (12): 1103–13. [https://doi.org/10.1061/\(ASCE\)EE.1943-7870.0000444](https://doi.org/10.1061/(ASCE)EE.1943-7870.0000444).
- Hathaway, J. M., W. F. Hunt, R. M. Guest, and D. T. McCarthy. 2014. "Residual Indicator Bacteria in Autosampler Tubing: A Field and Laboratory Assessment." *Water Science and Technology* 69 (5): 1120–26. <https://doi.org/10.2166/wst.2014.035>.

- Hathaway, J. M., W. F. Hunt, and O. D. Simmons. 2010. "Statistical Evaluation of Factors Affecting Indicator Bacteria in Urban Storm-Water Runoff." *Journal of Environmental Engineering* 136 (12): 1360–68. [https://doi.org/10.1061/\(ASCE\)EE.1943-7870.0000278](https://doi.org/10.1061/(ASCE)EE.1943-7870.0000278).
- Hayes, Gail M., Charles R. Burgis, Wuhuan Zhang, Derek Henderson, and James A. Smith. Forthcoming. "Runoff Reduction by Four Green Stormwater Infrastructure Systems in a Shared Environment." *Journal of Sustainable Water in the Built Environment*. <https://doi.org/10.1061/JSWBAY.0000932>.
- Hrenovic, Jasna, and Tomislav Ivankovic. 2009. "Survival of Escherichia Coli and Acinetobacter Junii at Various Concentrations of Sodium Chloride." *EurAsian Journal of Biosciences*, no. 3 (December): 144–51. <https://doi.org/10.5053/ejobios.2009.3.0.18>.
- Hunt, W. F., J. T. Smith, S. J. Jadlocki, J. M. Hathaway, and P. R. Eubanks. 2008. "Pollutant Removal and Peak Flow Mitigation by a Bioretention Cell in Urban Charlotte, N.C." *Journal of Environmental Engineering* 134 (5): 403–8. [https://doi.org/10.1061/\(ASCE\)0733-9372\(2008\)134:5\(403\)](https://doi.org/10.1061/(ASCE)0733-9372(2008)134:5(403)).
- Hunt, William F., Allen P. Davis, and Robert G. Traver. 2012. "Meeting Hydrologic and Water Quality Goals through Targeted Bioretention Design." *Journal of Environmental Engineering* 138 (6): 698–707. [https://doi.org/10.1061/\(ASCE\)EE.1943-7870.0000504](https://doi.org/10.1061/(ASCE)EE.1943-7870.0000504).
- Jeng, Hueiwang C., Andrew England, and Henry B. Bradford. 2005. "Indicator Organisms Associated with Stormwater Suspended Particles and Estuarine Sediment." *Journal of Environmental Science and Health, Part A* 40 (4). <https://pubmed.ncbi.nlm.nih.gov/15792299/>.
- Jetten, Mike S. M. 2008. "The Microbial Nitrogen Cycle." *Environmental Microbiology* 10 (11): 2903–9. <https://doi.org/10.1111/j.1462-2920.2008.01786.x>.
- Kawasaki, Nobuyuki, Kazuhiro Komatsu, Ayato Kohzu, Noriko Tomioka, Ryuichiro Shinohara, Takayuki Satou, Fumiko Nara Watanabe, et al. 2013. "Bacterial Contribution to Dissolved Organic Matter in Eutrophic Lake Kasumigaura, Japan." *Applied and Environmental Microbiology* 79 (23): 7160–68. <https://doi.org/10.1128/AEM.01504-13>.
- Kim, Myung Hee, Chan Yong Sung, Ming-Han Li, and Kung-Hui Chu. 2012. "Bioretention for Stormwater Quality Improvement in Texas: Removal Effectiveness of Escherichia Coli." *Separation and Purification Technology* 84 (January): 120–24. <https://doi.org/10.1016/j.seppur.2011.04.025>.
- Kinnaman, Alison R., Cristiane Q. Surbeck, and Danielle C. Usner. 2012. "Coliform Bacteria: The Effect of Sediments on Decay Rates and on Required Detention Times in Stormwater BMPs." *Journal of Environmental Protection* 03 (08): 787–97. <https://doi.org/10.4236/jep.2012.328094>.
- Krometis, Leigh-Anne H., Gregory W. Characklis, Otto D. Simmons III, Mackenzie J. Dilts, Christina A. Likirdopulos, and Mark D. Sobsey. 2007. "Intra-Storm Variability in Microbial Partitioning and Microbial Loading Rates." *Water Research* 41 (2): 506–16. <https://doi.org/10.1016/j.watres.2006.09.029>.
- Li, Houng, and Allen P. Davis. 2009. "Water Quality Improvement through Reductions of Pollutant Loads Using Bioretention." *Journal of Environmental Engineering* 135 (8): 567–76. [https://doi.org/10.1061/\(ASCE\)EE.1943-7870.0000026](https://doi.org/10.1061/(ASCE)EE.1943-7870.0000026).
- Mallin, Michael A., Mary I.H. Turner, Matthew R. McIver, Byron R. Toothman, and Hunter C. Freeman. 2016. "Significant Reduction of Fecal Bacteria and Suspended Solids Loading by Coastal Best Management Practices." *Journal of Coastal Research* 320 (July): 923–31. <https://doi.org/10.2112/JCOASTRES-D-15-00195.1>.
- McCarthy, D.T., A. Deletic, V.G. Mitchell, T.D. Fletcher, and C. Diaper. 2008. "Uncertainties in Stormwater E. Coli Levels." *Water Research* 42 (6–7): 1812–24. <https://doi.org/10.1016/j.watres.2007.11.009>.
- Mohanty, Sanjay, Andrew Torkelson, Hanna Dodd, and Kara Nelson. 2013. "Engineering Solutions to Improve the Removal of Fecal Indicator Bacteria by Bioinfiltration Systems during Intermittent Flow of Stormwater." *Environmental Science & Technology* 47: 10791–98.

- NRC (US). 1999. "Size Limits of Very Small Microorganisms: Proceedings of a Workshop." Workshop Proceedings. National Research Council (US) Steering Group for the Workshop on Size Limits of Very Small Microorganisms. <https://www.ncbi.nlm.nih.gov/books/NBK224751/>.
- Petersen, T. M., H. S. Rifai, M. P. Suarez, and A. R. Stein. 2005. "Bacteria Loads from Point and Nonpoint Sources in an Urban Watershed." *Journal of Environmental Engineering-Asce* 131 (10): 1414–25. [https://doi.org/10.1061/\(ASCE\)0733-9372\(2005\)131:10\(1414\)](https://doi.org/10.1061/(ASCE)0733-9372(2005)131:10(1414)).
- Rippy, Megan A. 2015. "Meeting the Criteria: Linking Biofilter Design to Fecal Indicator Bacteria Removal: Linking Biofilter Design to FIB Removal." *Wiley Interdisciplinary Reviews: Water* 2 (5): 577–92. <https://doi.org/10.1002/wat2.1096>.
- USEPA. 2012. "Recreational Water Quality Criteria." 820-F-12–058. Environmental Protection Agency: Office of Water.
- USGS. 2017. "Bacteria and Their Effects on Ground-Water Quality." USGS: Science for a Changing World. January 2017. <https://mi.water.usgs.gov/h2oqual/GWBactHOWeb.html>.
- VDOT. 2018. "Average Daily Traffic Volumes with Vehicle Classification Data on Interstate, Arterial, and Primary Routes." Virginia Department of Transportation. http://www.virginiadot.org/info/resources/Traffic_2018/AADT_PrimaryInterstate_2018.pdf.
- Voisin, Jérémy, Benoit Cournoyer, Antonin Vienney, and Florian Mermillod-Blondin. 2018. "Aquifer Recharge with Stormwater Runoff in Urban Areas: Influence of Vadose Zone Thickness on Nutrient and Bacterial Transfers from the Surface of Infiltration Basins to Groundwater." *Science of The Total Environment* 637–638 (October): 1496–1507. <https://doi.org/10.1016/j.scitotenv.2018.05.094>.
- Willard, L. L., T. Wynn-Thompson, L. H. Krometis, T. P. Neher, and B. D. Badgley. 2017. "Does It Pay to Be Mature? Evaluation of Bioretention Cell Performance Seven Years Postconstruction." *Journal of Environmental Engineering* 143 (9): 04017041. [https://doi.org/10.1061/\(ASCE\)EE.1943-7870.0001232](https://doi.org/10.1061/(ASCE)EE.1943-7870.0001232).
- Wright Water Engineers, Inc. 2010. "International Stormwater Best Management Practices (BMP) Database: Pollutant Category Summary: Fecal Indicator Bacteria." International Stormwater BMP Database. <http://www.bmpdatabase.org/Docs/BMP%20Database%20Bacteria%20Paper%20Dec%202010.pdf>.
- Zhang, Kun, and Ting Fong May Chui. 2019. "A Review on Implementing Infiltration-Based Green Infrastructure in Shallow Groundwater Environments: Challenges, Approaches, and Progress." *Journal of Hydrology* 579 (December): 124089. <https://doi.org/10.1016/j.jhydrol.2019.124089>.
- Zhang, Lan, Eric A. Seagren, Allen P. Davis, and Jeffrey S. Karns. 2011. "Long-Term Sustainability of *Escherichia Coli* Removal in Conventional Bioretention Media." *Journal of Environmental Engineering* 137 (8): 669–77. [https://doi.org/10.1061/\(ASCE\)EE.1943-7870.0000365](https://doi.org/10.1061/(ASCE)EE.1943-7870.0000365).

5. Dissertation Conclusions

Green infrastructure (GI) is a widely used stormwater management technique, but there are still knowledge gaps on in situ performance of GI systems in the mitigation of runoff volume and contaminants. This dissertation addressed these knowledge gaps by characterizing the water quality and water quantity improvements of four green infrastructure (GI) systems used in roadside stormwater management. The four analyzed GI systems, a bioretention (BR), bioswale (BS), compost-amended grass channel (CAGC), and a grass channel (GC), were within 1 km of each other along Lorton Road in Fairfax County, VA. Total runoff volume reduction was measured for each system for its first year of operation. Analyses of water quality improvements included identifying the potential mobilizing impacts of road salts on trace metals and also quantifying the mitigation of fecal contamination.

The runoff volume study showed that in their first full year of operation, the GI systems all reduced runoff volume by 43% – 78% such that the GC had the highest reduction, followed by the BR, BS, and CAGC. However, the BR had predictably large volume reductions in most events, making it a good choice where space allows and high loading ratios are required. The BR also showed the narrowest variation in runoff reduction as it was uninfluenced by event rainfall depth and marginally so by season. The GC also showed minimal influence from seasonality but, like the other two swales, its volume reductions were significantly influenced by rainfall depth. The simple design of the GC in combination with its relatively high runoff reductions shows that it would be a good stormwater management choice over swales with more complex designs such as the BS and CAGC. While the GC could be a good replacement for piped infrastructure, the BR is a promising solution for larger spaces where the ratio of contributing drainage area to footprint is large. Suggestions for future research include analyzing performance with respect to the age of the GI system as well as maintenance costs and performance benefits.

The study on the interactions of trace metals (chromium, copper, nickel, and lead) and road salts (primarily sodium chloride) showed little evidence that metals were mobilized from the GI soils during

the monitoring period in the stormwater, soil, and groundwater analyses. The influent metal concentrations in the stormwater were typically very low, so irreducible concentrations were likely reached or nearly reached, causing consistently negative EMC reductions, regardless of salt content. Over the winter of 2019 – 2020, some deposition of road salt was found in the soils, but increases were not significant. Over this same period, metal content of the soils did not decrease but mulch metal content fell significantly. There was no evidence that road salts displaced metals from the soils, though the loading of salt over the sampling period was possibly too small to make a difference. It is recommended to replace mulch in BR systems prior to winter to avoid release of metals as the mulch decomposes or comes into contact with high salt flows. The groundwater did show surges in road salt in two wells in conjunction with a wintry event, but there was no corresponding detectable surge in metal content of those wells. Future research is suggested that uses increased frequency of groundwater testing immediately following a wintry event to capture small and quick changes in groundwater chemistry resulting from road salt intrusion.

The fecal contamination study revealed that the BR significantly reduced *E. coli* (EC) EMC and loading in spite of its high inflow concentrations. However, the swales (even with low inflow concentrations) had consistently negative reductions, indicating that their footprints were potential sources of the contamination. Correlations between outflow EC concentrations and temperature, dissolved organic carbon, and total dissolved nitrogen imply predictability of EC in the GI outflows. These patterns in GI outflow quality also indicate a significance with the carbon and nitrogen cycles that was previously underappreciated in the stormwater community. Suggestions for future research include analyzing GI systems on the watershed scale to determine significance in EC outflow concentrations and adherence to government water quality requirements.

Increases in urbanization as well as climate change make it essential to protect our waterways from pollution. Overall, this dissertation has shown that GI systems can be effective stormwater management

techniques through improvements in runoff volume and water quality. This dissertation addressed the important knowledge gap in comparing the volume reductions of various GI types, finding that simple designs often work as well if not better than more complex systems. Secondly, it addressed the conflicting results of current research on whether or not road salts can mobilize trace metals from GI systems, finding that in a climate such as Lorton Road, such an occurrence is unlikely. Lastly, it answered questions on fecal contamination using robust sampling methods not deployed on such a scale before, finding that some designs of GI systems might be sources of fecal contamination. Most significantly, this dissertation advanced our understanding of GI system operation, providing insight into their benefits and limitations. It is important to understand the capabilities of GI systems in order to adjust expectations and future designs to meet stormwater quality and quantity management needs.

6. Appendices

6.1 APPENDIX A: GI DESIGN DETAILS AND MONITORING METHODS

Fig. A.1, Fig. A.2, Fig. A.3, and Fig. A.4 are cut-away schematics of the grass channel, compost-amended grass channel, bioswale, and bioretention, respectively. Overland inflow is represented by triple arrows. These illustrations were created by Gail Hayes using Microsoft PowerPoint.

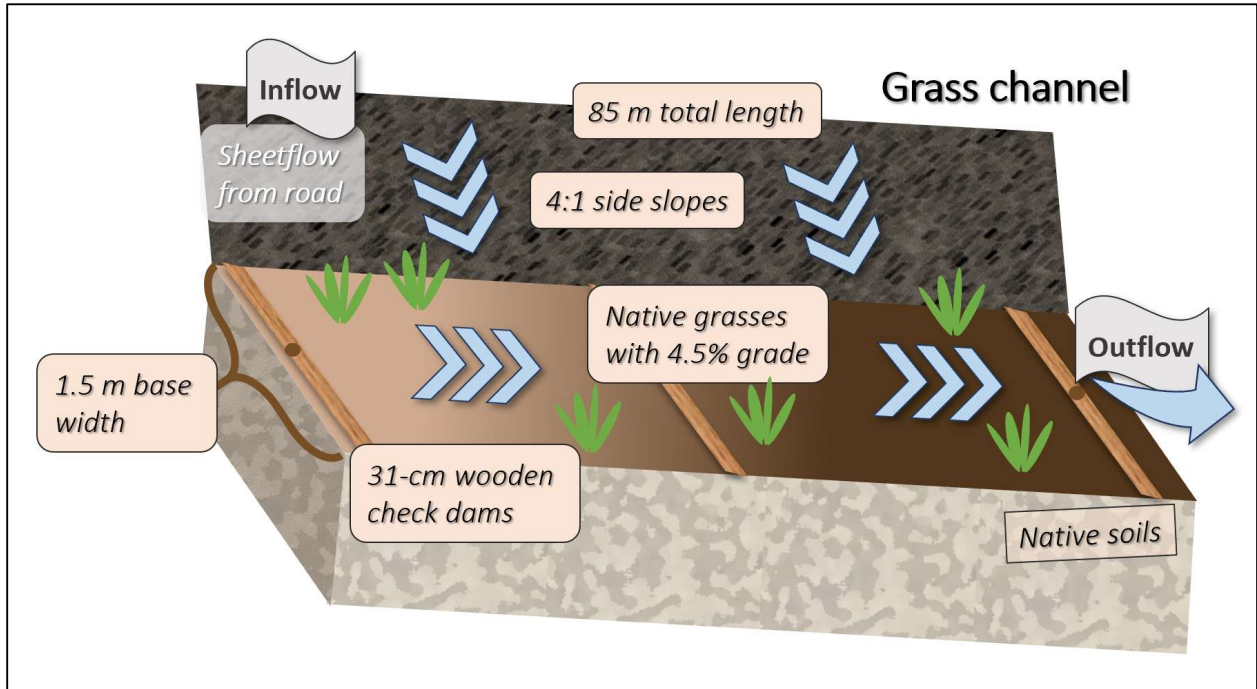


Figure A.1. Grass channel design and flow cut-away schematic.

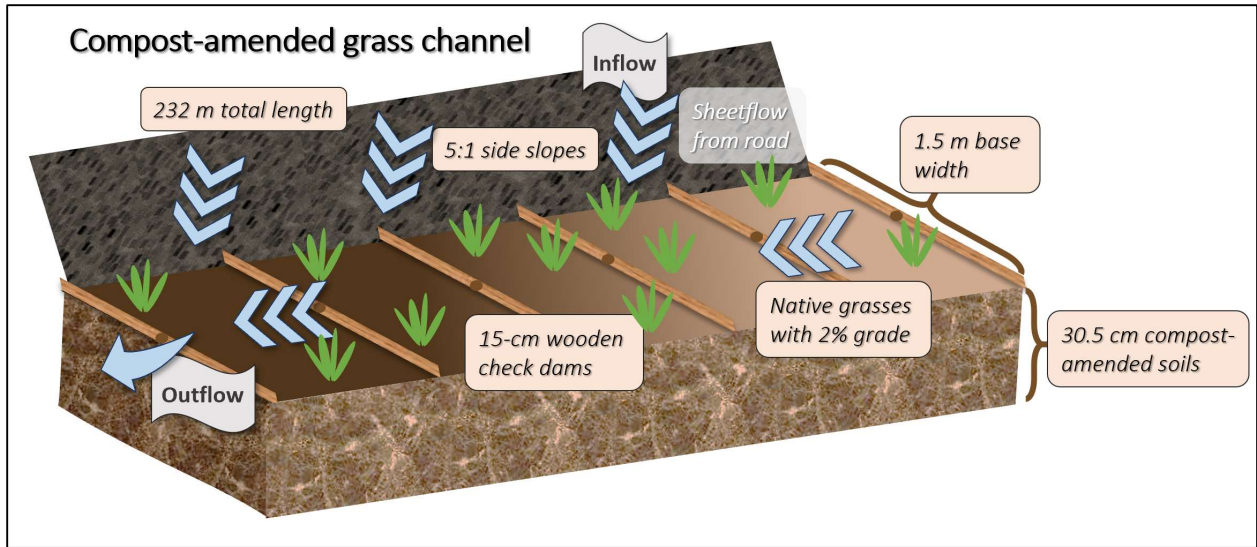


Figure A.2. Compost-amended grass channel design and flow cut-away schematic.

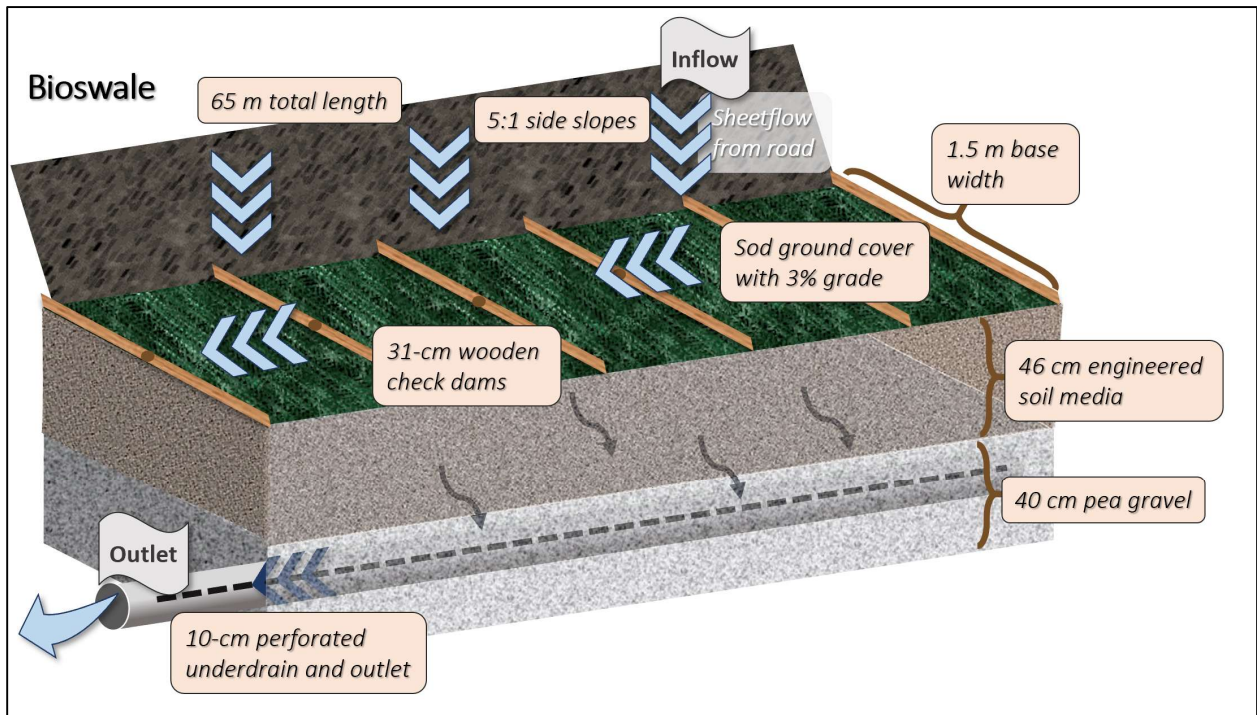


Figure A.3. Bioswale design and flow cut-away schematic.

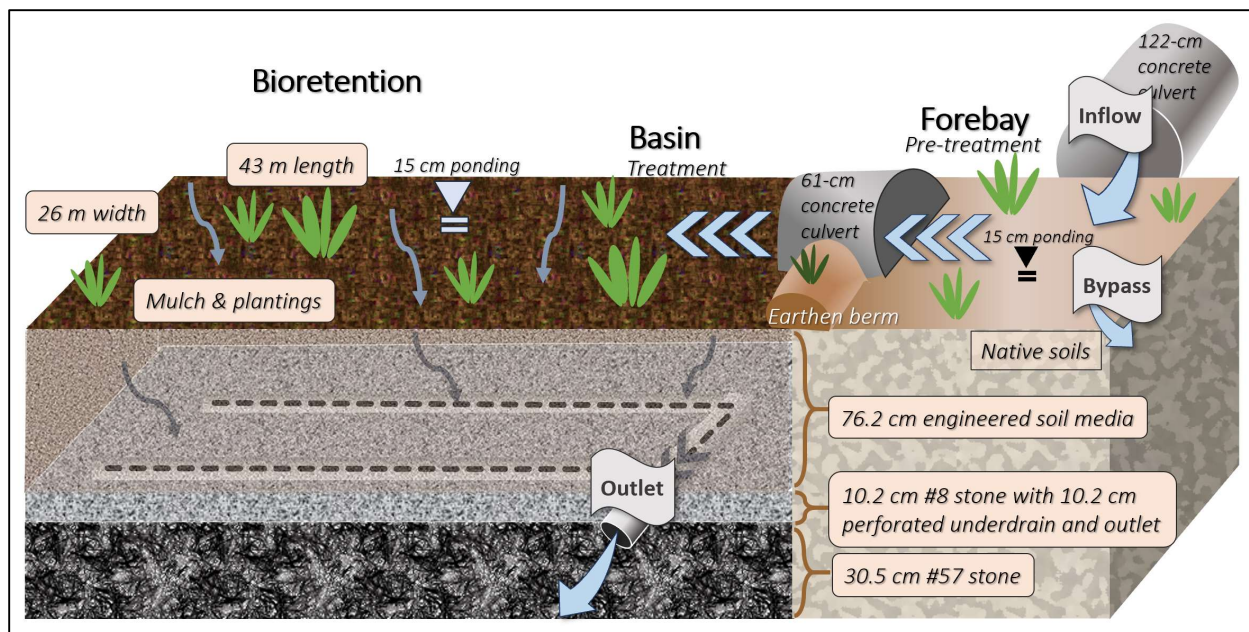


Figure A.4. Bioretention design and flow cut-away schematic.

Table A.1 lists vegetation types for each of the four monitored GI system. Swale vegetation was planted via seeding and the bioretention received plug planting additions. Not every plant is found in its respective system, but selections from the list are chosen.

Table A.1. Plantings for each GI system

Grass channel	Compost-amended grass channel	Bioswale	Bioretention
Common yarrow	Upland bentgrass	Upland bentgrass	Blue wild indigo
Partridge pea	Rough bentgrass	Deertongue	Marsh marigold
Lanceleaf tickseed	Partridge pea	Swamp milkweed	Fox sedge
Golden tickseed	Lanceleaf tickseed	Blue wild indigo	Cardinal flower
Sheep fescue	Deertongue	Squarrose sedge	Rough avens
Italian ryegrass	Purple coneflower	Fox sedge	Dense blazing star
Blackeyed susan	Canada wildrye	Indian woodoats	Talus slope penstemon
	Virginia wildrye	Lanceleaf tickseed	New England aster
	Dense blazing star	Purple coneflower	
	Italian ryegrass	Riverbank wildrye	
	Wild bergamot	Dense blazing star	
	Talus slope penstemon	Wild bergamot	
	Blackeyed susan	Talus slope penstemon	
	Little bluestem	Blackeyed susan	
	Indiangrass	Little bluestem	
	Purpletop tridens	American senna	
		Flat-top goldentop	
		New England aster	
		Bluejacket	
		Swamp verbena	
		Golden zizia	

Table A.2 lists the flow equations used for each type of flume that are provided by the flume manufacturer. “H flume” refers to the standard size flume while “HS flume” refers to the smaller, narrower flume. H refers to the height of water within the flume (m).

Table A.2. Flume flow equations

Flume type	Flow (L/s) =
0.12-m HS flume	$0.003086536 - 0.06693418 \times H^{0.5} + 12.33204684 \times H^{1.5} + 366.8872845 \times H^{2.5}$
0.15-m H Flume	$0.003171487 - 0.10001658 \times H^{0.5} + 28.15410639 \times H^{1.5} + 894.3863793 \times H^{2.5}$
0.2-m H flume	$0.014781694 - 0.30876915 \times H^{0.5} + 51.92697619 \times H^{1.5} + 1004.480343 \times H^{2.5}$
0.46-m H flume	$-0.00396436 - 0.07231968 \times H^{0.5} + 79.89379128 \times H^{1.5} + 900.3765227 \times H^{2.5}$
0.91-m H flume	$-0.01019406 - 0.10384217 \times H^{0.5} + 160.4613601 \times H^{1.5} + 891.4730165 \times H^{2.5}$

Fig. A.5 contains photographs of the overland flow collector gutter installed along Lorton Road. The overland flow collector consists of a 9-m HDPE-aluminum gutter that channels sheetflow to a monitoring station that is then extrapolated to compute inflow for each of the three swales.

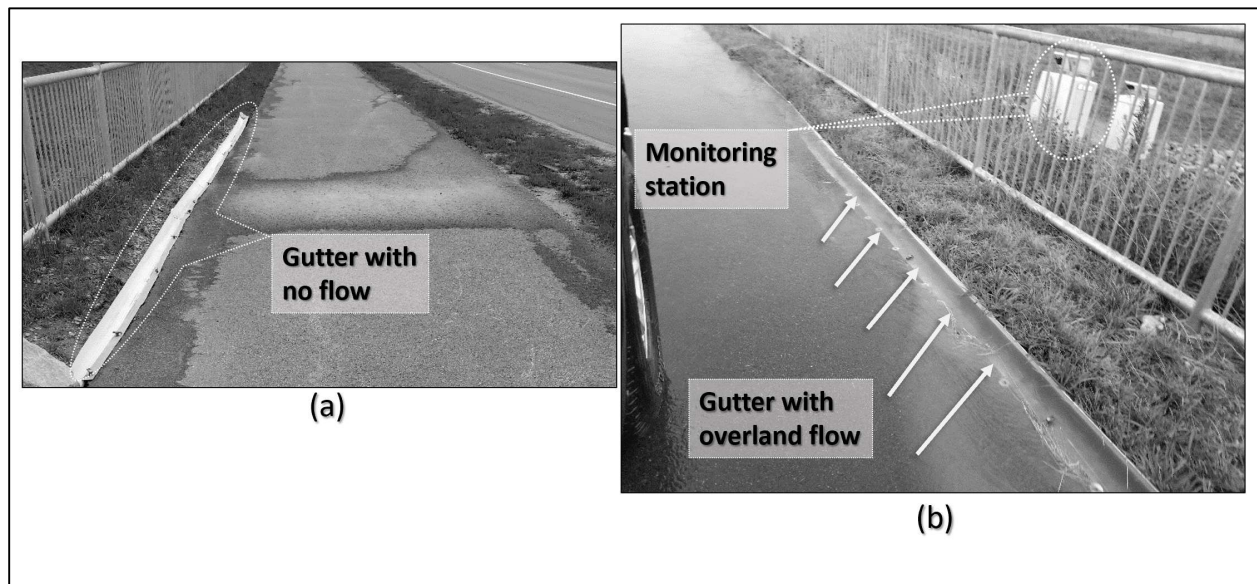


Figure A.5. Overland flow collector with 9-m aluminum-HDPE gutter connected to sampling station in no flow conditions (a) and flowing conditions (b)

6.4 APPENDIX B: FLOW DATA FOR REPORTED EVENTS

Table B.1 – B.5 presents the flow data for each monitored event. The superscript ^a of Table B.1 indicates flooding in the BS flume that was adjusted according to Appendix D. The flow values were adjusted to reflect baseflow and instrument sensitivity (low flow) (Appendix D) and swale inflow is split between pervious (CDA_p) and impervious (CDA_i) flow. Blanks indicate no data and – indicates the value measured was 0 or below the detection limit.

Table B.1. Rain data for each reported event and significant flow data from each monitoring station.

AMC = antecedent moisture conditions

Date	Depth (mm)	Duration (h)	Intensity (mm/h)	AMC (mm)	Antec. dry period (h)	Overland flow collector Peak flow (L/s)
6/2/2018	51.1	51.3	1.0	0.0	221	1.2
7/17/2018	7.9	7.7	1.0	4.1	452	1.1
7/20/2018	96.5	11.0	8.8	7.9	93	1.2
7/22/2018	38.1	18.0	2.1	104.4	15	0.9
7/23/2018	45.5	7.2	6.3	134.0	20	0.8
7/25/2018	49.8	3.9	12.9	179.0	30	0.9
7/30/2018	24.4	8.7	2.8	49.8	115	1.0
8/1/2018	13.5	6.5	2.1	24.4	20	1.8
8/2/2018	33.5	1.8	18.6	37.8	35	1.6
8/4/2018	8.4	11.0	0.8	71.4	25	1.8
8/21/2018	72.1	17.2	4.2	2.0	27	1.9
8/31/2018	72.6	7.5	9.7	0.3	237	1.7
9/2/2018	20.8	3.8	5.4	72.6	14	1.3
9/8/2018	28.4	1.3	21.3	1.0	140	1.6
9/9/2018	52.1	41.7	1.2	28.4	16	2.4
9/25/2018	70.9	59.8	1.2	19.8	145	0.6
9/26/2018	7.4	3.3	2.2	70.9	28	0.9
9/28/2018	39.9	18.8	2.1	43.4	18	1.4
10/11/2018	86.1	17.8	4.8	1.3	314	1.4
10/26/2018	39.6	21.2	1.9	0.0	135	1.3
11/10/2018	14.0	13.7	1.0	67.3	305	1.0
11/13/2018	32.0	12.7	2.5	14.5	70	0.7
11/15/2018	71.6	19.5	3.7	32.3	56	1.5
11/24/2018	47.0	6.0	7.8	0.0	194	1.2
11/26/2018	11.2	5.8	1.9	47.0	38	0.7
12/1/2018	8.4	19.2	0.4	0.5	119	0.1
1/19/2019	24.4	13.0	1.9	3.8	1140	1.9
1/25/2019	27.4	11.8	2.3	24.1	91	2.4
2/12/2019	15.2	35.0	0.4	0.8	90	0.6
2/24/2019	32.8	21.5	1.5	2.0	270	1.7
3/9/2019	11.9	7.5	1.6	16.3	326	2.4
3/21/2019	64.8	26.2	2.5	0.5	258	1.8
4/5/2019	7.9	17.8	0.4	7.9	338	0.4
4/8/2019	3.6	1.5	2.4	1.0	66	0.4
4/13/2019	16.0	19.8	0.8	8.1	90	1.1
4/15/2019	10.4	7.5	1.4	16.0	40	1.7
4/20/2019	10.4	11.7	0.9	4.1	102	1.9
4/26/2019	10.2	4.3	2.4	0.3	156	1.9
6/18/2019	19.1	5.5	3.5	36.6	1272	1.9
6/19/2019	2.8	7.8	0.4	44.2	17	1.0
6/25/2019	8.4	10.3	0.8	3.6	113	2.1
6/29/2019	9.4	19.7	0.5	10.9	109	0.9
7/2/2019	4.6	5.7	0.8	11.9	55	1.5
7/4/2019	6.6	6.2	1.1	13.7	41	0.5
7/6/2019	7.9	12.3	0.6	11.2	39	1.5
7/8/2019	19.1	6.8	2.8	14.5	28	1.6
7/11/2019	25.1	5.2	4.8	23.4	74	1.3
7/17/2019	23.6	6.3	3.7	0.0	140	1.8

Table B.2. Grass channel flow data

Date	Inflow: CDA _i (liters)	Inflow: CDA _p (liters)	Outflow (liters)	Peak Outflow (L/s)	% Volume Reduction
6/2/2018	204,130	-	24,150	2.50	88%
7/17/2018	46,749	-	-		100%
7/20/2018	299,472	4,876	86,536	15.20	72%
7/22/2018	27,175	13,649	2,450	1.50	94%
7/23/2018	37,681	20,025	46,495	25.30	19%
7/25/2018	57,679	24,067	28,059	9.20	66%
7/30/2018	78,415	-	1,239	0.83	98%
8/1/2018	120,990	-	2,672	2.00	98%
8/2/2018	66,501	378	35,830	23.70	46%
8/4/2018	67,973	-	27	0.05	100%
8/21/2018	84,213	447	41,124	30.64	51%
8/31/2018	182,535	492	87,617	41.50	52%
9/2/2018	115,942	2,468	23,436	4.20	80%
9/8/2018	26,500	-	11,505	7.80	57%
9/9/2018	301,270	-	53,552	3.40	82%
9/25/2018	112,782	14,898	100,094	4.10	22%
9/26/2018	30,063	-	770	0.40	97%
9/28/2018	117,500	15,121	48,172	4.90	64%
10/11/2018	198,616	2,447	49,067	19.40	76%
10/26/2018	134,795	-	27,072	0.90	80%
11/10/2018	30,103	324	15,155	1.30	50%
11/13/2018	111,612	217	40,960	1.74	63%
11/15/2018	323,770	46,953	75,110	2.80	80%
11/24/2018	158,345	-	52,803	4.60	67%
11/26/2018	29,568	16	17,037	1.80	42%
12/1/2018	19,849	-	2,146	0.10	89%
1/19/2019	151,953	-	17,304	1.50	89%
1/25/2019	203,507	0	16,462	2.10	92%
2/12/2019	87,626	-	13,144	1.00	85%
2/24/2019	122,987	-	26,821	5.20	78%
3/9/2019	172,527	-	5,334	1.20	97%
3/21/2019	288,965	33	59,096	4.40	80%
4/5/2019	7,632	-	422	0.04	94%
4/8/2019	4,466	-	492	0.06	89%
4/13/2019	45,394	-	721	0.04	98%
4/15/2019	52,221	-	1,165	0.20	98%
4/20/2019	45,788	-	1,117	0.04	98%
4/26/2019	26,725	-	412	0.04	98%
6/18/2019	42,642	-	5,116	3.89	88%
6/19/2019	24,290	-	-		100%
6/25/2019	45,653	-	-		100%
6/29/2019	17,218	-	-		100%
7/2/2019	12,195	-	-		100%
7/4/2019	13,938	-	-		100%
7/6/2019	28,387	-	-		100%
7/8/2019	39,180	-	-		100%
7/11/2019	47,029	-	1,006	0.11	98%
7/17/2019	35,134	-	37	0.06	100%

Table B.3. Compost-amended grass channel flow data

Date	Inflow: CDA _i (liters)	Inflow: CDA _p (liters)	Outflow (liters)	Peak Outflow (L/s)	% Volume Reduction
6/2/2018	196,721	-	137,119	9.40	30%
7/17/2018	45,052	-	-		100%
7/20/2018	288,602	16,830	222,946	25.40	27%
7/22/2018	26,188	47,109	20,619	3.00	72%
7/23/2018	36,313	69,114	180,162	61.90	-71%
7/25/2018	55,585	83,067	159,955	41.70	-15%
7/30/2018	75,569	-	17,600	4.95	77%
8/1/2018	116,599	-	20,968	4.41	82%
8/2/2018	64,087	1,306	110,122	17.10	-68%
8/4/2018	65,506	-	11,738	1.90	82%
8/21/2018	81,157	1,542	30,672	84.01	63%
8/31/2018	175,910	1,699	144,306	64.40	19%
9/2/2018	111,734	8,518	47,034	8.10	61%
9/8/2018	25,538	-	26,127	9.60	-2%
9/9/2018	290,336	-	109,155	6.60	62%
9/25/2018	108,689	51,419	184,408	9.20	-15%
9/26/2018	28,972	-	8,863	1.00	69%
9/28/2018	113,236	52,188	116,901	10.10	29%
10/11/2018	191,407	8,444	192,349	25.10	4%
10/26/2018	129,903	-	27,907	1.50	79%
11/10/2018	29,011	1,120	15,103	2.10	50%
11/13/2018	107,561	749	68,379	3.02	37%
11/15/2018	312,019	162,054	125,014	125.30	74%
11/24/2018	152,598	-	121,093	13.20	21%
11/26/2018	28,495	55	22,340	3.30	22%
12/1/2018	19,128	-	2,263	0.10	88%
1/19/2019	146,438	-	92,242	5.30	37%
1/25/2019	196,120	0	82,459	7.50	58%
2/12/2019	84,446	-	80,870	3.40	4%
2/24/2019	118,524	-	100,430	14.20	15%
3/9/2019	166,265	-	29,663	3.60	82%
3/21/2019	278,477	112	195,285	12.30	30%
4/5/2019	7,355	-	77	0.04	99%
4/8/2019	4,304	-	69	0.05	98%
4/13/2019	43,747	-	1,092	0.13	98%
4/15/2019	50,326	-	12,662	1.60	75%
4/20/2019	44,126	-	751	0.10	98%
4/26/2019	25,755	-	20	0.03	100%
6/18/2019	41,094	-	17,777	5.74	57%
6/19/2019	23,409	-	270	0.08	99%
6/25/2019	43,996	-	-		100%
6/29/2019	16,593	-	-		100%
7/2/2019	11,753	-	3,988	0.10	66%
7/4/2019	13,433	-	4,950	0.09	63%
7/6/2019	27,357	-	5,032	0.10	82%
7/8/2019	37,758	-	5,618	0.08	85%
7/11/2019	45,322	-	13,771	2.46	70%
7/17/2019	33,859	-	8,550	2.15	75%

Table B.4. Bioswale flow data. ^a Flood correction.

Date	Inflow: CDA _i (liters)	Inflow: CDA _p (liters)	Outflow (liters)	Peak Outflow (L/s)	% Volume Reduction
6/2/2018 ^a	204,227	-	152,112	10.80	26%
7/17/2018	46,771	-	43	0.04	100%
7/20/2018 ^a	299,614	-	158,652	16.40	47%
7/22/2018	27,188	721	15,098	2.70	46%
7/23/2018 ^a	37,699	2,462	81,105	24.10	-102%
7/25/2018 ^a	57,706	3,908	86,019	10.60	-40%
7/30/2018	78,452	-	2,864	3.80	96%
8/1/2018	121,048	-	18,322	2.52	85%
8/2/2018 ^a	66,532	-	59,712	6.30	10%
8/4/2018	68,005	-	8,968	0.96	87%
8/21/2018 ^a	84,253	-	53,670	6.30	36%
8/31/2018 ^a	182,621	-	35,156	9.94	81%
9/2/2018	115,997	-	23,759	3.10	80%
9/8/2018	26,512	-	13,021	4.66	51%
9/9/2018	301,413	-	67,372	4.80	78%
9/25/2018 ^a	112,836	61	178,809	6.10	-58%
9/26/2018	30,077	-	3,757	0.50	88%
9/28/2018	117,556	1,052	64,634	6.30	46%
10/11/2018	198,710	-	8,203	11.60	96%
10/26/2018	134,859	-	41,602	1.60	69%
11/10/2018	30,118	-	14,040	1.10	53%
11/13/2018	111,665	-	55,894	2.82	50%
11/15/2018 ^a	323,923	15,191	193,121	8.90	43%
11/24/2018 ^a	158,420	-	91,733	11.20	42%
11/26/2018	29,582	-	11,582	1.00	61%
12/1/2018	19,858	-	4,996	0.20	75%
1/19/2019	152,025	-	83,634	5.10	45%
1/25/2019 ^a	203,603	-	78,464	7.30	61%
2/12/2019	87,668	-	47,527	1.30	46%
2/24/2019 ^a	123,046	-	106,784	10.90	13%
3/9/2019	172,609	-	13,895	1.10	92%
3/21/2019 ^a	289,102	-	128,846	10.40	55%
4/5/2019	7,636	-	-		100%
4/8/2019 ^a	4,468	-	-		100%
4/13/2019	45,416	-	4,710	0.72	90%
4/15/2019	52,246	-	7,666	0.80	85%
4/20/2019	45,810	-	918	0.50	98%
4/26/2019	26,738	-	73	0.02	100%
6/18/2019	42,662	-	11,183	2.40	74%
6/19/2019	24,302	-	5,391	0.71	78%
6/25/2019	45,674	-	5,174	0.13	89%
6/29/2019	17,226	-	6,354	0.13	63%
7/2/2019	12,201	-	1,336	0.03	89%
7/4/2019	13,945	-	1,783	0.08	87%
7/6/2019	28,401	-	4,195	0.80	85%
7/8/2019	39,199	-	12,135	2.96	69%
7/11/2019	47,051	-	19,826	4.35	58%
7/17/2019	35,151	-	4,575	1.69	87%

Table B.5. Bioretention flow data. No adjustment for baseflow in BR inlet shown in **bold**.

Date	Inflow (liters)	Max inflow (L/s)	Outlet (liters)	Max outlet flow (L/s)	Bypass (liters)	Peak bypass flow (L/s)	% Volume Reduction
6/2/2018	536,065	85.0	117,315	7.0	37,704	3.0	71%
7/17/2018	104,925	70.3	9,422	5.7			91%
7/20/2018	2,433,792	333.0	249,905	7.0			90%
7/22/2018	232,959	124.0	57,655	6.0			75%
7/23/2018	1,372,662	331.1	391,333	6.8	226,963	59.3	55%
7/25/2018	1,998,160	498.2	242,090	6.7	350,807	76.2	70%
7/30/2018	310,398	129.0	75,834	6.9	48,565	32.5	60%
8/1/2018	138,809	117.5	31,341	6.7	20,940	24.6	62%
8/2/2018	622,388	383.3	107,518	6.9	75,964	55.8	71%
8/4/2018	97,376	47.3	18,059	0.6	5,328	0.6	76%
8/21/2018	1,322,976	340.7	252,435	7.0	186,735	64.5	67%
8/31/2018	854,638	364.1	182,464	34.5	34,127	6.5	75%
9/2/2018	285,864	123.4	92,607	6.3	35,054	47.5	55%
9/8/2018	540,247	398.4	89,130	6.7	808	6.7	83%
9/9/2018	1,359,591	32.1	296,999	6.2	2,985	0.5	78%
9/25/2018	1,962,158	73.3	135,804	101.6	30,752	4.1	92%
9/26/2018	81,798	33.5	15,480	4.9	3,697	0.4	77%
9/28/2018	551,727	92.5	204,304	5.1	36,197	75.5	56%
10/11/2018	1,535,168	326.3	261,455	5.0	383,525	55.2	58%
10/26/2018	410,006	4.6	138,550	0.6	12,192	1.1	63%
11/10/2018	247,456	45.7	50,005	6.2	16,287	1.2	73%
11/13/2018	470,146	33.4	173,047	5.7	29,034	1.0	57%
11/15/2018	890,427	53.6	324,495	6.0	34,421	11.3	60%
11/24/2018	930,086	107.0	232,777	6.4	148,371	23.7	59%
11/26/2018	122,822	27.6	42,827	5.5	3,602	0.7	62%
12/1/2018	63,478	17.5	8,128	0.7	355	0.1	87%
1/19/2019	426,117	42.2	142,564	0.6	25,238	0.5	61%
1/25/2019	419,692	56.8	134,092	6.0	19,122	1.8	63%
2/12/2019	528,110	30.7	97,907	6.7	20,771	35.5	78%
2/24/2019	570,992	139.4	170,304	6.1	36,401	16.2	64%
3/9/2019	166,984	34.9	50,611	6.3	7,498	1.0	65%
3/21/2019	1,201,655	100.7	265,087	5.1	147,918	18.8	66%
4/5/2019	156,666	11.5	4,744	0.6	143	0.0	97%
4/8/2019	45,569	26.2	1,631	0.9	1,072	0.1	94%
4/13/2019	172,840	48.3	36,300	5.8	4,447	1.3	76%
4/15/2019	84,894	43.0	10,564	4.2	3,870	0.6	83%
4/20/2019	116,423	74.9	15,027	5.3	5,527	0.3	82%
4/26/2019	62,718	78.7	26,824	5.0	5,185	1.3	49%
6/18/2019	376,315	134.8	71,293	5.6	69,077	80.4	63%
6/19/2019	45,815	21.2	1,567	0.6	1,264	0.1	94%
6/25/2019	102,523	17.2	4,760	0.8	1,772	0.0	94%
6/29/2019	158,111	148.4	14,398	5.0	8,661	6.0	85%
7/2/2019	77,411	49.2	2,168	0.4	2,583	0.1	94%
7/4/2019	93,455	19.7	3,126	0.5	3,841	0.1	93%
7/6/2019	98,569	28.5	3,401	0.6	4,050	0.1	92%
7/8/2019	207,621	162.2	34,247	5.3	54,917	46.1	57%
7/11/2019	335,001	183.6	71,758	5.4	46,188	28.7	65%
7/17/2019	293,645	264.3	38,308	4.9	73,126	57.0	62%

6.2 APPENDIX C: APPLICATION OF CURVE NUMBER METHOD

When rainfall depth was below the initial abstraction, inflow to swales from pervious surfaces (CDA_p) was assumed to be zero. Otherwise, CDA_p was calculated using the CN method. CN values were chosen according to the antecedent moisture condition (AMC), or rainfall depth in the 5 days preceding an event, as defined in Mays (2011) (Chapter 2). Low AMC values were ≤ 12.5 mm (dormant season) or ≤ 35.56 mm (growing season), average AMC values were $12.5 \text{ mm} < \text{AMC} < 27.94$ mm (dormant) or $35.56 \text{ mm} < \text{AMC} < 53.34$ mm (growing), and high AMC values were ≥ 27.94 mm (dormant) or ≥ 53.34 mm (growing). Accordingly, CN values for the GC and CAGC (with similar soils) with increasing AMC were 45, 65, and 83 and the CN values for the BS were 25, 43, and 63.

6.3 APPENDIX D: FLOW DATA REPAIR

Data Repair – BS flooded flume

In some cases, data repair on the BS flooded flume was possible because of its similar sized underdrain to the BR. Because the BS and BR had underdrains of identical diameter (10.2 cm) but the BS did not have the pressure from ponded water or as large of a CDA, its maximum outflow is assumed to be no greater than that of the BR (7 L/s). Specifically, when the BR basin ponding was at its maximum (therefore maximum hydraulic head), its 10.2-cm outlet pipe was consistently flowing at 7 L/s. So, when the BS outflow results showed flow rates greater than 7 L/s, the data was adjusted to its assumed maximum flow of 7 L/s as noted at the BR. It is highly unlikely for the BS to have a higher hydraulic head than the BR because of its sloping surface and lack of ponding space. Verification that the BS outflow flume was flooded occurred during events not included in this study by positioning its ultrasonic sensor such that it measured the depth of water surrounding the flume and those results indicated water depths above the bottom of the flume. This repair occurred in the events marked in Table D.1.

Data Repair – BR baseflow

It should be noted that the BR had nearly continual flow through both its inlet and outlet pipes. In dry periods, the BR outlet read at most 0.3 L/s and the inlet read 1.3 L/s by both visual inspection of the flumes and recorded data. The reason for the continual inlet reading is attributed to a slow draining storm sewer. The continual outflow may have been due to a variety of reasons including but not limited to continually saturated soils and gravel surrounding the underdrain, and the native, compacted clayey soils underlying the BR slowing if not preventing infiltration. Groundwater depths from monitoring wells surrounding the BR and adjacent to its underdrain outlet indicate that the intrusion of groundwater into the bioretention outflow pipe is unlikely if not impossible since the distance from the groundwater to the underdrain for all monthly readings is between 0.9 m and 2.5 m. While the BR does have a low level of constant base flow, the flow is not low enough relative to the stormflow that it is considered negligible and is therefore subtracted from the event flow data. As with the other monitored systems, the flow summation for the BR is ended once the outlet flow rate is consistent with flow prior to the rain event. This correction was performed on all BR inflow and outlet flow data except those bolded in Table D.1 – D.5 of Appendix D where the baseflow was not present. The BR bypass data received no constant baseflow, so it was not adjusted.

6.5 APPENDIX E: DESIGN TO AVOID FLOW BYPASS AT THE GRASS CHANNEL

Fig. E.1 is a photo of the grass channel with cinderblocks in place that direct flow in the swale into the flume.



Figure E.1. Grass channel flume with cinder blocks preventing flow-around

6.7 APPENDIX F: WELL DATA

Table F.1 gives the well depths of each well below the bioretention forebay.

Table F.1. Depths of wells around and inside bioretention system

Well	1	2	A	A.2	B	C	D	E	E.2	F
Depth (Cm)	350	330	370	520	450	540	500	740	860	530

Table F.2 gives the groundwater data used in this study. ND indicates a non-detect reading and a “-“ indicates that the reading was not performed.

Table F.2. Groundwater data including salts, metals, and DOC

Date	Well ID	Sodium	Chloride	Chromium	Nickel	Copper	Lead
8/31/2018	Well 1	-	795.0	1.3	7.5	5.7	2.6
10/31/2018	Well 2	-	-	34.8	42.9	80.9	306
12/9/2018	Well 1	263.0	471.0	2.1	3.9	8.3	5.4
	Well 2	126.0	244.0	29.0	23.6	63.4	60.9
1/11/2019	Well 1	190.0	307.0	3.8	3.6	12.7	11.2
	Well 2	114.0	198.0	24.2	23.2	53.6	42.1
2/22/2019	Well 1	-	-	2.5	1.9	13.0	8.5
	Well 2	-	-	5.9	18.6	22.7	20.8
4/15/2019	Well 1	229.0	390.0	4.3	3.2	19.5	12.4
	Well 2	65.0	160.0	1.8	19.2	10.2	3.0
	Well A	375.0	1032.0	19.2	116.5	26.2	4.8
	Well A.2	-	-	-	-	-	-
	Well B	57.7	132.9	53.2	19.5	27.9	19.7
	Well C	95.0	201.0	52.6	24.8	39.6	50.7
	Well D	140.0	293.0	25.6	16.1	13.2	6.1
	Well E	87.5	294.0	3.7	25.8	11.6	1.4
	Well E.2	-	-	-	-	-	-
6/7/2019	Well 1	198.0	345.0	2.9	2.1	8.3	3.6
	Well 2	62.0	180.0	22.1	24.1	33.3	14.2
	Well A	338.0	1043.0	12.4	83.8	21.8	5.7
	Well A.2	184.0	612.4	44.2	55.5	36.3	6.1
	Well B	57.0	146.3	23.5	9.8	13.2	6.5
	Well C	89.0	209.0	14.8	13.1	13.2	5.2
	Well D	130.0	286.0	5.6	9.3	8.0	1.1
	Well E	91.7	326.0	1.8	16.8	8.4	0.5
	Well E.2	10.8	59.0	25.6	10.2	14.8	3.8
7/10/2019	Well 1	153.0	303.0	1.1	1.7	7.7	5.2
	Well 2	53.0	166.0	5.5	17.7	15	9.1
	Well A	362.0	1164.0	6.8	67.7	18.7	4.6
	Well A.2	286.0	983.5	2.5	61.2	16.7	1.6
	Well B	54.6	149.5	4.0	6.4	6.4	3.3
	Well C	91.0	215.0	3.1	9.4	5	3.3
	Well D	114.0	255.0	1.6	5.5	4.3	1.2
	Well E	79.7	315.0	0.8	15.2	6	0.6
	Well E.2	9.6	65.0	7.5	5.9	6.1	2.0
Well F	36.7	156.2	25.4	16.6	14.7	13.5	

Table F.2 (continued). Groundwater data including salts, metals, and DOC

Date	Well ID	Sodium	Chloride	Chromium	Nickel	Copper	Lead
9/4/2019	Well 1	236.0	447.0	0.7	1.1	8.6	6.1
	Well 2	86.0	150.0	1.9	7.1	16.2	18.1
	Well A	403.0	1250.0	2.4	66.1	15.2	2.1
	Well A.2	264.0	899.6	2.7	52	14.9	1.0
	Well B	73.3	157.3	10.1	5.9	8.4	4.4
	Well C	110.0	233.0	0.4	9.1	4.2	0.4
	Well D	97.1	201.0	3.0	4.7	3.8	0.9
	Well E	97.5	325.0	0.8	14.8	6.6	0.4
	Well E.2	23.6	93.0	12.3	7.3	7.2	2.9
	Well F	40.4	159.4	6.6	36.2	10.2	2.5
10/11/2019	Well 1	234.0	455.0	1.8	1.4	18.3	11.9
	Well 2	75.0	166.0	1.0	11.8	12.2	5.8
	Well A	358.0	1115.0	3.8	62.9	25.3	3.0
	Well A.2	270.0	902.6	1.9	53.2	16.8	0.7
	Well B	72.3	153.8	8.6	5.4	10	4.1
	Well C	110.0	243.0	2.4	10.2	6.5	2.9
	Well D	93.9	178.0	1.9	3.4	4.7	0.7
	Well E	109.3	347.0	0.7	13.9	5.3	0.3
	Well E.2	24.1	103.0	2.9	6.8	4.8	0.7
	Well F	54.6	184.2	8.4	13.1	9.6	2.6
11/13/2019	Well 1	288.0	486.0	16.5	5.3	91.4	45.2
	Well 2	177.0	300.0	5.5	17.4	28.1	57.5
	Well A	1398.0	4503.0	4.6	62.6	22.9	2.4
	Well A.2	940.0	2922.7	6.0	46.8	19.1	1.3
	Well B	104.2	220.7	5.5	5.6	8.3	2.6
	Well C	162.0	365.0	1.1	8.9	9.8	0.6
	Well D	142.0	261.0	9.0	4.3	10.5	3.0
	Well E	161.8	501.0	2.4	14	7.5	1.1
	Well E.2	47.7	167.0	2.9	7.7	5.9	0.5
	Well F	72.7	226.8	4.7	10.7	6.3	1.4
1/28/2020	Well 1	-	202.8	8.7	1.8	28.5	19
	Well 2	-	326.1	10.2	21.1	35.1	18.1
	Well A	-	807.5	7.1	55.4	26.1	3.7
	Well A.2	-	697.2	7.6	63.3	24.9	0.8
	Well B	-	216.8	8.5	5.8	9.1	2.2
	Well C	-	182.6	12.8	11.7	15.9	8.2
	Well D	-	124.9	14.2	5	10.1	4.8
	Well E	-	245.5	5.1	14.4	8.3	0.4
	Well E.2	-	121.3	11.6	10.6	11.7	1.5
	Well F	-	127.1	11.7	9.2	12.6	5.0

Table F.2 (continued). Groundwater data including salts, metals, and DOC

Date	Well ID	Sodium	Chloride	Chromium	Nickel	Copper	Lead
5/12/2020	Well 1	-	103.6	2.3	1.3	21.4	12.0
	Well 2	-	142.4	2.4	4.3	29.1	13.8
	Well A	-	762.4	3.0	57.6	19.4	1.6
	Well A.2	-	890.3	2.9	69.6	22	0.8
	Well B	-	111.0	3.0	5.7	5.3	1.8
	Well C	-	185.0	1.5	9.9	5.2	1.2
	Well D	-	78.9	2.2	2.4	4.1	0.5
	Well E	-	256.9	0.7	12.4	5.7	0.2
	Well E.2	-	100.1	0.4	8.8	4.1	0.1
	Well F	-	173.6	2.5	17.4	6.4	0.8
7/2/2020	Well 1	-	130.3	6.6	2.9	42.1	23.3
	Well 2	-	125.5	5.6	6.5	38.5	14.3
	Well A	-	853.5	2.5	50.9	18.8	0.2
	Well A.2	-	877.8	1.6	58.6	18.3	ND
	Well B	-	108.4	3.1	4.9	5.6	ND
	Well C	-	164.9	1.9	7.4	5.7	ND
	Well D	-	71.7	4.8	2.2	5.2	0.9
	Well E	-	202.6	1.2	9.7	5.6	ND
	Well E.2	-	86.0	0.6	6.9	4.3	ND
	Well F	-	171.6	1.5	15.1	5.4	ND

The well depths over the study period are summarized in Fig. F.1. Groundwater flowed from highest to lowest hydraulic head. The datum was the bottom of Well 1. Well B is the furthest upgradient.

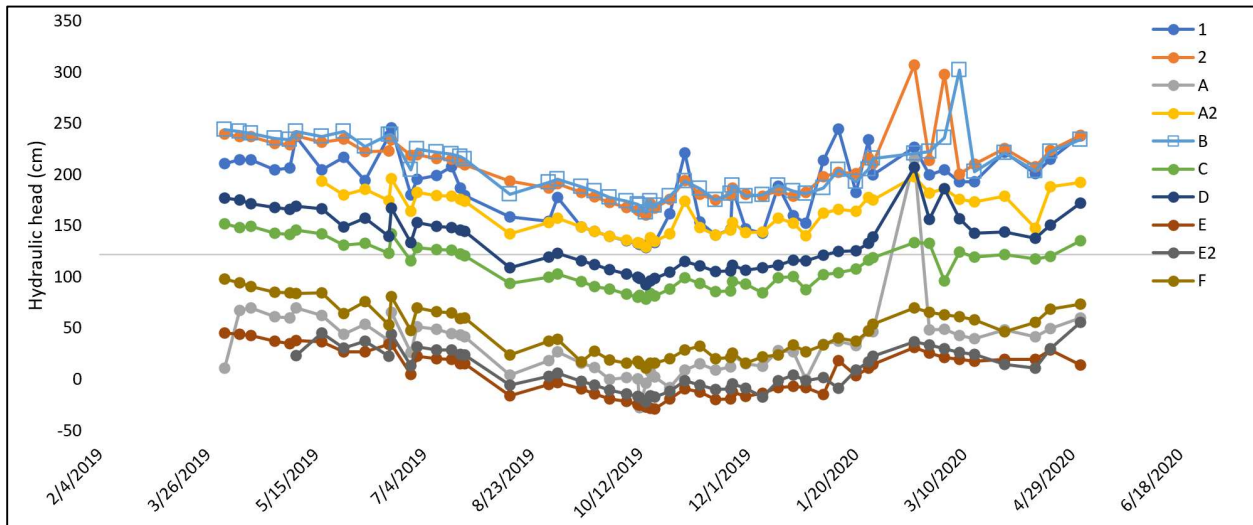


Figure F.1. Hydraulic head measurements of the wells at the bioretention (cm)

6.8 APPENDIX G: EVENT MONITORING RESULTS (CHAPTER 3)

Tables G.1 – G.8 gives the average daily temperature, precipitation depths, and water quality data. Blank spaces indicate the event was not monitored at that system.

Table G.1. List of monitored events. ^a likely road salt event, ^b rain data from Ronald Reagan National Airport, ^c snowmelt

Date	Temp (C)	Precip. (mm)	Bioretention	Bioswale	Compost-amended grass channel	Grass channel
3/20/2018 ^a	1.7	60.7	✓			
4/16/2018	12.4	94.5	✓			
4/27/2018	14.1	26.4	✓			
5/19/2018 ^b	20.1	93.5	✓		✓	
5/23/2018	21.2	21.8	✓	✓	✓	
6/2/2018	21.8	51.1	✓	✓	✓	✓
7/23/2018	25.4	104.9	✓			
7/30/2018	24.0	24.4	✓	✓	✓	
8/21/2018	25.1	72.1	✓			
8/31/2018	26.9	72.6	✓	✓	✓	✓
9/26/2018	24.4	7.4	✓		✓	
9/28/2018	17.6	39.9	✓	✓	✓	✓
10/11/2018	20.3	86.1	✓		✓	✓
10/26/2018	8.9	39.6	✓		✓	✓
11/10/2018	7.9	14	✓	✓	✓	✓
11/13/2018	7.4	32	✓		✓	✓
11/15/2018 ^{ab}	4.2	43.7	✓			
12/15/2018	9.6	103.6	✓	✓		✓
1/16/2019 ^{abc}	1.1	24.1	✓	✓	✓	
1/19/2019 ^a	3.7	24.4	✓	✓		✓
1/25/2019	6.3	27.4	✓	✓	✓	✓
2/12/2019 ^{ab}	2.1	15.2	✓	✓	✓	✓
2/20/2019 ^{abc}	5.6	22.9	✓	✓	✓	✓
2/24/2019	6.3	32.8	✓	✓	✓	✓
3/21/2019	8.0	64.8	✓	✓	✓	✓
4/26/2019	18.6	10.2	✓			
5/5/2019 ^b	19.4	78.7	✓			✓
6/18/2019	23.9	19.1	✓	✓	✓	✓
10/17/2019	14.4	40.6	✓	✓		✓
11/23/2019	7.4	22.1	✓	✓	✓	✓
2/7/2020	7.6	47	✓	✓	✓	✓
4/13/2020 ^b	14.8	70.9	✓	✓	✓	✓
8/3/2020 ^b	25.0	73.7	✓	✓	✓	✓

Table G.2. Bioretention inlet data from monitored events.

Bioretention inflow										
Date	Cl	Na	Ca	Mg	DOC	TSS	Cr	Ni	Cu	Pb
	mg/L						µg/L			
3/20/2018	2080.4	1308.9	7.7	0.7		58.2	2.4	1.0	15.3	1.9
4/16/2018	35.0	32.7	2.9	0.2	5.8	176.0	1.4	1.1	11.1	2.9
4/27/2018	44.7	51.1	7.1	1.0	5.2	66.0	1.1	0.9	10.9	3.1
5/19/2018	41.2	43.2	9.0	1.0	6.2	60.7	1.5	0.7	11.0	2.4
5/23/2018	49.7	49.0	11.0	1.5	6.5	64.0	2.7	1.1	13.1	2.9
6/2/2018	50.8	41.1	12.9	1.7	5.6	17.0	1.1	0.7	8.7	2.2
7/23/2018	22.0	29.8	11.4	1.7	6.7	35.0	1.1	0.6	9.0	1.7
7/30/2018	28.7	29.0	8.9	1.1	4.8	24.8	1.3	0.7	7.8	1.9
8/21/2018	12.5	20.5	5.9	0.9	5.0	40.8	1.5	0.7	9.6	1.6
8/31/2018	3.9	14.5	2.4	0.6	4.8	22.0	0.9	0.6	6.5	0.8
9/26/2018	61.4	47.9	23.7	2.8	5.8	13.0	0.9	0.9	7.9	0.9
9/28/2018	22.5	28.0	15.2	1.8	4.2	24.0	1.0	0.8	7.7	2.5
10/11/2018	12.9	22.1	8.3	0.9	4.7	31.0	1.6	1.1	10.8	1.4
10/26/2018	17.1	21.1	7.5	0.8	4.7	19.0	1.0	0.7	8.8	1.1
11/10/2018	44.5	37.6	15.1	1.7	4.6	19.5	1.1	0.9	9.3	2.0
11/13/2018	13.5	18.7	7.8	0.8	4.5	9.5	0.7	0.6	6.8	2.3
11/15/2018	547.4	335.5	14.5	1.5	3.3		3.4	1.3	12.5	2.6
12/15/2018	11.3	17.0	6.4	0.9	4.7	37.8	1.0	0.7	8.4	2.6
1/16/2019	7395.3	4345.6	59.8	3.6	4.7		2.8	3.4	9.6	2.4
1/19/2019	641.6	390.2	11.0	1.1		144.3	4.5	2.7	16.1	7.2
1/25/2019	216.0	129.3	14.9	1.9	6.0	66.0	2.4	1.9	15.5	4.9
2/12/2019	1056.0	598.8	22.4	2.5	6.0	57.7	2.0	1.9	13.6	2.6
2/20/2019	2744.2	1527.1	38.2	3.2	4.7		2.3	3.0	7.9	1.7
2/24/2019	147.9	97.8	16.3	1.3	4.6	73.8	1.7	1.5	11.2	4.2
3/21/2019	45.7	29.8	6.6	0.8	5.1	148.7	2.8	1.7	12.7	3.7
4/26/2019	45.8	27.1	10.8	1.9	21.4	302.0	6.9	4.7	40.6	9.5
5/5/2019	31.4	24.0	7.6	1.1	5.5	120.7	1.5	0.9	9.2	1.7
6/18/2019	25.6	19.4	8.0	1.2	13.9		1.8	0.8	11.3	2.6
10/17/2019	7.8	10.2	3.6	1.0	4.4	20.0	1.3	0.4	10.6	1.2
11/23/2019	10.9	11.6	4.6	0.8	4.0	19.2	0.7	0.0	7.7	1.0
2/7/2020	18.1				3.5	122.0	2.1	2.2	12.1	3.8
4/13/2020	6.5				5.8	54.0	0.7	0.6	6.9	2.3
8/3/2020	5.9						0.7	0.7	10.7	0.9

Table G.3. Bioretention outlet data from monitored events.

Bioretention outlet										
Date	Cl	Na	Ca	Mg	DOC	TSS	Cr	Ni	Cu	Pb
	mg/L						µg/L			
3/20/2018	113.4	67.9	19.7	5.5		15.2	1.6	2.1	16.6	2.3
4/16/2018	549.6	246.6	82.0	25.8	13.4	29.5	2.2	6.0	32.1	5.5
4/27/2018	71.5	59.3	17.8	4.3	10.0	32.0	3.2	6.9	50.5	9.5
5/19/2018	43.0	49.7	12.1	2.7	0.0	11.0	1.5	5.1	34.0	8.1
5/23/2018	49.8	68.6	14.6	3.4	9.1	15.0	1.5	4.9	32.4	7.4
6/2/2018	37.9	54.7	11.7	2.3	8.3	10.0	1.1	4.1	24.0	6.9
7/23/2018	25.9	42.7	9.9	2.0	8.4	15.0	0.7	2.7	15.7	3.1
7/30/2018	40.3	54.9	14.7	2.7	7.9	13.2	1.1	3.2	21.3	4.5
8/21/2018	16.9	35.3	12.4	2.2	10.6	22.3	1.3	3.9	28.5	6.7
8/31/2018	20.1	36.9	13.3	2.3	8.0	23.0	2.6	4.7	30.4	4.6
9/26/2018	51.7	51.1	16.2	2.8	5.3	4.8	0.8	1.8	10.9	1.5
9/28/2018	25.1	37.8	14.6	2.7	4.7	3.0	0.8	1.8	11.7	1.6
10/11/2018	21.0	31.2	10.3	1.6	10.1	4.8	1.2	2.6	17.9	2.9
10/26/2018	21.6	30.8	11.1	1.9	6.4	6.8	1.0	1.7	12.2	2.8
11/10/2018	31.6	36.4	11.8	1.9	4.4	3.3	0.9	1.8	14.4	2.5
11/13/2018	23.4	31.2	5.1	1.5	3.4	3.0	0.7	1.3	12.0	1.9
11/15/2018	395.8	116.8	85.1	24.9	2.3		0.6	3.8	6.2	1.6
12/15/2018	20.5	30.7	7.4	1.2	4.8	6.7	0.8	1.5	14.0	2.6
1/16/2019	3747.5	1788.7	311.8	42.2	2.6		0.0	8.5	3.2	1.2
1/19/2019	1489.9	721.4	113.8	26.2	3.0	5.9	0.3	6.5	5.2	0.6
1/25/2019	345.2	186.1	25.5	7.6	3.6	3.0	0.3	1.7	5.7	1.4
2/12/2019	618.1	334.4	27.5	6.1	6.7	3.1	0.2	1.2	7.2	0.5
2/20/2019	865.3	457.8	31.4	6.1	4.7		0.5	0.4	4.7	0.3
2/24/2019	406.9	213.6	31.5	8.5	3.7	1.5	0.4	2.2	7.1	1.6
3/21/2019	74.7	57.6	5.5	1.3	6.1	11.1	1.4	1.9	18.6	2.1
4/26/2019	58.3	72.1	9.9	1.9	15.4	28.2	3.9	8.3	63.1	7.8
5/5/2019	27.0	38.5	8.3	1.3	7.2	29.0	4.2	8.0	56.2	6.8
6/18/2019	18.7	34.3	5.6	1.1	18.2		1.6	5.2	30.3	5.9
10/17/2019	10.7	31.6	6.9	1.8	17.8	42.5	3.0	5.8	45.8	6.9
11/23/2019	10.0	30.8	7.7	1.5	9.5	15.4	0.6	0.3	7.4	0.9
2/7/2020	30.0				5.5	7.8	1.1	3.4	18.6	2.3
4/13/2020	7.4				7.7	12.9	0.7	2.8	23.1	3.3
8/3/2020	6.6						2.9	6.7	39.6	4.8

Table G.4. Bioretention bypass data from monitored events.

Bioretention bypass										
Date	Cl	Na	Ca	Mg	DOC	TSS	Cr	Ni	Cu	Pb
	mg/L						µg/L			
3/20/2018	131.0	82.9	2.9	11.6		17.5				
4/16/2018	48.4	35.3	0.5	3.7	4.2	99.5	1.1	0.6	7.5	253.7
4/27/2018	48.8	39.8	1.1	5.9	6.0	39.2	0.7	0.7	7.3	192.2
5/19/2018	52.2	47.4	1.7	9.6	9.7	22.7	1.0	1.2	9.4	160.8
5/23/2018	17.8	32.3	0.9	5.1	7.1	37.7	2.9	0.9	7.7	107.7
6/2/2018	28.8	41.1	2.0	10.7	8.2	24.8	0.5	0.8	6.3	81.9
7/23/2018	6.0	16.0	0.9	4.8	5.3	20.7				
7/30/2018	9.0	16.6	0.8	4.7	4.1	8.7				
8/21/2018	4.6	14.3	0.6	3.1	4.6	21.5				
8/31/2018	5.7	15.4	0.7	3.9	6.4	15.2	0.9	0.6	9.6	1.9
9/26/2018										
9/28/2018	20.0	27.9	2.7	13.2	ND	20.0	0.6	0.8	5.5	1.3
10/11/2018	4.2	13.8	0.6	4.9	4.1	11.8	1.2	0.6	7.7	1.2
10/26/2018	29.8	28.5	2.0	9.5	9.3		0.6	0.6	6.1	1.2
11/10/2018	22.4	28.3	2.3	11.7	7.3		0.7	0.8	6.7	1.5
11/13/2018	19.3	23.0	1.9	8.8	5.7	7.2	0.5	0.5	5.6	1.5
11/15/2018	271.6	144.3	5.3	20.7	3.6		0.8	0.4	4.3	0.6
12/15/2018			0.9	6.4						
1/16/2019	410.6	195.0	15.9	62.6						
1/19/2019	584.1	323.4	8.6	34.7	6.0	38.7	0.3	0.5	3.8	0.7
1/25/2019	214.6	122.6	3.4	13.8	7.2	22.7	0.4	0.5	4.9	2.3
2/12/2019	273.9	144.0	4.0	15.5	3.9	20.0	0.2	0.4	5.9	2.6
2/20/2019	2299.2	1230.8	14.5	64.4		22.8	0.6	0.9	4.3	0.8
2/24/2019	145.2	92.0	1.5	10.7	3.8	70.3	1.4	1.2	8.1	4.1
3/21/2019	55.9	35.2	0.9	6.3	5.6	30.7	1.4	0.6	6.8	1.7
4/26/2019	72.4	46.0	1.5	8.3	23.0		1.4	1.5	9.6	1.5
5/5/2019	18.1	15.4	0.9	5.1	10.2	36.3	1.1	0.8	7.5	1.4
6/18/2019	3.7	2.7	0.4	1.7	10.4		1.4	0.6	6.1	2.1
10/17/2019	11.7	13.4	4.4	1.4	6.6	10.1	1.0	0.7	8.0	0.6
11/23/2019	26.7	22.4	6.7	1.7	8.3	11.3	2.0	4.4	36.5	6.1
2/7/2020	9.6				4.0		2.2	2.0	11.9	3.2
4/13/2020	2.5				5.1	24.9	0.5	0.4	5.4	1.5
8/3/2020	3.4						0.6	0.9	8.4	0.8

Table G.5. Road runoff entering swales data from monitored events.

Road runoff into swales										
Date	Cl	Na	Ca	Mg	DOC	TSS	Cr	Ni	Cu	Pb
	mg/L					µg/L				
3/20/2018										
4/16/2018										
4/27/2018										
5/19/2018	52.5	44.0	8.9	1.1	8.0	35.0	0.7	2.1	7.5	109.2
5/23/2018	31.9				7.9	121.0	1.9	1.6	9.5	4.9
6/2/2018	24.7	29.5	4.9	0.8	5.1	105.0	1.1	0.8	7.3	6.7
7/23/2018										
7/30/2018	19.3	22.1	3.5	0.6	6.6	64.2	0.7	0.7	7.7	3.1
8/21/2018	9.8				6.0					
8/31/2018	10.9	19.5	3.1	0.6	6.8	128.0	1.3	0.8	11.9	2.5
9/26/2018	29.9				11.2	217.0	2.3	2.2	12.3	5.1
9/28/2018	17.5	24.4	9.3	1.2	4.8	68.0	1.1	2.8	7.2	2.0
10/11/2018	9.6	19.6	4.0	0.5	4.4	116.0	1.5	1.1	7.7	3.5
10/26/2018	18.6	21.6	5.3	0.7	5.0	30.0	1.0	0.8	10.3	1.7
11/10/2018	20.5	24.2	6.6	0.6	4.6		1.6	1.1	8.4	2.5
11/13/2018	17.1	20.5	5.4	0.5	3.7	7.0	0.4	0.4	5.2	1.2
11/15/2018	3064.0	1848.0	15.9	1.1	3.0		4.3	1.2	10.8	2.1
12/15/2018	6.8	17.0	3.2	0.4	2.8	45.0	0.9	0.6	6.3	2.7
1/16/2019	8050.0	4976.0	63.7	3.5	6.9		0.2	1.3	4.2	1.0
1/19/2019	641.6	390.2	11.0	1.1	8.1	144.3	4.5	2.7	16.1	7.2
1/25/2019	241.0	142.7	8.0	1.0	8.5	63.0	1.4	1.2	9.5	2.8
2/12/2019	230.6	129.2	7.2	0.9	3.7		1.4	1.1	9.5	4.3
2/20/2019	4270.0	2420.0	22.6	0.8	5.7		2.5	1.6	8.7	2.3
2/24/2019	63.6	48.3	6.2	0.1	2.9	341.0	4.0	2.8	15.9	9.8
3/21/2019	65.4	39.8	3.0	0.3	3.3	106.3	2.2	1.4	9.9	3.7
4/26/2019										
5/5/2019	67.1	39.6	7.0	0.8	5.2	55.3	1.5	0.9	7.1	3.8
6/18/2019	48.6	26.2	3.7	0.6	11.8		2.4	1.5	10.8	5.5
10/17/2019	19.6	14.9	2.0	0.7	6.4	78.2	1.4	0.7	9.0	2.5
11/23/2019	35.0		4.6	0.8	3.7	94.0	1.1	0.4	7.7	2.8
2/7/2020	22.6				2.9	134.0	2.2	1.4	9.8	5.0
4/13/2020	6.5				5.8	54.0	0.7	0.6	6.9	2.3
8/3/2020	8.0				3.5	78.4	1.3	1.1	7.7	2.1

Table G.6. Grass channel outlet data from monitored events.

Grass channel										
Date	Cl	Na	Ca	Mg	DOC	TSS	Cr	Ni	Cu	Pb
	mg/L					µg/L				
3/20/2018										
4/16/2018										
4/27/2018										
5/19/2018										
5/23/2018										
6/2/2018	4.1				9.6	11.0	0.5	0.5	8.5	4.2
7/23/2018					11.7					
7/30/2018										
8/21/2018										
8/31/2018	2.1				9.9	50.0	2.0	1.6	7.6	3.7
9/26/2018										
9/28/2018	4.2				10.4	8.0	0.5	0.6	11.5	1.8
10/11/2018	1.6	14.5	6.1	1.5	8.6	27.0	0.7	0.6	8.5	2.6
10/26/2018	9.4	16.5	10.5	3.1	15.2	28.0	0.8	0.7	15.5	4.7
11/10/2018	3.3	15.3	9.6	2.5	8.8	13.0	0.7	0.7	12.2	3.2
11/13/2018	4.0	13.4	8.9	2.3	6.9	5.0	0.5	0.4	8.3	2.8
11/15/2018										
12/15/2018	1.7	13.7	6.3	1.5	5.3	18.0	0.4	0.3	5.1	2.5
1/16/2019										
1/19/2019	70.2	42.4	14.1	3.9	5.5	13.8	0.3	0.3	4.7	1.4
1/25/2019	41.5	17.8	9.2	2.9	6.8	17.0	0.5	0.3	6.3	6.5
2/12/2019	61.3	26.2	10.4	3.1	6.8		0.3	0.3	5.6	6.2
2/20/2019	313.4	133.8	35.9	9.4	2.9		0.3	0.6	4.7	2.1
2/24/2019	64.1	40.2	12.6	2.8	4.3	26.5	0.4	0.4	6.0	4.4
3/21/2019	16.8	12.2	5.4	1.3	7.2	36.3	1.2	0.5	8.1	6.3
4/26/2019										
5/5/2019	7.0	8.0	9.6	2.1	12.9	34.3	2.4	1.1	12.7	8.6
6/18/2019	3.8	5.1	8.1	1.9	25.7		0.6	0.5	15.8	5.7
10/17/2019	4.7	9.5	4.0	1.7	23.0		0.3	0.5	8.9	1.2
11/23/2019	5.9	10.8	5.1	1.7	10.7	13.9	0.5	0.0	9.2	1.7
2/7/2020	1.6				7.9	55.3	0.8	1.2	8.4	6.6
4/13/2020	0.7				7.4	35.9	0.1	0.2	6.6	3.6
8/3/2020	2.7				11.9	15.2	0.7	0.8	12.1	2.2

Table G.7. Compost-Amended grass channel outlet data from monitored events.

Compost-amended grass channel										
Date	Cl	Na	Ca	Mg	DOC	TSS	Cr	Ni	Cu	Pb
	mg/L						µg/L			
3/20/2018										
4/16/2018										
4/27/2018										
5/19/2018							1.2	2.1	21.0	330.6
5/23/2018	37.0				20.9	59.0	1.2	1.5	15.5	4.9
6/2/2018	30.2				20.4	36.0	1.1	1.6	13.1	5.0
7/23/2018					20.0					
7/30/2018	34.4				23.4	54.7	0.7	1.3	14.8	1.9
8/21/2018										
8/31/2018	19.1				21.3	45.0	5.2	9.4	83.9	15.0
9/26/2018	27.7				30.0	136.0	1.7	2.7	11.8	4.1
9/28/2018	15.0				21.5	79.0	1.4	1.9	9.6	3.8
10/11/2018	11.1	28.2	10.1	2.7	15.1	31.0	1.3	1.4	11.3	2.3
10/26/2018	44.8	36.6	16.0	5.3	20.6	41.0	1.3	1.1	14.0	3.2
11/10/2018	22.8	29.8	19.4	5.7	14.9	39.0	1.4	1.2	10.1	4.5
11/13/2018	16.0	30.5	16.1	4.6	11.8	18.0	0.8	0.8	6.4	3.4
11/15/2018										
12/15/2018										
1/16/2019	518.3	221.7	79.2	26.5	7.8		0.0	0.5	3.6	0.8
1/19/2019	364.3	198.8	41.1	12.2	9.9	40.0	2.4	1.3	8.0	2.2
1/25/2019	166.7	77.6	21.1	7.1	11.8	40.0	0.6	0.6	7.3	3.1
2/12/2019	396.0	178.3	44.0	14.0	10.2	23.7	0.4	0.5	6.1	2.7
2/20/2019	1049.6	540.3	56.4	15.7	6.6		0.5	0.8	5.6	1.6
2/24/2019	118.2	74.4	15.3	3.8	7.1	83.6	0.9	0.7	6.7	4.4
3/21/2019	61.7	42.3	9.1	2.4	10.5	76.0	1.4	0.8	7.6	4.8
4/26/2019										
5/5/2019										
6/18/2019	32.3	28.8	11.9	3.1	33.3		1.0	1.3	12.0	4.1
10/17/2019										
11/23/2019	75.3	45.0	13.6	4.3	18.9	19.8	0.9	0.4	11.8	2.0
2/7/2020	20.7				11.8	33.8	1.2	1.5	8.4	3.5
4/13/2020	2.7				10.1	59.7	0.3	0.5	6.8	2.5
8/3/2020	15.4				24.3	17.6	1.4	1.7	16.9	1.7

Table G.8. Bioswale outlet data from monitored events.

Bioswale										
Date	Cl	Na	Ca	Mg	DOC	TSS	Cr	Ni	Cu	Pb
	mg/L						µg/L			
3/20/2018						14.0				
4/16/2018										
4/27/2018										
5/19/2018	23.0	30.9	15.5	3.6	10.6	10.0				
5/23/2018					12.9	54.7	1.8	6.5	49.8	16.3
6/2/2018	28.8	103.3	41.3	9.3	12.5	19.0	1.2	4.7	35.4	10.7
7/23/2018	22.7				11.6	20.0				
7/30/2018	28.0	47.3	23.3	4.4	13.6	46.7	2.1	6.9	62.8	17.4
8/21/2018										
8/31/2018	8.8	34.5	12.4	2.3	12.8	52.0	1.6	1.5	14.3	3.6
9/26/2018										
9/28/2018	14.8	32.6	25.6	4.7	8.7	12.0	1.3	3.0	26.8	3.5
10/11/2018										
10/26/2018										
11/10/2018	12.9	27.2	16.8	2.7	7.6	5.5	1.8	3.0	31.4	5.8
11/13/2018										
11/15/2018										
12/15/2018	13.1	31.5	11.1	1.9	7.3	21.0	1.3	2.3	24.2	5.1
1/16/2019	7112.3	3501.3	524.5	59.3	4.5		0.0	23.4	5.5	0.9
1/19/2019	1765.5	863.5	147.3	31.2	5.9	5.5	0.3	10.8	8.5	0.6
1/25/2019	808.2	378.8	69.7	16.0	6.4	17.0	0.5	7.1	11.4	1.4
2/12/2019	1041.4	539.1	58.5	11.9	6.1	10.0	0.4	3.3	9.5	1.8
2/20/2019	1717.0	822.8	109.2	20.8	4.1		2.5	2.9	13.1	1.8
2/24/2019	402.1	225.7	29.8	5.6	5.6	14.8	0.7	1.9	13.7	2.8
3/21/2019	140.6	91.6	10.1	1.8	6.5	16.3	1.2	1.8	18.5	3.2
4/26/2019										
5/5/2019										
6/18/2019	51.5	49.9	15.3	2.2	22.0		1.8	6.4	57.7	12.5
10/17/2019	51.6	49.2	6.4	1.6	15.5	31.2	2.2	4.6	63.1	9.0
11/23/2019	75.9	51.6	14.0	2.2	9.2	8.3	1.6	2.6	36.9	7.7
2/7/2020	21.1				6.9	88.3	1.4	2.6	27.8	4.8
4/13/2020	8.0				10.5	43.0	1.0	3.3	36.2	6.5
8/3/2020	7.9				13.5	22.7	2.3	5.3	49.2	6.0

6.9 APPENDIX H: IRREDUCIBLE CONCENTRATIONS

Linear regression analyses (Figure H.1) indicated that the bioretention inflow metal concentrations were significantly positively correlated with their respective EMC reductions according to the equations listed below.

- Chromium: $P = .02$ ($R^2 = 0.2$); $y = 32x - 59$
- Copper (omits outlying inflow of $41 \mu\text{g/L}$): $P = .07$ ($R^2 = 0.1$); $y = 19x - 302$
- Nickel: $P = .01$ ($R^2 = 0.2$); $y = 142x - 479$
- Lead ($R^2 = 0.2$): $P = .01$; $y = 43x - 203$

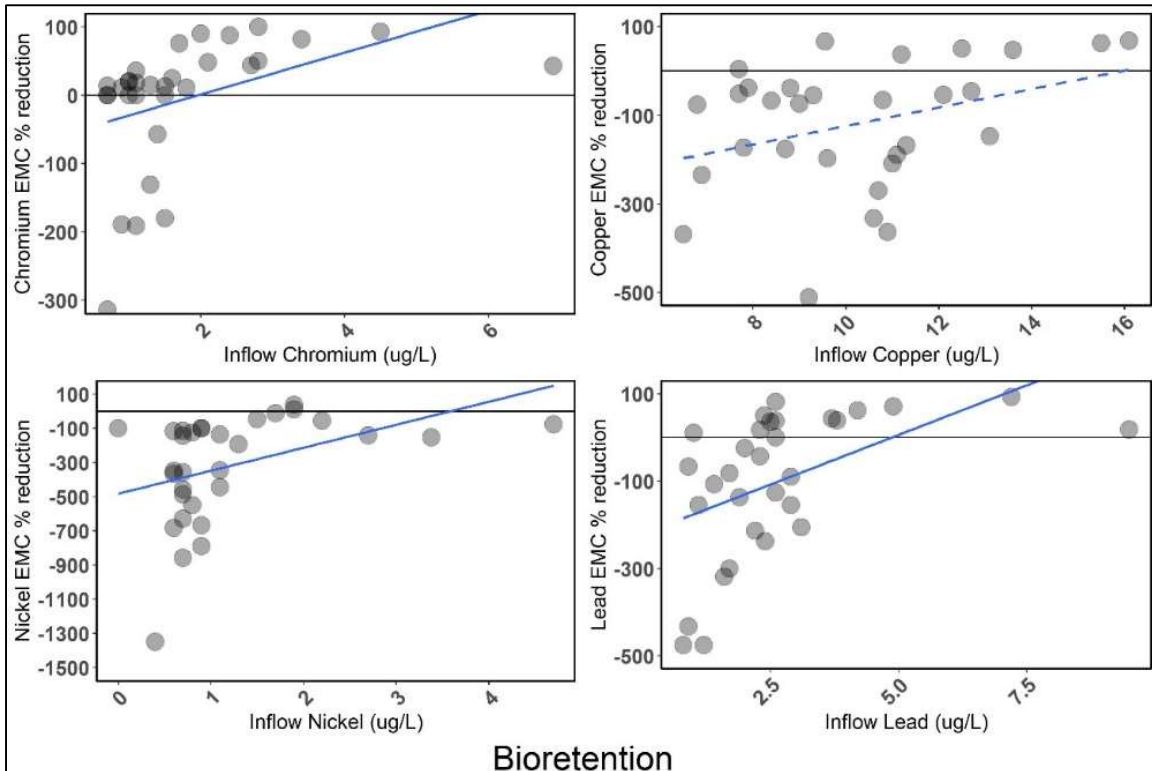


Figure H.1. Linear regression analyses showing relationship between inflow metal concentrations and EMC % reductions at the bioretention. Long dashes indicate omission of large negative reduction. Dots are partially transparent such that darker dots indicate overlapping data points.

Linear regression analyses (Figure H.2) indicated that the bioswale inflow metal concentrations were significantly positively correlated with their respective EMC reductions according to the equations listed below. The equation for nickel omits the large negative reduction (-1700% shown in the figure). Lead is not significant even after eliminating the large negative EMC reduction (-500%).

- Chromium: $P = .03$ ($R^2 = 0.2$); $y = 33x - 57$
- Copper: $P = .06$ ($R^2 = 0.2$); $y = 34x - 570$
- Nickel (omits -1700%): $P = .01$ ($R^2 = 0.3$); $y = 188x - 543$
- Lead: not significant

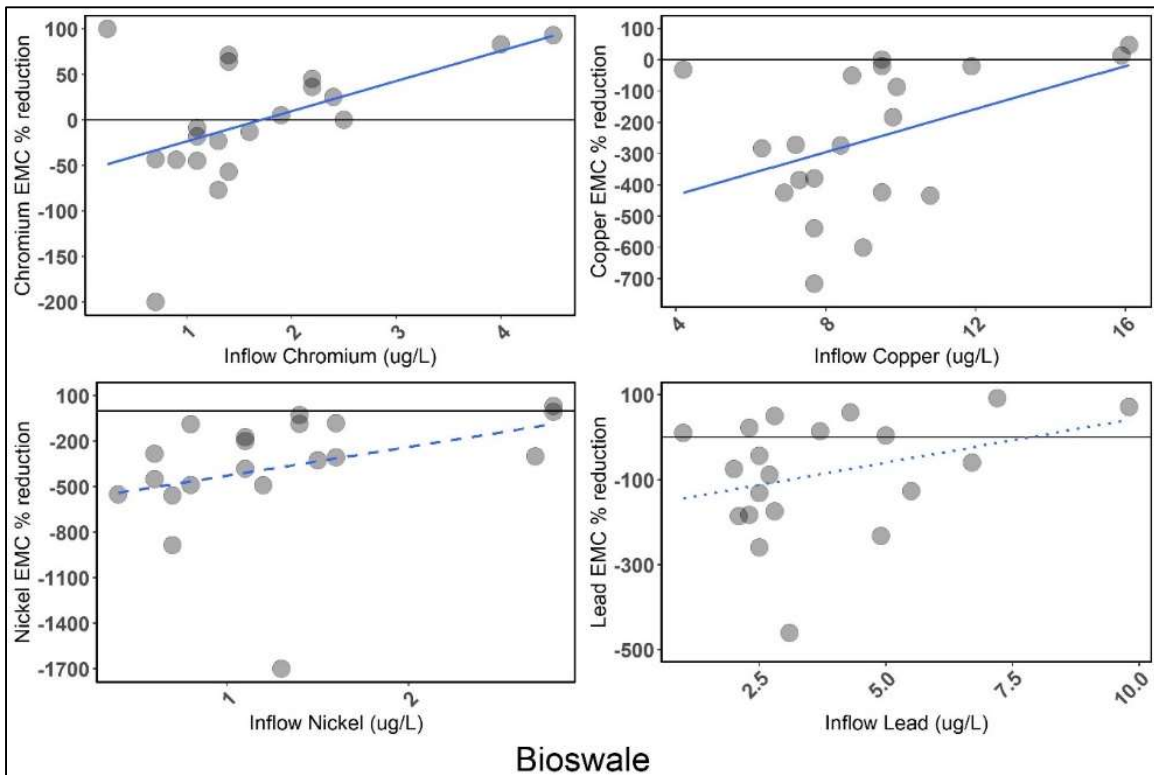


Figure H.2. Linear regression analyses showing relationship between inflow metal concentrations and EMC % reductions at the bioswale. Long dashes indicate omission of large negative reduction. Short dashes indicate no significance. Dots are partially transparent such that darker dots indicate overlapping data points.

Linear regression analyses (Figure H.3) indicated a significant positive correlation between inflow metal concentrations and their respective EMC reductions at the compost-amended grass channel according to the equations below. All regressions required dropping some data point(s) to be significant as indicated. Dashed lines indicate omission of large negative reduction value or high inflow concentration.

- Chromium (omits -300%): $P = .04$ ($R^2 = 0.2$); $y = 21x - 11$
- Copper (omits -600%): $P = .08$ ($R^2 = 0.2$); $y = 9.6x - 110$
- Nickel (omits -1070%): $P = .02$ ($R^2 = 0.3$); $y = 39x - 54$
- Lead (omits -500% and high inflow (109 ppb)): $P = .02$ ($R^2 = 0.3$); $y = 15x - 61$

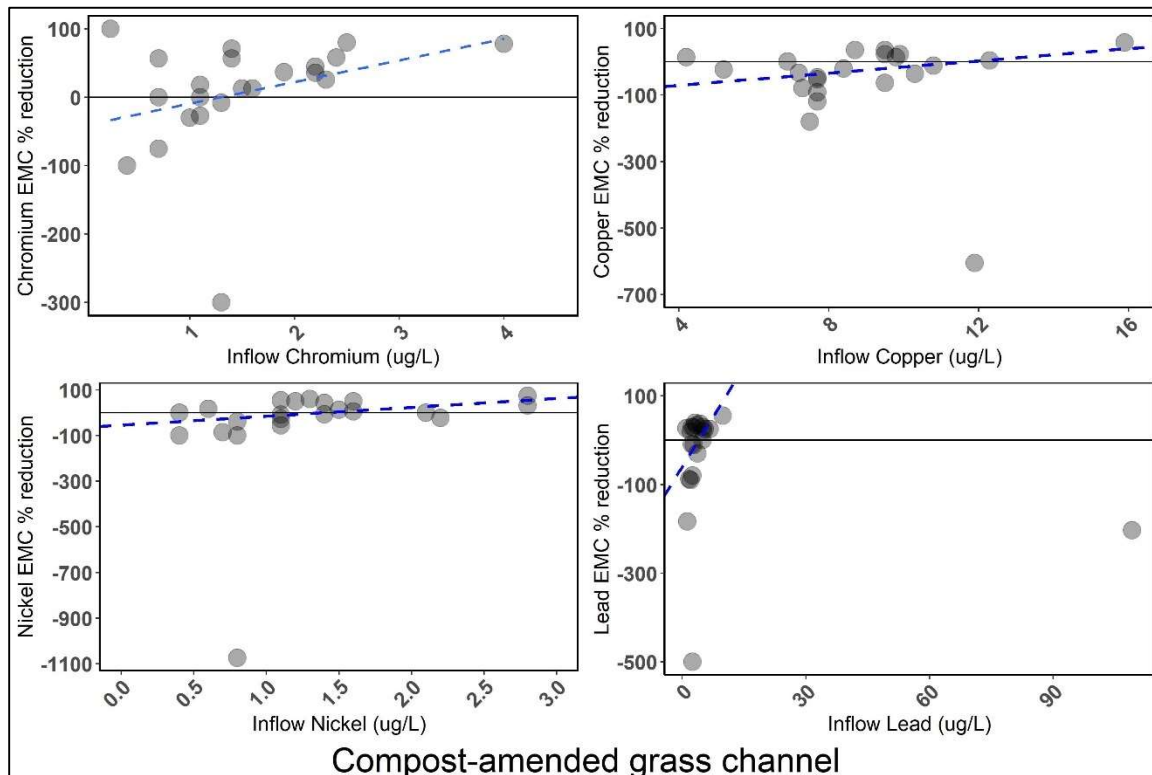


Figure H.3. Linear regression analyses showing relationship between inflow metal concentrations and EMC % reductions at the compost-amended grass channel. Long dashes indicate omission of large negative reduction. Lead also omitted the high inflow concentration. Dots are partially transparent such that darker dots indicate overlapping data points.

Linear regression analyses showed significant positive relationships between inflow metal concentrations and EMC reductions at the grass channel.

- Chromium: $P = .06$ ($R^2 = 0.2$); $y = 18x + 17$
- Copper: $P = .003$ ($R^2 = 0.4$); $y = 10x - 96$
- Nickel: $P = .06$ ($R^2 = 0.2$); $y = 26x + 10$
- Lead: $P = .02$ ($R^2 = 0.2$); $y = 16x - 85$

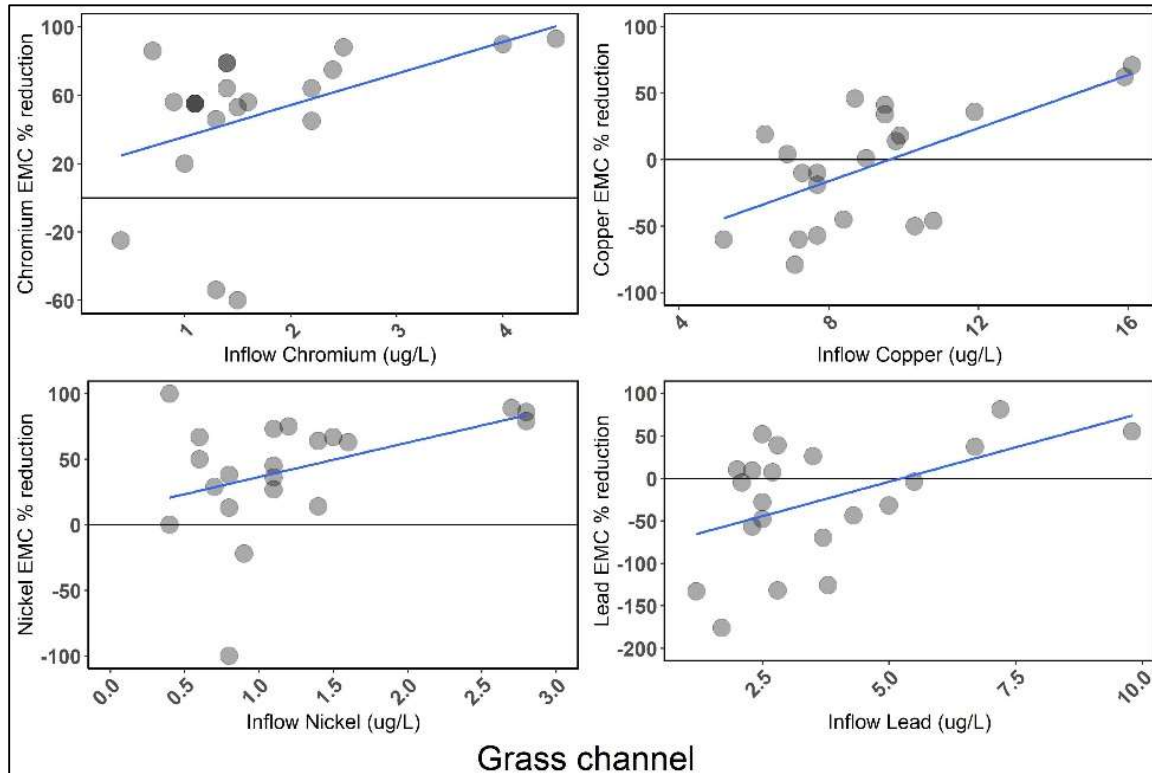


Figure H.4. Linear regression analyses showing relationship between inflow metal concentrations and EMC % reductions at the grass channel. Dots are partially transparent such that darker dots indicate overlapping data points.

6.10 APPENDIX I: SOIL DATA

The data for soils characterization is provided in Table I.1 and Table I.2. Due to methodology limitations, the salt and pH were not measured for the mulch of the bioretention.

Table I.1. Average and standard deviation of soil metal content for GI systems

Date	GI	Depth	Chromium (mg/kg)		Copper (mg/kg)		Nickel (mg/kg)		Lead (mg/kg)	
			Av.	Stand. Dev.	Av.	Stand. Dev.	Av.	Stand. Dev.	Av.	Stand. Dev.
2019-Oct	BR	Sub-surface	2.9	0.7	56.7	11.7	10.0	1.9	6.5	2.2
2019-Oct	BR	Top soil	3.1	1.4	54.4	17.7	8.4	2.6	6.2	2.6
2019-Oct	BR	Mulch	8.0	1.6	24.6	3.8	4.9	1.0	8.8	1.2
2019-Oct	BS	Sub-surface	3.7	2.5	44.6	32.6	7.2	4.2	9.9	1.8
2019-Oct	BS	Top soil	10.3	4.5	44.9	16.6	9.3	2.4	15.6	5.1
2019-Oct	CAGC	Sub-surface	7.2	2.6	9.4	4.7	1.7	1.0	13.3	2.4
2019-Oct	CAGC	Top soil	9.4	3.1	15.9	11.5	2.5	0.9	17.4	3.8
2019-Oct	GC	Sub-surface	6.9	2.2	5.2	1.1	1.7	0.6	21.8	2.7
2019-Oct	GC	Top soil	8.6	2.4	7.0	1.5	2.0	0.7	40.5	8.7
2020-Mar	BR	Sub-surface	4.1	1.5	65.0	29.1	12.4	4.7	7.9	2.9
2020-Mar	BR	Top soil	5.1	1.5	46.4	17.9	8.6	3.9	8.2	1.6
2020-Mar	BR	Mulch	2.8	1.0	11.0	4.1	2.2	0.8	3.9	1.0
2020-Mar	BS	Sub-surface	7.6	7.6	38.0	36.0	6.2	4.8	9.0	2.5
2020-Mar	BS	Top soil	15.4	6.5	32.0	22.1	9.1	2.0	16.8	4.9
2020-Mar	CAGC	Sub-surface	11.8	4.1	8.9	2.9	2.1	0.9	13.0	3.1
2020-Mar	CAGC	Top soil	11.8	2.6	21.6	9.8	3.5	0.8	14.6	3.1
2020-Mar	GC	Sub-surface	5.4	1.7	5.1	1.3	1.5	0.5	22.0	4.9
2020-Mar	GC	Top soil	8.0	2.2	9.7	4.7	2.7	0.4	43.6	33.5

Table I.2. Salt, organic percent, pH, SAR, and CEC of soils of GI systems reported as averages for each soil depth for each sampling session. SAR = sodium adsorption ratio. CEC = cation exchange capacity.

Date	GI	Depth	Chloride (mg/kg)		Sodium (mg/kg)		Organic percent (%)		pH		SAR		CEC	
			Av.	Stand. Dev.	Av.	Stand. Dev.	Av.	Stand. Dev.	Av.	Stand. Dev.	Av.	Stand. Dev.	Av.	Stand. Dev.
2019-Oct	BR	Sub-surface	3.9	2.4	711.3	89.6	2.5	0.1	6.4	0.2	39.8	27.1	16.0	2.0
2019-Oct	BR	Top soil	6.0	6.1	175.1	143.7	3.6	0.2	5.5	0.4	8.3	5.2	18.1	1.6
2019-Oct	BS	Sub-surface	25.5	36.2	220.0	60.0	3.6	0.5	6.0	0.9	9.9	7.8	12.5	5.4
2019-Oct	BS	Top soil	19.5	11.9	69.1	37.6	7.8	2.7	5.5	0.4	2.5	1.3	14.9	2.6
2019-Oct	CAGC	Sub-surface	101.5	83.9	133.5	75.5	5.6	0.7	5.8	1.1	7.2	4.1	11.6	1.0
2019-Oct	CAGC	Top soil	61.5	39.6	119.9	61.4	7.2	1.4	6.3	0.2	5.4	3.0	11.9	2.8
2019-Oct	GC	Sub-surface	5.4	0.4	19.2	3.4	3.9	0.5	5.7	0.3	0.8	0.3	6.3	0.6
2019-Oct	GC	Top soil	4.9	0.6	17.9	2.7	4.6	0.7	5.5	0.4	0.7	0.2	7.4	1.1
2020-Mar	BR	Sub-surface	4.2	4.6	462.5	445.3	2.7	0.3	6.0	0.2	14.3	14.1	15.7	3.0
2020-Mar	BR	Top soil	22.2	17.7	232.3	263.8	3.3	0.5	5.7	0.4	6.9	7.3	14.3	3.7
2020-Mar	BS	Sub-surface	4.2	2.6	75.2	29.4	3.1	0.2	6.2	0.1	3.2	2.4	10.9	8.2
2020-Mar	BS	Top soil	16.9	14.1	46.1	35.2	9.5	1.7	5.3	0.1	1.9	1.7	11.6	3.6
2020-Mar	CAGC	Sub-surface	15.2	4.5	121.0	58.1	7.1	3.5	5.8	0.1	4.6	2.9	11.7	2.8
2020-Mar	CAGC	Top soil	32.2	5.4	106.6	30.8	11.4	6.5	6.5	0.2	3.7	1.4	11.2	2.0
2020-Mar	GC	Sub-surface	1.6	0.4	28.4	10.1	3.8	0.1	5.0	0.4	1.9	0.8	4.7	0.1
2020-Mar	GC	Top soil	3.8	1.1	26.9	3.0	5.2	0.5	5.2	0.1	1.3	0.1	8.3	0.6

6.11 APPENDIX J: BACTERIA DATA

Table J.1 gives each *E. coli* and weather data for the monitored events. Table J.2 gives the other water quality constituents for the monitored events.

Table J.1. Data from each monitored event (April 2018 – February 2019). AMC: Antecedent moisture conditions. ^a Rainfall data from Ronald Reagan Airport.

	4/15/2018	4/27/2018	5/22/2018	6/2/2018	7/23/2018	7/30/2018	8/21/2018	9/28/2018	10/26/2018	11/10/2018	11/12/2018	12/15/2018	1/19/2019	1/25/2019	2/12/2019 ^a	2/23/2019	
Temp. (C)	12.4	14.1	21.2	21.8	25.4	24.0	25.1	17.6	8.9	7.9	7.4	9.6	3.7	6.3	2.1	6.3	
Rain (mm)	94.5	26.4	21.8	51.1	96.5	24.4	72.1	39.9	39.6	14.0	32.0	104	24.4	27.4	15.2	32.8	
AMC (mm)	1.0	28.2	44.7	0.0	134.0	179.0	2.0	43.4	0.0	67.3	14.5	0.3	3.8	24.1	0.8	2.0	
EMC (MPN/100 mL)	BR inlet	461	1046	9600 ^a	2000	6300 ^a	687	13400 ^a	6300 ^a	770	299	365		361	32	34	
	BR outlet	154	167	1553	1553	488	649	2419.6 ^a	411	1120	308	98	22	172	26	56	
	BR bypass	99	649	14600 ^a	3100 ^a	2419.6 ^a	1986	22300 ^a	1120	35500 ^a	3100 ^a	1000	6	142	10	272	
	Road runoff	365	7	1203	308		1414	980	236	201	78	5	19	16	35	1	
	GC out				2000	1986			980	15400 ^a	1300		138	86	150	39	31
	CAGC out			866	2000	6300 ^a	2419.6 ^a		276	17500 ^a	1733	3000 ^a		276	161	13	43
	BS out	16	387	12000 ^a	980	3000 ^a	17300 ^a		228		299		461	649	225	21	16
	Loading (MPN/event)	BR inlet	8.6E+08	4.4E+08	3.7E+09	1.1E+09	1.8E+10	2.1E+08	1.8E+10	3.5E+09	3.2E+08	7.4E+07	1.0E+09		1.5E+08	1.7E+07	2.0E+07
		BR outlet	4.6E+07	2.1E+07	1.7E+08	1.8E+08	2.6E+08	4.9E+07	6.1E+08	8.4E+07	1.6E+08	1.5E+07	4.4E+07	3.1E+06	2.3E+07	2.5E+06	9.5E+06
BR bypass		6.6E+07	2.4E+07	4.2E+08	1.2E+08	1.5E+09	9.6E+07	4.2E+09	4.1E+07	4.3E+08	4.7E+07	2.9E+07	1.6E+05	2.7E+06	2.0E+05	9.9E+06	
GC in		5.4E+07	1.2E+06	6.8E+07	6.3E+07		1.1E+08	8.3E+07	3.1E+07	2.7E+07	2.4E+06		2.4E+06	2.8E+06	3.2E+06	3.1E+06	1.2E+05
GC out					4.8E+07	1.6E+08			4.7E+07	4.2E+08	2.0E+07		1.0E+07	3.3E+05	2.6E+05	4.6E+05	2.7E+04
CAGC in		5.6E+07	1.2E+06	6.6E+07	6.1E+07		1.1E+08	8.1E+07	3.9E+07	2.6E+07	2.4E+06		2.4E+06	2.7E+06	3.1E+06	3.0E+06	1.2E+05
CAGC out				2.6E+07	2.7E+08	2.4E+09	4.3E+07		3.2E+07	4.9E+08	2.6E+07	2.1E+08		2.0E+06	1.3E+06	2.8E+06	1.0E+05
BS in		5.2E+07	1.2E+06	6.8E+07	6.3E+07		1.1E+08	8.3E+07	2.8E+07	2.7E+07	2.3E+06		2.3E+06	2.8E+06	3.2E+06	3.1E+06	1.2E+05
BS out		1.3E+06	2.0E+07	4.5E+08	1.5E+08	5.6E+08	5.0E+07		1.5E+07		4.2E+06		1.4E+08	1.6E+06	1.2E+06	1.7E+06	1.1E+05

Table J.1 (continued). Data from each monitored event (March 2019 – April 2020)

		3/21/2019	5/5/2019 ^a	10/17/2019	11/23/2019	2/7/2020	4/13/2020 ^a
	Temp. (C)	8.0	19.4	14.4	5.7	7.6	14.8
	Rain (mm)	64.8	78.7	40.6	22.1	47.0	70.9
	AMC (mm)	0.5	16.3	2.8	5.1	6.1	0.3
EMC (MPN/100 mL)	BR inlet	488	8200 ^a	1046	29500 ^a	345	2000
	BR outlet	105	1414	27900 ^a	6300 ^a	199	921
	BR bypass	649	1000	8600 ^a	1000	260	2000
	Road runoff	32	214	7	13	19	
	GC out	13	12200 ^a	44300 ^a	921	48	387
	CAGC out	435			291	88	199
	BS out	21		172000 ^a	248	21	250
Loading (MPN/event)	BR inlet	5.9E+08	5.4E+09	5.2E+08	1.2E+10	2.9E+08	4.0E+09
	BR outlet	2.8E+07	3.0E+08	3.9E+09	4.4E+08	4.5E+07	2.3E+08
	BR bypass	9.6E+07	4.7E+07	2.3E+08	2.4E+07	1.4E+07	9.7E+08
	GC in	9.3E+06	7.0E+07	1.3E+06	5.8E+05	1.9E+06	
	GC out	1.9E+06	5.0E+06	1.1E+04	9.4E+04	1.5E+06	2.8E+07
	CAGC in	9.0E+06	6.9E+07	1.3E+06	5.6E+05	1.9E+06	
	CAGC out	6.3E+06			4.7E+05	9.6E+06	2.9E+07
	BS in	9.3E+06	7.0E+07	1.3E+06	5.8E+05	1.9E+06	
BS out	4.2E+06		1.9E+05	3.5E+05	1.9E+06	5.3E+07	

Table J.2. TSS, TN, DOC, and chloride GI outlet values of monitored events used in linear regression analyses (April 2018 – March 2019)

		4/15/2018	4/27/2018	5/22/2018	6/2/2018	7/23/2018	7/30/2018	8/21/2018	9/28/2018	10/26/2018	11/10/2018	11/12/2018	12/15/2018	1/19/2019	1/25/2019	2/12/2019 ^a	2/23/2019	3/21/2019
BR out	TSS	29.5	32.2	15.0	10.2	15.2	13.2	22.3	3.2	6.8	3.3	3.0	6.7	5.9	3.2	3.1	1.5	11.1
	TN	0.7	0.5	0.7	0.4	0.4	0.5	0.6	0.6	0.9	0.7	0.6	0.5	1.0	0.9	1.1	0.8	0.7
	DOC	13.4	10.0	9.1	8.3	8.4	7.9	10.6	4.7	6.4	4.4	3.4	4.8	3.1	3.6	3.9	3.7	6.1
	Cl-	549.6	71.5	49.8	37.9	25.9	40.3	16.9	25.1	21.6	31.6	23.4	20.5	1489.9	345.2	618.1	406.9	74.7
GC out	TSS				11.3	11.5			8.2	28.2	12.5	5.0	18.0	13.8	16.7		26.5	36.3
	TN				0.4	0.5			0.5	0.8	0.5	0.4		0.0	0.0	0.3	0.2	0.4
	DOC				9.6	11.7			10.4	15.2	8.8	6.9	5.3	5.5	6.8	6.8	4.3	7.2
	Cl-			26.3	4.1	3.3			4.2	9.4	3.3	4.0	1.7	70.2	41.5	61.3	64.1	16.8
CAGC out	TSS			58.7	35.7	20.0	54.7		79.0	40.8	38.8	17.6		40.0	39.8	23.7	83.6	76.0
	TN			1.0	0.9	1.0	2.0		1.1	0.9	0.7	0.7		0.6	0.0	0.5	0.4	0.6
	DOC			20.9	20.4	20.0	23.4		21.5	20.6	14.9	11.8		9.9	11.8	10.2	7.1	10.5
	Cl-			37.0	30.2	16.7	34.4		15.0	44.8	22.8	16.0		364.3	166.7	396.0	118.2	61.7
BS out	TSS	115.7	47.8	54.7	19.3	36.5	46.7		11.8		5.5		20.7	5.5	17.0	10.0	14.8	16.3
	TN	0.3	0.5	0.7	0.6	0.7	0.8		0.5		0.4		0.5	0.5	0.5	0.5	0.4	0.4
	DOC	11.8	11.8	12.9	12.4	11.6	13.6		8.7		7.6		7.3	5.9	6.4	6.1	5.6	6.5
	Cl-			46.3	28.8	22.7	28.0		14.8		12.9		13.1	1765.5	808.2	1041.4	402.1	140.6

Table J.2. TSS, TN, DOC, and chloride GI outlet values of monitored events used in linear regression analyses (May 2019 – April 2020)

		5/5/2019 ^a	10/17/2019	11/23/2019	2/7/2020	4/13/2020 ^a
BR out	TSS	29.0	10.1		7.8	12.9
	TN	0.8	0.9	1.1	0.9	0.8
	DOC	10.8	17.8	9.5	5.5	7.7
	Cl-	27.0	10.7	10.0	30.0	
GC out	TSS	34.3			55.3	38.9
	TN	0.8	2.5	1.2	0.5	0.5
	DOC	13.6	23.0	10.7	7.9	7.4
	Cl-	7.0	4.7	5.9	20.7	
CAGC out	TSS				33.8	59.7
	TN			1.0	0.7	0.5
	DOC			18.9	11.8	10.1
	Cl-			75.3	21.1	
BS out	TSS		31.2		83.3	43.0
	TN		1.3	1.0	0.7	0.8
	DOC		15.5	9.2	6.9	10.5
	Cl-		51.6	75.9	22.6	

Field Blanks

Field blanks consisted of distilled water passed through the autosampler tubing via the grab sample command after the cleaning procedure was completed. In September 2018, field blanks for the BR inlet and bioswale were both 0 MPN/100 mL. In March 2019, field blanks for the bioswale and BR outlet were both 0 MPN/100 mL. In June 2020, readings of *E. coli* taken to verify cleaning procedure were 0 MPN/100 mL for all autosamplers except for the bioretention inlet which had 2 MPN/100 mL and 1 MPN/100 mL for the bioswale.